ATLAS Deliverable 3.2

Water masses controls on biodiversity and biogeography

Project acronym:	ATLAS
Grant Agreement:	678760
Deliverable number:	Deliverable 3.2
Work Package:	WP3
Date of completion:	28.02.2019
Author:	Lea-Anne Henry (lead for D3.2), Patricia Puerta
Contributors	(alphabetical, all contributors are also authors) Sophie Arnaud-Haond, Barbara Berx, Jordi Blasco, Marina Carreiro-Silva, Laurence de Clippele, Carlos Domínguez-Carrió, Alan Fox, Albert Fuster, José Manuel Gonzalez-Irusta, Konstantinos Georgoulas, Anthony Grehan, Cristina Gutiérrez-Zárate, Clare Johnson, Georgios Kazanidis, Francis Neat, Ellen Kenchington, Pablo Lozano, Guillem Mateu, Lenaick Menot, Christian Mohn, Telmo Morato, Ángela Mosquera, Francis Neat, Covadonga Orejas, Olga Reñones, Jesús Rivera, Murray Roberts, Alex Rogers, Steve Ross, José Luis Rueda, David Stirling, Karline Soetaert, Javier Urra, Johanne Vad, Dick van Oevelen, Pedro Vélez-Belchí, Igor Yashayaev

This project has received funding from the European Union's Horizon 2020 research and innovation programme under grant agreement No 678760 (ATLAS). This output reflects only the author's view and the European Union cannot be held responsible for any use that may be made of the information contained therein.

Contents

1. Executive Summary

The oceanographic and hydrographic conditions of the North Atlantic are predicted to dramatically change by this century's end. The Atlantic Meridional Overturning Circulation (AMOC) is anticipated to slow, and many of the waters that currently bathe vulnerable marine ecosystems (VMEs) are predicted to be warmer, have reduced oxygen and food supply, and be more acidic. Among the many ways in which impacts of climate change on VMEs are being studied in ATLAS is the empirical approach, whereby effects of present day oceanographic variables are directly related to VME biodiversity through systematic review or statistical analyses. Deliverable 3.2 adopts this empirical approach: first, D3.2 reviews what is known about effects of oceanographic variables on VME biodiversity across the North Atlantic to derive a basin-scale synoptic view of key ocean controls on system biodiversity; second, D3.2 examines the statistical significance of these variables in selected regional ATLAS Case Studies covering several Exclusive Economic Zones (EEZs) and Areas Beyond National Jurisdiction (ABNJ).

Our review concluded that VMEs in several ATLAS Case Study areas will likely be impacted by critical changes and multiple stressors, even without additional human activities from the Blue Economy. VMEs in the western North Atlantic that are predicted to experience critical changes in sea temperatures and food supply (Flemish Cap and Davis Strait) are also the Case Studies that the review and empirical analyses identified as having temperature and food supply playing significant roles in the occurrence of VMEs and biodiversity of their associated communities, which seem to depend on relatively cooler water at least on the Flemish Cap. Projected critical declines in oxygen, pH, and a shoaling of the aragonite saturation horizon for the Davis Strait however need further in-depth investigations to ascertain impacts on future VMEs. Many VMEs in the mid- to eastern North Atlantic are also projected to experience multiple critical changes (Reykjanes Ridge, Norway, Faroe Shetland Channel, Rockall, Porcupine Seabight, Mingulay Reef Complex, and the Azores), which our review and empirical analyses strongly suggest will impact VMEs. Targeted studies at our eastern Atlantic Case Studies showed warmer oceans are likely to alter the biogeographic affinities of cold-water coral communities at Mingulay, the biodiversity and density of sponge grounds in the Faroe Shetland Channel, while reductions in food supply could significantly reduce the density of octocorals and black corals at Rockall, and result in species loss of sponge grounds and coral gardens in the Azores.

Deliverable 3.2 shows that a backdrop of climate change will narrow the margins for safe ecological and thus operational limits of existing and emerging ocean industries. It is understood that biodiversity enhances ecosystem resilience by contributing to both climate change mitigation and adaptation. Thus, we make the policy recommendation under the Convention on Biological Diversity Aichi Target 15 that regulatory frameworks for licensing and planning such as Environmental Impact Assessments and Strategic

Environmental Assessments explicitly incorporate climate change impacts to assist blue economy sectors to avoid, minimise, restore or offset biodiversity loss resulting from resource exploration or exploitation.

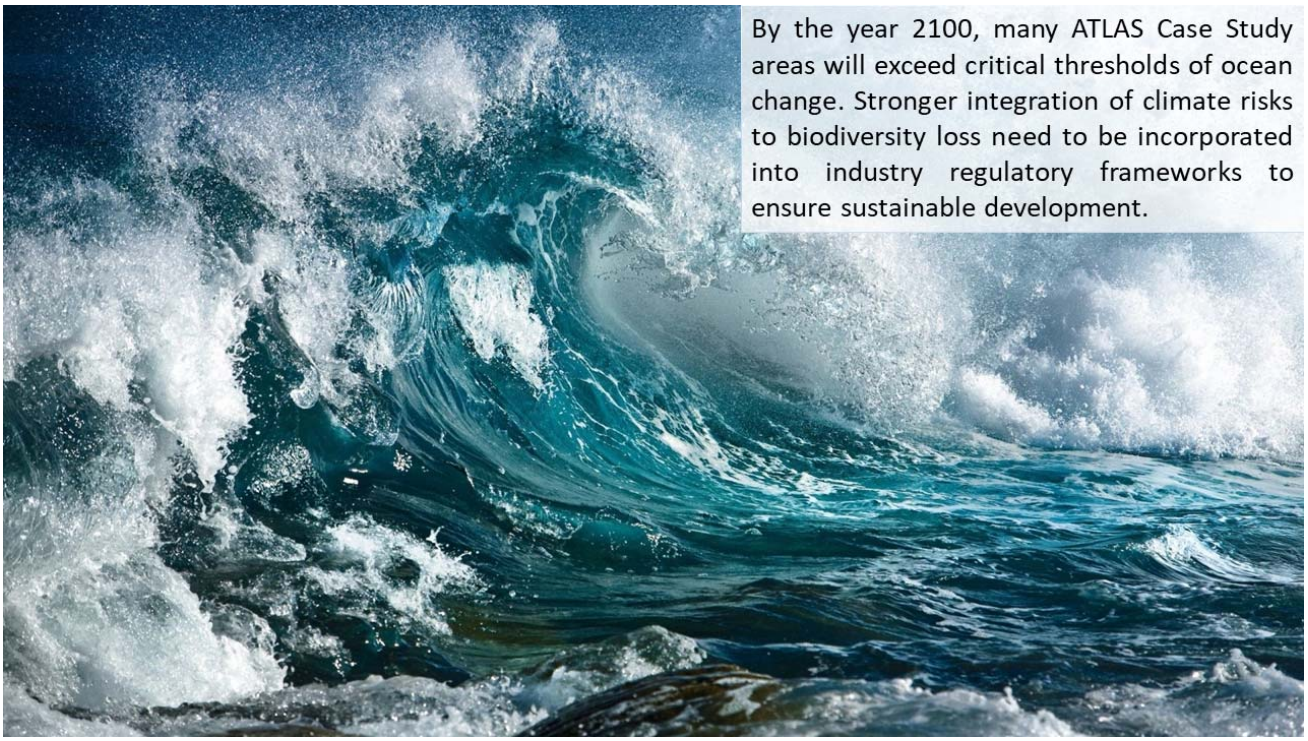

By the year 2100, many ATLAS Case Study areas will exceed critical thresholds of ocean change. Stronger integration of climate risks to biodiversity loss need to be incorporated into industry regulatory frameworks to ensure sustainable development.

2. Review: Influence of water masses on deep-sea biodiversity and biogeography of the North Atlantic

Authors: Patricia Puerta, Covadonga Orejas, Marina Carreiro-Silva, Clare Johnson

Contributors: Lea-Anne Henry, Telmo Morato, Georgios Kazanidis, José Luis Rueda, Javier Urra, Pablo Lozano, Ellen Kenchington, Igor Yashayaev, Dick van Oevelen, Lenaick Menot, David Stirling, José Manuel Gonzalez-Irusta, Steve Ross, Christian Mohn, Alan Fox, Sophie Arnaud-Haond, Anthony Grehan and J. Murray Roberts

Acknowledgements: Luis Rodrigues, Carlos Domínguez-Carrió

Summary

Different water masses and their characteristic properties are major drivers of biodiversity and biogeography patterns in the deep sea. Circulation patterns and water mass characteristics along the North Atlantic have changed and re-organized multiple times since the genesis of this ocean, affecting the composition and functioning of deep-sea ecosystems. We reviewed the evolution of the North Atlantic circulation and water mass properties, such as temperature, salinity, oxygen or organic matter content, and their impacts on VMEs occurring from the continental shelves to the bathyal regions of the deep sea. Eleven case studies, spanning different features and habitats across the North Atlantic, have been included as examples to illustrate how different water masses shape VME biodiversity and biogeography. Finally, we forecasted conditions in several water mass properties to explore how these changes might affect VMEs and their associated deep-sea benthic communities, with a particular focus on critical cumulative changes in the case study areas. This review and the assessment of future conditions might help identify areas likely to experience the biggest changes in oceanic properties to help us learn how to better manage the deep North Atlantic as deepwater industries develop.

Setting the context: the North Atlantic Ocean

In the North Atlantic Ocean, the Atlantic Meridional Overturning Circulation (AMOC) re-distributes warm saline water masses northwards. These water masses are compensated by a deeper southerly circulation of cooler fresher waters, accounting for 25 % of global heat transport. Climate models forecast a slowing or even disappearing of the AMOC by the end of the century, which will modify water masses characteristics and circulation patterns. Thus, warmer temperatures of 1 or 2 °C, reduced organic carbon fluxes (up to 50 %), ocean acidification, shoaling of the aragonite saturation horizon (above 1000 m) and deoxygenation are expected to significantly impact the deep-sea benthic communities and VMEs, and even compromise their survival. This review will show that most, if not all, of the areas encompassed by Case Studies in ATLAS will experience a critical change in at least one of the variables but since the potential impacts on their VMEs has remained poorly investigated, this part of the Deliverable 3.2 begins by reviewing how VMEs might be impacted by looking at contemporary controls on VME biodiversity and biogeography.

Oceanic Drivers of Deep-sea Biodiversity and Biogeography Patterns

Deep-sea ecosystems have been traditionally considered vast habitats in the ocean characterised by stable and homogeneous environment (darkness and constant low temperatures) with lack of barriers for dispersal, resulting in large biogeographic areas with broad distributions of the deep-sea species (McClain & Hardy 2010, Smith et al. 2006b). In the last few decades, new technologies allowed us to overcome many of the challenges of sampling these remote ecosystems, revealing new discoveries and ecological paradigms in the deep sea (Cunha et al. 2017, Danovaro et al. 2014), including the discovery of geormorphological features and ecosytems such as submarine canyons (Fernandez-Arcaya et al. 2017), seamounts (Morato et al. 2013), hydrothermal vents (Ramirez-Llodra et al. 2007b) or cold-water coral (CWC) reefs (Roberts et al. 2006). High habitat complexity (Beazley et al. 2013, Buhl-Mortensen et al. 2010, Henry et al. 2010), the role on carbon recycling (Duineveld et al. 2012, Guihen et al. 2013, Hofmann & Schellnhuber 2009, Rix et al. 2016, Wild et al. 2009), the recently discovered ecological interactions (Buhl-Mortensen & Mortensen 2004, Carreiro-Silva et al. 2017, Henry & Roberts 2017) or chemosynthetic production in the deep-sea (Levin et al. 2016, Ramirez-Llodra et al. 2007a, Rodrigues et al. 2013) for instance, have been proved to enhance biodiversity, allowing us to reject the old picture of low diversity, food-poor and metabolic inactivity of the largest ecosystem on Earth (Cunha et al. 2017, Danovaro et al. 2014, Ramirez-Llodra et al. 2010).

Many of the factors that drive biodiversity and biogeography in the deep sea are inherent or related to the water masses characteristics. These included factors such as temperature (Yasuhara & Danovaro 2014), flow regime (Mienis et al. 2007, van Haren et al. 2014), seafloor topography and sedimentary features (Collart et al. 2018, Levin & Sibuet 2012, Tong et al. 2012), oxygen (Levin 2003, Woulds & Cowie 2007), organic matter supply (Guihen et al. 2013, Guinotte et al. 2006) or circulation patterns (Henry et al. 2014, Somoza et al. 2014), among others. The presence of different water masses influences the biodiversity, distribution and connectivity of the deep-sea habitats including VMEs (Henry et al. 2014, Radice et al. 2016). In addition, the properties and spatial extent of these water masses in the North Atlantic present inter-annual to decadal variability in response to atmospheric forcing (such as, the North Atlantic Oscillation or NAO, and the Atlantic Multidecadal Oscillation or AMO) and create a fluctuating environment that varies at local, regional and basin scales. Thus, changes in the deepwater circulation in the Atlantic Ocean are of particular interest in order to understand deep-sea species distribution, community composition, ecosystem functioning

and dynamics, but also to shed light on the past and future climate changes and how they might affect deep-sea organisms.

Re-organisations in North Atlantic water mass structure have been occurring since the Atlantic's genesis 200 My ago, and we know that VMEs such as the distribution of cold-water coral reefs and their biodiversity can be driven by re-organisations in water mass structure caused by AMOC and Sub-Polar Gyre (SPG) dynamics (Henry et al. 2014, Wienberg & Witschack 2017). To preserve deep-sea biodiversity and ensure a sustainable socio-economic development in the Atlantic Ocean, ecosystem-based management is needed on the same spatial and temporal scales as the key ocean circulation features (e.g. AMOC, SPG) and atmospheric drivers such as those driven by the NAO and AMO. This requires that we be able to disentangle effects of regional and basin-scale changes in oceanography on VME biodiversity and biogeography from impacts of more localised human activities. We need to understand which, and how, ocean variables affect biodiversity and biogeography of VMEs in the North Atlantic, and then to determine how these key ocean drivers are likely to change the focal VMEs in our Case Study areas in the future.

North Atlantic Circulation and Key Water Masses

Atlantic Meridional Overturning Circulation (AMOC)

The Atlantic is Earth's youngest ocean, its genesis rooted in the splitting of Pangaea 200 My ago. The opening of the Norwegian-Greenland Sea during the Late Paleocene to Early Eocene created a new pathway for the exchange of water between the Arctic and North Atlantic Oceans that forever impacted the global ocean-climate system (Thiede 1979). Deglacial-Holocene changes were crucial for the current configuration of the AMOC and the global ocean convenyor belt. The main warm and saline water mass transport through the AMOC goes from eastern to western basin via the North Atlantic Current (NAC). With the strength of the SPG partly controlling the inflow of NAC into the Rockall Trough, the pathways and properties of the NAC can therefore be altered by shifting the position of the eastern limb of the subpolar front (Lozier & Stewart 2008).

A moderate to strong AMOC probably persisted in the intermediate water mass layers during the last glacial maximum 19 – 21 kyr ago (Lippold et al. 2009, Lynch-Stieglitz et al. 2007, Ritz et al. 2013), which was followed by a slowdown of the AMOC throughout the deglacial period 12 – 19 kyr coinciding with the Younger Dryas. This period represents one of the most well-known abrupt climate changes on Earth, shifting from a cold glacial world to a warmer interglacial state in the North Atlantic

14 kyr ago. Fossil records indicate that the currently widespread CWC *Lophelia pertusa* remained relegated to a few refugia during the Last Glacial Maximum (LGM) and deglacial times when AMOC was reduced (Henry et al. 2014). Relative strong SPG at mid-depths characterized the early Holocene (Colin et al. 2010, Montero-Serrano et al. 2011), and a strong AMOC was re-established after the Younger Dryas (Rogerson et al. 2006, Xie et al. 2012), probably due to the enhanced export of Mediterranean and Caribbean water masses into the Atlantic (Henry et al. 2014), which increased both deep-water convection and production in the Nordic Seas (Rogerson et al. 2006). This rapid spin-up of overturning during the early Holocene coincided with a rapid and widespread return of *L. pertusa* to northern Europe after a hiatus of over 65 kyr (after Frank et al. 2011). Thus, CWCs achieved the fastest postglacial range re-expansion ever recorded, covering 7500 km in under 400 years alongside a re-invigorated AMOC.

Today, the AMOC is still a crucial part of the climate regulation by balancing Earth's net radiation budget, mediating 25 % of global heat transport via intense air-sea interactions. As a critical component of global ocean thermohaline exchange (Khélifi & Frank 2014), with a northward flowing of warm, saline upper waters which converts to denser cold waters returning southward at depth, the kinetics of the AMOC also connects much of the living marine resources across the ocean basin.

Key Water Masses and Gyre Dynamics affecting North Atlantic VMEs

In the upper limb of the AMOC, warm and salty waters are transported northwards within the Gulf Stream and across the Mid-Atlantic Ridge into the eastern basins via the NAC (Fig. 1). Around 40 % of this water flows northward over the Greenland-Scotland Ridge into the Nordic Seas (8.4 Sv; i.e. 8.4 million $m^3 s^{-1}$), whilst 12.7 Sv recirculates cyclonically around the SPG (Sarafanov et al. 2012). The SPG is the dominant feature of the surface subpolar North Atlantic with an anticyclonic circulation (Berx & Payne 2017, Hátún et al. 2017). As the upper waters circulate in the SPG they are cooled and freshened via air-sea fluxes leading to an increase in density. The upper waters that enter the Nordic Seas are further subject to winter heat loss and storms which mix these waters with denser underlying waters trapped by the bathymetry. Hence, in the Nordic Seas upper waters are converted to denser intermediate and bottom waters (Fig. 1).

These deeper water masses are, in the main, trapped to the north of the Greenland Scotland Ridge; however, 6.5 Sv is estimated to low into the Atlantic through channels in the ridge (Beaird et al. 2013, Hansen et al. 2016, Jochumsen et al. 2017). The other 12.7 Sv of upper waters that recirculate within the North Atlantic are also subject to winter storms, mainly in the Labrador Sea but also in the Irminger Sea (Jong & Steur 2016, Yashayaev 2007). The upper waters are converted here to denser intermediate water masses, termed Labrador Sea Water, which circulates both within the SPG and southwards along with the overflow waters in the Deep Western Boundary Current also known as the lower limb of the AMOC (Fig. 1).

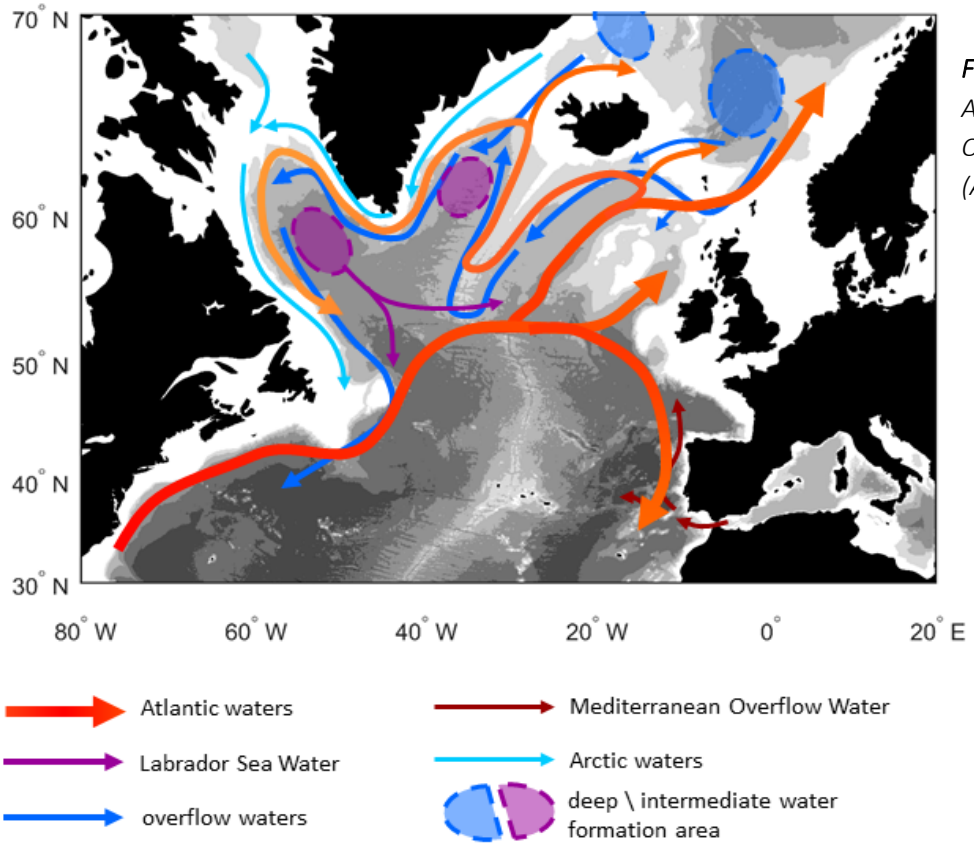

Figure 1. Schematic of the Atlantic Meridional Overturning Circulation (AMOC) in the North Atlantic.

The predominant water mass in the upper 500 – 1000 m is North Atlantic Central Water (NACW) (Fig. 2), which is warm and salty although its properties vary spatially. For example, the NACW east of the Mid-Atlantic Ridge (so-called ENACW or ENAW) is formed by winter convection in the intergyre region (Pollard et al. 1996) and is warmer and saltier (8 – 16°C and 35.5 – 36.2 psu; Pollard et al. 2004, Ríos et al. 1992) than that found further west (named WNACW or WNAW). The nutrient concentrations of the two water masses also differ, being considerably higher in the west (Johnson et al. 2013). Moving northward into the SPG, the upper waters are cooler and fresher due to air-sea fluxes and are sometimes referred to as Subpolar Mode Waters (SPMW). Again, salinities and

temperatures decrease east-to-west, while nitrate and phosphate concentrations increase (García-Ibáñez et al. 2015, Read 2000). Finally, fresher (< 34.9 psu) Subarctic Intermediate Water (SAIW) is also observed in the upper layers of the Irminger and Labrador Seas (García-Ibáñez et al. 2015).

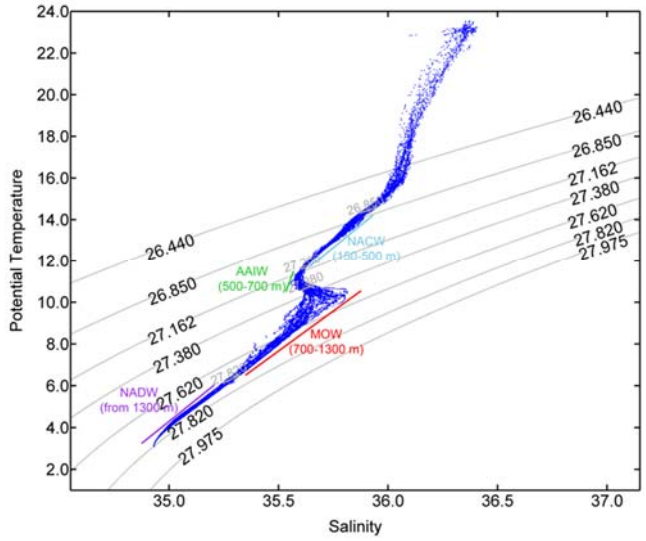

Figure 2. Temperature/Salinity diagram showing different water masses in the Formigas Seamount (Azores). Depth range where water masses were detected is indicated in the figure. Abbreviations: AAIW, Antarctic Intermediate Water; NACW,North Atlantic Central Water; NADW, North Atlantic Deep Water; MOW, Mediterranean Outflow Water.

Below the upper waters, four main intermediate water masses are observed (Fig. 2; example of intermediate water masses observed in the Azores): Mediterranean Outflow Water (MOW), SAIW, Antarctic Intermediate Water (AAIW), and Labrador Sea Water (LSW). MOW is a salty water mass (35.5-35.6 psu; Fig. 2) with a low dissolved oxygen concentration (~200 µmol kg^{-1}) that overflows the Straits of Gibraltar and spreads out at around 1000 m depth in the Atlantic (Bower et al. 2002, Reid 1979). Although SAIW exists as an upper water mass in the Irminger and Labrador Sea; further east it is found below the upper waters (Pollard et al. 1996, Wade et al. 1997). AAIW has been observed as far north as 60° N (Tsuchiya 1989), being identifiable by a slightly higher salinity than surrounding water masses and an elevated silicate concentration (11.0 – 11.5 µM; Read 2000). The intermediate water column present a wide-spread biochemical feature centered upon 500 – 1200 m: the mid-depth oxygen minimum (~220 µmol kg^{-1}) and the associated but less-well defined local nutrient maximum and elevated organic matter remineralization (Crocket et al. 2018, Read 2000). Finally, LSW is found between 500 – 2000 m, being predominantly formed by deep winter convection in the Labrador Sea (Yashayaev 2007), although evidence suggests, it is also formed in the Irminger Sea (Jong & Steur 2016, Pickart et al. 2003). Due to its formation mechanism, it is characterised by a broad salinity minimum (< 34.9 psu), potential vorticity minimum, and higher oxygen concentrations (~290 µmol kg^{-1}). However, its exact signature, density and volume varies inter-annually with changes

in the convection depth (Yashayaev 2007). LSW spreads out from the Labrador Sea into the subpolar North Atlantic, and also southward both as a component of the Deep Western Boundary Current and via interior pathways (Bower et al. 2009, Fischer et al. 2004).

The deepest water masses in the North Atlantic are: Iceland Scotland Overflow Water (ISOW), Denmark Strait Overflow Water (DSOW), and Antarctic Bottom Water (AABW). ISOW is formed as Norwegian Sea Deep Water overflows the Iceland-Scotland Ridge. Although small volumes flow over the Wyville-Thomson and Iceland-Faroe Ridge, the main flow is through the Faroe Bank Channel (2.2 Sv) into the north-eastern Iceland Basin (Dickson & Brown 1994, Hansen et al. 2016). From here, ISOW flows cyclonically around the northern and western boundaries of the Iceland Basin, through fracture zones in the Mid-Atlantic Ridge, and into the Irminger Sea. Here, it is joined by DSOW that overflows through the Denmark Strait. DSOW is cooler, fresher and denser than ISOW (Fogelqvist et al. 2003, García-Ibáñez et al. 2015). DSOW and ISOW move cyclonic around the Labrador Sea and then southward within the Deep Western Boundary Current where they are termed North Atlantic Deep Water (NADW; Fig. 2). The last water mass we consider is AABW, also sometimes known as Lower Deep Water (LDW). This water mass, which has been heavily modified since its formation in the Southern Ocean, is most easily identified by its high silicate concentration (> 30 μmol kg^{-1}). It is most prevalent in the areas south of the subpolar basins (Read 2000), although a diluted form can also be observed in the Rockall Trough and Iceland Basins (New & Smythe-Wright 2001, Van Aken & De Boer 1995).

Variability of North Atlantic water masses

The properties and spatial extent of water masses in the North Atlantic exhibit interannual to decadal variability. An important source of variability is the strength and extent of the SPG, which is also linked to the atmospheric forcing such as the NAO (Lozier & Stewart 2008; Fig.3). The variability in SPG affects water masses contribution, North Atlantic circulation and nutrient concentrations. When the SPG is strong, it expands eastward increasing the amount of cooler and fresher subpolar waters within the eastern basins and reducing the contribution of warmer and saltier ENACW. Oppositely, when the gyre is weaker, it contracts westward leading to increased temperatures and salinities in the eastern basins. The SPG variability affects the pathways and spread of both MOW and LSW (Fig.3). During a weak state, more MOW flows northwards into the Rockall Trough (Bozec et al. 2011, Lozier & Stewart 2008). When the SPG is strong, the northward pathway of MOW is curtailed but more LSW is able to enter the Rockall Trough from the west (Lozier & Stewart 2008).

Another important mechanism is the strength of air-sea fluxes over the Labrador and Irminger Seas, and the associated intensity of winter convection. Stronger atmospheric cooling leads to deeper winter convection, and the production of cooler, fresher and denser LSW in greater volumes (Yashayaev 2007).

A strong SPG is additionally associated with elevated nitrate and phosphate concentrations, and a weaker gyre with lower values in the upper 800 m (Johnson et al. 2013, Sherwin et al. 2012). Silicate concentrations in the upper waters of the subpolar North Atlantic also varied with SPG with a more complex mechanism linked to the depth of winter convection. The silicate concentrations have decreased by 1.5 – 2.0 µM over the past 25 years (Hátún et al. 2017). Finally, changes in the dissolved oxygen content (Stendardo & Gruber 2012) and carbon chemistry (Vazquez-Rodriguez et al. 2012) have also been observed. In the eastern SPG dissolved oxygen concentrations have decreased in the upper waters (-5 µmol kg^{-1} $decade^{-1}$) and increased below 1500 m (2.5 µmol kg^{-1} $decade^{-1}$), over the past 50 years; whilst in the Labrador Sea an increase of between 0 and 4 µmol kg^{-1} $decade^{-1}$ is observed in the very top of the water column. In the STG, concentrations are again lower and higher in the upper waters and LSW respectively, but there is also a mid-depth peak (5 µmol kg^{-1} $decade^{-1}$) centred upon ~450 m. Overall, in the Atlantic as a whole, oxygen reduction in upper waters is linked to a change in the solubility associated with warming, whilst at deeper levels this mechanism is only dominant in the south-

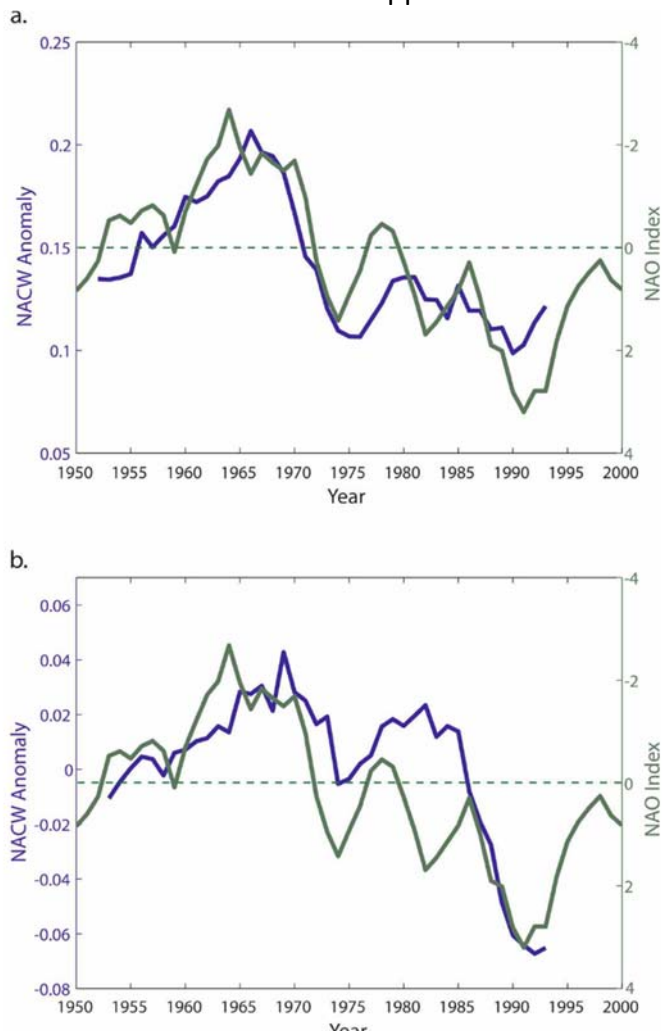

Figure 3. Time series of salinity anomalies (psu, blue) in the Rockall Trough and the NAO index (green) (a) at the MOW level (on σ_1 = 32.10) 5-yr running mean, 2-yr lag [r^2 = 0.72 ($p < 0.01$)] and (b) at the LSW level (on $\sigma_{1.5}$ = 34.66) 5-yr running mean, 3-yr lag [r^2 = 0.60 ($p < 0.01$)]. Note that the NAO index is plotted on a reverse y axis and that the 0 position is marked by a green dashed line (Lozier & Stewart 2008).

western North Atlantic, with changes in circulation and ventilation being more important elsewhere. Widespread changes in carbon chemistry have also been observed with a general decrease in pH over all areas and all depth ranges between 1981 and present (Perez et al. 2018, Vazquez-Rodriguez et al. 2012). In the upper waters the largest reduction is observed in the Irminger Sea ($-1.85 \cdot 10^{-3}$ yr^{-1}), with a less pronounced acidification in the more eastern basins ($-0.94 \cdot 10^{-3}$ yr^{-1}) due to partial compensation of the anthropogenic signal by increased primary productivity. Decreases in pH are also observed in the recently ventilated LSW, ISOW and DSOW with rates of change between -1.0 – $1.7 \cdot 10^{-3}$ yr^{-1} in these water masses. For LSW it is estimated that 50 % of the observed change is associated with anthropogenic effects and 50 % with changes in organic matter remineralisation. Changes are much less pronounced in the AABW which has been isolated from the atmosphere for a considerable period.

Current state-of-the-art: effects of water mass properties on biodiversity and biogeography patterns in the North Atlantic

Our current knowledge of biodiversity and biogeography patterns in the deep North Atlantic is strongly shaped by studies from soft sediment ecosystems, but increasingly studies from VMEs are emerging and helping to shape ecological paradigms. Seamounts and CWC reefs are, for example, biodiversity hotspots and increase alpha, beta and gamma diversity (Bongiorni et al. 2010, Danovaro et al. 2009, Henry & Roberts 2017, Hovland 2008, Smith et al. 2006a). But these studies are still over-shadowed by trends for soft sediment ecosystems.

Marine biodiversity generally follows a decreasing pattern of biodiversity with increasing water depth (Costello & Chaudhary 2017, Rex et al. 2006, Roberts 2009) and increasing latitude (Gage 2004, Lambshead et al. 2000, Rex et al. 1993). Decreased organic carbon flux to the seafloor has been usually related to the depth pattern (Rex et al. 2005). However, deep-sea biodiversity in the tropics, where productivity is low to moderate, is generally higher than temperate and polar biodiversity where productivity is higher and more seasonal (Willig et

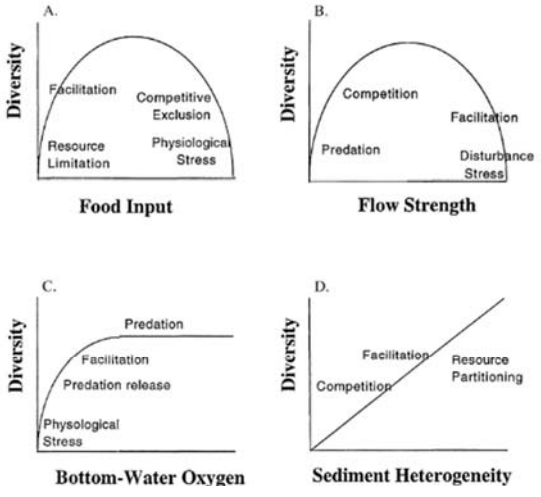

Figure 4. Schematic examples of patterns of biodiversity along different environmental gradients. A) Productivity, B) Flow, C) Bottom-water oxygen concentration, D) Sediment heterogeneity, E) Biotic disturbance (Levin et al. 2001).

al. 2003). In addition, water temperature has been also related to biodiversity latitudinal patterns, but its influence would not explain either biodiversity patterns observed at depth, where temperature tends to be lower and constant, and not latitude-dependent (Lambshead et al. 2000). This illustrates the complexity of large-scale patterns in deep-sea biodiversity and the difficulty to interpret these patterns as the product of a single mechanism (Costello & Chaudhary 2017, Lambshead et al. 2000). Indeed, some studies have demonstrated that not all biodiversity patterns are unimodal and follow those trends (e.g. Gage 2004, Stuart & Rex 2009). Biodiversity can increase, decrease or show no relationship with depth or latitude (Costello & Chaudhary 2017; Fig 4). For instance, polychaetes, bivalves and foraminifera increase with depth in the western North Atlantic (Allen & Sanders 1996, Olabarria et al. 2005, Sanders 1968). Biodiversity of deep-sea gastropods in the North Atlantic varied between regions (Stuart & Rex 2009), while no depth or latitudinal trends has been found for asteroids (Price et al. 1999). Patterns can also be irregular where large-scale environmental heterogeneity is imposed by topography, bottom currents and strong variation in nutrient input (Kendall & Haedrich 2006, Willig et al. 2003), or interrupted where oxygen minimum zones impinge on the continental slope and depress biodiversity (Levin & Gage 1998, Rogers 2000).

Mechanisms that control biodiversity patterns at large-scales are still not well understood (Costello & Chaudhary 2017, Stuart & Rex 2009), but simple latitudinal or bathymetric zonation (as zones with similar ecological conditions) is clearly insufficient to explain them (Danovaro et al. 2009). Gaps in this knowledge also limit the understanding of biogeographic patterns, where species richness and endemicity are likely to play an important role (Costello & Chaudhary 2017, McClain & Hardy 2010, Moalic et al. 2012, Watling et al. 2013). For intance, in the classic view of deep-sea biogeography, the homogeneity of habitats (e.g. constant dark and cold conditions) at large-scales, compared with coastal environments, should lead to broad distributions across ocean-basin scales in many deep-sea taxa. Indeed, this broad distribution pattern has been observed among soft-bottom taxa inhabiting the vast abyssal plains (Smith et al. 2006a). However, it also occur in highly patchy and specialised environments, such as hydrothermal vents and seamounts, with an elevated number of endemic species (Clark et al. 2010b, McClain 2007, Van Dover et al. 2002), challenging the classical concepts of deep-sea biogeographic patterns. Genetic homogeneity has been observed in several taxa inhabiting different vents and seamounts separated by large distances (McClain & Hardy 2010) and references therein). It is worth noting also that the large undersampling of the deep-sea (only

around 5 % of seafloor; Ramirez-Llodra et al. 2010), prevents the full characterization of species ranges and might misslead the observed biogeographic patterns (Costello & Chaudhary 2017).

Existing knowledge of biodiversity trends in complex deep-sea habitats such as VMEs

Many studies (including observations and models) now illustrate deep-sea ecosystems as highly complex, diverse and characterised by high spatial and temporal variability (Danovaro et al. 2014 and references therein) related to the characteristics of the surrounding water masses (Levin & Gage 1998, Levin et al. 2001, Mohn et al. 2014, Yasuhara & Danovaro 2014). For instance, water mass properties have been tightly related to the occurrence of CWC gardens (Mortensen et al. 2001), massive sponge grounds (Beazley et al. 2015, Howell et al. 2016, Murillo et al. 2012) and other deep-sea habitat-forming organisms such as oyster reefs (Van Rooij et al. 2010). Strong evidence of the importance of the environmental effects in the deep-sea communities, also comes from the geological perspective of CWC reefs formation. Evidence from drilling of CWC mounds has shown that they formed over periods of thousands to hundreds of thousands years (Roberts et al. 2006). For instance, Norwegian reefs date from after the retreat of the last ice sheet, some 10 to 14 ky ago. However, the formation of other reefs in the North Atlantic (Dorschel et al. 2005, Matos et al. 2015), occurred during several glacial-interglacial periods extending back to >300 kyr BP or even >2 My in the Porcupine Seabight (Kano et al. 2007). These long time series allow for interesting inferences regarding environmental conditions that allow mound growth. It´s been observed that reef formation during several glacial-interglacial cycles imply that mound growth has been intermittent with periods of non-growth or even erosion. Interestingly, the temporal cycles of mound formation and erosion do not align in time for coral mounds across the globe (Frank et al. 2011, Henry et al. 2014), as mound growth in the NE Atlantic (Dorschel et al. 2005) and Gulf of Mexico (Matos et al. 2015) occurred during the interglacial, while mound growth off the coast of Mauritania occurred during the glacial period (Eisele et al. 2011). This asynchronous formation of mounds is suggested to be related to surface productivity (Eisele et al. 2011), oxygen limitation (Wienberg et al. 2018), current regime (Dorschel et al. 2005) and larval supply and connectivity (Henry et al. 2014). Thus, a combination of ecological, oceanographic and historical processes influence deep-sea biodiversity and biogeography on different spatial and temporal scales.

Physical, chemical and biological properties of the water masses, such as flow velocities, temperature, oxygen concentration or quantity and quality of food supply, are overall drivers of diversity, abundance and distribution of deep-sea species (Levin et al. 2001, Willig et al. 2003). The

relative importance of these factors seems to vary between taxonomic groups and regions (Buhl-Mortensen et al. 2015b and references therein). For instance, temperature is usually one of the leading drivers of deep-sea biodiversity and biogeography at the global scale (Buhl-Mortensen et al. 2015b, Watling et al. 2013, Yasuhara & Danovaro 2014). However, the dominant driver may vary at different time and spatial scales. Water mass structure and the associated characteristics also varies temporally and spatially, creating fluctuating environmental parameters that can affect the benthic deep-sea organisms even at scales of several hundred meters (Radice et al. 2016). Thus, for instance, temperature effects may be stronger over longer time scales but food supply flux effect may be stronger over shorter time scales (Yasuhara & Danovaro 2014). At medium scales (10s of km), the presence of large geomorphological features such as submarine canyons, nodule fields or habitat forming biological structures are significant (Buhl-Mortensen et al. 2010, Henry & Roberts 2007), while sediment substrate characteristics and food resources appear more important finer spatial scales (m to km; Collart et al. 2018, McClain & Barry 2010, Vetter & Dayton 1998).

Another example illustrating this variability of the environmental effects can be observed in response curves. These models provide direct information about the effect of the explanatory variables in the habitat suitability of the species of interest and can help to understand the environmental restriction of these species in the environment (e.g. depth niche, thermal niche, etc.). For instance, the response curves of *Lophelia pertusa* to depth niche and environmental variables (Fig. 5) in the North Atlantic differ among studies, with peaks for the habitat suitability varying from 170 to 800 m depth (De Clippele et al. 2017a, Georgian et al. 2014, Howell et al. 2011, Rengstorf et al. 2013).

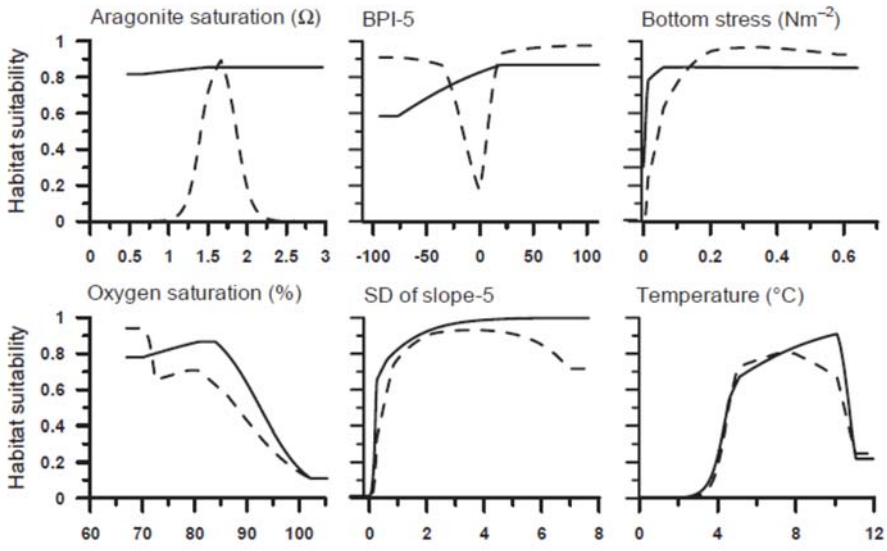

Figure 5*. Response curves showing the relationships between predictor variables and habitat suitability scores for* Lophelia pertusa *reefs in the Irish continental margin. The solid curves show how a model's prediction changes as each environmental variable is varied, keeping all other environmental variables at their average sample value. The dashed curves represent models built using only the correspondent variable (Rengstorf et al. 2013).*

Usually, depth-driven patterns result from poor or incomplete sampling and understanding of the environment. Depth is a proxy for hydrostatic pressure, temperature, oxygen or even food availability. It is also strongly linked to the different water masses in the water column, but many other factors might co-vary with depth and can be expected to define these vertical patterns (Mortensen et al. 2001). Therefore, when direct variables are not available, proxies such as depth can be used as surrogates of the real environmental drivers to understand species distribution and ecology. In general, *L. pertusa* seems to prefer a seafloor with positive topographic relief where colonies and reefs would be exposed to moderate currents (Fig. 5). In fact, when the habitat suitability for *L. pertusa* is modelled considering current speed together with a complete depth gradient, the occurrence of CWCs increases with current speed up to a certain threshold value (Rengstorf et al. 2014). Despite the demonstrated usefulness of species distribution models in deep-sea ecology, and even considering some of the best-known deep-sea species, our knowledge about the ecological niche and factors influencing deep-sea biota is still scarce. The insufficient information of the species such as inter- and intra-specific differences in the response to environmental parameters (Howell et al. 2016), the absence of good environmental data, the colinearity of different environmental variables and the lack of large scale studies prevent us from finding general patterns and making robust conclusions about effect of water masses, habitat suitability or forecasting climate change effects in deep-sea ecosystems.

Effects of Sea Temperature on VMEs

The relative spatial and temporal stability of water temperature in the deep sea has historically led to paradigms that deep-sea biodiversity is not related to temperature (Yasuhara & Danovaro 2014). However, an increasing number studies now show significant temperature–diversity relationships in the deep sea (Danovaro et al. 2004, O'Hara & Tittensor 2010, Yasuhara & Danovaro 2014). Indeed, it is very likely that temperature stability makes deep-sea organisms highly sensitive even to small temperature changes (Yasuhara & Danovaro 2014). Thus, temperature is probably the most important factor shaping recent large-scale biodiversity patterns (at least at the alpha diversity level) in deep-sea taxa (Tittensor et al. 2010, Yasuhara & Danovaro 2014). Over a broad range of temperatures, the response of deep-sea diversity is unimodal with a peak at around 5–10°C (Yasuhara & Danovaro 2014; Fig. 6). Responses to temperature might be also size dependent. Small species such as nematodes, with very short generation times from days to months (Danovaro et al. 2004), react strongly and rapidly to temperature changes but also may adapt to such changes

through generations. Indeed, thermal niche is also size dependent in some deep-sea taxa such as the mussel *Bathymodiolus azoricus*, whose intermediate sizes have a broader thermal niche than small or large mussels (Husson et al. 2017). In contrast, large taxa with longer generation times of years, such as molluscs, corals, or echinoderms (Rowe et al. 1992) are more resistant to the effects of rapid changes, but then may be unable to adapt over short time scales (Yasuhara & Danovaro 2014).

Effects of the Gulf Stream and MOW warm the North Atlantic to temperatures higher than 10°C. It remains the warmest of the major basins at 3500 m, with about 2.5°C across most of the bathyal zone (Watling et al. 2013). Each deep-sea species has probably an optimal temperature for living and they (firstly) colonise a bathymetric range in response to that temperature.

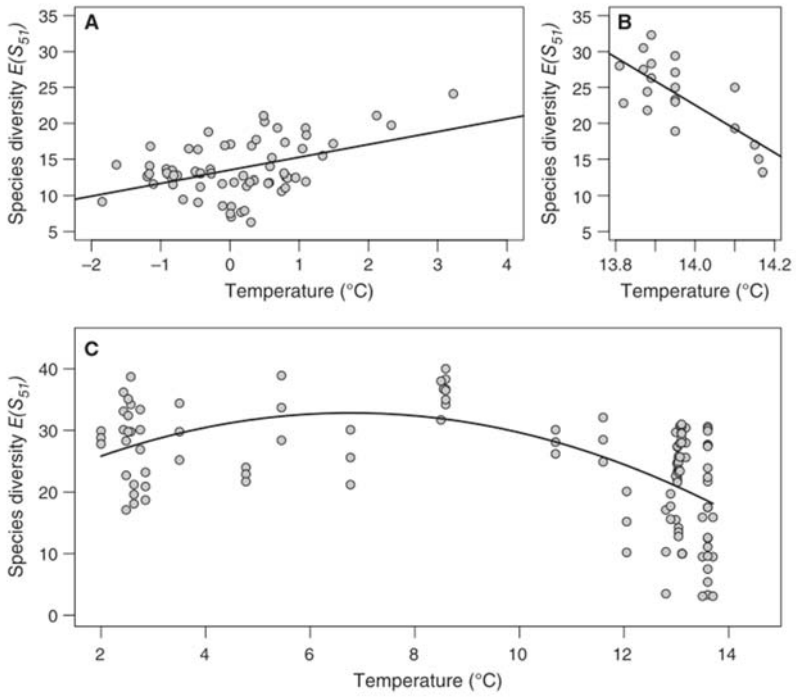

Figure 6. Examples of deep-sea temperature – diversity relationships at 1000 – 4000 m depth. A) Positive relationship from North Atlantic palaeo-time-series dataset. B) Negative relationship from Mediterranean Sea biological time-series dataset. C) Unified unimodal relationship from present-day Atlantic Ocean and Mediterranean Sea. Species diversity shown as E(S51), species richness rarefied to 51 individuals (Yasuhara & Danovaro 2014).

Thermal boundaries of the several reef-forming CWCs, such as *L. pertusa* and *Madrepora oculata,* (4 – 12°C; Davies & Guinotte 2011, Freiwald 2002, Gass & Roberts 2006; see also Fig.5) match the North Atlantic water temperature range. These conditions are generally found in relatively shallow waters (50 to 1000 m) at high latitudes, and at great depths (up to 4000 m) at low latitudes (Roberts et al. 2006; 2009). As a consequence, regional maximum depths of *L. pertusa* generally reflect different maximum depths of water masses with suitable temperatures (Mortensen et al. 2001). However, thermal ranges also vary between populations of the same species in different geographic regions. For example, *L. pertusa* is commonly found in the Mediterranean Sea between

12.5–14°C (Freiwald et al. 2009, Tursi et al. 2004). Likewise, Mediterranean colonies of *M. oculata* can tolerate, at least temporarily, elevated seawater temperatures up to 20°C (Keller & Os'kina 2008). Other VME species such as the octocorals *Radicipes gracilis*, *Acanella arbuscula* and *Acanthogorgia armata* can be found at lower temperatures 1.5–6.1°C or present lower maximum limit (10°C), such as *Paragorgia arborea* (Buhl-Mortensen et al. 2015b).

Studies on potential impacts of climate change so far have mostly focused on scleractinian corals, while other ecosystem-forming CWCs (e.g. gorgonians, soft corals, black corals) have been considerably less studied. Studies on potential impacts on sponges are also very limited. Increased temperatures at the seafloor (+4°C) have been related to mass mortalities of the habitat-forming sponge *Geodia barretti* observed in 2006 and 2008 on the Tisler Reef in Norway (Guihen et al. 2012). However, a subsequent *ex-situ* experiment exposing the same species to acute thermal conditions (up to 5°C above ambient temperature for 14 days) did not record sponge mortality nor changes in the associated microbial community although physiological and cellular effects were noted, with all parameters returning to pre-experimental levels upon a recovery phase (Strand et al. 2017). Sponges are hypothesised to be more tolerant to ocean acidification than corals, with bioeroding sponges potentially becoming more efficient under future conditions, thereby weakening reef framework (Wisshak et al. 2012, 2014).

Specific tolerances, together with the magnitude and time of exposure to increased temperature, are also important and might define the response of the deep-sea organisms (Dodds et al. 2007, Mienis et al. 2014). For instance, a natural increment of 4°C in 24 h was observed at Tisler Reef causing a mass mortality of the sponge *Geodia baretti*, although it did not affect *L. pertusa* reef despite of exceeding its typical physiological temperature limits (Guihen et al. 2012). More recent experimental and *in situ* data suggested that the upper lethal temperature limit for *L. pertusa* is near 15°C and that it can survive short term (24 h) considerable temperature spikes up to 20°C (Brooke et al. 2013). However, temperature changes have a strong effect on CWC metabolism and the adaptation to the new temperature conditions also varied among taxa. The experimental study by Naumann et al. (2014) showed that *L. pertusa* has a greater capacity to change its respiratory metabolism and acclimate to decreased temperature (from 12 to 6°C) than *M. oculata*. This result suggests a species-specific rapid acclimatation to different temperature ranges. The scleractinian coral *Dendrophyllia cornigera*, common in the eastern Atlantic and the Mediterranean Sea at a warmer temperature range (11-17°C) than many other CWCs (Gori et al. 2014), also experiences

reductions in metabolic rate (respiration) and calcification when temperature is experimentally lowered to 8°C (Gori et al. 2014). However, growth rates of this CWC increased when temperature was elevated from 12 to 17.5°C (Naumann et al. 2013); In contrast, growth rates did not show any significant differences under the two temperature regimes for *Desmophyllum dianthus* (Naumann et al. 2013). These studies provide support for the geographical and bathymetrical distribution of the different species, with *M. oculata* as the dominant reef-building species in warmer Mediterranean waters, and *L. pertusa* being more prevalent in colder regions like the North Atlantic (Freiwald et al. 2009, Roberts 2009, Tursi et al. 2004). Results may also explain the absence of *D. cornigera* from most of the NE Atlantic, where temperatures range from 5 to 10°C (Dullo et al. 2008, Purser et al. 2013, Roberts et al. 2009) and the general occurrence of *D. dianthus* in waters with temperatures below 14°C (Forsterra & Haussermann 2003, Freiwald et al. 2009). In addition to reducing metabolic rates (Drazen & Seibel 2007, Glover & Smith 2003, Rowe et al. 1992), low temperatures tend to diminish reproduction and larvae connectivity potential (Woolsey et al. 2013), favoring species with wide temperature tolerance or those with physiological adaptations to cold.

Together with temperatures, organic carbon transport into the deep ocean, dissolved oxygen and other factors are likely to explain the depth limits of CWCs (Buhl-Mortensen et al. 2015b, Mortensen & Buhl-Mortensen 2004, Mortensen et al. 2006) and other deep-sea organisms (Yasuhara & Danovaro 2014). Indeed, temperature might trigger more important effects on deep-sea biota in combination with other factors or stressors (synergies) such as ocean acidification, low food availability or reduced oxygen (e.g. Gori et al. 2016, Lunden et al. 2014) than its isolated effects. Adaptations to combined stressors have occurred in the past over evolutionary time and are currently exhibited by stress-tolerant organisms at present conditions (Levin & Le Bris 2015).

Effects of Hydrodynamic Features on VMEs

Occurrence of benthic suspension feeders, such as corals and sponges, are frequently associated with high energy environments characterised by strong current velocities (Khripounoff et al. 2014, Mienis et al. 2007, Roberts et al. 2009, Van Haren et al. 2014, White & Dorschel 2010) or unique current patterns such as recirculation gyres that increase concentrations of particles (Howell et al. 2016, Serrano et al. 2017b). Numerical hydrodynamic models showed intensified near-bottom currents in areas where living CWC are observed in comparison with coral absence and random background locations (Mohn et al. 2014). Areas inhabited by suspension feeders in the North Atlantic registered flow rates of 15 cm s^{-1} on average (Davies et al. 2009, Duineveld et al. 2007, Mienis et al.

2012), which can peak up to 25 cm^{-1} in the Gulf of Cadiz (Wienberg et al. 2009), 51 cm^{-1} in the Irish margin (Dorschel et al. 2007a, Mienis et al. 2007) or 80 cm^{-1} in Mingulay reef complex (Davies et al. 2009). These high flow rates increase the food supply, and prevent the living suspension feeders from burial by sediments (Mienis et al. 2007, Roberts et al. 2006, White et al. 2005). Such flow rates are usually found on the continental slope (Thiem et al. 2006, Tong et al. 2016) and areas with particular topographic features such as seamounts (Lavelle & Mohn 2010, White et al. 2007a) and submarine canyons (Canals et al. 2006, Mulder et al. 2012, Palanques et al. 2006). For instance, the rugged seabed and slopes > 0.6° of the mid-Norwegian shelf-slope region concentrate up to nine *L. pertusa* reefs per km^2, each of them covering an area of 5,628 m^2 on average (Mortensen et al. 2001). Conspicuous concentrations of deep-sea sponge grounds (Klitgaard et al. 1997, Rice et al. 1990) and *L. pertusa* reefs (Frederiksen et al. 1992) have been found on the upper slope all around NW Europe, where the combination of a steep slope and the hydrographic conditions cause internal waves that accelerates local currents (Mienis et al. 2007).

Breaking internal waves (Dorschel et al. 2007a, Mienis et al. 2007, Wienberg et al. 2009) enhance local food availability by re-distributing suspended particles in the bottom mixed layer (Frederiksen et al. 1992) and helping to pump food through the coral framework (White et al. 2005, 2007b). Internal waves generally occur at the interface between two water masses of different densities and propagate along the pycnocline (Pomar et al. 2012). The importance of water mass boundaries and internal waves on coral mound formation has been proposed for the Porcupine Seabight based on the fossil record (Raddatz et al. 2014). In this region, mound aggradation was active when the boundary between the MOW and the ENAW was placed towards the depth level of the mounds, whereby the stable water mass stratification between both water masses caused enhancing of food supply (e.g., Raddatz et al. 2014). Internal waves have also been hypothesised to positively influence the formation of the coral mound province, the Campeche Bank, in the Gulf of Mexico (Matos et al. 2017). Here, mound formation was restricted to interglacial periods, when internal waves propagated along the pycnocline between the AAIW and the Tropical Atlantic Central Water, whereas during glacial times this water mass boundary was replaced by an homogeneous water mass (Matos et al. 2017). Resuspension of particles can be enhanced by other mechanisms as well, such as the collision of water masses against seamount walls (bottom trapping (Genin & Dower 2008), or the water cascading in submarine canyons (Canals et al. 2006), which also ensure food

supply and trophic enrichment for corals and sponges (Huvenne et al. 2011, Rowden et al. 2010, Thiem et al. 2006, Wagner et al. 2011).

However, CWCs seem to prefer areas with periodically varying currents (Dorschel et al. 2007a, Duineveld et al. 2007, Mienis et al. 2007, Van Haren et al. 2014) and/or strong flow speed variations (Davies et al. 2009; Mienis et al. 2007, 2012; Fig. 7), allowing high food supply on peak currents and high capture rates during lower flow (Orejas et al. 2016). These periods of strong currents are often short and driven by the tide or stochastic events (Davies et al. 2009). Thus, to maximise encounter rates with food particles, CWCs can adjust their colony growth morphologies to face into the prevailing bottom current (Mortensen & Buhl-Mortensen 2004, Roberts et al. 2009). Indeed, the forcing of seabed currents is magnified if the diurnal tides are resonant with stratification and seabed slope and might lead to an alignment of coral mound structures in the direction of diurnal tides (White et al. 2007b). The processes associated with oscillatory flow interacting with the topography can also trigger food supply mechanisms to CWC by promoting large amplitude local vertical mixing. The vertical flux or downwelling of fresher, warmer and chlorophyll richer waters from surface layers can be an additional important food source for deep-sea benthic organisms (Davies et al. 2009, Wagner et al. 2011). Large seasonal and annual variability in the flux of phytodetritus and carbon have been observed for instance in the Galicia Bank (Duineveld et al. 2004). In addition, the opposite mechanism, stratification of the water column, can modify the local oceanography in some cases. In the NE Atlantic, the presence of the warm and saline MOW at mid depths creates a permanent thermocline at the upper level of the MOW that promotes local current intensification (White & Dorschel 2010). For instance, coral banks in the Porcupine Seabight are located in the themorcline depth range (De Mol et al. 2005) and its occurrence has been associated to the presence of the MOW.

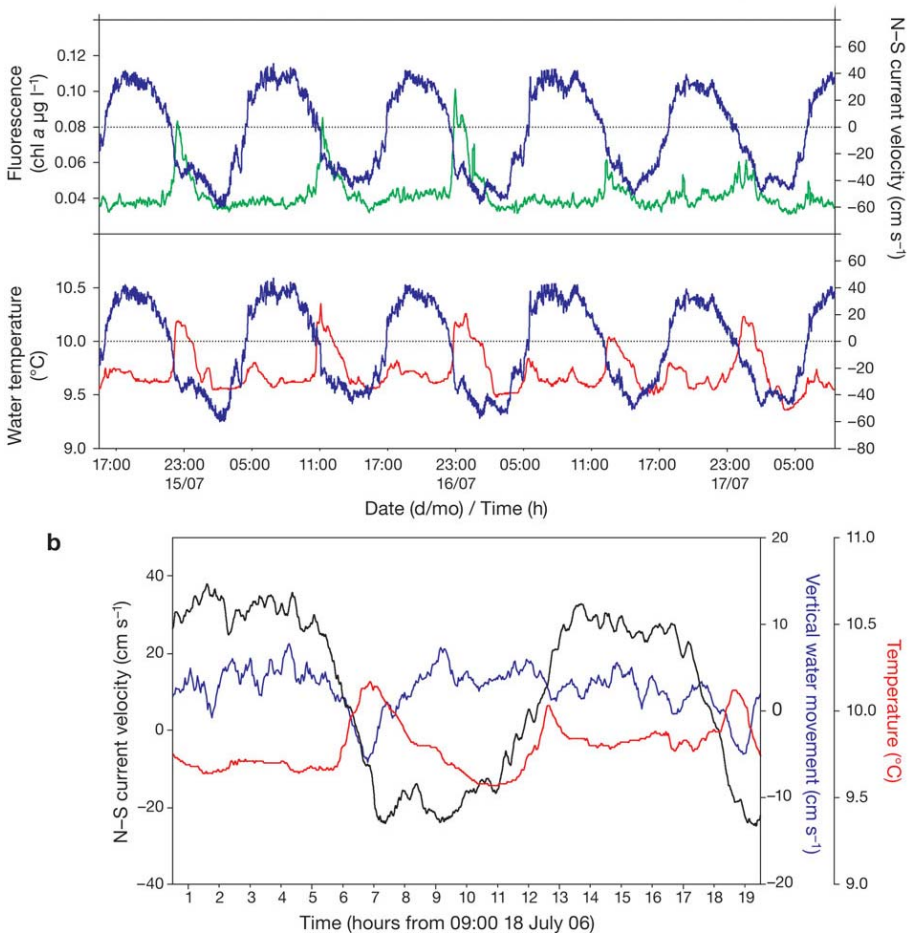

Figure 7. Relationship between the N–S current velocity (blue line), fluorescence as proxy of phytodetritus (green line) and temperature (red line) in Mingulay Reef Complex (Roberts et al. 2009).

Effects of Organic Matter and Food Supply on VMEs

Food availability is one of the main drivers of the occurrence and distribution of living organisms, including deep-sea taxa and, as described above. It is strongly linked to large scale and local hydrodynamics regardless of the mechanism that enhance current velocities (e.g. downstream of upwelled water, cascading, internal waves). The magnitude of the organic matter (OM) flux can affect the abundance and diversity of deep-sea biota (Pape et al. 2013a, Pusceddu et al. 2016; Fig. 8). For instance, OM flux was found to be a more important factor than temperature in shaping the biodiversity patterns of molluscs in the Atlantic Ocean (Tittensor et al. 2011).

Except for chemosynthetic habitats (hydrothermal vents and some cold seeps), the food supply for deep-sea biota below 200 m depth is ultimately derived from an attenuated 'rain' of detritus from remote surface waters (typically 1 – 10 g *C org* m^{-2} yr^{-1}; Glover & Smith 2003). Detrital food particles range from the fresh remains of phytoplankton produced in the photic zone to the carcasses of whales (Glover & Smith 2003, Watling et al. 2013). CWC usually occur in areas where surface waters present an above-mean concentrations of chlorophyll *a* (> 94 mg m^{-3}; Guinotte et al. 2006), evidencing the importance of surface OM supply for survival in the deep-sea.

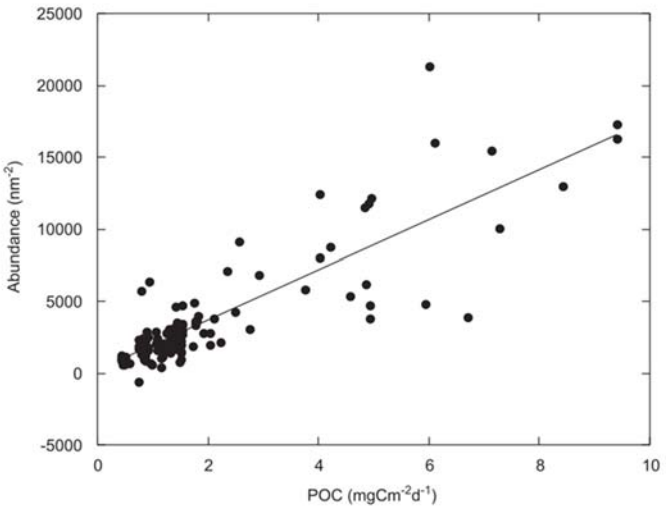

Figure 8. Relationship between estimated POC flux and abundance of the deep-sea macrobenthos in the western North Atlantic. Regression: P<0.001, r^2 = 0.672 (Johnson et al. 2007).

In addition to vertical transport, food particles are also transported laterally by advective fluxes, improving the capture of food by suspension feeder organisms and facilitating their distributional range to areas not necessarily being beneath of regions with high primary productivity to receive adequate levels of nutrition (Davies et al. 2009, Hebbeln & Wienberg 2016, Mienis et al. 2009). Indeed, CWC locations are also frequently found under oligotrophic areas (< 3mg *Chl-a* m^{-3}), with surface-derived particulate organic carbon (POC) often being the main carbon source of CWC skeletal carbon for some species (e.g., *Lophelia pertusa*, *Gerardia* spp., *Paragorgia johnsoni* and *Corallium noibe*, *Leiopathes* spp., *Primnoa* spp; Griffin & Druffel 1989, Roark et al. 2009, Sherwood et al. 2005). This fact supports the importance of advective fluxes for CWC growth. The deep-sea is subject to considerable temporal and spatial fluctuations in the pulses of OM derived from both vertical (e.g. seasonal upwelling; Gil 2008, Lavaleye et al. 2002) and advective fluxes (e.g. nepheloid layers; Mienis et al. 2007, Wilson et al. 2015); canyon funneling, (Khripounoff et al. 2014, Sorbe 1999); estuarine outwelling, (Lopez-Jamar 1992).

Recent studies have also evidenced reciprocal feedback between the suspension feeders and the enhancement of food supply at locations where these organisms are present. For instance,

sponges play a significant role in ecosystem functioning by recycling dissolved organic matter (DOM) and transforming it to particulate organic matter (POM) that becomes available to detritivores, and ultimately higher trophic levels (de Goeij et al. 2013, McIntyre et al. 2016, Rix et al. 2016). By contrast, as the topography formed by CWC framework or mound structures, may create a positive feedback on OM supply that indeed improves the trophic quality of the environment in which they are found. The areas where *Lophelia* colonies thrive at Tisler Reef presented a higher degree of particle resuspension than the coral rubble or areas outside the reef (Guihen et al. 2013), providing more food particles to the corals. Similarly, several studies have shown that the interaction of tidal currents with the bottom topography formed by the CWC induced downwelling of rich OM surface waters towards the living corals at Mingulay reef complex (Davies et al. 2009, Duineveld et al. 2012) and Rockall margin (Soetaert et al. 2016). Thus, the formation of CWC reefs are not only just controlled by the surrounding environmental conditions, whereby food supply is enhanced, but exert an environmental control of their habitats.

Effects of Ocean Salinity on VMEs

Salinity along with temperature are indicators of particular water masses, which potentially influence species distributions overall and also in the deep sea. However, the strong collinearity of depth, temperature, salinity and dissolved oxygen, make very difficult to discern between the role of hydrostatic pressure and other depth-correlated variables (Lundsten et al. 2010, Mortensen et al. 2001). Thus, results on the distribution of deep-sea species are often difficult to interpret and should be taken with caution (Huff et al. 2013). For instance, in the *L. pertusa* reefs off Norway, it is almost impossible to determine whether temperature (up to 10°C) or salinity (down to 32 psu) is the limiting factor for the upper bathymetrical distribution (Mortensen et al. 2001).

Watling et al. (2013) presented an overall biogeography of the world´s deep oceans (800 – 3500 m) based on the many physical water mass variables, including salinity structure of the ocean, yet the salinity in deep waters only varies up to 1 psu worldwide. Some areas of distinct salinity were identified in the main ocean basins. Thus, the salinity in the North Atlantic is characterized by the influence of the saline Gulf Stream and the northward spreading of the saltier MOW. This high salinity water mass extends as far north as the Iceland-Faeroes Ridge on the eastern side of the Atlantic. In contrast, salinity becomes more uniform in deeper waters, with some influence of upper water layers up to 2000 m depth and values between 34.5 and 35 psu below 3500 m (Watling et al. 2013). However, long term data series (1986 – 2000) highlighted that salinity, among other factors, played

an important role on changes in the large scale spatial distribution of the shallower (50 – 100 m) macrofaunal communities, such as the North Sea (Kröncke et al. 2011) or the coral reefs in the Norway margin (Mortensen et al. 2001).

The occurrence of CWCs in the NE Atlantic has been correlated with a parameter directly linked with salinity and temperature, the water density (Dullo et al. 2008). Thus, CWC reefs seem to be limited by different intermediate water masses and indeed, most corals inhabit environments with salinities ranging between 34 and 37 psu (Bryan & Metaxas 2006, Mortensen et al. 2001). While conditions such as temperature, dissolved oxygen or current speed can vary relatively wide in areas inhabited by CWCs, Dullo et al. (2008) found that living reefs in the NE Atlantic occurred in a narrow water density envelope of sigma-theta (potential density; σ_θ = 27.35 – 27.65 kg m^{-3}), indicating the importance of physical boundary conditions for CWC growth and distribution. However, works published after this one revealed the occurrence of CWC reefs outside this density envelope in the NW (σ_θ = 27.1 – 27.2 kg m^{-3}, Davies et al. 2010) and other areas of the NE Atlantic (σ_θ = 27.62 – 27.84 kg m^{-3} (Huvenne et al. 2011, Kenchington et al. 2017). However, presence and peak abundances of other deep-sea taxa has been found in the depth range (800-1300 m) where usually the MOW is found (Schönfeld & Zahn 2000), being abundances linked to variations in near-bottom MOW current strength (Zenk & Armi 1990).

Studies of salinity gradients in deep-sea communities need also to consider effects on larval stages of the benthic organisms. An experimental work conducted with *L. pertusa* demonstrated that larvae can survive for long periods of time (up to 10 months) in environments with salinity values of 25 psu, being also able to cope with salinity gradients of up to 5 psu without displaying unusual behavior nor mortality (Strömberg & Larsson 2017). The same authors documented that *Lophelia* larvae can migrate to the surface, revealing that larvae are likely to be exposed to density gradients in nature. Indeed, larvae from deep populations of *L. pertusa* may encounter density gradients since water mass boundaries are present in the deep ocean interior especially in more southerly latitudes (e.g. Stewart 2008). This behaviour observed in the laboratory revealed a high plasticity for *L. pertusa* larvae regarding salinity gradients and a great longevity which could allow a wide geographical dispersal range for this species. Other studies conducted in the laboratory with larvae of different invertebrates (from shallow waters), revealed the presence of haloclines that inhibit larvae vertical migration (Sameoto & Metaxas 2008). A negative correlation between early benthic larvae of

decapods/stomatopoda and salinity was found in the field, revealing the different environmental conditions that can be supported by larvae and adults of the same species (Brandão et al. 2015).

Effects of Ocean Carbonate Chemistry on VMEs

Seawater pH influences marine organisms through its critical role in mediating physiological reactions and by changing the availability of carbonate ions needed for biocalcification of the skeletons (Doney et al. 2012, Pörtner & Farrell 2008). Hence, ocean acidification (OA), i.e., the reduction in ocean pH and carbonate mineral saturation states due to the absorption of anthropogenic carbon dioxide (CO_2) into seawater, has been identified as one of the greatest threats to marine ecosystems (Doney et al. 2009). Since pre-industrial times, the average surface ocean pH has declined by 0.12 units (Hennige et al. 2014).

Marine calcifying organisms (e.g. corals, molluscs, echinoderms) inhabiting cold and deep waters may be particularly sensitive to decreases in carbonate chemistry. The higher CO_2 and lower pH of deep waters resulting from organic matter microbial respiration make their natural content in carbonate ions low. Carbonate saturation in seawater is a critical parameter for the precipitation (in saturated waters, $\Omega > 1$) and dissolution (in unsaturated waters, $\Omega < 1$) of calcium carbonate mineral forms (i.e. aragonite, calcite). Solubility of calcium carbonate increases at higher pressure and lower temperature, which means that Ω decreases with increasing depths and at higher latitudes. Indeed, the distribution of important deep-sea habitat building organisms with carbonate skeletons, such as CWC, is largely found in waters above the carbonate saturation horizon, the boundary between waters promoting biocalcification above and carbonate dissolution below (Davies & Guinotte 2011, Guinotte et al. 2006, Yesson et al. 2012). Other calcifying taxa, such as echinoderms, are found throughout the world´s oceans, but are far less abundant or even absent from undersaturated waters (Lebrato et al. 2010). The carbonate saturation horizon in the North Atlantic is still very deep > 2000 m depth (Guinotte et al. 2006), but still constrains the distribution of multiple deep-sea calcifying organisms.

One of the most reported responses of benthic organisms to OA is the dissolution of the tissue unprotected shells and skeletons (Doney et al. 2012, Rodolfo-Metalpa et al. 2015). Dissolution and deformation of exposed tissue-free skeletons under low pH has also been demonstrated for the CWC *L. pertusa* (Hennige et al. 2015, Wall et al. 2015). However, acidification can also cause mortality or compromised reproduction (Verkaik et al. 2017) and development of early life stages (Byrne 2011,

Dupont & Thorndyke 2009, Kurihara 2008), or even induce no response at all, being the response highly variable depending on the taxa (Ries et al. 2009). Some species protect their carbonate skeletons with tissue (e.g. *Paragorgia arborea*) or proteinaceus covers (e.g. the mussel *Bathymodiolus brevior)* in acidic environments (Tunnicliffe et al. 2009).

Experimental studies with the reef-building CWCs *L. pertusa* and *M. oculata* from NE Atlantic and Mediterranean sea have shown their ability to calcify and grow under acidic and even undersaturated conditions (Büscher et al. 2017, Form & Riebesell 2012, Hennige et al. 2014, Maier et al. 2012, 2013, Movilla et al. 2014; Fig. 9).

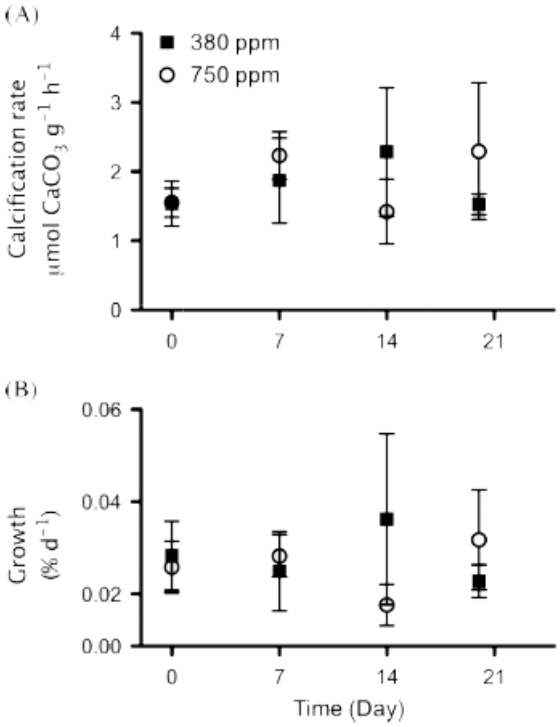

Figure 9*. Net calcification rate ± SE of L. pertusa fragments exposed to control conditions (380 ppm, 9 1C) and acidified conditions (750 ppm, 9 1C) over 21 days calculated from the alkalinity anomaly technique expressed as A) mmol $CaCO_3$ g^{-1} tissue dry weight h^{-1}, and B) as % d^{-1}* (Hennige et al. 2014).

In contrast, *L. pertusa* from the Gulf of Mexico and California margins living under low carbonate or understaturated conditions showed great susceptibility to OA with decreased calcification rates and skeletal dissolution (Georgian et al. 2016, Gómez et al. 2018, Kurman et al. 2017, Lunden et al. 2014) but some coral genotypes seem to be more resistant that others (Kurman et al. 2017). There is also evidence of a geographic effect in CWC ability to cope with OA conditions, with the Norwegian populations of *L. pertusa* being able to increase feeding rate to maintain growth at low pH, while populations of the Gulf of Mexico reduce their feeding and calcification rates (Georgian et al. 2016).

The ability of CWCs to cope with OA has been related to their ability to increase internal pH at the site of calcification (McCulloch et al. 2012a, Raybaud et al. 2017). However, it remains unclear

whether calcification can be sustained indefinitely, as this is an energy demanding process (20 – 30% of CWC energy budget, Cohen & Holcomb 2009) and OA has been shown to affect coral metabolism (Hennige et al. 2014). Furthermore, it is unknown how OA may affect other important physiological processes such as reproduction and the development of early life stages, as observed for shallow water organisms (Byrne 2011, Dupont & Thorndyke 2009, Kurihara 2008, Verkaik et al. 2017). The impact of OA on other habitat-builders such as octocorals has been little studied, but the limited experimental evidence suggests reduced calcification and growth of temperate octocoral *Corallium rubrum* (Cerrano et al 2013) and reduced metabolism in the deep-sea octocoral *Dentomuricea meteor* (Carreiro-Silva pers. comm) suggesting that gorgonians may also be negatively affected by OA. Synergic effects of acidification and other factors are also scarcely studied yet. But an experimental study combining elevated temperature and low pH revealed significantly effects on the metabolic and calcification rates in the CWC *D. dianthus* (Gori et al. 2016).

Effects of Oxygen Concentration on VMEs

Most of the global ocean has dissolved oxygen (DO) values near saturation, with the highest values generally associated with the colder, deeper, and more recently formed waters. However, there are extensive midwater regions (100–1200 m depth) where oxygen is depleted and thus, limiting (< 1ml l^{-1} ; Levin et al. 2001, Stramma et al. 2010) for living organisms. These hypoxic zones (0.2–0.5 ml l^{-1}), referred to as oxygen minimum zones (OMZs), are usually formed by microbial degradation of OM beneath highly productive waters (Levin et al. 2001) and may last for thousands of years (Ramirez-Llodra et al. 2010, Reichart et al. 1998).

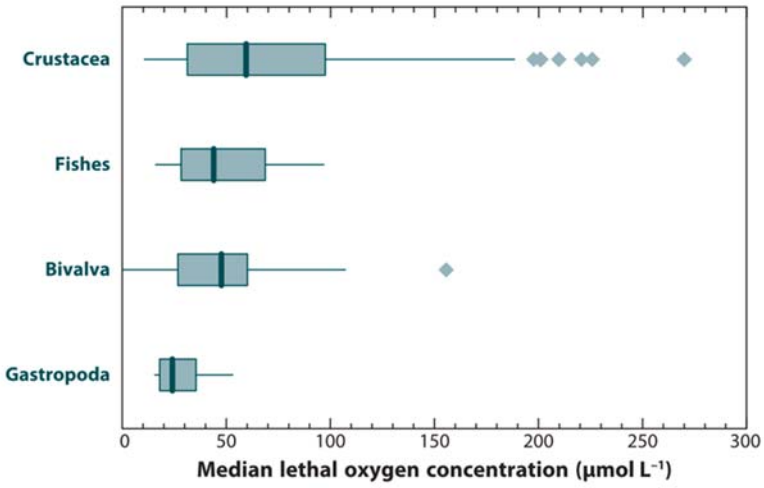

Figure 10. Median lethal oxygen concentration (LC50,in µmol l^{-1}) among four different taxa (Keeling et al. 2010). Copyright (2008) National Academy of Sciences, USA.

Most organisms are not very sensitive to variations in DO as long as the concentrations are above tolerance levels. But when oxygen drops below a certain threshold, the organisms suffer from a variety of stresses, leading ultimately to death if low oxygen concentrations are maintained for too long (Keeling et al. 2010). Thresholds for hypoxia vary greatly between marine taxa (Fig. 10). Above a threshold of probably 0.45 ml l^{-1}, oxygen effects on macrobenthic diversity are minor relative to OM influence, but below, oxygen becomes a critical factor (Levin & Gage 1998). For the bathyal fauna in the Atlantic, hypoxia might have more influence on species richness while organic carbon regulates species distribution and community evenness (Levin & Gage 1998). Thus, within OMZs the macrofauna exhibit low species richness and very high dominance, although annelid species are often prevalent (Levin et al. 2001, Ramirez-Llodra et al. 2010, Rogers 2000, Soltwedel 2000). However, macro- and megafauna often exhibit dense aggregations at OMZ edges since they favor from high OM fluxes and still suitable DO levels (Levin 2003). The major cause of reduced species richness within OMZs is the loss of taxa that are less or intolerant to hypoxia, such as echinoderms, crustaceans and molluscs. Taxa with calcified shells or exoskeletons in particular, tend to be absent from the cores of OMZs (Rogers 2000).

Notably however, living colonies of *L. pertusa* and *M. oculata* have been found in OMZ at oxygen levels of 1.1 to 0.6 ml l^{-1}, respectively (Hebbeln et al. 2017). Tolerance to hypoxia also varies with body size, with meiofauna being more tolerant to low oxygen than most macro- or megafauna (Levin et al. 2001). There is evidence that OMZ benthic organisms maximise oxygen uptake through morphological and physiological adaptations, such as raised ventilation rates, increased respiratory surface, reduced diffusion distance, development of respiratory pigments, vertical migrations or enzymatic adaptation to anaerobic metabolism (Levin 2003). OMZs may represent a barrier, disrupting species distribution in the OMZ region or isolating communities and populations across the inhospitable waters (Rogers 2000). However, genetic studies revealed that, although it occurred in the past, it is not likely that OMZs influence speciation at present (Rogers 2000). Thus, oxygen exerts tremendous control on marine biodiversity through effects on evolution, physiology, reproduction, behavior, and species interactions (Levin & Le Bris 2015).

Hypoxic, suboxic, and anoxic conditions are common in all of the oceans (Kamykowski & Zentara 1990), not only occurring as permanent zones, but also as oxygen gradients that might vary over geological time, interannually, seasonally, daily or as an episodic feature (Levin 2018, Rogers 2000), which might drive different adaptations and tolerance levels in bethic taxa. In addition, as

water temperature increases, the solubility and thus, the concentration of DO declines, being in some cases the level of DO associated with water masses characteristics. For instance, MOW presents higher salinity and lower-oxygen concentrations than surrounding NACW and NADW (Serrano et al. 2017b, Wienberg et al. 2009). Indeed, a drastic drop in DO, from 6.85 to 5.40 mg l^{-1} at water depths between 800 and 1200 m, associated with the presence of MOW has been observed in the Galicia Bank at these depths. The habitat of living *L. pertusa* reefs in this area, indeed, correspond to the boundary between the MOW and ENACW water masses (Somoza et al. 2014).

North Atlantic minimum oxygen concentrations occur at much higher concentrations than a proper OMZ, ranging from 2.5 ml l^{-1} off SW Africa to 6 ml l^{-1} in the NW Atlantic (Watling et al. 2013). However, permanent OMZs are present in the South Atlantic off Namibia (< 0.5 ml l^{-1}) and Angola (< 1 ml l^{-1}; (Hebbeln et al. 2017). The majority of *L. pertusa* reefs found in the North East Atlantic coincide with the range of relatively low DO (3 – 5 ml l^{-1}), which occurs between 500 and 1600 m water depth. However, the actual importance of oxygen stress and the high organic suspended matter in these regions is difficult to distinguish as the responsible factor for the presence of *L. pertusa* (Freiwald 2002, Levin & Gage 1998, Roberts et al. 2006, White et al. 2005). Reduced diversity of CWC has been observed on the summits of seamounts relative to the surrounding slopes, thought to be influenced in part by extreme hydrological forces, exposure to OMZs, or the fine-scale topography of the summit (Clark et al. 2010a, Georgian et al. 2014). Lower DO values of 2.6 – 3.2 ml l^{-1} have also been recorded at sites inhabited by CWC (*L. pertusa*, *Enallopsammia profunda)* in the Gulf of Mexico (Hebbeln et al. 2014). Experimental and modeling data suggest that oxygen levels may be a limiting factor in the distribution of *L. pertusa*, being absent in waters with DO less than 2.37 ml l^{-1} (Davies et al. 2008, Dodds et al. 2007). However, more recent research in the South Atlantic OMZ, revealed a lower oxygen limit for living *L. pertusa* of 0.6 ml l^{-1}, being relatively abundant at 0.8 ml l^{-1} and completely disappearing at oxygen levels < 0.5 ml l^{-1} (Hebbeln et al. 2017).

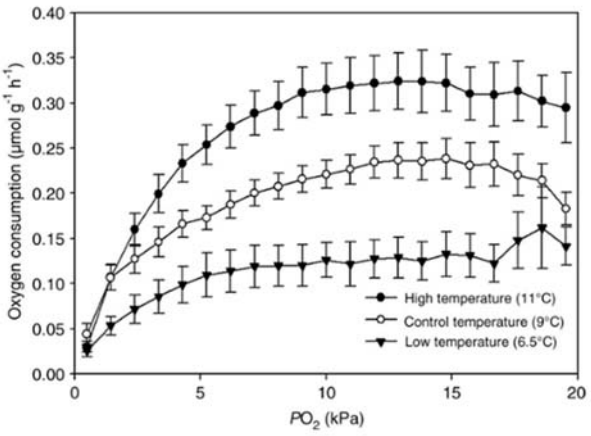

Figure 11. The relationship between the mean rate of oxygen consumption (± SE) of Lophelia pertusa and oxygen partial pressure (PO_2) at three different temperatures: 6.5°C, n=6; 9°C, n=6; 11°C, n=4 (Dodds et al. 2007).

Experimental research also revealed that *L. pertusa* mantains constant rates of oxygen consumption over a range of DO concentrations and colonies are able to survive short-time periods of anoxia (1 h) and hypoxia (up to 96 h). However, both oxygen consumption and the survivorship are sensitive to temperatures changes (6.5–9°C; Dodds et al. 2007; Fig. 11). Indeed, a different experimental study observed that oxygen consumption of *L. pertusa* recorded at 11°C was 50 % higher than that recorded at 9°C (Dodds et al. 2007; Fig. 11). Complete mortality of *L. pertusa* nubbins has been observed at DO levels of 1.5 ml l^{-1} and temperatures of 14°C (Lunden et al. 2014). Recent studies carried out in the South Atlantic revealed thriving CWC reefs off Angola, dominated by *Lophelia pertusa* at water depths between 470 and 330 m; Oxygen concentrations where about 0.5 ml L^{-1} values that are below of any other reported live occurrence of *L. pertusa* (Hebbeln et al. 2017). Thus, field and experimental studies demonstrated a wide tolerance of *Lophelia pertusa* with respect to DO values.

Oceanographic Drivers of VME Biodiversity and Biogeography in ATLAS Case Studies

This section of the review synthesises existing knowledge on how the biodiversity of VMEs and the biogeographical affinities of their biological communities can vary over space and time due to regional and basin-scale changes in oceanographic conditions. The goal here was to identify which variables affect VME biodiversity the most so that a statement could made at the end as to whether future ocean changes are likely to cause even more change, aside from any type of blue economy development in that Case Study.

Cold-water Coral Reefs on Shelves, Slopes and Banks

1. Norway

The Norwegian shelf covers around 2 million km^2 with a depth range from 100 to 500 m and harbor a high concentration of CWC reefs from Skagerrak Strait, ~57° N to Sørøya Island, ~70.5° N. The shelf is dominated by shallow plains and valleys (400 m depth). On the continental slope, unstable sediments form small slides. Major ice streams active during the glacial periods have shaped the Norwegian continental shelf into its current shape. Oil and gas are resources are under exploration and development in Norway, and the LoVe observatory ATLAS Case Study is an example of an area being carefully monitored by the industry. The wider shel region is itself already heavily exploited by the oil and gas industry, which also influence the chemical state in the sediments (Buhl-Mortensen et al. 2015a). The Norwegian continental margin also supports highly productive fisheries

(Skjoldal 2004). Ocean circulation is characterised by the northward transport of warm water (6 – 14°C) to high latitudes by a branch of the NAC (Dullo et al. 2008). This current is overlain by the Norwegian Coastal Current (NCC), which flows northward parallel to the coast gathering freshwater discharge from the Norwegian landmass (Freiwald 2002) and reaching salinities lower than 35 psu. Below, the Arctic Intermediate Water (AIW) constitutes a salinity minimum at depths of ~600 m (Blindheim 1990) and bottom waters on the continental slope present temperatures below 0°C (Peterson & Rooth 1976).

Norwegian reefs (Fig. 12) are mainly formed by *Lophelia pertusa*, which can grow up to 35 m high and several km long (Freiwald 2002, Lindberg et al. 2007). Here, reefs are present in waters with salinities higher than 34 ‰ and temperatures between 4 and 8°C, matching approximately a depth range of 100 – 400 m (Buhl-Mortensen et al. 2015b, Dullo et al. 2008, Mortensen et al. 2001). *Lophelia* reefs vary from scattered colonies to vast reef complexes (e.g. the giant Sula reef, Fig. 12). The deepest *Lophelia pertusa* ocurrence coincides with the shallowest boundary of warm NAC and the cold AIW (Buhl-Mortensen et al. 2015b). Bubblegum corals (*Paragorgia arborea*) also form vast coral garden VMEs here (Buhl-Mortensen et al. 2015b, Tong et al. 2012), reaching up to 2 – 3 m in height and being also important structuring species among the CWC *Lophelia* reefs.

The water masses at different depths, the small scale turbulence (Hovland et al. 2002, Thiem et al. 2006), internal waves and tidal cycles are the main factors shaping the distribution of the reefs (Guihen et al. 2013, Ruggeberg et al. 2011) and the associated fauna (Mortensen & Fosså 2006, Purser et al. 2013). Indeed, reefs are only present on certain parts of the Norwegian shelf, although adjacent areas might present similar topographic and oceanographic conditions (Hovland et al. 2002). The relatively strong current over particular topographical formations which can form eddies might enhance continuous and regular food supply (usually zooplankton) for CWC in specific areas, but also geological conditions, such as seepage activity, has been suggested to influence the reef distribution (Hovland et al. 2002).

The northernmost *Lophelia* record lies in the Fugløy reef (70° N, Lindberg et al. 2007), where age measurements of the reefs suggest that they established just after the end of the last Ice Age, ~ 10 kyr ago (Freiwald et al. 1999, López Correa et al. 2012).

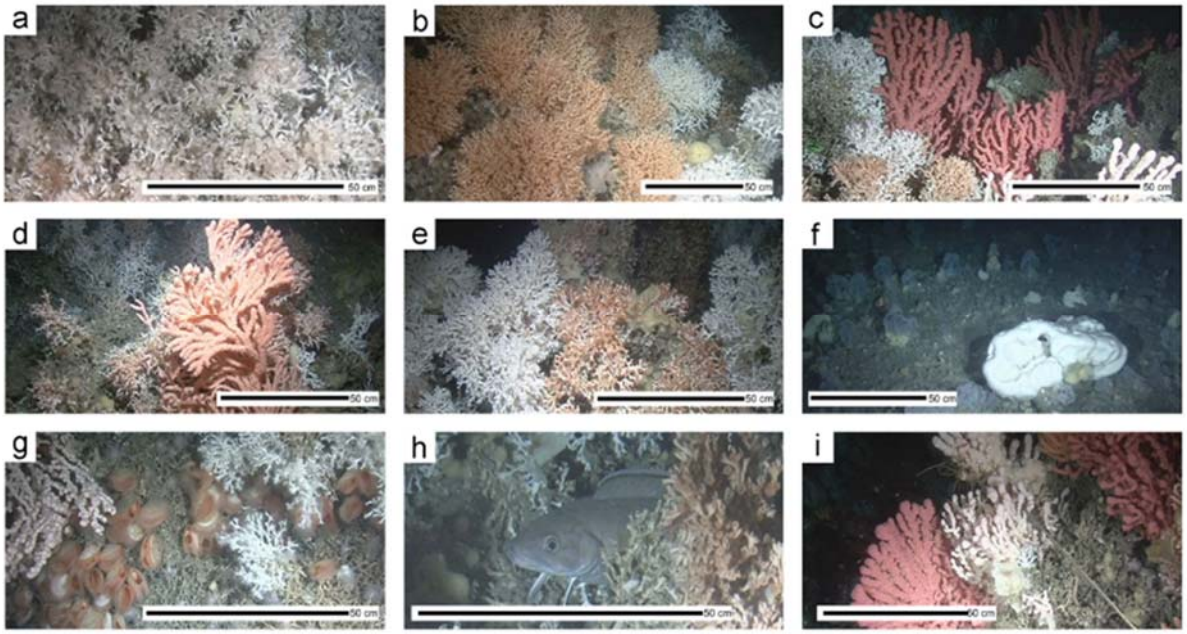

Figure 12. Cold-water coral and associated species in the reefs of the Norwegian continental margin: a) Lophelia pertusa*, b)* Madrepora oculata*, c)* Paragorgia arborea*, d) Primnoa resedaeformis, e)* Mycale lingua *within* L. pertusa *framework, f)* Geodia baretti*, g)* Acesta excavata*, h) Fish with coral framework and i) Rope trapped within coral framework and* P. arborea *colonies. Scale bar represent 50 cm (Purser et al. 2013).*

The northern reefs (approximately from Lofoten, 68° N to Nørd Fugloya Island, 70° N) thrive in the Norwegian branch of NAC at 140 – 320 m (Fosså et al. 2002, Freiwald et al. 2004, Ruggeberg et al. 2011). In this area, CWC reefs are strongly shaped by the currents regime, forming elongated features called 'cigar reefs' (Spezzaferri et al. 2013).

In the 'cigar reefs' the living front face the main current, growing uni-directionally, while dead coral extends for some hundred meters at the tail in the direction of the current (e.g. Traena reef, Fosså & Skjoldal 2010). Currents near the seabed seem to influence even the internal structure of the reef as observed in the Korallen region, where velocities vary from 6.5 cm s^{-1} in areas dominated by coral ruble (reef bottom) to 8.9 cm s^{-1} in the living part (reef top; Buhl-Mortensen 2017). The isopycnal of 27.5 kg m^{-3} marks the boundary between Atlantic and Norwegian coastal waters (with high freshwater discharges) setting the upper limit for living corals in the northern reefs (Ruggeberg et al. 2011). Indeed, no living coral reefs have been found in this areas above and below the density belt of 27.51 – 27.63 kg m^{-3} (Dullo et al. 2008).

On the mid-Norwegian shelf (approximately from Mørebankene, 62° N to Lofoten, 68° N) large and patched *L. pertusa* bioherms (carbonates mounds of biological origin) rise up 25 m of the surroundings across an area of ~ 1700 km^2 (Hovland et al. 1994, Mortensen et al. 1995). In those living reefs, gorgonians (e.g. *Paramuricea placomus)* are also abundant and prevail perpendicular to the currents, being a good proxy for current direction (Mortensen et al. 1995). On the down-current sides of the bioherms, gorgonians were less uniform oriented, indicating a turbulent water movement. The associated fauna showed a gradual increase in diversity from the up-current to the down-current side, particularly sponges and gorgonians (Mortensen et al. 1995). The slope and the local topography, such as ridges (Thiem et al. 2006), mounds or sills (Guinan et al. 2009, Wilson et al. 2007), locally amplified the current velocity and mixing, which may promote the advection of food particles for utilization by suspension feeders (Tong et al. 2012, Wagner et al. 2011). Even structural *Lophelia* frameworks increase local turbulence, resuspension and particle trapping (de Haas et al. 2009, Mienis et al. 2009, van Oevelen et al. 2009) favoring food supply and the presence of associated fauna, as for instance the gorgonians *P. arborea* and *P. resedaeformis* in Traena and Røst reefs (Tong et al. 2012).

In the southern region, CWCs in the Oslo Fjord develop in very shallow waters between 90 – 140 m and thrive in the saline and well oxygenated AWI, only a few tens of meters below the permanently brackish surface Baltic waters (Svanson 1975, Wisshak et al. 2005). Also in the Skagerrak Strait is Tisler Reef, one of the most studied *Lophelia* reefs in the Norwegian shelf that is thought to be ~8.7 kyr old (Wisshak et al. 2005). Tisler Reef is a dynamic region, despite the lack of strong tidal currents (3 – 8 cm s^{-1} amplitude; (White et al. 2012). The strong resuspension of OM in the bottom (Lavaleye et al. 2009) facilitates the presence of CWC. A bottom residual current of 3.5 cm s^{-1} was recorded at Tisler reef. However, speeds observed inside the live reef were much lower than that outside or in the dead framework, suggesting a significant baffling by the coral colonies (Guihen et al. 2013), which might facilitate particle capture. The local hydrodynamics and food supply affect the reef's growth and morphology (De Clippele et al. 2017b). Downwelling occurs at the downstream sides of the reef sill, providing more labile POM as a food source available (De Clippele et al. 2017b, Wagner et al. 2011). The southeastern side of Tisler Reef is exposed more frequently and for longer periods of time to downwelling, where warmer and more chlorophyll-rich water is transported to the corals from surface waters, creating more favourable growing conditions for *L. pertusa* and sponges (Wagner et al. 2011). But also, carbon fluxes and POC concentrations varied along the reef (Lavaleye et al. 2009,

Wagner et al. 2011, Wild et al. 2009; Table 1). This fact was not only influencing the food quality for the CWC at different locations within Tisler Reef, but also showed the importance of relative small reefs in the biogeochemical processes in the ocean (Lavaleye et al. 2009).

2. Porcupine Seabight

The Porcupine Seabight is an embayment in the continental margin to the SW Ireland. It extends for about 230 km in the N-S direction, and is 100 km wide at most (Huvenne et al. 2002). Depth range goes from 400 m to more than 3000 m in the SW, where the embayment opens into the Porcupine Abyssal Plain. Overall, ENAW dominates the upper 750 m, with a northward flow along the NE Atlantic continental margin. SAIW might be present between 500 – 800 m depth. A core of MOW is found below down to ~1500 m, which presents a marked salinity maximum and oxygen minimum (Rice et al. 1991). The northward extension of MOW along the Irish continental slope appears to be limited in periods of strong SAIW, which is connected to long-term shifts of NAO (Ullgren & White 2010). Deeper waters are dominated by the LSB.

The Porcupine Seabight is characterized by the presence of large carbonate mounds, which are exclusively found in this region and the Rockall- Hatton Plateau (Wheeler et al. 2007). The origin of the mound formation has been related to hydrocarbon seeps, but in recent geological times, ocean circulation and carbonate contribution from scleractinian CWC have shaped the mounds (De Mol et al. 2002, Dorschel et al. 2007b). Carbonate mounds occur in water depths between 500 - 1200 m and vary from small structures of a few meters to over 300 m in height (De Mol et al. 2002). Three carbonate mound provinces have been described in Porcupine Seabight with different morphologies, distribution and associated coral banks and macrofaunal (De Mol et al. 2002, Henry & Roberts 2007, Roberts et al. 2003, Wheeler et al. 2007) that might be related with the different local scale hydrodynamics in each province (Huvenne et al. 2005).

High densities of living CWC banks of *Lophelia pertusa, Madrepora oculata* and (to a minor degree) *Desmophyllum cristagalli* are patchly distributed on top and the upper flanks of the mounds (De Mol et al. 2002). On-mound habitats host higher associated biodiversity than off-mound ones, with a clear dominance of suspension (e.g. *L. pertusa*) and deposit feeders (e.g. *Pliobothrus symmetricus*), respectively (Henry & Roberts 2007).

Due to the close relation between the carbonate mounds and the CWC banks, the spatial distribution of both have been related to oceanographic boundary conditions. The depth range of the CWC banks coincides with the MOW depth distribution (De Mol et al. 2005), with the largest coral banks are located in steep channels directed contour current (700 – 900 m depth; De Mol et al. 2002) and close to the ENAW-MOW boundary. The peak of demersal fish richness (1100 – 2000 m) also occurs in the presence of the MOW (Priede et al. 2010). The stratification of water column at the ENAW-MOW boundary combined with the complex bottom topography intensify the near-bottom currents in the mound provinces a (White 2003), with peak velocities up to 40 - 70 cm s^{-1} (Henry & Roberts 2007, Rüggeberg et al. 2007; see also Table 1) and creates internal waves (White 2003). That create favourable settlement sites for deep-sea coral by increasing food supply favoring the settlement sites for CWC (De Mol et al. 2005). Indeed, the intensification of currents and the increased MOW into the NE Atlantic after last glacial period is thought to allow Mediterranean CWC to repopulate the Porcupine Seabight (De Mol et al. 2005, Henry & Roberts 2008, Henry et al. 2014). It has been also suggested that this enhanced localised currents with the tidal signature brings alternating pulses of relatively cold and warm waters on the mounds, is important for CWC growth since it brings phyto-detritus (Duineveld et al. 2007, Mienis et al. 2007, Van Haren et al. 2014, White et al. 2007b).

Separate from the CWC reefs of the Porcupine Seabight are its sponge grounds. Dense sponge aggregations (~1.5 ind m^{-2}; Rice et al. 1990), such as the hexactinellid *Pheronema carpenteri* are also found the Porcupine Seabight. This aggregation was found close to, but not within, areas of the upper continental slope with increased tidal energy since sponges may not be able to cope with the increased current velocity but may be benefited from the resuspended POC transferred to them (Purser et al. 2013, Rice et al. 1990).

3. Rockall Bank

The Hatton-Rockall Plateau lies to the eastern margin of the north-eastern North Atlantic Ocean and is comprised of two relatively shallow banks. One of these, Rockall Bank, has supported a fishery for more than 200 years (Newton et al. 2008). This area is situated at the boundary between the STG and SPG influence (McGrath et al. 2012). The physical oceanography of this area is dominated by the changes in the strength and extent of the SPG (Hátún et al. 2009a). During strong SPG conditions the NAC

predominantly flows to the east of the plateau exposing it to the subarctic front, while during weak SPG conditions it predominantly flows to the west, bathing the plateau in warmer and more saline modified WNACW (Johnson et al. 2013).

Many different VME indicator species, including corals, sponges and chemosynthetic species, have been recorded in the Hatton-Rockall Plateau and the UK and Irish continental shelf edge (Fig. 13) as bottom trawl by-catch, but also a large proportion come from seabed imagery techniques.

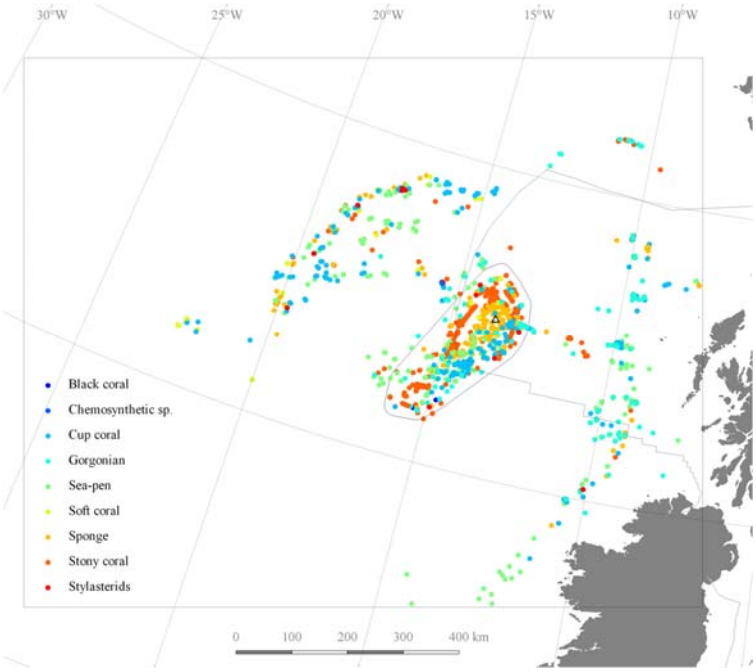

Figure 13. Vulnerable Marine Ecosystems by taxa in the Rockall Bank (ICES VME data).

Lophelia pertusa, is the most studied species. It occurs along the shelf break ridge at 400 to 600 m depth in Rockall Bank and on the 'growing tip' of carbonate mounds adjacent to the bank (Rengstorf et al. 2013, Rogers 1999, White et al. 2007b). While *L. pertusa* has been found in water temperatures from 4 – 12°C and depths of 40 – 1200 m, most reefs occur in 8 – 9°C (Freiwald 1998; see also Table 1). Soetaert et al. (2016) suggest two different mechanisms, using model simulations that serve to transport OM down from surface layers in these two types of locations. On the shelf break ridge, the dominant transport mechanism appears to be the downslope transport of OM rich waters above Rockall Bank. While at the carbonate mounds the topography acts to influence tidal currents and internal waves inducing vertical downwelling events and the formation of nepheloids layers, coupling *L. pertusa* reefs to surface productivity (Duineveld et al. 2007, Mienis et al. 2007). A recent study suggests *L. pertusa* is

most abundant on west facing slopes (Fernandes & Stirling, pers. comm.). Indeed, Johnson et al. (2013) found a decline in nutrient concentrations (particularly nitrate and phosphate; Table 1) in the east of Rockall Bank related to the strength of the SPG. Thus, west facing slopes may be more sensitive to the SPG dynamics and might represent a more suitable habitat with more favourable food supply and water chemistry. However, the available data on the distribution of *L. pertusa* around Rockall Bank is not of sufficient temporal resolution to allow the effects of SPG dynamics be linked with the life-history traits. While there is a paucity of information in the literature describing the distribution of other benthic taxa in relation to the distribution of water masses around Rockall Bank, the fauna associated with CWC reefs in the area has been well described. A typical assemblage of benthic fauna associated with CWC around the Hatton Rockall Plateau include: actiniarians, hydroids, hexactinellids and demosponges as well as crinoids and brisingiids, as described for western Rockall Bank (Wienberg et al. 2008), Hatton Bank (Roberts et al. 2008) and Rockall Trough (Masson et al. 2003). It is likely that the same factors (food availability, suitable substrate and water temperature) that determine the distribution of CWCs also prove favourable for this associated fauna.

More data are available on the spatial and temporal distribution of fish in the area and studies have linked these spatio-temporal dynamics to SPG strength. For instance, the spawning distribution of blue whiting, *Micromesistius poutassou*, is constrained along the European continental slope during years with strong SPG and the accompanying spread of cold, fresh water over the Hatton-Rockall Plateau. By contrast, weak SPG conditions spread warmer and more saline in the plateau moving the spawning distribution of blue whiting northwards and westward (Hátún et al. 2009b, Payne et al. 2012). Changes in SPG have been also linked tochanges across trophically connected levels in the food chain, ranging from phytoplankton to pilot whales (Hátún et al. 2009a). Finally, the declining of the SPG strength since the early 1990s has been correlated to fish abundances, suggesting a shift in the fish assemblages of Rockall Bank from one more characteristic of subpolar regions to a more boreal one in recent years (Stirling, pers. comm.).

4. Mingulay Reef Complex

The Mingulay Reef Complex (MRC) is an inshore seascape of reef mounds formed by *L. pertusa* in the east of Mingulay Island, western Scotland. It is located in a topographically complex deep-water

channel connecting the Scottish continental shelf and the Atlantic Ocean. This seascape contains hollows 250 m deep and rocky ridges that rise more than 100 m above the surrounding seafloor (Navas et al. 2014), which are surrounding by three main water masses: Atlantic water propagating northward from the west of Ireland, Irish Sea water passing northward through the North Channel, and coastal water created by the high volume of river runoff from the Scottish mainland (Cunha et al. 2013) and references therein. Current speeds, sedimentation rates and food supply in the MRC are also affected by the strength and position of the SPG (Douarin et al. 2016) and NAC inflow, which have controlled the occurrence and growth of the reefs over geological timescales.

The MRC encompasses five reef-mounds at relative shallow waters (100 – 250 m depth; Roberts et al. 2005, 2009), with low salinity (35.3 – 35.1 psu) and temperatures peaking at ~ 10^{o}C during spring, matching the peaking time of fluorescence (~ 0.08 μg *Chl-a* l^{-1}; see also Table 1). The Mingulay Reef 1 is the best studied reef within the MRC, which covers ~ 4 km long and ~500 m wide east-west. It has a steep southern slope, which gets gentler in the north (Davies et al. 2009, Roberts et al. 2009). The more recently discovered Banana Reef forms a ~ 2.5 km long ridge with an east-west orientation and despite its proximity to the Mingulay Reef 1, it has very different communities and dynamics.

Multiple studies on the biodiversity of the MRC benthic communities revealed a mosaic of habitats including framework of living *L. pertusa* usually hosting a small number of species e.g. *Mycale* sp. and *Hymedesmia* sp. sponges, *Eunice* sp. polychaetes (De Clippele et al. 2017a, Roberts et al. 2009), fine to coarse sediments with crinoids, coarse substrates (gravel, boulder rocks) with erect sponges (Duineveld et al. 2012, Roberts et al. 2005, Vad 2013), coral rubble and dead coral framework with the latter one being colonized by a species-rich community which is dominated by suspension and filter feeding organisms in terms of species richness (Henry et al. 2010, 2013b; Van Soest & De Voogd 2015) and biomass (Kazanidis & Witte 2016, Kazanidis et al. 2016). *L. pertusa* living reefs are also the spawning grounds for sharks, such as *Galeus melastomus*, a recreationally valuable resource in the MRC (Henry et al. 2013a). Most of the species in the area are typical representatives of the temperate inshore British fauna, but some sponge species have Lusitanian distributions reaching up to the Mediterranean basin (Roberts et al. 2009). The variability in the macrobenthic communities occurs at both large (across reefs) and small spatial (within reef) scales. While hydrographic (i.e. current speed) and topographic (i.e. rugosity, slope or depth) gradients shaped the broad scale assembly of taxa and functional traits (i.e.

feeding types); species´autoecology (i.e. recruitment, mating, foraging) played a more important role in shaping assemblies at fine spatial scales (Henry et al. 2010, 2013b).

Coral communities in Mingulay Reef 1 are more developed on its north side as a response to the gentler slope, local hydrographic and food supply conditions (Davies et al. 2009, Duineveld et al. 2012, Roberts et al. 2009; see also Fig. 7). Recently, (De Clippele et al. 2017a) recorded living coral colonies in the center of Mingulay Reef 1 associated with particular topographic and current speed (peak at ~ 40 cm s^{-1}) conditions. In the Banana reef, 24 % of area surveyed area is formed by dead coral (vs only 5 % in Mingulay reef 1; Duineveld et al. 2012) and sponges (erect and encrusting) and galatheid crabs are less common than in Mingulay Reef 1 (Duineveld et al. 2012, Van Soest & De Voogd 2015). The massive sponge *Spongosorites coralliophaga* colonizes dead fragments of *L. pertusa* (Kazanidis et al. 2016). However, higher densities of this sponge have been found in Mingulay Reef 1 (up to 14 ind m^{-2}) than in the Banana Reef (up to 1.7 ind m^{-2}). Therefore, although direct evidence is not available, it is very likely that between-reef differences in current conditions (maximum speed of 65 cm s^{-1} in Banana reef) play more important role than dead coral substrate in the distribution of *S. coralliophaga*. Indeed, corals (suspension feeders) rely more on current speed than sponges (Kazanidis et al. 2018, Orejas et al. 2016, Van Oevelen et al. 2018). Differences in food supply, in terms of polyunsaturated fatty acids concentration of the suspended POM, between the two reefs are very small (Duineveld et al. 2012). However, corals at the Banana Reef had lower concentrations of lipids, suggesting that they might be under less favourable food conditions than those in Mingulay Reef 1 (Duineveld et al. 2012). Davies et al. (2009) showed that tidally induced downwelling of fresher, warmer and chlorophyll richerwater fromsurface layers (Fig. 7) is important for the reef nutrition of the MRC.

Cold-water Coral Reefs in Submarine Canyons

5. Bay of Biscay

The continental margin of the Bay of Biscay extends from the Goban Spur off South Ireland to the Ortegal Spur off North Spain (Bourillet et al. 2006). From north to south, the area is divided into the Celtic, Armorican and Aquitaine margins. The Celtic and the Armorican margins are characterized by a wide continental shelf of up to 250 km and a canyon-dominated slope. The Aquitaine margin has a much narrower shelf of 70 km wide and a tectonic-dominated slope; thus, canyons in this margin are smoother,

wider and with weaker slope. Four water masses with different origins and densities can be found in the Bay of Biscay (van Aken 2000a,b). The ENAW (200 – 600 m depth) Iis originated from the Labrador Current and may contain a significant amount of AAIW transported to the NE Atlantic by the AMOC. Below (700 – 1300 m) the more saline and denser MOW is found and LSW flows down to approximately 2000 m depth. LSW is usually mixed with the MOW by internal tidal waves near the continental slope and therefore this water mass is less remarkable. Finally, the NEADW occurs approximately between 2000 and 2600 m water depth.

In the Bay of Biscay, the reef-building corals *M. oculata* and *L. pertusa* systematically co-occur with an appartent dominance of *M. oculata* (Arnaud-Haond et al. 2017, De Mol et al. 2011). The first contributions to the distribution of these two species was published in 1922 by (Joubin 1922), and in order to warn fishermen against those corals that might damage trawling nets. Aggregations of the two corals are commonly found in canyons of the Celtic and Armorican continental margins but absent from the Aquitaine margin, south of 46° N (van den Beld et al. 2017). These aggregations are small compared to the large carbonate mounds of the Porcupine and Rockall basins and usually do not exceed a linear of a hundred meters. Dense or isolated colonies of living and dead colonies of *L. pertusa* and *M. oculata* were observed from 650 m down to 1225 m depth, while coral rubbles were regularly recorded starting from 220 m. Thus, shallow coral rubbles are older (7.4 – 9.7 kyr) than the deeper living corals (1.2 – 2.3 kyr), suggesting a deepening of scleractinian depth distribution since the last maximum glacial period 11.5 kyr ago (De Mol et al. 2011). However, the impact of trawling, already mentionned by (Joubin 1922) can not be ruled out to explain these depth and age distribution patterns.

According to De Mol et al. 2011, the contemporary distribution of living *L. pertusa* and *M. oculata* in two canyons of the Bay of Biscay coincides with the lower limit of the physical boundary between the ENACW and the MOW (Fig. 14). It also matches the range of potential density (σ_θ between 27.35 and 27.65 kg m^{-3}) encompassing the realized niche of *L. pertusa* along the Norwegian margin and in the Porcupine Seabight (Flögel et al. 2014). However, (van den Beld et al. 2017) suggested a wider bathymetric and potential density ranges for the niche of *L. pertusa* and *M. oculata* based on the distribution of cold-water coral in 24 canyons of the Bay of Biscay.

The general circulation, and in particular the MOW cyclonic circulation interacts with the topography of the canyons resulting in an intensification of bottom currents and erosion on the right flanks of the canyons where sessile suspension feeders preferentially develops, including corals (De Mol et al. 2011, Van Rooij et al. 2010). Indeed, contourite depostional systems generated by the MOW have been repeatedly associated with the occurrence of CWC ecosystems in the NE Atlantic, from the southern Ortegal spur to the northern Porcupine Seabight (Hernández-Molina et al. 2009, Van Rooij et al. 2007b,a). In addition, on the continental slope of the Bay of Biscay, tidal currents are generated in the continental slope containing the most energetic internal waves in the world (Jézéquel et al. 2002).

These currents trapped and funneled by the canyon can reach speeds up to 1 m s^{-1} with a current residual parallel to the axis of the canyon and directed upstream or downstream (Khripounoff et al. 2014, Mulder et al. 2012; Table 1). Internal waves, generated by canyon topography, resuspend sediments and create nepheloid layers that propagate in particular at interfaces with the permanent thermocline and the MOW (Wilson et al. 2015).

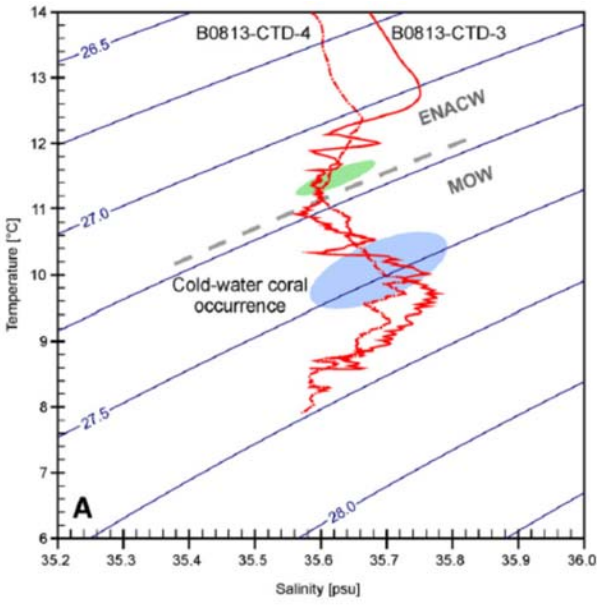

Figure 14. Temperature/salinity profile showing the occurrence of Lophelia pertusa and Madrepora oculata in canyons of the Bay of Biscay, with two different envelopes for shallow-water (green) and deep-water (blue) cold-water corals. The boundary (dashed grey line) between the Eastern North Atlantic Central Water (ENACW) and the Mediterranean Outflow Water (MOW) is indicated (De Mol et al. 2011).

6. Mid-Atlantic Bight, western North Atlantic

The western North Atlantic Ocean between Cape Hatteras and Cape Cod (USA, Middle Atlantic Bight) spans an area about 850 km of latitude, and the slope here is characterised by numerous and diverse submarine canyons (Brothers et al. 2013). The southern half of this region includes major canyon,

seep, hardground and open slope habitats that have been particularly well sampled, especially for fish assemblages. In ATLAS, we are focusing mostly on the unique Hatteras middle slope (Ross et al. 2001) and the most studied canyons, Norfolk and Baltimore, and their nearby surroundings (CSA Ocean Sciences et al. 2017, Obelcz et al. 2014). The Gulf Stream influences the oceanography of the Middle Atlantic Bight, particularly south of Cape Hatteras, which delimits a biogeographic boundary between warm-temperate and cool-temperate regions. Mean surface currents are derived from Gulf Stream flow southwestward over the Middle Atlantic Bight (MAB). Near Cape Hatteras, this flow turns back northward entraining colder, lower salinity water in a cyclonic gyre boundary current. Thus, the oceanography of the Hatteras middle slope is so complex and different from other areas that it seems very likely to have mediated observed ecological differences. Underneath, the Western Boundary Undercurrent flows southward generally along the 4000 m contour. On a smaller and more local scale, the MAB canyons are influence by the water movement, tides and internal waves, but topography also plays roles in the complex water flow around and within canyons (CSA Ocean Sciences et al. 2017).

Although the physical oceanography of the area has been well studied, the influence of oceanography on the benthic slope fauna has rarely been addressed directly. Distribution and community structure usually only involved depth zones due to water mass characteristics are frequently unavailable. The large differences in benthic habitats (corals and carbonate structures, seeps, and mud canyons) and oceanography suggests the benthic fauna is widely tolerant and community composition most likely influenced by food and habitat availability. The Hatteras middle slope (HMS) is biologically unusual related to the unique oceanography noted above. This is a transition region for many faunal groups where species reach their southern and northern limits. Some of the common benthic taxa occurring on the HMS include: the foramaniferan *Bathysiphon filiformis*, the anemone *Actinauge verilli*, the ophiuroid *Ophiura sarsii*, red crab *Chaceon quinquedens*, squids *Illex* spp., and the fishes *Myixine glutinosa*, *Helicolenus dactylopterus, Lycenchelys verrillii, Nezumia bairdii, Lophius americanus*, and *Glyptocephalus cynoglossus*. While the benthic species composition is similar to that of the overall Mid-Atlantic slope, the fauna of the Hatteras middle slope displays high densities but low species richness (Blake et al. 1985, Sulak & Ross 2006). In addition to these characteristics, the benthic fishes also display unusually small sizes and low activity attributed potentially to DO limitations (Moser et al. 1996, Sulak &

Ross 2006; see also Table 1). This possible low oxygen may be more a result of local high benthic respiration (Blair et al. 1994, Schaff et al. 1992) rather than an inherent water mass characteristic.

The Baltimore and Norfolk canyons are influenced by similar, large scale hydrographic conditions, mostly driven by the shelf-slope front (CSA Ocean Sciences et al. 2017). Thus, benthic fish (Ross et al. 2015) and invertebrate (CSA Ocean Sciences et al. 2017) assemblages were also similar between the two canyons, exhibiting clear patterns related to habitat characteristics (rugged *vs* simple) and depth zones (roughly above and below 1200 m). Some of the dominant species in these canyons included sea pens (*F. quadrangularis*), octocorals (*P. arborea*, *Anthothela grandiflora*), soft coral (*Duvia florida*), cerianthid anemones, red crab (*Chaceon quinquedens*), squat lobsters (*Eumunida picta, Munida* spp.), Jonah crab (*Cancer borealis*), sergestid shrimps, hyperiiid amphipods (*Themisto* sp.), squids and octopods (*Illex illecebrosus, Brachioteuthis beani, Bathypolypus bairdii*) and fishes (*Synaphobranchus* spp., *Dysommina rugosa, Arctozenus risso, Laemonema barbatulum, Phycis chesteri, Lophius americanus, Helicolenus dactylopterus, Hoplostethus mediterraneus, Brosme brosme, Nezumia bairdii, Glyptocephalus cynoglossus*) (CSA Ocean Sciences et al. 2017, Ross et al. 2015). Water mass influence on faunal structure was not readily apparent, although depth zonation is closely related to temperature. Hundreds of methane seeps were recently discovered on the slope of the MAB (including two near the Baltimore Canyon, 380 – 430 m depth, and Norfolk Canyon, 1460 – 1610 m depth, respectively), with well-developed chemosynthetic communities (CSA Ocean Sciences et al. 2017, Skarke et al. 2014). These sites promote extensive habitat complexity and food web diversity (Ross et al. 2015), but they occur in two very different water masses (or depth zones). The seeps share the dominant chemotrophic mussel *Bathymodiolus childressi*, but do not share any other fauna (CSA Ocean Sciences et al. 2017, Ross et al. 2015). This complete separation appears due to the great differences in depth and temperature (~8 *vs* 4°C).

Proxy studies from fossil scleractinians have shown clear glacial-interglacial cycles of CWC biodiversity in the Mid-Atlantic canyons. The most conspicuous switch was found between solitary corals, such as *D. dianthus* (mainly glacial) and colonial taxa, such as *L. pertusa* (interglacial). Variations in the water mass geometry and currents could effectively switch on/off a supply of coral larvae, accompanied by changes in food supply, nutrients, temperature, and salinity (Robinson et al. 2007). More recently it has been inferred that *D. dianthus* distribution depends on oxygen levels (Thiagarajan

et al. 2013). Today it is absent from OMZs, but it boomed during times when AAIW was high in oxygen and productivity, spreadind as far north as the mid-Atlantic canyons (Thiagarajan et al. 2013). Off the temperate eastern US coast, *L. pertusa* growth history was also forced by AMOC dynamics, whereby the warmer more saline limb of the AMOC, the Gulf Stream, migrated coastward and established present-day conditions by 7.5 kyr BP after the final sea level rise and the displacement of the Gulf Stream to its present location (Matos et al. 2015).

Coral Gardens on Seamounts and Banks

7. Azores

The Azores is a volcanic archipelago in the northeast Atlantic composed of nine islands, lying above a tectonically active triple junction between the North American, Eurasian and African plates. The rough seafloor topography comprises island slopes, seamounts, mid-ocean ridges, deep fracture zones, trenches, and abyssal plains exceeding 5,000 m depth (Tempera et al. 2012). Seamounts are prominent topographic features in the Azores, with 460 seamount-like features identified to date that may occupy 37 % of the total area of the ~1 million km^2 Economic Exclusive Zone (Morato et al. 2008, 2013). The archipelago is located in the vicinity of the North Atlantic subtropical convergence. Thus, this region is influenced by two eastward currents branching from the Gulf Stream: the cold NAC in the north and the warm Azores Current to the south (Alves & Colin de Verdière 1999, Bashmachnikov et al. 2004, Martins et al. 2007). Almost permanent complex mesoscale eddies with meanders and recirculation pattern are also important oceanographic features (Reverdin et al. 2003). Intermediate (NACW, NSPW and MOW) and deep water masses (Amorim et al. 2017, Johnson & Stevens 2000) are thought to shape the distribution of benthic communities in the seamounts slopes. Productivity is low in general with maximum values reported for upper water column in spring (Santos et al. 2013), but it can be enhanced by local upwelling associated with island slopes and seamounts (Bashmachnikov et al. 2004, Morato et al. 2008).

CWC diversity associated with seamounts and slopes is particularly high in the Azores (Fig. 15), with 184 species identified to date (Braga-Henriques et al. 2013, Sampaio et al. 2018) and sheltering the 75 % of the Octocorallia species recorded in European waters (Costello et al. 2001).

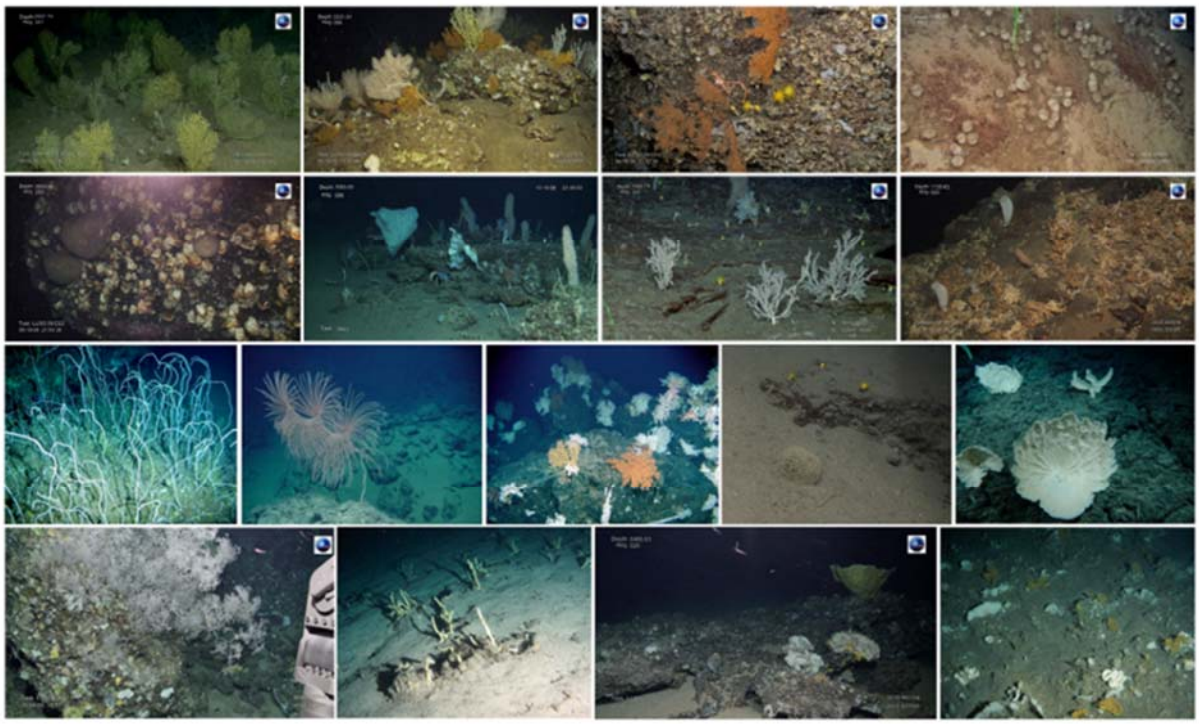

Figure 15. Examples of diverse deep-sea communities of the Azores seamounts (Tempera et al. 2012). Image credits: EMEPC; IMAR/DOP-UAz; GreenPeace ©Gavin Newman; SEAHMA.

A strong bathymetric gradient (upper 1000 m depth) in CWC species composition and diversity has been reported in the Azores based on historical and recent records (Braga-Henriques et al. 2013), with maximum diversity of different CWC groups occurring at different depths: 400–500 m for Antipatharia (7 species), mainly *Leiopathes* spp.; 500 – 600 m for Alcyonacea (29 species) where *Viminella flagellum*, *Dentomuricea meteor*, *Callogorgia verticillata* and *Acanthogorgia armata* are the most common species; 500 – 800 m for Scleractinia (24 species) dominated by *Caryophyllia cyathus*, *Madrepora oculata* and *Lophelia pertusa*. Finally, 800 –1000 m for Stylasteridae (6 species), such as *Errina dabneyi* (Fig. 16). The bathymetric distribution of CWCs may be related with water masses properties, with antipatharian distribution coinciding with the cold and less dense NACW, and octocorals with the less saline NSPW; whereas scleractinian and stylasterids appear to be more diverse and abundant where the saltier and warmer MOW waters occur, but more robust analysis are needed to confirm these relationships.

CWCs form important mono- and multi-specific coral gardens, with more than twenty different types identified to date (Braga-Henriques et al. 2013, Tempera et al. 2013), that are essential fish

habitats for commercially important species in the Azores (Pham et al. 2015). In contrast, large coral reefs are not common, but instead large extents of dead reefs and coral rubble accumulation are conspicuous throughout the region, potentially suggesting the demise of coral reefs during the last deglaciation event (Norbert Frank and Marina Carreiro-Silva, pers. comm.).

Biogeographic studies indicate that CWC in the Azores show mixed zoographic affinities with a greater affinity to the Lusitanian-Mediterranean biogeographic region (71 % shared species) and to a lesser extent to the western North Atlantic (Braga-Henriques et al. 2013). This same trend has also been found for deep demersal fish assemblages (Menezes et al. 2006), likely reflecting higher proximity of the Azores to the eastern continental margin, the past surface currents and glacial events (Crowley 1981).

Changes in biogeographic affinities are also observed in depth and likely related to water mass properties (Table 1). The proportion of amphi-Atlantic and cosmopolitan CWC and fish species increases at depth. In addition, while number of species increases with depth at high latitudes a concomitant decrease occur at low latitudes (Braga-Henriques et al. 2013, Menezes et al. 2006), in agreement with trends observed at ocean basin scales, possibly as a result of more constant environments (Etter et al. 2011).

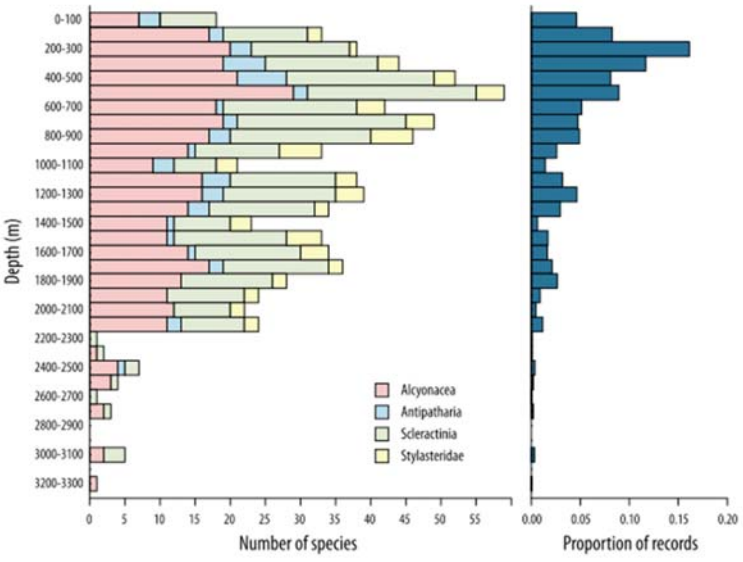

Figure 16. Summary of depth ranges and records for Alcyonacea, Antipatharia, Scleractinia and Stylasteridae in the Azores seamounts (Braga-Henriques et al. 2013).

This pattern is also consistent with the presence of permanent thermocline in the NE Atlantic (600 – 1000 m) and the predominance of colder and fresher deep-water masses formed at high latitudes (i.e. the SAIW and the LSW) beneath its lower boundary. The distribution of demersal fish in slopes and seamounts at depth have been tentatively related to the distribution of water masses and their properties (Menezes et al. 2006). However, no clear association between fish

bathymetric distribution and environmental factors (e.g. temperature, salinity, oxygen) other than depth has been found up to date (Parra et al. 2017). Intermediate upper slope assemblages (200 – 600 m) dominated by *Helicolenus dactylopterus* and *Pagellus bogaraveo* coincide with the core distribution of the colder and fresher NACW, delimited from other water masses by its lower density. The intermediate and deep mid-slope fish assemblages (600 – 800 and 800 – 1200 m) dominated by the species *Moro moro* and *H. dactylopterus* match the distribution of MOW (higher salinity and low oxygen content) and the presence of oxygen local minimum zone in the region (Johnson & Stevens 2000), which decrease diversity and fish abundance at 800 – 900 m depth (Menezes et al. 2006). An increase in biomass and diversity observed at 1000 m depth has been related with the limit of the permanent thermocline, increased oxygen concentrations and the influence of the subpolar intermediate waters (SAIW and LSW) and high abundance of deep mesopelagic microneckton prey enhances benthopelagic fish (Menezes et al. 2006).

Longitudinal differences in fish assemblages have been also found along the 600 km NW-SE longitudinal spread of the Azores archipelago, with higher abundance of subtropical shelf species in the southern islands (São Miguel, Santa Maria) and higher abundance of temperate shelf species in the western and northern most islands of Flores and Corvo (Menezes et al. 2006). In contrast, no clear differences in CWC species composition has been detected along this longitudinal strip or in relation to the Mid-Atlantic Ridge (MAR; which separates the western from central and eastern sections of the archipelago, Braga-Henriques et al. 2013). However, preliminary results may indicate higher species richness and distinct CWC communities in the eastern most sampled area of the Azores region around the Formigas bank (Santana 2018). There has been considerably less sampling on west of MAR than on the Euro-Asian plate. Thus, we cannot rule out the hypothesis that dissimilarities between the CWC on both sides of the MAR exist, in particular in lower bathyal and abyssal fauna as suggested for other studies (Gebruk et al. 2010, Mironov et al. 2006). Longitudinal gradients for some environmental variables point out for dissimilarities in environmental conditions on both sides of the MAR (Amorim et al. 2017). DO and oxygen saturation where higher to the west of the MAR, while inorganic nutrient concentrations presented the opposite pattern. That might reflect the presence of a topographic discontinuity created by the MAR, but also an oceanographic transition zone between water masses (Amorim et al. 2017). More sampling effort and information on larvae biology and dispersal potential

will help to clarify the role of the MAR as a barrier between the western and the eastern parts and in shaping trans-Atlantic deep-sea biogeography. No clear latitudinal gradient has been found for demersal fishes and CWC species composition at scale of the Azores (Braga-Henriques et al. 2013, Menezes et al. 2006). This is likely because of the narrow latitudinal range (2.5°) of the archipelago, since studies covering a wider region of the northern MAR have found significant differences in demersal fish assemblages (e.g. Bergstad et al. 2008, 2012) and in bathyal invertebrate fauna (Gebruk et al. 2010). Investigations on the northern and southern sections of the MAR will likely reveal latitudinal gradients in fauna distribution that are currently not detected at the regional scale of the Azores.

8. Galicia Bank

The Galicia Bank (GB) is a non-volcanic deep-seamount located on the north-western continental margin off the Spanish coast. The GB creates an intra-slope of of ca. 3000 m depth and other morpho-structural provinces (Vázquez et al. 2008) with dispersed highs (up to 800 m in relief; (Ercilla et al. 2006, 2011; Vázquez et al. 2008). The dome-shaped GB seamount has a relatively flat summit at 600 m depth, followed by a bank break (significant increase in slope) at 1000 – 1400 m (Serrano et al. 2017b) and getting to 5000 m depth. High current velocities have been recorded above the summit (5 – 30 cm s^{-1}; Duineveld et al. 2004). The surface waters originated in the Atlantic circulates southward in the GB during spring-summer, and northward during autumn-winter (Iberian Poleward Current). Beneath in the intermediate layers, ENACW and MOW are found. MOW present higher salinities than surrounding waters to 1500 – 1600 m and moves as a contour current reaching velocities of 5 – 10 cm s^{-1} (Iorga & Lozier 1999, Pingree & Le Cann 1990). LSW, NADW and LDW can be detected in the deeper water strata (Huthnance et al. 2002, van Aken 2000a, Van Aken 2002). This area is characterized by a relatively high primary productivity (~ 220 g C m^{-2} yr^{-1}; Joint et al. 2002), caused by intense, wind driven seasonal upwelling (McClain et al. 1986).

Depth, substrate type and the influence of water masses determine the distribution of the deep-sea assemblages in GB (Altuna 2017, Serrano et al. 2017a). A deep summit surrounded by abyssal areas with very low fishing activity make the 75.6 % of the bathyal fauna known in the region occurs in GB (Cairns & Chapman 2001). GB presents one of the highest coral biodiversity in the northeast Atlantic (Altuna 2017; Fig. 17), encompassing Macaronesian, Mediterranean, NE and NW Atlantic species, due to

the confluenced of different intermediate and deep water masses (Ruiz-Villarreal et al. 2006). As other seamounts, it also presents high number of endemic species. (Souto et al. 2016) found 25 species of Cheilostomata in GB with an unusual high endemicity (48 – 60 %) when comparing with other taxonomic groups in GB or areas. For instance, in Gorringe Bank (off Portugal), Demospongia, a group with limited dispersal capacity as bryozoans, displayed only 28 % endemicity (Xavier & Van Soest 2007). Ecological differentiation among species of the same genus has been observed for decapod crustaceans (*Polycheles typhlops - Polycheles laevis and Munida sarsi-Munida tenuimana*), bivalves (*Limopsis minuta - Limopsis cristata*) and fish (*Uropthychus rubrovittatus - Uropthychus concolor*) in GB, showing a clear preference for shallower or deeper depth. A generalized species substitution occur with depth (Serrano et al. 2017a). The 56 % of species appeared in a depth range narrower than 25 % of the total explored depth range. In contrast, the 29 % of species were distributed along 75 % or more of the total depth, being *M. oculata*, *D. dianthus* and *L. pertusa* the most widely distributed species in GB (721, 868 and 436 m depth range, respectively).

The summit of GB matches the boundary between ENACW and MOW and contains large biomass of Ophiacanthidae ophiuroids (1985 kg km^{-2}, Fig. 17). Also, in the soft bottoms, *Amphiura grandisquama,* the solitary corals *Deltocyathus moseleyi* and *Flabellum chunii*, and the bivalve *Limopsis minuta* are frequently present. Ophiuroids are replaced by shrimps and crabs when getting deeper into the sands and MOW core, and coinciding with the disappearance of the moderate slope current (Serrano et al. 2017b). MOW flowing along GB contour favor nutrient afflux from the Atlantic mass waters to deep waters allowing to coral colonies to growth (Somoza et al. 2014). Thus, under the MOW influence, CWC communities dominated by *L. pertusa* and *M. oculata*, (315.5 and 306 kg km^{-2}, respectively) are found in rocky plain substrates. These two species intermingle in some locations, growing on each other. The summit assemblage also include other scleractinians (*Desmophyllum dianthus*), gorgonians (*Acanthogorgia armata*, *Swiftia rosea)*, black corals (*Parantipathes* sp.), bivalves (*Lima marioni*, *Asperarca nodulosa)* and decapod crustaceans (*Munidopsis* spp., *Munida tenuimana* and *Bathynectes maravigna*) (Altuna 2017; Serrano et al. 2017a,b). The turbulent boundary between ENACW and MOW allows the transport of coral larvae along the NE Atlantic margins (Somoza et al. 2014). Highly variable (seasonal and inter-annual) flux of phytodetritus and other OM (e.g. faecal pellets, copepods,

amphipods) has been detected in this area ranging from 17 to 37 mg C m^{-2}, although isotopic signatures indicate that sinking algae are not main food source in CWC (Duineveld et al. 2004).

The bank break (1000 – 1400 m) recorded the highest diversity in hard-bottom assemblages. Hexactinellids, demosponges and bamboo corals present a higher occurrence in the bank break than in the summit (Fig. 17). Fauna in these substrates is typified by the bamboo coral *Acanella arbuscula*, and with several sponge species associated in low number (*Aphrocallistes beatrix, Phakellia robusta,* Geodiidae and Hexactinellida), gorgonians (*Anthothela grandiflora*), and the sea star *Brisinga endecacnemos* (Serrano et al. 2017b). Flow acceleration in upper flanks and the enrichment from northern LSW arriving to GB might increase zooplankton biomass at vertical-steep walls by "bottom trapping" (Genin & Dower 2008), explaining the higher diversity of CWC at the rocky break. However, low OM content was observed in soft sediments (Serrano et al. 2017a).

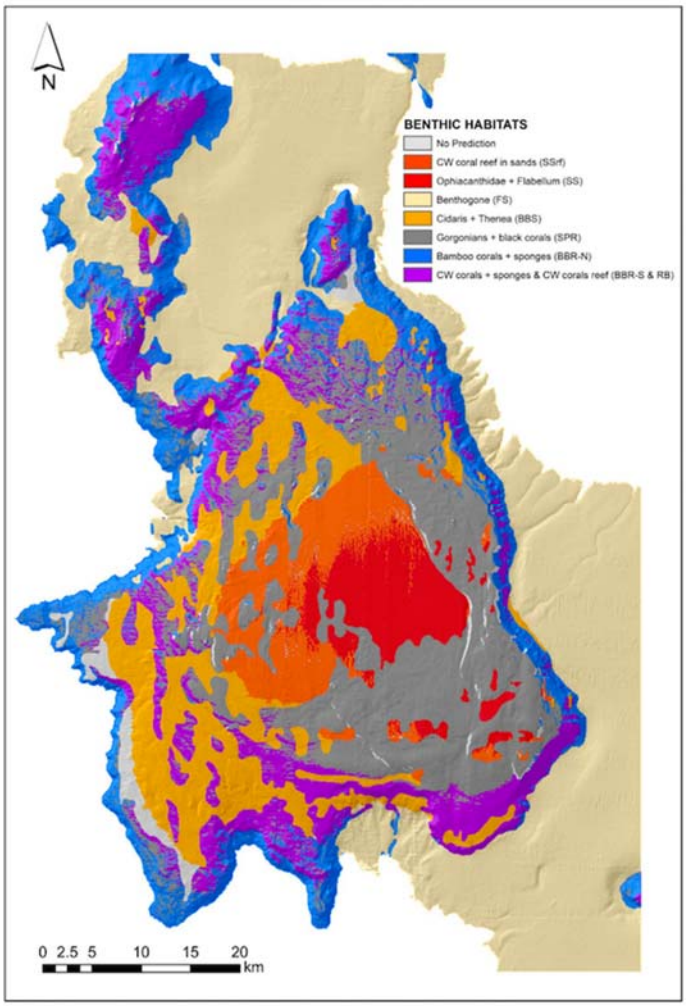

Figure 17. *Habitat map (showing highest probability of presence) of benthic communities in the Galicia Bank* (Serrano et al. 2017b).

In addition, lower phytopigment concentrations ($7{\cdot}10^{-3}$ ± $0.6{\cdot}10^{-3}$ µg *Chl-a* g^{-1}) than in deeper strata were found in the break, resulting in also lower abundance of infauna such as nematodes. The decoupling between pelagic and benthic processes in the GB seems to be due to the strong hydrodynamic forcing, that sweep away fine phytodetrital matter (Pape et al. 2013b,a). Patches of sandy bottoms are dominated by the urchin *Cidaris cidaris,* with high presence of the sponge *Thenea muricata* and the seastar *Plinthasther dentatus* and the benthopelagic shrimps *Aristaeopsis edwardsiana* and *Systellaspis debilis.* The influence of MOW core here might lead to a

general impoverishment of fauna and of biomass (Serrano et al. 2017a, Table 1). In the southern bank break, *L. pertusa* and *M. oculata* banks are also present, forming complex three-dimensional structures that support a diverse associated macro- and megafauna (Serrano et al. 2017b).

The deep flanks (1400 – 1800 m) are highly influenced by LSW, presenting fine sands with high OM contents. The permanent thermocline (4°C) and the boundary between MOW and LSW, can cause changes in food supply and the increase in OM (Howell et al. 2010). Main assemblage here is composed by high biomass of the holothurian *Benthogone rosea* (628.2 kg·km^{-2}, Fig. 17), accompanied by the urchin *Araeosoma fenestratum* and a very distinct arthropod fauna (the crabs *Neolithodes grimaldii, Glyphocrangon longirostris* or the giant sea spider *Colossendeis colossea*), the scaphopod *Fissidentalium capillosum*, and several anthozoans including the solitary coral *Stephanocyathus crassus*, the seapen *Umbellula* sp., the bamboo coral *A. arbuscula* and the gorgonian *S. rosea*. Live colonies of the scleractian *Solenosmilia variabilis* are also found in this depth interval.

Coral Gardens and Cold Seeps on Mud Volcanoes

9. Gulf of Cádiz

The main oceanographic context of the Gulf of Cádiz (GoC) is represented by the exchange of Atlantic and Mediterranean water masses through the Strait of Gibraltar. The Atlantic Inflow Water (composed by North Atlantic Surface Water NASW down to 150 m depth and NACW from ~150 to 450 – 550 m depth (Sánchez & Relvas 2003) flows inside the Mediterranean with average temperatures of 12 – 16˚C and salinities of 34.7 – 36.25 psu, but displaying clear seasonal variations and current speeds between 0.3 – 0.4 m s^{-1}. Below, at depths of 500 – 800 m with saline dense water averaging 13˚C and 36.5 – 36.9 psu (Fernández-Salas et al. 2012, García et al. 2009, Nelson et al. 1999), the MOW flows north-westwards into the Atlantic Ocean (Hernández-Molina et al. 2016, Nelson et al. 1999) at speeds up to 3 m s^{-1} (Mulder et al. 2003; see also Table 1). The GoC represents an extensive seepage area, with more than 60 mud volcanos identified to date. In fluid venting areas, the bacterial activity promotes the formation of Methane-Derived Authigenic Carbonates (MDACs) such as chimneys and slabs that can be exhumed by the bottom currents and transform completely the seabed. These stable hard bottoms favor the settlement of suspension feeders (e.g. sponges and CWCs) that are favored by the strong hydrodynamics, which provides continuous food supply and burial prevention (Díaz-del-Río et al. 2003,

León et al. 2007). MOW circulation contributes significantly to sediment transport and deposition, seafloor erosion, destabilization of gas-hydrate rich sediments and development of seafloor structures (e.g. channels, erosive depressions) and, therefore, it influences the presence of different types of deep-sea habitats (Hernández-Molina et al. 2016, Pinheiro et al. 2003, Rueda et al. 2016).

CWCs are scarce and restricted to specific areas in the GoC (Álvarez-Pérez et al. 2005, Wienberg et al. 2009). Mostly dead colonies and coral graveyards were found to date as a result of the strong decline of these organisms after the last ice-age due to the recent warming and oligotrophic conditions of the GoC (Van Rooij et al. 2011, Wienberg et al. 2009). One of the very few still living *M. oculata* banks (10 colonies m^{-2} on average) occurs in Gazul mud volcano related to the low temperature (13.1°C) and salinity (35.9 – 36.0 psu) at the summit, the strong hydrodynamic conditions (speed > 0.3 m s^{-1}) and the low trawling activity (González-García et al. 2012; Table 1). Gazul mud volcano is dominated by large suspension feeders (e.g. *M. oculata, Asconema setubalense, Poecillastra compressa, Antipathella dichotoma*) and represents a biodiversity hotspot in the GoC with more than 400 associated species (versus ~50 spp. in the surrounding soft bottoms; Ramalho et al. 2018, Rueda et al. 2016, Sitjá et al. 2018). Several studies have pointed specific assemblages in the GoC with a low MOW influence (e.g. *Leptometra-Asconema-Madrepora* assemblage in Gazul mud-volcano; Fernández-Salas et al. 2012, J.E. García-Raso 1996, Salas 1996) and the presence of about 26 species previously known from deep-sea Mediterranean locations bathed by the MOW (Sitjá et al. 2018), including the species *Coelosphaera cryosi* and *Petrosia raphida*. These discoveries highlight the importance of MOW in structuring the distribution of deep-sea fauna and the natural export of Mediterranean deep-sea benthos.

In the northern sector of the GoC, the community composition on the slope varies with the intensity of the trawling activities and the influence of the MOW (Fig. 18). Flat muddy and sandy bottoms are widespread in the upper slope and dominated by burrowing megafauna such as Cerianthiids, sabellids, the decapods *Nephrops norvegicus*, *Munida* spp. and *Goneplax rhomboides together with sea-pens* (*Kophobelemnon stelliferum*) and small sponges (*Thenea muricate;* Díaz del Río et al. 2014, Fig. 18). The low presence of suspension feeders in these areas cannot be disentangled from low hydrodynamic conditions (< 0.1 m s^{-1}) and high trawling impact, with more than 50 vessels operating along the year (Díaz del Río et al. 2014). However, sea-pens such as *K. stelliferum*, *Funiculina quadrangularis* and *Pennatula aculeata*, are abundant in soft bottoms with low trawling activity and high hydrodynamic

conditions (0.2 – 0.3 m s^{-1}, Sánchez-Leal et al. 2017). Dense sea-pen communities in the upper slope have been correlated with the percentages of OM content and mud (González-García et al. 2015), as well as the presence of deposit feeders, such as the bivalve *Abra longicallus* and the polychaete *Spiochaetopterus typicus* (Díaz del Río et al. 2014).

Aggregations of the bamboo coral *Isidella elongata* occur in the middle slope where MOW influence is higher and the trawling activity is minimal due to the large distances to the fishing ports (> 20 nm, Rueda et al. 2016). Other suspension feeders are also abundant in these areas, including gorgonians (*Radicipes* sp.), small (*K. stelliferum*) and large sea-pens (*Protoptilum* sp.) and hexactinellid sponges (*Pheronema carpenter*; Rueda et al. 2016, Fig. 18). In areas with high MOW influence and hydrodynamic conditions such as in channels and furrows (0.3 – 0.6 m s^{-1}), the sediments are coarser and dominated by the echinoderm *Leptometra phalangium*, the coral *Flabellum chunii* or hormathiidae organisms (*Actinauge richardi*). In these areas, the seafloor may contain ripples due to the near bottom currents and the associated erosive processes (Díaz del Río et al. 2014). Also, cidaroid type sea-urchins (*Cidaris cidaris)* are very common, probably due to the easy anchoring provided by these sediments.

The Atlantic-Mediterranean transition at the Strait of Gibraltar is one of the most important potential barrier for gene flow in the world's oceans at different temporal and spatial scales (Galarza et al. 2009a). Multiple studies have analyzed genetic structure in Atlanto-Mediterranean invertebrates e.g. (Pérez-Losada et al. 2007, Wangensteen et al. 2012) and fishes e.g. (Carreras-Carbonell et al. 2006, Galarza et al. 2009b). However, studies regarding deep-sea species are scarce (Taboada & Pérez-Portela 2016). Recently, (Sitjá et al. 2018) recorded several deep-water Mediterranean sponge species in the GoC bathed by the MOW, representing their first records in Atlantic waters, which could suggest that the natural export of Mediterranean deep-sea benthos by the MOW might be promoting population connectivity between geographically distant locations.

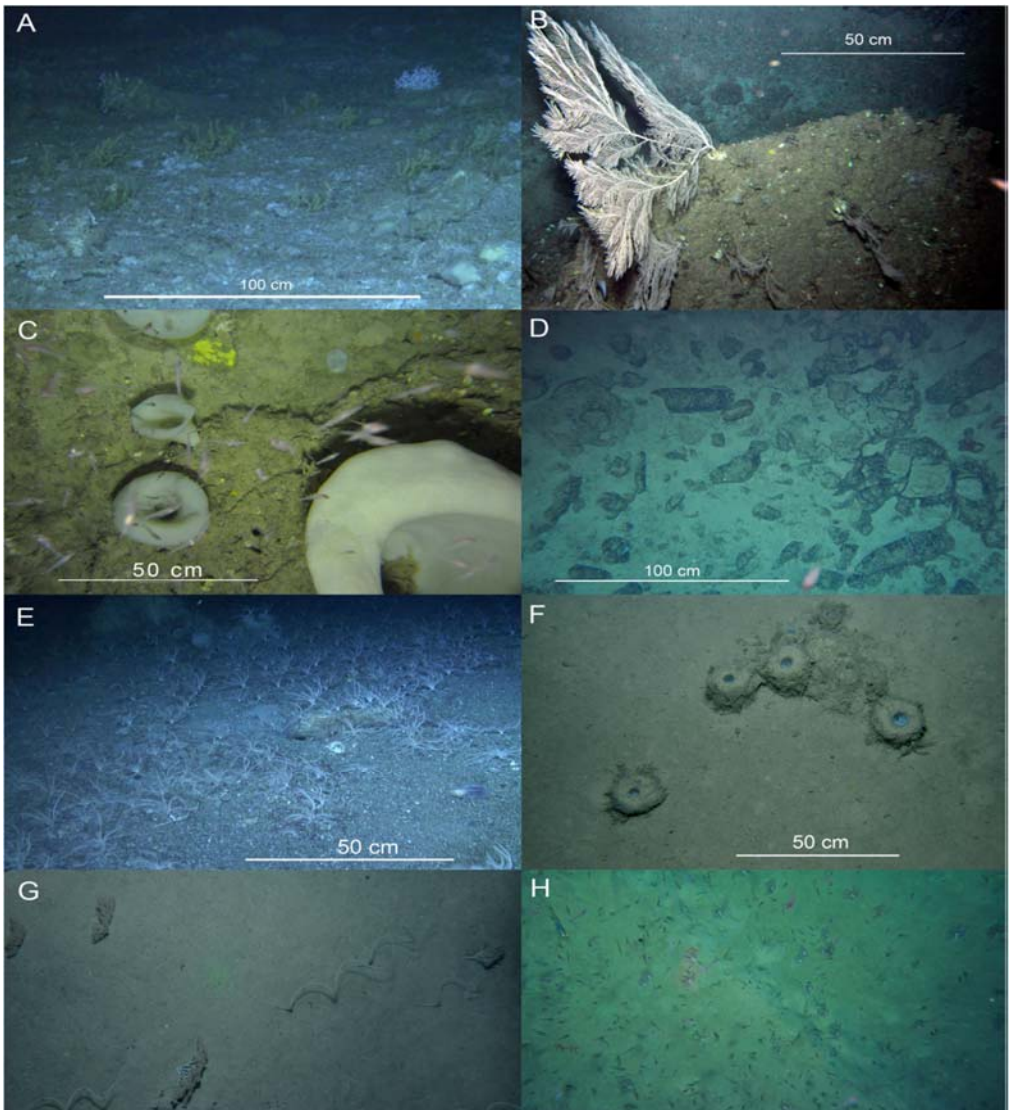

Figure 18. *Deep-sea habitats in the Golf of Cadiz mud-volcanos. Bathyal rocky bottoms with a) Bebryce mollis, b) Callogorgia verticillate, c) large hexactinellid sponges (*Asconema setubalense*), d) authigenic carbonate (chimneys and slabs), e) bathyal detritic bottoms with Leptometra phalangium, f) bathyal muds with* Pheronema carpenter*, g) with* Isidella elongata *and* Radicipes *and h) with sea-pens* (Rueda et al. 2016).

Deep-sea Sponge Grounds in Deep Sedimentary Plains

10. Davis Strait

The Davis Strait connects the Arctic Ocean in the north via Baffin Bay and the Atlantic Ocean in the south via the Labrador Sea; and separates southwestern Greenland and south-eastern Baffin Island (the largest island in the Canadian Arctic Archipelago). It is considered the world's largest strait renowned for exceptionally strong tides (9 – 18 m) and a complex hydrography. The slopes at the Labrador Sea flank of the ridge drop to more than 2500 m. The Labrador Sea is a key basin of the Atlantic Ocean with respect to receiving and mixing the Arctic and Atlantic waters, sea-ice coverage, Greenland freshwater flux and continental runoff (Yashayaev et al. 2015), and recurrent production gas and freshwater enriched cold and dense intermediate water masses (deep-water convection) ventilating the deep and abyssal layers of the North Atlantic (Rhein et al. 2017; Yashayaev & Loder 2016, 2017) and the AMOC (Thornalley et al. 2018).

These processes administer climate and ecosystem of the subpolar region, shaping and maintaining its deep-sea communities from top (Fragoso et al. 2016, 2018) to bottom (Kenchington et al. 2017). The particular characteristics of this region make it shelter benthic species unique to the area and the western subpolar North Atlantic as a whole. Epibenthic megafauna in the Canadian waters of Davis Strait revealed a total of 480 taxa from diverse phyla (Baker et al. 2018). In both Davis Strait and Baffin Bay sponges and sponge grounds can make up the majority of the benthic biomass (Murillo et al. 2018), as usually occurs along the continental slopes of the northwest Atlantic. Sponge communities include arctic and boreal astrophorid-demospongia grounds and at least 112 species have been identified from the region (Brøndsted 1933). (Murillo et al. 2018) have identified 93 sponges from trawl catches, while (Kenchington et al. 2016) have also identified significant concentrations of VME indicators (sponges, large and small gorgonian corals and sea pens) in the Canadian portion of the David Strait.

Recently, the first reported *L. pertusa* reef from Greenlandic waters was found at 886 – 932 m depth on a steep continental slope off southwest Greenland (Kenchington et al. 2017). Analyses of hydrographic data showed that the reef was located in a layer of Atlantic Water of stable temperature (3.5 – 4.5°C) and salinity (34.88 – 34.94 psu) with water density slightly higher (27.63 – 27.75 kg m^{-3}) than reported for the northeast Atlantic, and exceptionally high currents of > 15 cm s^{-1} at 1000 m (Table 1).

The intermediate salinity maximum, in the near-bottom water mass characteristics, was found in the depth range where the corals were found. Signals of consistent vertical and horizontal transport at 700 – 900 m over the reef area have been also discovered. Although this area is not directly influenced by intermediate and deep-water convection in the Labrador Sea, the seasonal evolution of near-bottom temperature, salinity and density in this depth range revealed strong seasonal patterns related to local convection from the surface and advection of cooled and freshened waters at depth.

Benthic communities are affected by a number of different biological and physical parameters; with temperature, depth, food input (nutrient concentration and composition), sediment composition, particle load, disturbance level (e.g. ice scouring) and hydrographical regime (including currents and turbulence) being the most prominent (e.g. Wlodarska-Kowalczuk et al. 2004). Benthic fish assemblages are linked to depth and temperature and 78 species of fish have been identified from in trawl surveys in this region (Jørgensen et al. 2005, 2011). Circulation and inflow of Atlantic Waters (warmer than 4°C) are vital for the coral and sponge colonies documented along the continental slope. Macrobenthic fauna is usually tightly linked to food availability in Artic and sub-Artic regions (e.g. Piepenburg et al. 1997). Thus, a high benthic-pelagic coupling and an efficient transport of food from surface to the sea floor is expected in areas with important deep benthic communities. In the Davis Strait the senescent algal blooms and zooplankton faecal pellets provide high levels of nutrients and food input to the sedimentary organic carbon flux. Intense phytoplankton blooms occur in the northern Labradors Sea south of Davis Strait during spring in the ice-free waters triggered by ice-melt and water column stability (Frajka-Williams & Rhines 2010). Prior extensive deep winter convection and strong surface freshening can enhance the spring blooms. The high biomass of phytoplankton blooms feed a community of grazers dominated by large copepods, i.e. *Calanus* (Head et al. 2003). Most higher trophic levels in the Arctic feed directly on *Calanus* (Falk-Petersen et al. 2009). But also, the vertical flux of faecal pellets sinking fast to the sea floor is a key food source for benthic communities and particularly, suspensive feeders such as corals and sponges (Juul-Pedersen et al. 2006, Turner 2002).

11. Flemish Cap, Flemish Pass and the Grand Banks

The continental margin offshore of Newfoundland, eastern Canada, comprises the areas of the Grand Banks, Flemish Pass and Flemish Cap. The Grand Banks are a series of shallow, sandy plateaus

extending for 730 km along the Newfoundland continental shelf. The southeast slope of the Grand Banks lead to the Flemish Pass, a sandy-muddy channel of approximately 1200 m depth, that separates this area from Flemish Cap (Murillo et al. 2011 and references therein), another relative shallow sandy-muddy bank offshore. These areas are important spawning, nursery and feeding grounds for a large number of fish and shellfish species. They have been fished at least since the beginning of the 15th century (Lear 1998) and continues to be fished today, primarily with bottom-contact trawls (Murillo et al. 2016a), strongly regulated and managed by the Northwest Atlantic Fisheries Organization (NAFO). The Grand Banks shelf is separated from the Flemish Cap by the cold (3 – 4.8°C and salinities 34 – 35 psu) southward flow of the Labrador Current (Colbourne & Foote 2000), while the warmer waters of the Gulf Stream crosses both areas. Around the tail of the Grand Bank these two currents meet giving rise to the NAC (Gil et al. 2004).

Massive occurrences of sponges are commonly found along the Labrador Slope to the southern Davis Strait (e.g. Kenchington et al. 2014, Knudby et al. 2013, Murillo et al. 2012, 2016b), including both hexactinellids and demosponges, and particularly from the family Geodidae. Studies in the Grand Banks and Flemish Cap recorded structure-forming sponge grounds (Fig. 19), with similar composition to those in the east, from 880 to 1400 m depth with densities varying from 0.078 to 0.311 kg m^{-2} (Murillo et al. 2012, 2016b). These aggregations coincide with the flow of the lower limit of the Labrador Current, presenting bottom temperature and salinity values ranging between 3.38 and 3.84°C and between 34.85 and 34.90 psu. Further studies evidenced the relationship between dense sponge aggregations and warm (~3.0 – 3.5°C), salty (~34.85 – 34.90 psu) water masses in the area at ~1300 and 1723 m depth (Beazley et al. 2015; see also Table 1) that could be a remnant of the Irminger Current. Thus, megafaunal communities in the area are dominated by large numbers of ophiuroids and sponges. On the slope of the Flemish Cap, sponge grounds were dominated by axinellid and polymastid sponges, while the deeper sponge ground in the southern Flemish Pass was formed mainly by geodiids and *Asconema* sp. The presence of structure-forming sponges was associated with a higher biodiversity and abundance of associated megafauna compared with non-sponge habitat (Beazley et al. 2013). According to models developed by (Knudby et al. 2013), the distribution of *Geodia* spp. sponges and deep-sea sponge grounds in the North-west Atlantic (Baffin Bay, Hudson Strait, Newfoundland and Labrador, Flemish Cap) are related to depth and bottom minimum salinity. However, similar models produced for the

Newfoundland and Labrador shelves and slopes (Guijarro et al. 2016) found primary production levels to be important determinants of both presence and biomass consistent with the requirements for a high food supply to produce and maintain the high biomasses observed (Beazley et al. 2013, Klitgaard & Tendal 2004).

In addition to the sponge grounds, soft corals (order Alcyonacea) are also common in the soft-bottoms of this region (Fig. 19), with highest species richness and biomass found between 600 – 900 m depth (Murillo et al. 2011). The northeastern slope of the Grand Banks present a high biomass of large gorgonians (Fig. 19; Isididae, Paragorgidae, Plexauridae, and Primnoidae), while pennatulaceans (*Anthoptilum grandiflorum*, *F. quadrangularis*, *Pennatula aculeata*, and *Halipteris finmarchica*) are more frequent in Flemish Pass and Flemish Cap (Murillo et al. 2011; Fig. 19). Radiocarbon methods showed that many gorgonian species such as, *A. arbuscula*, *Keratoisis ornata*, *Paramuricea* spp., *P. arborea* and the antipatharian *Stauropathes arctica* rely on exported POM (Sherwood & Edinger 2009, Wang et al. 2014). The grow rates in these corals vary with the local oceanography, being higher in areas with stronger currents. The fastest growth rates were recorded in the Northeast Channel where tidal currents average 1 m s^{-1}, versus the Hudson Strait where currents average about 0.4 m s^{-1} (Sherwood & Edinger 2009).

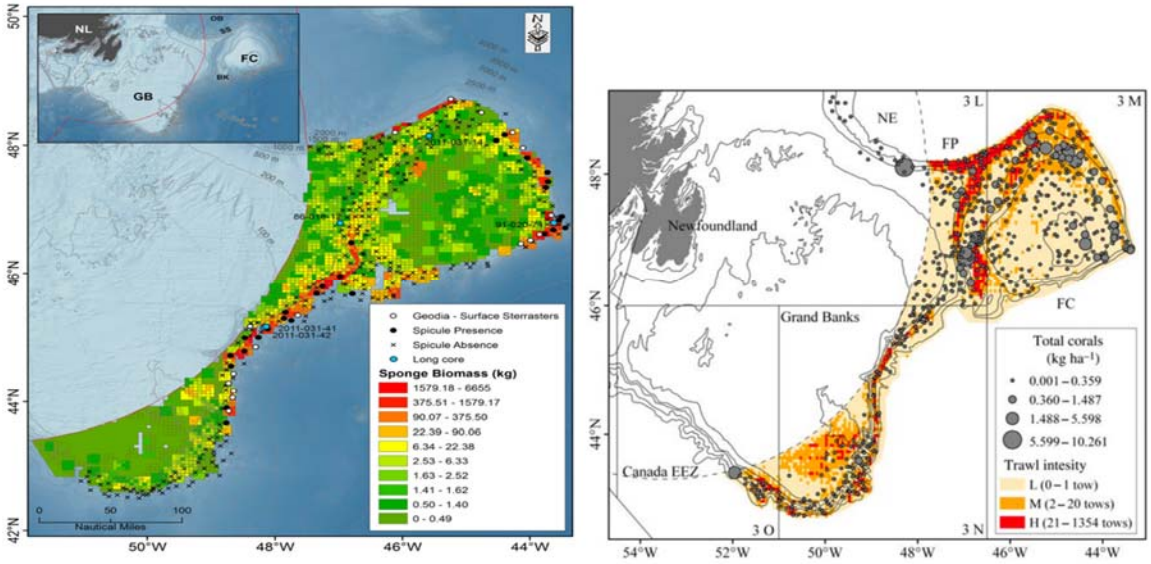

Figure 19. Records of habitat forming deep-sea taxa in the Flemish Cap and the Grand Banks area (outside Canadian Economic Exclusive Zone). Grey lines indicate depth contours at 50, 100, 200, 500, 1000, and 1500 m. Left image: Sponge biomass (Murillo et al. 2016a). Right image: Cold-water corals biomass and trawling fisheries footprint; L, Lightly–never trawled; M, moderately trawled; H, heavily trawled (Murillo et al. 2011).

Nutrient variability (see Table 1) in this region is closely related to climate forcing, such as NAO, and recent climate changes (Sherwood et al. 2011). Warm and nutrient-rich waters of the slope have persisted in this region over the last century in line with a shift in the NAO towards a predominantly positive NAO mode and away from the cooler nutrient-poor waters of the Labrador Sea Water. This study also suggested that this large regime shift between subpolar to subtropical water dominance, reflect a change in the source of nitrate used by the gorgonian *Primnoa resedaeformis*, with no not noticeably impact in its persistence over time (Sherwood et al. 2011).

Over millennial timescales, eastern Canada's deep-sea sponge grounds have also persisted despite variable environmental conditions. Geodiid sponge grounds off the Flemish Cap and Grand Banks have persisted for the last 130 kyr (Murillo et al. 2016a), despite large shifts in water mass structure alternating between the warmer North Atlantic Drift and the cooler Labrador Current. Notably, the strength of the Labrador Current increased during the deglaciation, and may explain the significant biogeographic range expansion of geodiids as observed from sediment cores in this region (Murillo et al.

2016a). In contrast, records of the solitary scleractinian corals *D. dianthus* from the Flemish region were absent over the last MIS 2, MIS 4 and MIS 6 (Hillaire-marcel et al. 2017). However, southern specimens off the New England region were also able to persist throughout the last 70 kyr, despite large deglacial intermediate water mass re-organisations over the Younger Dryas (Smith et al. 1997), and it has been suggested that this species generally seems to undergo population booms during such periods of abrupt oceanic change (Thiagarajan et al. 2013). Hillaire-marcel et al. (2017) concluded that observed corals to date in this region might be linked to high food supply from either production in the overlying water column or to particulate and dissolved organic carbon transported by an active Western Boundary Undercurrent.

Possible Impact of Changes to Ocean Circulation: Pathways and Transport

Knowledge of deep-sea connectivity still remains limited, from both the physical and biological perspective. Duration of larvae in the plankton (from days up to a year) and the depth of dispersal have been proved to be decisive for connectivity patterns. Broad distribution patterns and genetic homogeneity are commonly observed in deep-sea taxa, including those from highly patchy and specialized environments, such as hydrothermal vents and seamounts, which also have an elevated number of endemic species. The widespread connectivity in the deep Atlantic is (non-exclusively) related to the high dispersal capabilities of taxa, the large-scale larval dispersal by the AMOC, the use of stepping stone habitats to cross vast geographic distances and the ancient connections between ocean basins.

Connectivity of marine ecosystems is fundamental to survival, growth, spread, recovery from damage and adaptation to changing conditions, on ecological and evolutionary timescales (Burgess et al. 2014, Cowen & Sponaugle 2009, James et al. 2002). Empirical evidence shows also the benefits of connectivity information to conservation management (Olds et al. 2012, Planes et al. 2009). Knowledge of the characteristics of marine connectivity is rapidly expanding, with recent studies using seascape genetics approaches combining particle tracking in high resolution ocean models with state-of-the art genetic techniques (Foster et al. 2012, Teske et al. 2016, Truelove et al. 2017). Many populations in the deep-sea are spatially fragmented and vulnerable to damage from increasing exploitation of the resources. Thus, understanding the connectivity between the subpopulations is critical for spatial management (Cabral et al. 2016). But knowledge of deep-sea connectivity remains limited, from both

the physical and biological perspective. Direct evidence of deep-sea population connectivity, through tagging and tracking, remains almost unknown, but indirect estimates of connectivity can be constructed by using genetic methods, elemental fingerprinting or particle modeling.

A common indirect method of estimating connectivity is through tracking of virtual adults, juveniles or, more usually, larvae, within a hydrodynamic model, so called 'Lagrangian', individual-based models or particle tracking modelling. To date, in the deep-sea, this approach is limited to relatively few studies (Breusing et al. 2016, Fox et al. 2016, Lavelle et al. 2010, McGillicuddy et al. 2010, Yearsley & Sigwart 2011, Young et al. 2012). Such modelled connectivity and dispersal estimates are reliant on knowledge of life history traits - timing of spawning, larval behavior, and most importantly, effective pelagic larval duration (PLD). Knowledge of these biological parameters important to dispersal and connectivity in the deep-sea is sparse. (Bradbury et al. 2008) review estimates of marine dispersal, for fish species these estimates are primarily based on otolith microstructure and a connection between PLD and depth is found. For non-fish species, PLD was largely estimated from biogeography and population separation distances. (Hilário et al. 2015) provides an updated and thorough review of the challenges of estimating dispersal distances in the deep-sea. They found estimates of PLD for fewer than 100 species living below 200 m, over 80 % of these estimates are for species on sedimentary slopes, predominantly echinoderms. PLDs from a few days to over a year were found. Duration of larvae in the plankton (Bradbury et al. 2008) increase with depth, that maximize the chance of larvae finding suitable food-supply in a nutrient-poor and vast habitat and thus, explaining why deep-sea species are relatively widespread (Costello & Chaudhary 2017). Several studies of larval dispersal from deep-sea methane seeps (Arellano et al. 2014, Mullineaux et al. 2005) have included direct observation of larval position in the water column information that can be used to infer PLD and spawning times and to ground-truth larval dispersal models.

Beyond PLD, depth of dispersal is also a critical parameter for models of deep-sea connectivity, since current speeds and directions differ significantly with depth in an extensive water column. For instance, larvae of the deep-sea mussel *Bathymodiolus childressi* drifting in the upper water layers of the Gulf of Mexico can potentially seed most known seep metapopulations on the Atlantic continental margin, whereas larvae drifting demersally cannot (McVeigh et al. 2017). Indeed, Young et al. (2012) found that the majority of bathyal invertebrate larvae exported out of the Caribbean and Gulf of Mexico

are retained in natal geographic areas and not capable of trans-Atlantic dispersal. However, genetic studies on vesicomyid clams revealed these larvae may use stepping stone habitats, instead of long distance dispersal, to cross vast geographic distances (LaBella et al. 2017). In addition, Fox et al. (2016) showed how *L. pertusa* larvae following vertical swimming behavior traits predicted from observations in the laboratory (Larsson et al. 2014, Strömberg & Larsson 2017) may disperse much more widely than passive larvae. The occurrence of seep species of mollusks, crustaceans, and other taxonomic groups across the Atlantic Ocean suggest broad connectivity (Cordes et al. 2007, Olu-Le Roy et al. 2004). The AMOC can achieve large-scale larval dispersal across ecological timescales as infered in the cold-water-coral *L. pertusa* (Henry et al. 2014). Dispersal modelling, coupled with pelagic larval duration estimates and population genetics, has also recently (Breusing et al. 2016, Young et al. 2012) been used to predict the existence of further vent ecosystems between neighbouring known sites on the mid-Atlantic ridge. Strong population genetic divergence above and below 3000 m depth has been documented for multiple protobranch bivalves in the western North Atlantic, which is likely driven by larval behaviors, mortality and selective processes that limit dispersal and recruitment from some depths (Wilson & Mcmahon 2015).

Genetic variation is essential for the survival and adaptability of populations in a continuosly changing environment and that variability can inform us about potential dispersal, persistance and evolution of the population. Despite a burgeoning literature on deep-sea genetic connectivity, studies are geographically disparate, taxonomically diverse, plagued by low sample sizes, and poor in spatial and temporal replication, making it hard to draw general conclusions in the deep-sea (Miller & Gunasekera 2017). In general, marine populations were believed to be highly connected (Cowen et al. 2000), resulting in weak genetic structures. Some exceptions exist however at large biogeographic breaks, such as the one observed at the entrance of the Baltic sea (Johanneson & André 2006) or between the Mediterranean Sea and the Atlantic Ocean. The shifts in the distribution of polymorphism between the Atlantic and Mediterranean waters were long thought to be the consequence of the current physical barrier imposed by Gibraltar Straight. However, the barrier effects on the ability of larvae (and adults) to disperse were even more important during the glacial periods of the Quaternary. This disruption was shown by a meta-analysis on 70 mostly coastal studies, which coincide more often with the water mass transition occurring Eastern Gibraltar at the entrance of the Alboran Sea (Patarnello et al. 2007). As a

result, genetic discontinuities are often the consequence of a combination of causes including paleo-climatic changes, the present-day circulation and compositions of water masses along with species life history traits. Studies of *L. pertusa* (Le Goff-Vitry et al. 2004) showed moderate genetic differentiation over the eastern Atlantic continental margin, indicating that the majority of recruitment was localized, but some gene flow occurs over large distances. However, strong genetic differentiation was reported for this species among regions in the east and west Atlantic, with restricted gene flow at large scales (Morrison et al. 2011). These divergent results are likely to be related to the use of different genetic markers (Costantini et al. 2017). A similar differentiation between the Mediterranean and the Atlantic Ocean was also found for both *L. pertusa* and *M. oculata* (Boavida et al., under review). In contrast, when reducing the analysis to basin scales, a relative homogeneity of *L. pertusa* at the scale of the Atlantic was observed, whereas genetic differentiation of a similar habitat-forming cold-water-coral species, *M. oculata,* at basin and regional scales was evident (Boavida et al., under review). Gorgonians and black corals showed a wide geographic distribution of haplotypes reflecting a high dispersal capabilities and/or ancient connections between ocean basins (Herrera et al. 2012, Thoma et al. 2009), challenging the paradigm of high endemisms in the seamounts across North Atlantic basin-scale. However, dispersal ranges limited to a few kilometers seems to be common in the deep-sea invertebrates (Costantini et al. 2017). Other factors can also explain genetic divergence among populations. For instance, Zarduset al. (2006) found that genetic variability in the deep-sea bivalve *Deminucula atacellana* was much greater among populations at different depths within the same basin, than among those at similar depths but separated by thousands of kilometers. These results might be related to the characteristics of water masses at different depths.

Projections of Future Oceanographic Conditions in the North Atlantic

Climate models forecast that anthropogenic climate change will modify the Atlantic Ocean considerably by 2100 in terms of circulation patterns and fluxes, energy flow and water mass characteristics such as temperature, pH and oxygen (Sweetman et al. 2017). In particular, model forecast of future climate change predicts a 25 % slowing or even disappearing of the AMOC by the end of the 21st century (Schmittner 2005, Thornalley et al. 2018) owing to anthropogenic greenhouse gas emissions. Similar reorganisation of the AMOC occurred during the last glacial period associated with large and abrupt climatic changes (Henry et al. 2014; see also section 2.1). These long-term changes will

likely have strong ecosystem implications. Recent model simulations show increased supply of acidified waters to deep waters via AMOC compared with pre-industrial times, which is predicted to expose 75 % of CWCs below 1000 m in the North Atlantic to undersaturated waters as soon as 2060 (Perez et al. 2018). The SPG is a key feature to monitor, as changes in gyre strength, properties and transport through the Rockall Trough have profoundly affected the North Atlantic ecosystems including those in the deep-sea. However, reconstructions are lacking from key SPG locations, and a lack of palaeo-records to explore decadal variability in the deep components of the AMOC (e.g. the Nordic Overflows or Labrador Sea Water) makes it difficult to place modern observations and the exceptional 20th century slowdown of the AMOC in context.

The deep ocean is already experiencing important changes in physical and chemical variables due to warming, OA and deoxygenation, which are predicted to impact deep-sea ecosystems (Levin & Le Bris 2015). Reduction of the flux POC from the surface to the deep seafloor as a consequence of these altered conditions will also likely significantly impact benthic communities and deep-sea biodiversity (Ruhl & Smith 2004). In this section we review the present and predicted future conditions in the North Atlantic seafloor based on modelling exercises and the expected impacts in the deep-sea ecosystems, focusing on CWC reefs and gardens and sponge grounds and the Case Studies.

We simulated different projections for future environmental changes in the deep ocean used 3D fully coupled earth system models. Environmental variables of present-day and future seafloor conditions were compiled for the deep waters of the North Atlantic basin, from 32° N to 76° N and 20° W to 78° W. These variables included POC flux at 100 m depth (*epc100*, mg $C \cdot m^{-2} \cdot d^{-1}$), DO concentration at seafloor (ml l^{-1}), pH at seafloor, and potential temperature at seafloor (°C), which were downloaded from the Earth System Grid Federation (ESGF) Peer-to-Peer (P2P) enterprise system (https://esgf-node.llnl.gov). The *epc100* was converted to export POC flux (*epc*) at the seafloor using the Martin curve (Martin et al. 1987) following the equation: $epc = epc100*(water\ depth/export\ depth)^{-0.858}$, where the export depth was set to 100 m. Aragonite and calcite saturation state at seafloor were computed by dividing the carbonate ion concentration (mol m^{-3}) by the carbonate ion concentration ($mol \cdot m^{-3}$) for seawater in equilibrium with pure aragonite and calcite, respectively. Yearly means of these parameters were calculated for the periods 1951-2000 (historical simulation) and 2081 – 2100 (RCP8.5 or business-as-usual scenario) using the average values obtained from the Geophysical Fluid Dynamics Laboratory's

ESM 2G model (GFDL-ESM-2G; Dunne et al. 2012), the Institut Pierre Simon Laplace's CM6-MR model (IPSL-CM5A-MR; Dufresne et al. 2013) and Max Planck Institute's ESM-MR model (MPI-ESM-MR; Giorgetta et al. 2013) within the Coupled Models Intercomparison Project Phase 5 (CMIP5). Environmental variables were available at a 0.5° resolution and re-scaled to 3x3km cell size.

Here we show present day (1951 – 2000) and predicted future (2080 – 2100) values of the different environmental parameters in the North Atlantic, as well as changes measured as the difference between those two periods in absolute values and proportion of changes. We also highlighted those areas in the North Atlantic predicted to attain critical environmental parameters, which may compromise growth and survival of benthic ecosystems. Critical values were: reduction of pH greater than 0.3, values of aragonite and calcite saturation <1; reduction of POC flux greater than 40% and 50%; and increase in temperature greater than 1°C and 2°C. Areas with dissolved oxygen reductions greater than 5% are also shown. Cumulative critical changes were measured by the number of parameters at a certain cell attaining critical values under future climate conditions.

Table 1. Present-day (year 2000) and predicted future (year 2100) values [range] of the main water masses and factors influencing deep-sea biodiversity in the North Atlantic at slope and bathyal regions (200 – 3000 m). Δ indicates change between present-day and predicted future conditions.

	2000		**2100**		**Δ**	
T (°C)	5.02	[0.50, 18.23]	5.78	[1.80, 20.76]	0.76	[-0.93, 4.29]
POC (mg C m^{-2} day^{-1})	9.12	[0.12, 77.86]	6.61	[0.28, 59.95]	-2.51	[-36.60, 2.71]
pH	8.07	[7.76, 8.14]	7.88	[7.46, 8.02]	-0.19	[-0.43, -0.01]
Aragonite	1.41	[0.57, 2.98]	0.96	[0.55, 2.09]	-0.45	[-1.36, 0]
Calcite	2.31	[0.97, 4.63]	1.57	[0.95, 3.19]	-0.74	[-2.15, -0.01]
DO (ml l^{-1})	5.94	[2.43, 7.06]	5.76	[2.36, 7.28]	-0.17	[-0.61, 0.41]

Table 2. Present-day (year 2000) and predicted future (year 2100) values [range] of the main water masses and factors influencing deep-sea biodiversity in the North Atlantic at abyssal regions (>3000 m). Δ indicates change between present-day and predicted future conditions.

	2000		2100		Δ	
T (°C)	3.78	[1.63, 11.63]	3.77	[1.69, 13.32]	-0.01	[-0.78, 1.69]
POC (mg C m^{-2} day^{-1})	1.60	[0.18, 34.41]	1.38	[0.15, 30.22]	-0.56	[-10.86, 0.97]
pH	7.98	[7.91, 8.10]	7.94	[7.90, 8.02]	-0.04	[-0.17, -0.01]
Aragonite	0.75	[0.49, 1.85]	0.69	[0.48, 1.46]	-0.06	[-0.51, 0.01]
Calcite	1.26	[0.80, 2.92]	1.15	[0.83, 2.24]	-0.11	[-0.82, 0.03]
DO (ml l^{-1})	5.37	[0.54, 4.26]	5.38	[4.47, 6.55]	0.01	[-0.61, 0.22]

Future Ocean Temperatures

Global warming due to the influx of anthropogenic carbon dioxide to the atmosphere is increasing global ocean temperatures both in surface layer and the deep ocean (Levitus et al. 2012, Purkey & Johnson 2010). Average global temperature of the upper ocean (0 – 2000 m) has warmed approximately 0.09°C between 1955 and 2010 (Levitus et al. 2012). Recent modelling efforts predicted greatest temperature increases at bathyal depths in the Pacific (3.6°C), Atlantic (4.4°C) and Arctic Oceans (3.7°C) by 2100 (Mora et al. 2013, Sweetman et al. 2017) and changes of ~1°C at the abyssal seafloor in the North Atlantic, Southern and Arctic Oceans (Sweetman et al. 2017). Modelling results show that the present-day values of seafloor temperature in the North Atlantic average 5.02°C bathyal areas and 3.78°C in the abyss (Fig. 20, Table 1-2). The seafloor temperature values by 2100 were predicted to increase to 5.78°C on average in bathyal areas but with no major changes in the abyss. Most areas of the North Atlantic will experience an increase in temperature greater than 1°C (Flemish Cap, Rockall Bank, Porcupine Seabight, Mingulay Reef and the Alboran Sea) or 2°C (Cape Hatteras, Labrador Sea, Davis Strait, Denmark Strait), but mostly below 1,000m depth (Fig. 20). However, a large bathyal area of the North Atlantic Ocean, between the Azores and Iceland with an extension to the Davis Strait, was

predicted to have seafloor temperatures decreased by 0.7°C. This is one of the few areas in the world's oceans where seafloor temperatures are predicted to decrease.

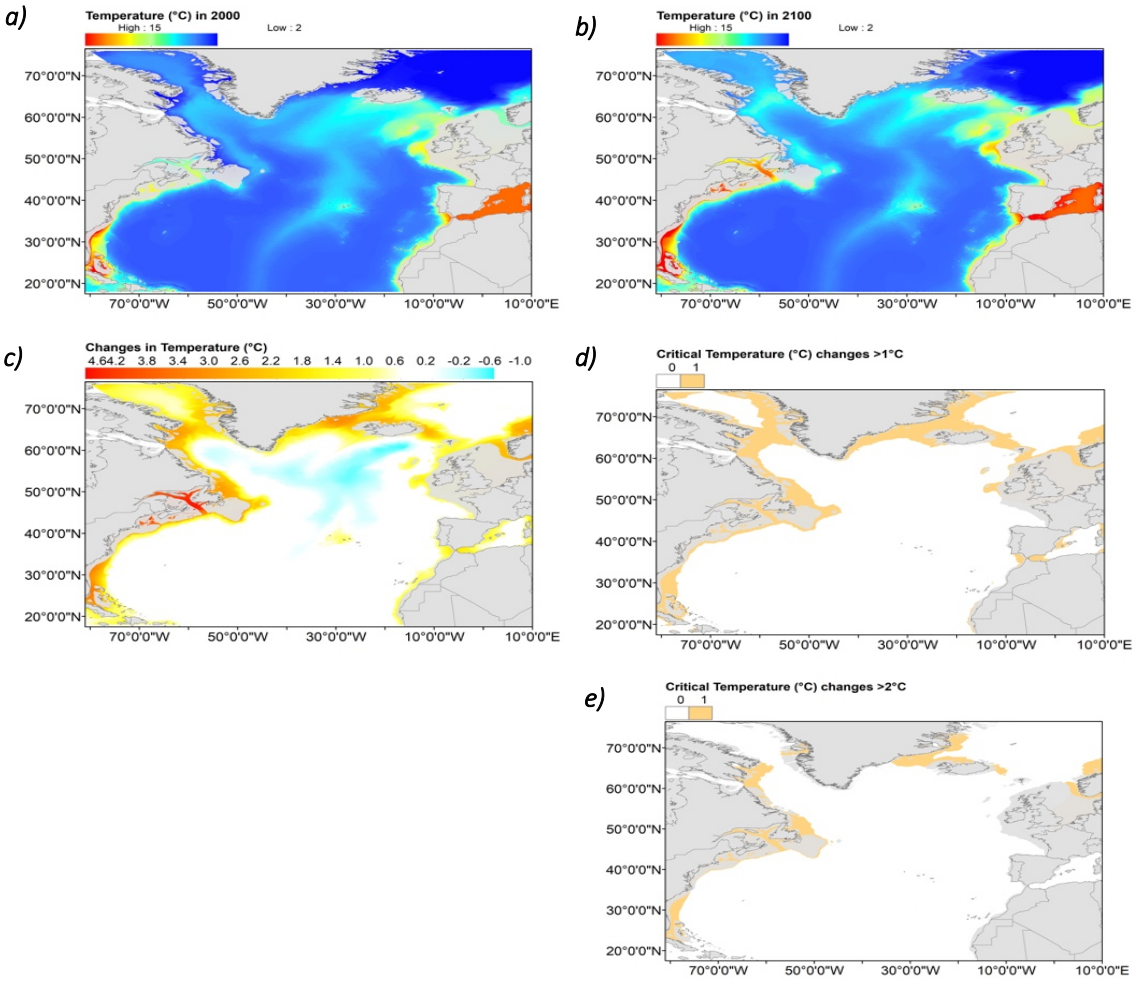

Figure 20. Temperature values at the seafloor in the North Atlantic Ocean. a) Present-day, b) predicted future, c) changes in temperature as the difference between present-day and modelled conditions by 2100, areas with critical changes in temperature of d) increment > 1°C, e) increment >2°C.

Future particulate organic carbon (POC) flux

With the exception of chemosynthetic habitats (e.g.,hydrothermal vents and cold seeps), deep-sea ecosystems largely depend on the export POC flux produced in the photic zone of the water column as a food source (McClain et al. 2012). Enhanced warming of the upper ocean, stratification, and ocean acidification, reduces the export flux and quality of POC that reaches the seafloor (Jones et al. 2014,

Smith et al. 2008, Sweetman et al. 2017). Modelling studies pointed the North Atlantic as one of the most impacted regions in the world´s oceans, with predicted reductions up to 40 % in POC export flux by 2100 in some areas (Jones et al. 2014, Sweetman et al. 2017).

The modelling predictions show that with the exception of the Azores and the Reykjanes Ridge, most North Atlantic deep-sea seafloor shallower than 3000 m is not currently food limited (POC flux >10 mg C m^{-2} day^{-1}). Present-day values of POC flux averaged 9.12 mg C m^{-2} day^{-1} (range 0.12 – 77.86) in the bathyal areas and 1.60 mg C m^{-2} day^{-1} (range 0.18 – 34.41) in the abyss (Table 2-3, Fig. 21).

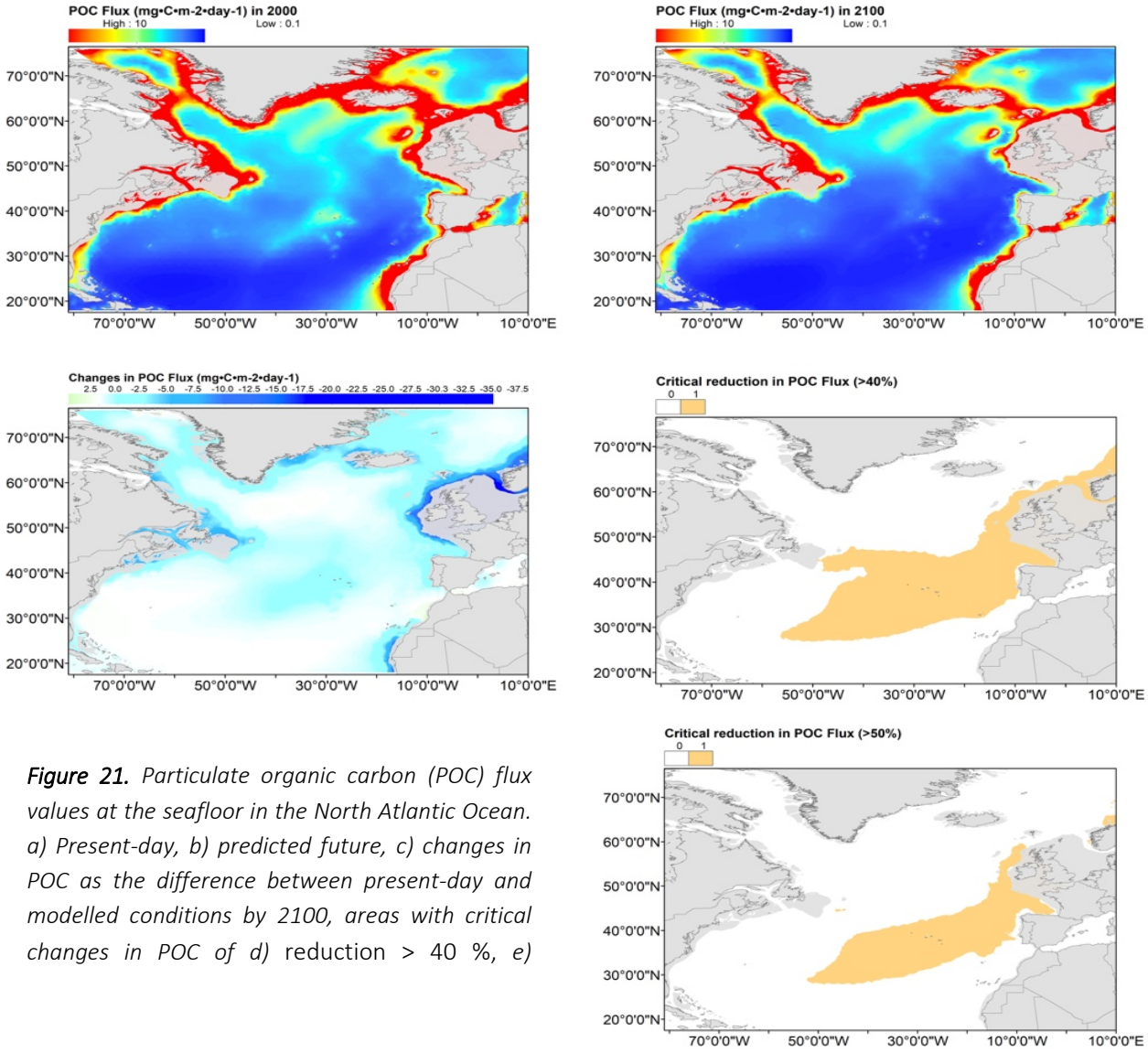

Figure 21. Particulate organic carbon (POC) flux values at the seafloor in the North Atlantic Ocean. a) Present-day, b) predicted future, c) changes in POC as the difference between present-day and modelled conditions by 2100, areas with critical changes in POC of d) reduction > 40 %, *e)*

In general, food availability in the deep-sea floor was predicted to decrease under future water masses conditions, with higher absolute changes occurring in the continental margins of the UK and Ireland, Iceland, Greenland and Eastern Canada. However, a critical decrease in POC flux (>50 % reduction) by 2100 was predicted to occur in the central-eastern Atlantic, mostly in a large area of the Azores, Bay of Biscay, Porcupine Seabight, and the Mingulay Reef (Fig. 21). The areas north and west of the Scotland including the Faroe Shetland Channel, and the southern part of the Flemish Cap will experience a 40 % reduction in food availability by 2100.

Future Ocean Carbonate Chemistry

The deep North Atlantic is the most alkaline seafloor in the world's ocean (Sweetman et al. 2017). Present-day values of pH averaged 8.07 (range 7.76 – 8.14) in bathyal areas (200 – 3000m) and 7.98 (range 7.91 – 8.10) in the abyss (Fig. 22).

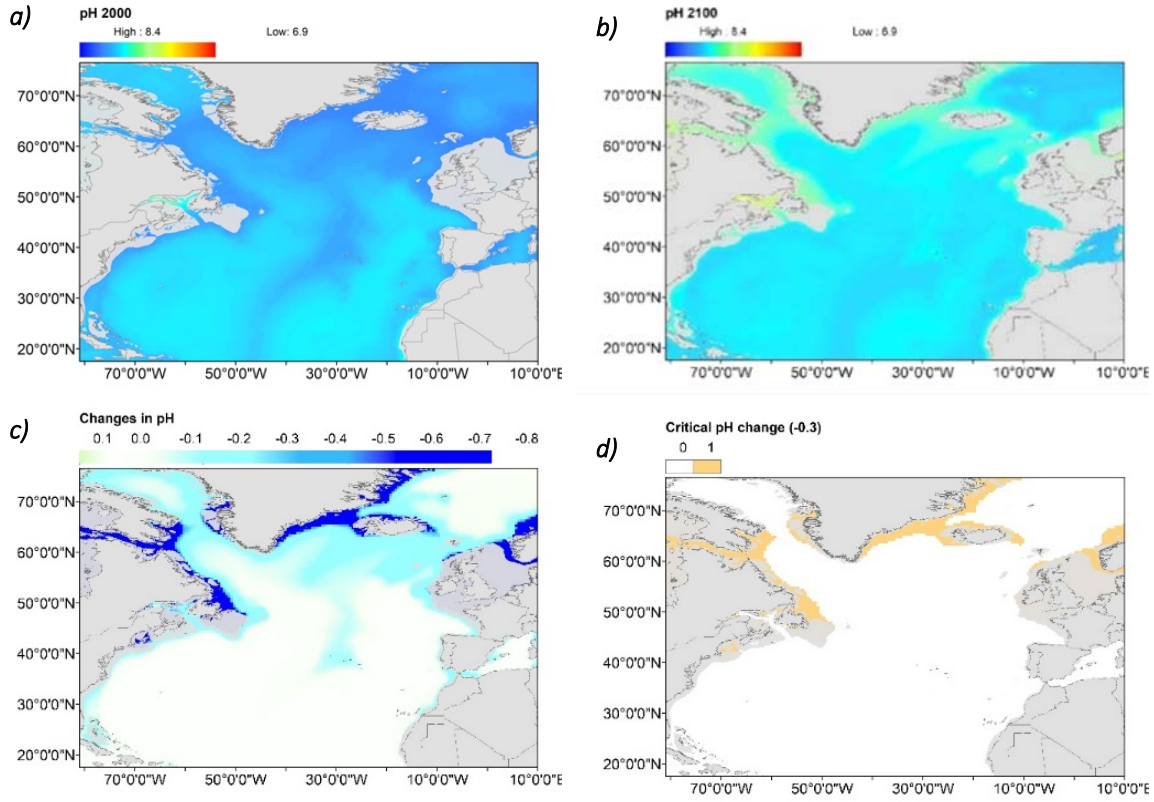

Figure 22. pH values at the seafloor in the North Atlantic Ocean. a) Present-day, b) predicted future, c) changes in pH as the difference between present-day and modelled conditions by 2100, d) areas with critical changes in pH values (reduction > 0.3).

However, absorption of anthropogenic CO_2 by the oceans is reducing seawater pH (-0.12 units since the preindustrial time) and the saturation of calcium carbonate ($CaCO_3$), a process termed ocean acidification (Caldeira & Wickett 2003, Orr et al. 2005). Model predictions indicate that pH at the seafloor will likely decrease to an average of 7.88 (7.46 – 8.02) and 7.94 (7.90 – 8.02) in abyssal and bathyal areas by 2100, respectively (Table 2-3).

Some areas of the North Atlantic, especially at higher latitudes, will experience the greatest pH reductions (> 0.3 units) as a result of the subduction of high-CO_2 waters via thermohaline circulation (Gehlen et al. 2014, Perez et al. 2018, Sweetman et al. 2017). This will be mostly the case in waters shallower than 1000 m depth in the northwest Atlantic, including the Labrador Sea (north of Newfoundland), Davis Strait, and Western Greenland. Notable reductions in pH (> 0.5 units) were also predicted in waters shallower than 1000 m in eastern Greenland, around Iceland and in Norwegian waters (Fig. 22). The average pH conditions at the Mingulay Reef were predicted to decrease by 0.38 units, although the entire reef complex is actually shallower than 200 m depth and experiences daily/tidal excursions in pH of up to 0.16 pH units already (Findlay et al. 2014). On the Reykjanes Ridge, Rockall Bank, in the Faroe Shetland Channel, Bay of Biscay, and in the Alboran Sea, average pH conditions were predicted to decrease by around 0.25, whereas in the Porcupine Seabight and the Azores may decrease by 0.15 units. Areas deeper than 3000 m will experience a reduction in pH from 0.01 to 0.17 units.

Model projections also reported large decreases in the calcium carbonate saturation state (Ω) in seawater throughout the world (Orr et al. 2005) with severe changes in the North Atlantic (Perez et al. 2018). Carbonate saturation in seawater is a critical parameter for the precipitation (in saturated waters, $\Omega > 1$) and dissolution (in unsaturated waters, $\Omega < 1$) of calcium carbonate mineral forms (i.e. aragonite, calcite). Solubility of calcium carbonate increases at higher pressure and lower temperature, which means that Ω decreases with increasing depths and at higher latitudes. As subsurface saturation state declines the depth separating undersaturated from oversaturated waters moves upwards, i.e. shoals. Recent model simulations showed that the present rate of supply of acidified waters to the deep Atlantic could cause the ASH to shoal by 1000 – 1700 m in the subpolar North Atlantic within the next three decades (Perez et al. 2018).

Model simulations show that the present-day Ω aragonite in the seafloor of the North Atlantic varied greatly with depth (Fig. 23). Seafloor conditions are in general supersaturated shallower than 3000 m and undersaturated in the abyssal areas (Table 3). However, Ω aragonite is expected to change significantly by 2100, decreasing by 32 % in areas shallower than 3000 m and by 8 % in the bathyal seafloor and thus, most of the deep North Atlantic will became undersaturated in aragonite (Fig. 23). ASH will shoal by approximately 800 m to depths around 3000 m in the western North Atlantic between Cape Hatteras and Cape Cod and in the Eastern Atlantic nearby the Alboran Sea, by approximately 1500 m to depths of 2000 m in the Azores region of the central North Atlantic, Bay of Biscay, and in the Porcupine Seabight.

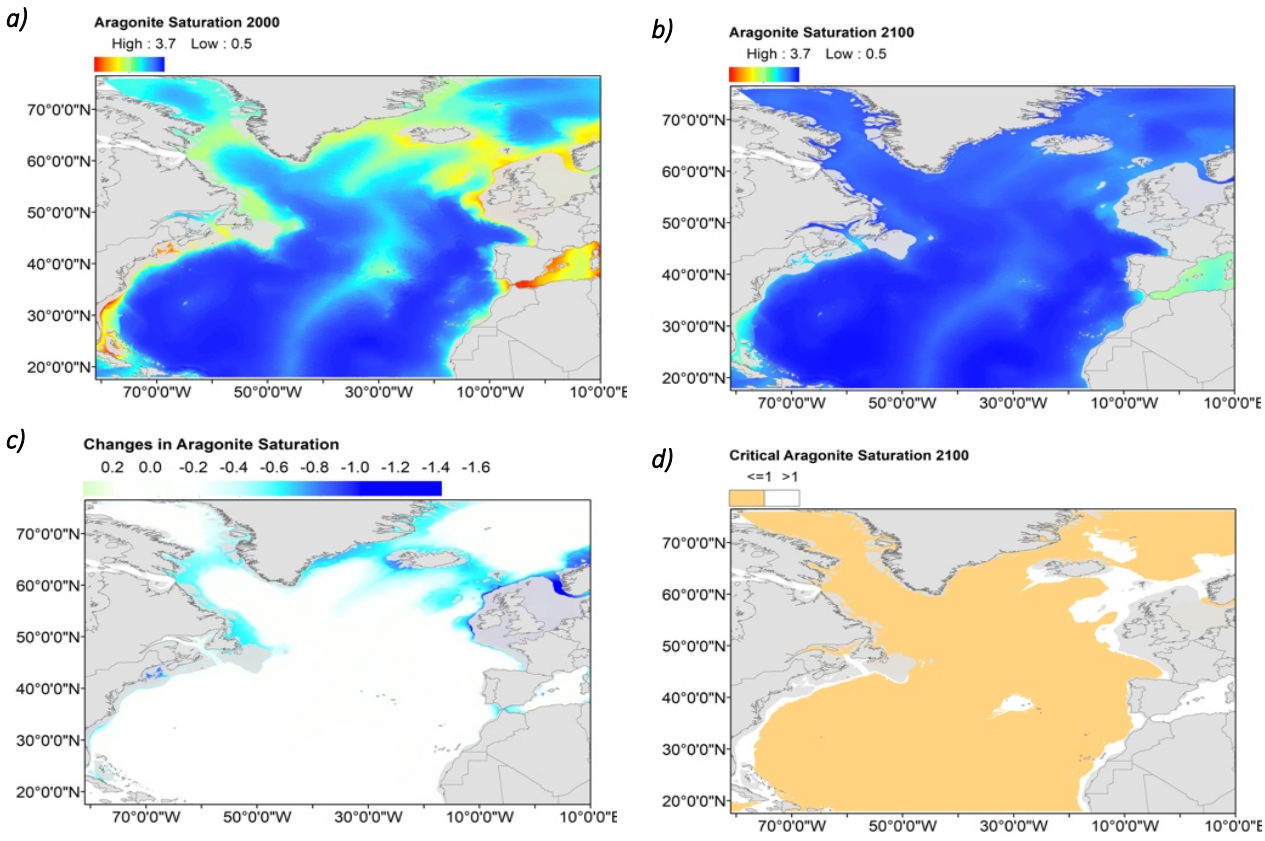

Figure 23. Aragonite saturation values at the seafloor in the North Atlantic Ocean. a) Present-day, b) predicted future, c) changes in pH as the difference between present-day and modelled conditions by 2100, d) areas with critical changes in aragonite saturation (< 1).

In the Reykjanes Ridge, the ASH will shoal by approximately 2500 m to 1000 m depth while in Labrador Sea, Davis Strait, and Western Greenland it will shoal by approximately 3000 m to depths as shallow as 200 m. Most of the Rockall Bank and the Mingulay Reef were predicted to maintain Ω aragonite > 1, while areas deeper than 3000 m will experience smaller changes.

Most of the seafloor of the North Atlantic is also currently supersaturated in calcite, with the exception of the abyssal areas below 5000 m (Fig. 24). The saturation levels were predicted to decrease in average by 32 % and 8 % for the bathyal and abyssal areas respectively, but most of the seafloor, including all the case study regions, will remain supersaturated. Calcite saturation horizon will shoal to 4500 m depth in the southernmost parts of the North Atlantic (Fig. 24).

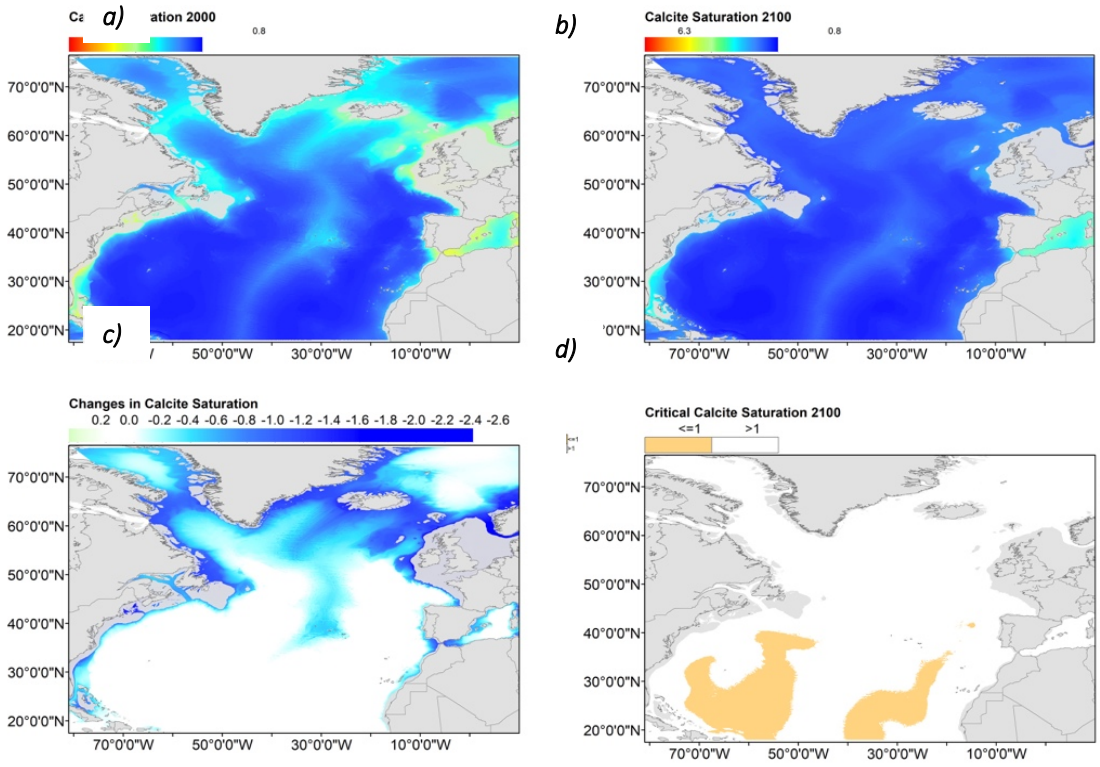

Figure 24. Calcite saturation values at the seafloor in the North Atlantic Ocean. a) Present-day, b) predicted future, c) changes in pH as the difference between present-day and modelled conditions by 2100, d) areas with critical changes in calcite saturation (< 1).

Future Oxygen Concentrations

Ocean warming also causes the loss of DO in ocean waters (deoxygenation), through reduced solubility, intensified biological respiration, and increased stratification of water masses (Keeling et al. 2010, Levin 2018). The open ocean has already lost on average 2 % of its oxygen content since the pre-industrial era, with the greatest reductions in intermediate waters (100 – 1000 m; (Bopp et al. 2013, Levin 2018, Stramma et al. 2010).

Recent model simulations predict decline in bottom-water oxygenation of 0.03 – 0.05 ml l^{-1} (0.7 % – 3.7 %) in bathyal seafloor habitats in the North Pacific, North Atlantic, Arctic and Southern Oceans (Levin 2018, Sweetman et al. 2017). In addition, expansion of OMZ present in along the continental margins of the East Pacific, Southeast Atlantic, West Pacific and North Indian Oceans are also expected, with severe consequences to benthic habitats on the fringes of these areas (Sweetman et al. 2017). Model simulations for the North Atlantic show that most of the seafloor below 200 m is currently well oxygenated, particularly from the West Shetlands to the Davies Strait. Present DO values averaged 5.94 ml l^{-1} in the bathyal regions and 5.37 ml l^{-1} (Fig. 25, Table 1).

Seafloor DO values were predicted to slightly decrease by 2100 in both abyssal and bathyal zones (Fig. 25, Table 1-2).

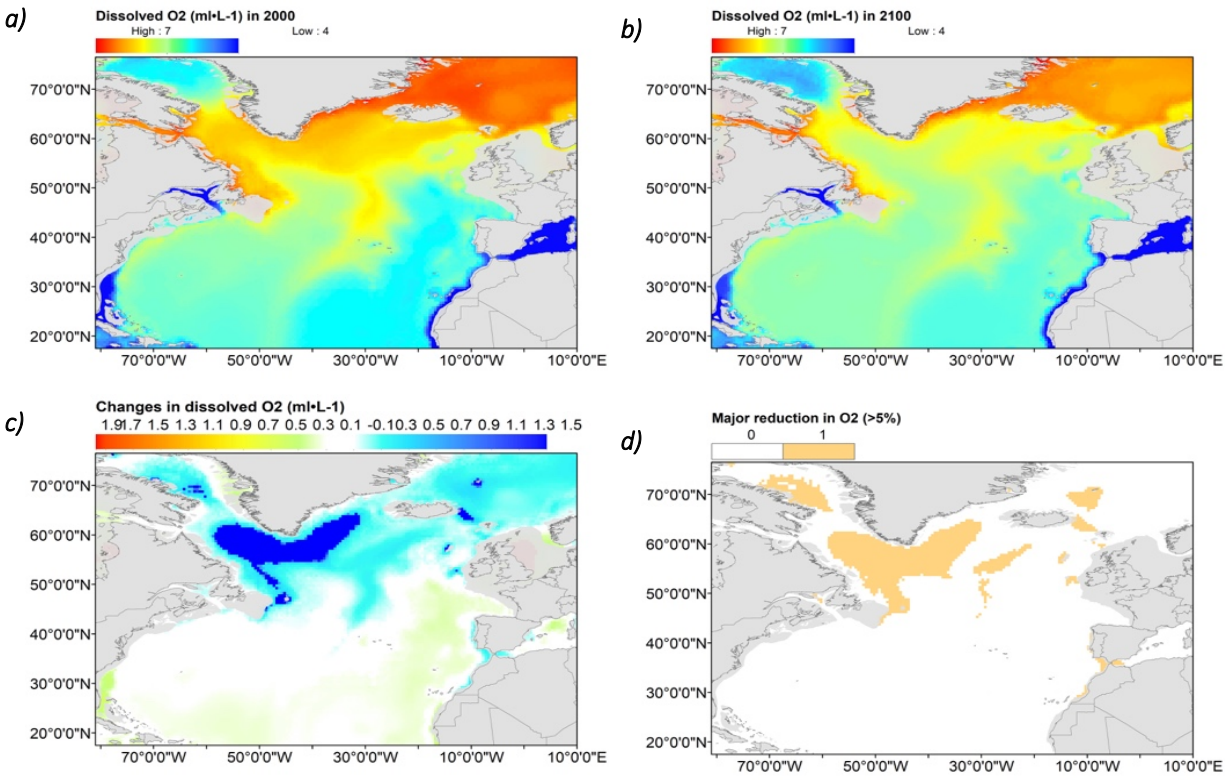

Figure 25. Dissolved oxygen values at the seafloor in the North Atlantic Ocean. a) Present-day, b) predicted future, c) changes in pH as the difference between present-day and modelled conditions by 2100, d) areas with critical changes in dissolved oxygen (reduction > 5 %).

A maximum of a 5 – 10 % decrease of DO is predicted to occur around Labrador Sea, Davis Strait, and Western Greenland, the Rockall Bank, and in the Porcupine Seabight. However, no area of the deep North Atlantic will experience moderately (~1.5 ml l^{-1}) or severely (< 0.5 ml l^{-1}) hypoxic conditions in the future.

VME Case Studies Most at Risk of Multiple Stressors by 2100

Cumulative critical changes in deep-sea conditions of the North Atlantic Ocean by the year 2100 (Fig. 26) were assumed to be (1) aragonite and (2) calcite saturation levels below 1, (3) pH reductions greater than 0.3, (4) POC flux reductions greater than 40 or 50 %, and (5) temperature increases greater than 1 or 2°C. Concentrations of DO will still not likely achieve hypoxic conditions values below 1.5 ml l^{-1} in 2100. The Labrador Sea, Davis Strait and Western Greenland will experience critical changes of pH, aragonite and temperature. The Bay of Biscay region will experience changes in aragonite, pH, and POC flux.

Several regions will also experience critical changes of at least two parameters. A large area of the Azores and a small portion of the Rockall Bank are expected to present critical changes in aragonite and POC flux, while western North Atlantic from Cape Hatteras north to Cape Cod, and the Flemish Cap will face critical changes in aragonite or temperature. By contrast, many regions will only present critical changes in at least one of the studied factors such as, Reykjanes Ridge (aragonite), Porcupine Seabight (aragonite or POC flux), the Mingulay Reef (pH or POC flux), Faroe Shetland Channel (pH), and the Alboran Sea (aragonite).

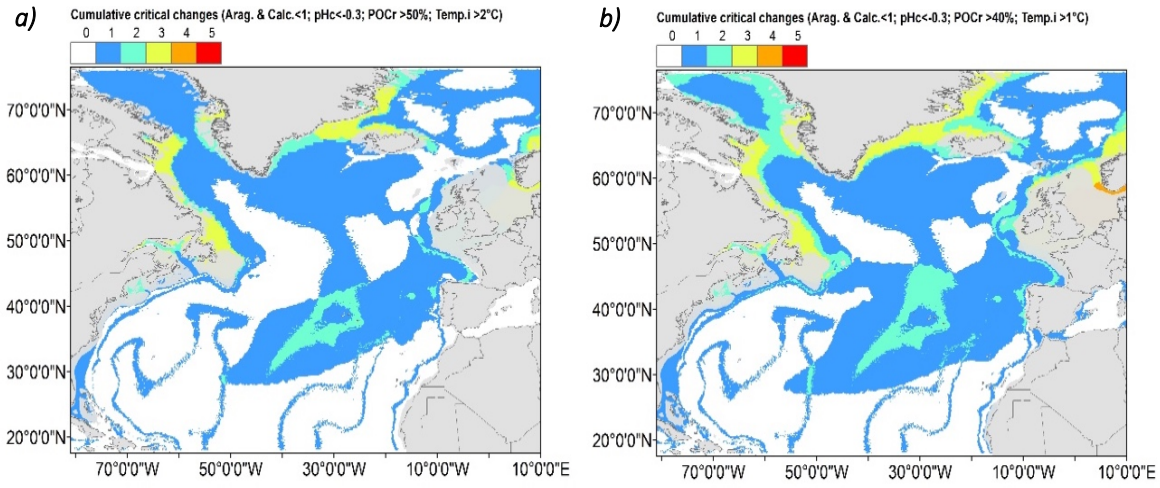

Figure 26. Predicted cumulative critical changes in seafloor conditions in the North Atlantic Ocean in the future (2100). Critical conditions include a) aragonite and calcite saturation levels < 1, pH reduction > 0.3, POC flux reduction > 50 % (or b) 40 %), and temperature increase > 2°C (or b) 1°C). Dissolved oxygen will not likely achieve hypoxic conditions values < 1.5 ml l^{-1} in 2100.

Model predictions indicated that the deep seafloor in high latitudes of the North Atlantic is likely to experience warming of 2°C. Despite many CWC reefs occurring in these regions, temperature is not expected to exceed the range (4 – 12°C) where *L. pertusa* is generally found in the North Atlantic (Gass & Roberts 2006, Roberts 2009). Mortality of *L. pertusa* has been reported to occur at temperatures > 14°C (Brooke et al. 2013, Lunden et al. 2014).

CWC are able to calcify and growth under conditions 3 – 4°C warmer, even when combined with acidified waters (Büscher et al. 2017, Hennige et al. 2014). However, the energetic cost of these process on such conditions may diminish other physiological processes or prevent to sustain growth over long-term periods (Dodds et al. 2007, Hennige et al. 2015), particularly when combined with aragonite

undersaturation and low food conditions. Thus, warming is more likely to impact CWC living close to their upper temperature limit of physiological tolerance (e.g. Gulf of Mexico; Brooke et al. 2013, Lunden et al. 2014; and Mediterranean Sea; Gori et al. 2016).

The predicted shoaling of the ASH is expected to lead to a loss of suitable habitat for slow-growing reef-forming CWC species (Davies & Guinotte 2011, Perez et al. 2018), which are commonly found at ASH depth at present (Davies & Guinotte 2011, Guinotte et al. 2006). According to model simulations, during the pre-industrial period 87 % of CWC reefs were surrounded by aragonite oversaturated waters, while projections for 2100 suggest that around 73 % of these reefs will suffer from undersaturated waters (Guinotte et al. 2006, Zheng & Cao 2014). CWC in Northeast Atlantic are predicted to be particularly vulnerable to ocean acidification, with 75 % of cold-water below 1000 m being exposed to undersaturated waters by 2060 under the "business as usual" RCP 8.5 scenario (Perez et al. 2018). According to our model predictions, areas within the Reykjanes Ridge below 1000 m and Davis Strait and western Greenland as shallow as 200 m depth may be exposed to corrosive waters in the future. Despite the physiologically resilience of CWCs to ocean acidification, the long-term survival of reefs may be impaired by the chemical dissolution and biological erosion of the unprotected tissue of the reef framework exposed to corrosive (i.e. aragonite understaturated) waters (Hennige et al., 2015; Schönberg et al., 2017). The balance between construction and erosion processes ultimately determines if the reef will grow or recede (Schönberg et al., 2017). Shifts towards net negative balances may lead to loss of reef growth potential, reef structural collapse, and diminished ecosystem service provisioning such as nutrient cycling, carbon storage and habitat provision, and severe consequences to the loss of biodiversity associated to these ecosystems.

These shoaling and reduction on habitat suitability for *L. pertusa* in the NW Atlantic due to ocean acidification can have important consequences to the connectivity pathway of *L. pertusa* populations between the NW and NE Atlantic (Kenchington et al. 2014). In contrast, Mingulay Reef and most of the Rockall Bank above 200 m will not be subjected to corrosive waters, thus providing a refuge for *Lophelia* reefs in the NE Atlantic. Protection of these areas within MPAs where trawling is banned provides additional support to ensure long-term survival of these habitats under regional predictions of 85 % CWC loss due to ASH shoaling for this area of the NE Atlantic (Jackson et al. 2014). Coral ecosystems in other ATLAS Case Studies in more southerly locations in the North Atlantic, including the western North

Atlantic below Cape Cod, the central North Atlantic region of the Azores and the Alboran Sea, and the Bay of Biscay, are located above the ASH shoaling depths predicted for 2100 and will thus be protected from corrosive waters. Coral gardens composed mainly of calcitic octocorals in the present case studies will also not be exposed to corrosive undersaturated conditions according to model predictions. However, the resilience of CWCs to warming and acidification may be reduced in areas with limited food as CWCs require extra energy for calcification (McCulloch et al. 2012b), compromising coral metabolism and even the survival of corals (Maier et al. 2016).

The model forecasting suggests large decreases in POC fluxes in areas where shoaling of the ASH and warming is also expected, including Iceland, Greenland and Eastern Canada, where the northernmost populations of *L. pertusa* are found, thus reducing the biogeographic distribution of this keystone habitat-structuring VME. POC reductions can have extreme effects in areas such as the Azores and Porcupine Seabight, where food availability is already limited (Jones et al. 2014). In particular, seamount features, such as many seamounts in the northern Mid-Atlantic Ridge, are projected to experience large declines in POC fluxes and benthic biomass (Jones et al. 2014). Global projections of changes POC export associated with other climate change effects suggest CWC ecosystems will suffer the greatest declines in benthic biomass and biodiversity and as a consequence, in ecological functioning and services provided (Jones et al. 2014).

References

Allen JA, Sanders HL. 1996. The zoogeography, diversity and origin of the deep-sea protobranch bivalves of the Atlantic: the epilogue. Prog. Oceanogr. 38:95–153

Altuna Á. 2017. Deep-Water Scleractinian Corals (Cnidaria: Anthozoa) from 2010-2011 INDEMARES Expeditions to the Galicia Bank (Spain, Northeast Atlantic). Zootaxa. 4353:257–93

Álvarez-Pérez G, Busquets P, De Mol B, Sandoval NG, Canals M, Casamor JL. 2005. Deep-water coral ocurrences in the Strait of Gibraltar. In Cold-Water Corals and Ecosystems, eds. A Freiwald, JM Roberts, pp. 207–21. Springer

Alves MLGR, Colin de Verdière A. 1999. Instability Dynamics of a Subtropical Jet and Applications to the Azores Front Current System: Eddy-Driven Mean Flow. J. Phys. Oceanogr. 29(5):837–64

Amorim P, Perán AD, Pham CK, Juliano M, Cardigos F, et al. 2017. Overview of the Ocean Climatology and Its Variability in the Azores Region of the North Atlantic Including Environmental Characteristics at the Seabed. Front. Mar. Sci. 4(56)

Arellano SM, Van Gaest AL, Johnson SB, Vrijenhoek RC, Youn CM. 2014. Larvae from deep-sea methane seeps disperse in surface waters. Proc. R. Soc. London B Biol. Sci. 281(1786):1–8

Arnaud-Haond S, Van den Beld IMJ, Becheler R, Orejas C, Menot L, et al. 2017. Two "pillars" of cold-water coral reefs along Atlantic European margins: Prevalent association of *Madrepora oculata* with *Lophelia pertusa*, from reef to colony scale. Deep. Res. Part II Top. Stud. Oceanogr. 145:110–19

Baker E, Beazley L, Mcmillan A, Rowsell J, Kenchington E. 2018. Epibenthic megafauna of the disko fan conservation area in the Davis Strait (Eastern Arctic) identified from in situ benthic image transects. Canadian Technical Report of Fisheries and Aquatic Sciences 3272, pp. 391

Bashmachnikov I, Lafon V, Martins A. 2004. SST Stationary Anomalies in the Azores Region. Proceedings of Remote Sensing of the Ocean and Sea Ice. 5569

Beaird NL, Rhines PB, Eriksen CC. 2013. Overflow Waters at the Iceland–Faroe Ridge Observed in Multiyear Seaglider Surveys. J. Phys. Oceanogr. 43(11):2334–51

Beazley L, Kenchington E, Yashayaev I, Murillo FJ. 2015. Drivers of epibenthic megafaunal composition in the sponge grounds of the Sackville Spur, northwest Atlantic. Deep. Res. Part I Oceanogr. Res. 98:102–14

Beazley LI, Kenchington EL, Murillo FJ, Sacau M. 2013. Deep-sea sponge grounds enhance diversity and abundance of epibenthic megafauna in the Northwest Atlantic. ICES J. Mar. Sci. 70:1471–90

Bergstad OA, Menezes G, Høines ÅS. 2008. Demersal fish on a mid-ocean ridge: Distribution patterns and structuring factors. Deep. Res. Part II Top. Stud. Oceanogr. 55(1):185–202

Bergstad OA, Menezes GMM, Høines ÅS, Gordon JDM, Galbraith JK. 2012. Patterns of distribution of deepwater demersal fishes of the North Atlantic mid-ocean ridge, continental slopes, islands and seamounts. Deep. Res. Part I Oceanogr. Res. 61:74–83

Berx B, Payne MR. 2017. The Sub-Polar Gyre Index - A community data set for application in fisheries and environment research. Earth Syst. Sci. Data. 9(1):259–66

Blair NE, Plaia GR, Boehme SE, DeMaster DJ, Levin LA. 1994. The remineralization of organic carbon on the North Carolina continental slope. Deep. Res. Part II Top. Stud. Oceanogr. 41(4):755–66

Blake J, Hecker B, F. Grassle J, Maciolek N, Brown B. 1985. Study of biological processes on the US South Atlantic slope and rise. Phase 1: Benthic characterization. Volume 2. Technical Report, U.S. Department of the Interior, Minerals Management Service. Contract No. 14-12-0001-30064, pp. 415

Blindheim J. 1990. Arctic intermediate water in the Norwegian sea. Deep. Res. Part I Oceanogr. Res. 37(9):1475–89

Boavida JRH, Becheler R, Choquet M, Frank N, Taviani M, et al. Out of the Mediterranean? Post-glacial colonisation pathways varied among cold-water coral species (under review)

Bongiorni L, Mea M, Gambi C, Pusceddu A, Taviani M, Danovaro R. 2010. Deep-water Scleractinian corals promote higher biodiversity in deep-sea meiofaunal assemblages along continental margins. Biol. Conserv. 143:1687–1700

Bopp L, Resplandy L, Orr JC, Doney SC, Dunne JP, et al. 2013. Multiple stressors of ocean ecosystems in the 21st century: Projections with CMIP5 models. Biogeosciences. 10(10):6225–45

Bourillet J-F, Zaragosi S, Mulder T. 2006. The French Atlantic margin and deep-sea submarine systems. Geo-Marine Lett. 26(6):311–15

Bower AS, Le Cann B, Rossby T, Zenk W, Gould J, et al. 2002. Directly measured mid-depth circulation in the northeastern North Atlantic Ocean. Nature. 419:603-607

Bower AS, Lozier MS, Gary SF, Böning CW. 2009. Interior pathways of the North Atlantic meridional overturning circulation. Nature. 459:243-247

Bozec A, Lozier MS, Chassignet EP, Halliwell GR. 2011. On the variability of the Mediterranean Outflow Water in the North Atlantic from 1948 to 2006. J. Geophys. Res. Ocean. 116:C09033

Bradbury IR, Laurel B, Snelgrove PVR, Bentzen P, Campana SE. 2008. Global patterns in marine dispersal estimates: The influence of geography, taxonomic category and life history. Proc. R. Soc. London B Biol. Sci. 275(1644):1803–9

Braga-Henriques A, Porteiro FM, Ribeiro PA, De Matos V, Sampaio Í, et al. 2013. Diversity, distribution and spatial structure of the cold-water coral fauna of the Azores (NE Atlantic). Biogeosciences. 10(6):4009–36

Brandão MC, Garcia CAE, Freire AS, Watling L, Guinotte J, et al. 2015. Large-scale spatial variability of decapod and stomatopod larvae along the South Brazil Shelf. Cont. Shelf Res. 107:11–23

Breusing C, Biastoch A, Drews A, Metaxas A, Jollivet D, et al. 2016. Biophysical and Population Genetic Models Predict the Presence of "Phantom" Stepping Stones Connecting Mid-Atlantic Ridge Vent Ecosystems. Curr. Biol. 26(17):2257–67

Brøndsted HV. 1933. The Godthaab Expedition 1928. Porifera. Meddelelser om Gronl. 79:1–25

Brooke S, Ross SW, Bane JM, Seim HE, Young CM. 2013. Temperature tolerance of the deep-sea coral *Lophelia pertusa* from the southeastern United States. Deep. Res. Part II Top. Stud. Oceanogr. 92:240–48

Brothers DS, ten Brink US, Andrews BD, Chaytor JD. 2013. Geomorphic characterization of the U.S. Atlantic continental margin. Mar. Geol. 338:46–63

Bryan TL, Metaxas A. 2006. Distribution of deep-water corals along the North American continental margins: Relationships with environmental factors. Deep. Res. Part I Oceanogr. Res. 53(12):1865–79

Buhl-Mortensen L, Hodnesdal H, Thorsnes T. 2015a. The Norwegian Sea Floor – New Knowledge from MAREANO for Ecosystem-Based Management. MAREANO 2015

Buhl-Mortensen L, Mortensen PB. 2004. Symbiosis in Deep-Water Corals. Symbiosis. 37:33–61

Buhl-Mortensen L, Olafsdottir SH, Buhl-Mortensen P, Burgos JM, Ragnarsson SA. 2015b. Distribution of nine cold-water coral species (Scleractinia and Gorgonacea) in the cold temperate North Atlantic: effects of bathymetry and hydrography. Hydrobiologia. 759(1):39–61

Buhl-Mortensen L, Vanreusel A, Gooday AJ, Levin LA, Priede IG, et al. 2010. Biological structures as a source of habitat heterogeneity and biodiversity on the deep ocean margins. Mar. Ecol. 31:21–50

Buhl-Mortensen P. 2017. Coral reefs in the Southern Barents Sea: habitat description and the effects of bottom fishing. Mar. Biol. Res. 13(10):1027–40

Burgess SC, Nickols KJ, Griesemer CD, Barnett LAK, Dedrick AG, et al. 2014. Beyond connectivity: How empirical methods can quantify population persistence to improve marine protected-area design. Ecol. Appl. 24(2):257–70

Büscher JV, Form AU, Riebesell U. 2017. Interactive Effects of Ocean Acidification and Warming on Growth, Fitness and Survival of the Cold-Water Coral *Lophelia pertusa* under Different Food Availabilities. Front. Mar. Sci. 4:101

Byrne M. 2011. Impact of ocean warming and ocean acidificati on marine in vertebrate life history stages: Vulnerabilities and potential for persistence in a changing ocean. Oceanogr. Mar. Biol. An Annu. Rev. 49:1–42

Cabral RB, Gaines SD, Lim MT, Atrigenio MP, Mamauag SS, et al. 2016. Siting marine protected areas based on habitat quality and extent provides the greatest benefit to spatially structured metapopulations. Ecosphere. 7(11):e01533

Cairns SD, Chapman RE. 2001. Biogeographic affinities of the North Atlantic deep-water Scleractinia. Proc. First Int. Symp. Deep. Corals, pp. 30–57. Ecology Action Centre and Nova Scotia Museum

Caldeira K, Wickett ME. 2003. Anthropogenic carbon and ocean pH. Nature. 425:365

Canals M, Puig P, de Madron XD, Heussner S, Palanques A, Fabres J. 2006. Flushing submarine canyons. Nature. 444:354–57

Carreiro-Silva M, Ocaña O, Stanković D, Sampaio Í, Porteiro FM, et al. 2017. Zoantharians (Hexacorallia: Zoantharia) Associated with Cold-Water Corals in the Azores Region: New Species and Associations in the Deep Sea. Front. Mar. Sci. 4(88)

Carreras-Carbonell J, Macpherson E, Pascual M. 2006. Population structure within and between subspecies of the Mediterranean triplefin fish Tripterygion delaisi revealed by highly polymorphic microsatellite loci. Mol. Ecol. 15(12):3527–39

Clark MR, Althaus F, Williams A, Niklitschek E, Menezes GM, et al. 2010a. Are deep-sea demersal fish assemblages globally homogenous? Insights from seamounts. Mar. Ecol. 31(Suppl. 1):39–51

Clark MR, Rowden AA, Schlacher T, Williams A, Consalvey M, et al. 2010b. The ecology of seamounts: structure, function, and human impacts. Ann. Rev. Mar. Sci. 2:253–78

Cohen AL, Holcomb M. 2009. Why corals care about ocean acidification: uncovering the mechanism. Oceanography. 22:118–27

Colbourne EB, Foote KD. 2000. Variability of the stratification and circulation on the Flemish cap during the decades of the 1950s-1990s. J. Northwest Atl. Fish. Sci. 26(1986):103–22

Colin C, Frank N, Copard K, Douville E. 2010. Neodymium isotopic composition of deep-sea corals from the NE Atlantic: implications for past hydrological changes during the Holocene. Quat. Sci. Rev. 29:2509–17

Collart T, Verreydt W, Hernández-Molina FJ, Llave E, León R, et al. 2018. Sedimentary processes and cold-water coral mini-mounds at the Ferrol canyon head, NW Iberian margin. Prog. Oceanogr. 169:48–65

Cordes EE, Carney SL, Hourdez S, Carney RS, Brooks JM, Fisher CR. 2007. Cold seeps of the deep Gulf of Mexico: Community structure and biogeographic comparisons to Atlantic equatorial belt seep communities. Deep. Res. Part I Oceanogr. Res. 54(4):637–53

Costantini F, Addamo AM, Machordom A, Abbiati M. 2017. Genetic Connectivity and Conservation of Temperate and Cold-Water Habitat-Forming Corals. In Marine Animal Forests. The Ecology of Benthic Biodiversity Hotspots, eds. S Rossi, L Bramanti, A Gori, C Orejas, pp. 1061–82. Springer

Costello M, Emblow C, White R. 2001. European Register of Marine Species, A Check-List of Marine Species in Europe and a Bibliography of Identification Guides., Vol. 50. Paris: Muséum National D'histoire Naturelle

Costello MJ, Chaudhary C. 2017. Marine Biodiversity, Biogeography, Deep-Sea Gradients, and Conservation. Curr. Biol. 27(11):R511–27

Cowen RK, Lwiza KMM, Sponaugle S, Paris CB, Olson DB. 2000. Conectivity of marine populations: open or closed? Science. 287:857–59

Cowen RK, Sponaugle S. 2009. Larval Dispersal and Marine Population Connectivity. Ann. Rev. Mar. Sci. 1(1):443–66

Crocket KC, Hill E, Abell RE, Johnson C, Gary SF, et al. 2018. Rare Earth Element Distribution in the NE Atlantic: Evidence for Benthic Sources, Longevity of the Seawater Signal, and Biogeochemical Cycling. Front. Mar. Sci. 5(147)

Crowley TJ. 1981. Temperature and circulation changes in the eastern North Atlantic during the last 150,000 years: Evidence from the planktonic foraminiferal record. Mar. Micropaleontol. 6(2):97–129

CSA Ocean Sciences I, Ross S, Brooke S, Baird E, Coykendall E, et al. 2017. Atlantic Deepwater hard Bottom Habitats and Shipwrecks with Emphasis on Canyons and Coral Communities: Atlantic Deepwater Canyons Study. Technical Report, U.S. Dept. of the Interior, Bureau of Ocean Energy Management, Atlantic OCS Region. OCS Study BOEM 2017-060 (Vol. I) & 061 (Vol. II), pp. 1000

Cunha MR, Hilário A, Santos RS, Hilario A, Santos RS. 2017. Advances in deep-sea biology: biodiversity, ecosystem functioning and conservation. An introduction and overview. Deep. Res. Part II Top. Stud. Oceanogr. 137:1–5

Cunha MR, Rodrigues CF, Génio L, Hilário A, Ravara A, Pfannkuche O. 2013. Macrofaunal assemblages from mud volcanoes in the Gulf of Cadiz: abundance, biodiversity and diversity partitioning across spatial scales. Biogeosciences. 10:2553–68

Danovaro R, Canals M, Gambi C, Heussner S, Lampadariou N, Vanreusel A. 2009. Exploring Benthic Biodiversity Patterns and Hot Spots on European Margin Slopes. Oceanography. 22(1):16–25

Danovaro R, Dell'Anno A, Pusceddu A. 2004. Biodiversity response to climate change in a warm deep sea. Ecol. Lett. 7(9):821–28

Danovaro R, Snelgrove P V, Tyler P. 2014. Challenging the paradigms of deep-sea ecology. Trends Ecol. Evol. 29:465–75

Davies AJ, Duineveld GCAA, Lavaleye MSSS, Bergman MJNN, Van Haren H, Roberts JM. 2009. Downwelling and deep-water bottom currents as food supply mechanisms to the cold-water coral Lophelia pertusa (Scleractinia) at the Mingulay Reef complex. Limnol. Oceanogr. 54(2):620–29

Davies AJ, Duineveld GCA, van Weering TCE, Mienis F, Quattrini AM, et al. 2010. Short-term environmental variability in cold-water coral habitat at Viosca Knoll, Gulf of Mexico. Deep. Res. Part I Oceanogr. Res. Pap. 57(2):199–212

Davies AJ, Guinotte JM. 2011. Global habitat suitability for framework-forming Cold-Water Corals. PLoS One. 6(4): e18483

Davies AJ, Wisshak M, Orr JC, Roberts JM. 2008. Predicting suitable habitat for the cold-water coral Lophelia pertusa (Scleractinia). Deep. Res. Part I Oceanogr. Res. 55:1048–62

De Clippele LH, Gafeira J, Robert K, Hennige S, Lavaleye MS, et al. 2017a. Using novel acoustic and visual mapping tools to predict the small-scale spatial distribution of live biogenic reef framework in cold-water coral habitats. Coral Reefs. 36(1):255–68

De Clippele LH, Huvenne VAI, Orejas C, Lundälv T, Fox A, et al. 2017b. The effect of local hydrodynamics on the spatial extent and morphology of cold-water coral habitats at Tisler Reef, Norway. Coral Reefs. 37(1): 253–26

de Goeij JM, van Oevelen D, Vermeij MJA, Osinga R, Middelburg JJ, et al. 2013. Surviving in a marine desert: the sponge loop retains resources within coral reefs. Science. 342:108–10

de Haas H, Mienis F, Frank N, Richter TO, Steinacher R, et al. 2009. Morphology and sedimentology of (clustered) cold-water coral mounds at the south Rockall Trough margins, NE Atlantic Ocean. Facies. 55:1–26

De Mol B, Henriet J-PP, Canals M. 2005. Development of Coral Banks in Porcupine Seabight: Do They Have Mediterranean Ancestors? In Cold-Water Corals and Ecosystems, eds. A Freiwald, J Roberts, pp. 515–33. Springer

De Mol B, Van Rensbergen P, Pillen S, Van Herreweghe K, Van Rooij D, et al. 2002. Large deep-water coral banks in the Porcupine Basin, southwest of Ireland. Mar. Geol. 188:193–231

De Mol L, Van Rooij D, Pirlet H, Greinert J, Frank N, et al. 2011. Cold-water coral habitats in the Penmarc'h and Guilvinec Canyons (Bay of Biscay): Deep-water versus shallow-water settings. Mar. Geol. 282(1–2):40–52

Díaz-del-Río V, Somoza L, Martínez-Frias J, Mata MP, Delgado A, et al. 2003. Vast fields of hydrocarbon-derived carbonate chimneys related to the accretionary wedge/olistostrome of the Gulf of Cádiz. Mar. Geol. 195(1–4):177–200

Díaz del Río V, Bruque G, Fernández Salas LM, Rueda JL, González E, et al. 2014. Volcanes de Fango Del Golfo de Cádiz, Proyecto LIFE+INDEMARES. Madrid, España: Fundación Biodiversidad del Ministerio de Agricultura, Alimentación y Medio Ambiente

Dickson RR, Brown J. 1994. The production of North Atlantic Deep Water: Sources, rates, and pathways. J. Geophys. Res. Ocean. 99:12319–41

Dodds LA, Roberts JM, Taylor AC, Marubini F. 2007. Metabolic tolerance of the cold-water coral *Lophelia pertusa* (Scleractinia) to temperature and dissolved oxygen change. J. Exp. Mar. Bio. Ecol. 349:205–14

Doney SC, Balch WM, Fabry VJ, Feely RA. 2009. Ocean acidification: A critical emerging problem for the ocean sciences. Oceanography. 22(4):16–25

Doney SC, Ruckelshaus M, Emmett Duffy J, Barry JP, Chan F, et al. 2012. Climate Change Impacts on Marine Ecosystems. Ann. Rev. Mar. Sci. 4(1):11–37

Dorschel B, Hebbeln D, Foubert A, White M, Wheeler AJ. 2007a. Hydrodynamics and cold-water coral facies distribution related to recent sedimentary processes at Galway Mound west of Ireland. Mar. Geol. 244:184–95

Dorschel B, Hebbeln D, Ruggeberg A, Dullo C. 2007b. Carbonate budget of a cold-water coral carbonate mound: Propeller Mound, Porcupine Seabight. Int. J. Earth Sci. 96:73–83

Dorschel B, Hebbeln D, Ruggeberg A, Dullo WC, Freiwald A. 2005. Growth and erosion of a cold-water coral covered carbonate mound in the Northeast Atlantic during the Late Pleistocene and Holocene. Earth Planet. Sci. Lett. 233:33–44

Douarin M, Elliot M, Noble SR, Moreton SG, Long D, et al. 2016. North Atlantic shifts in Meridional Overturning Circulation. Geophys. Res. Lett. 43:291–98

Drazen JC, Seibel BA. 2007. Depth-related trends in metabolism Metabolism Trends of Benthic and Benthopelagic Fishes. Limnol. Oceanogr. 52(5):2306–16

Dufresne J-L, Foujols M-A, Denvil S, Caubel A, Marti O, et al. 2013. Climate change projections using the IPSL-CM5 Earth System Model: from CMIP3 to CMIP5. Clim. Dyn. 40(9):2123–65

Duineveld GCA, Jeffreys RM, Lavaleye MSS, Davies AJ, Bergman MJN, et al. 2012. Spatial and tidal variation in food supply to shallow cold-water coral reefs of the Mingulay Reef complex (Outer Hebrides, Scotland). Mar. Ecol. Prog. Ser. 444:97–115

Duineveld GCA, Lavaleye MSS, Berghuis EM. 2004. Particle flux and food supply to a seamount cold-water coral community (Galicia Bank, NW Spain). Mar. Ecol. Prog. Ser. 277:13–23

Duineveld GCA, Lavaleye MSS, Bergman MJN, De Stigter H, Mienis F. 2007. Trophic structure of a cold-water coral mound community (Rockall Bank, NE Atlantic) in relation to the near-bottom particle supply and current regime. Bull. Mar. Sci. 81:449–67

Dullo WC, Flogel S, Ruggeberg A, Flögel S, Rüggeberg A. 2008. Cold-water coral growth in relation to the hydrography of the Celtic and Nordic European continental margin. Mar. Ecol. Prog. Ser. 371:165–76

Dunne JP, John JG, Adcroft AJ, Griffies SM, Hallberg RW, et al. 2012. GFDL's ESM2 Global Coupled Climate–Carbon Earth System Models. Part I: Physical Formulation and Baseline Simulation Characteristics. J. Clim. 25(19):6646–65

Dupont S, Thorndyke MC. 2009. Impact of CO2-driven ocean acidification on invertebrates early life-history – What we know, what we need to know and what we can do. Biogeosciences Discuss. 6(2):3109–31

Eisele M, Frank N, Wienberg C, Hebbeln D, Lopez Correa M, et al. 2011. Productivity controlled cold-water coral growth periods during the last glacial off Mauritania. Mar. Geol. 280:143–49

Ercilla G, Casas D, Vazquez JT, Iglesias J, Somoza L, et al. 2011. Imaging the recent sediment dynamics of the Galicia Bank region (Atlantic, NW Iberian Peninsula). Mar. Geophys. Res. 32(1):99–126

Ercilla G, Córdoba D, Gallart J, Gràcia E, Muñoz JA, et al. 2006. Geological characterization of the Prestige sinking area. Mar. Pollut. Bull. 53(5–7):208–19

Etter R, Boyle EE, Glazier A, Jennings RM, Dutra E, Chase MR. 2011. Phylogeography of a pan-Atlantic abyssal protobranch bivalve: implications for evolution in the Deep Atlantic. Mol. Ecol. 20(4):829–43

Falk-Petersen S, Mayzaud P, Kattner G, Sargent JR. 2009. Lipids and life strategy of Arctic Calanus. Mar. Biol. Res. 5(1):18–39

Fernandez-Arcaya U, Ramirez-Llodra E, Aguzzi J, Allcock AL, Davies JS, et al. 2017. Ecological Role of Submarine Canyons and Need for Canyon Conservation: A Review. Front. Mar. Sci. 4(5)

Fernández-Salas LM, Sánchez Leal RF, Rueda JL, López-González N, González-García E, et al. 2012. Interacción entre las masas de agua, los relieves submarinos y la distribución de especies bentónicas en el talud continental del Golfo de Cádiz Interaction between water masses, submarine relieves and distribution of benthic species in the continental. Geo-Temas. 13:569–72

Findlay, H.S., Hennige, S.J., Wicks, L.C., Navas, J.M., Woodward, E.M.S. and Roberts, J.M. 2014. Fine-scale nutrient and carbonate system dynamics around cold-water coral reefs in the northeast Atlantic. Nature Scientific Reports, 4:3671

Fischer J, Schott FA, Dengler M. 2004. Boundary Circulation at the Exit of the Labrador Sea. J. Phys. Oceanogr. 34(7):1548–70

Flögel S, Dullo W-CC, Pfannkuche O, Kiriakoulakis K, Rüggeberg A. 2014. Geochemical and physical constraints for the occurrence of living cold-water corals. Deep. Res. Part II Top. Stud. Oceanogr. 99:19–26

Fogelqvist E, Blindheim J, Tanhua T, Østerhus S, Buch E, Rey F. 2003. Greenland–Scotland overflow studied by hydro-chemical multivariate analysis. Deep. Res. Part I Oceanogr. Res. 50(1):73–102

Form AU, Riebesell U. 2012. Acclimation to ocean acidification during long-term CO2 exposure in the cold-water coral Lophelia pertusa. Glob. Chang. Biol. 18:843-853

Forsterra G, Haussermann V. 2003. First report on large scleractinian (Cnidaria: Anthozoa) accumulations in cold-temperate shallow water of south Chilean fjords. Zool. Verh. 117–28

Fosså J, Skjoldal H. 2010. Conservation of cold-water coral reefs in Norway. In Handbook of Marine Fisheries Conservation and Management, eds. GR Quentin, R Hilborn, D Squires, M Tait, M Williams, p. 770. New York: Oxford University Press

Fosså JH, Mortensen PB, Furevik DM. 2002. The deep-water coral Lophelia pertusa in Norwegian waters: distribution and fishery impacts. Hydrobiologia. 471:1–12

Foster NL, Paris CB, Kool JT, Baums IB, Stevens JR, et al. 2012. Connectivity of Caribbean coral populations: Complementary insights from empirical and modelled gene flow. Mol. Ecol. 21(5):1143–57

Fox AD, Henry L-A, Corne DW, Roberts JM. 2016. Sensitivity of marine protected area network connectivity to atmospheric variability. R. Soc. Open Sci. 3:160494

Fragoso GM, Poulton AJ, Yashayaev IM, Head EJH, Johnsen G, Purdie DA. 2018. Diatom Biogeography From the Labrador Sea Revealed Through a Trait-Based Approach. Front. Mar. Sci. 5(297)

Fragoso GM, Poulton AJ, Yashayaev IM, Head EJH, Stinchcombe MC, Purdie DA. 2016. Biogeographical patterns and environmental controls of phytoplankton communities from contrasting hydrographical zones of the Labrador Sea. Prog. Oceanogr. 141:212–26

Frajka-Williams E, Rhines PB. 2010. Physical controls and interannual variability of the Labrador Sea spring phytoplankton bloom in distinct regions. Deep. Res. Part I Oceanogr. Res. 57(4):541–52

Frank N, Freiwald A, López Correa M, Wienberg C, Eisele M, et al. 2011. Northeastern Atlantic cold-water coral reefs and climate. Geology. 39:743–46

Frederiksen R, Jensen A, Westerberg H. 1992. The distribution of the scleractinian coral *Lophelia pertusa* around the Faroe islands and the relation to internal tidal mixing. Sarsia. 77:157–71

Freiwald A. 1998. Geobiology of *Lophelia pertusa* (Scleractinia) reefs in the North Atlantic. Habilit. am Fachbereich Geowissenschaften der Univ. Bremen, 116pp

Freiwald A. 2002. Reef-Forming Cold-Water Corals. In Ocean Margin Systems, ed. BD Wefer G, Hebbeln D, Jorgensen, Schluter M, Van WeeringT, pp. 365–85. Springer Berlin Heidelberg

Freiwald A, Beuck L, Rueggeberg A, Taviani M, Hebbeln D. 2009. The white coral community in the central Mediterranean Sea Revealed by ROV Surveys. Oceanography. 22:58–74

Freiwald A, Fosså JH, Grehan A, Koslow T, Roberts JM. 2004. Cold-Water Coral Reefs. Cambridge, UK: UNEP-WCMC

Freiwald A, Wilson JB, Henrich R. 1999. Grounding Pleistocene icebergs shape recent deep-water coral reefs. Sediment. Geol. 125:1–8

Gage JD. 2004. Diversity in deep-sea benthic macrofauna: the importance of local ecology, the larger scale, history and the Antarctic. Deep. Res. Part II Top. Stud. Oceanogr. 51:1689–1708

Galarza JA, Carreras-Carbonell J, Macpherson E, Pascual M, Roques S, et al. 2009a. The influence of oceanographic fronts and early-life-history traits on connectivity among littoral fish species. Proc. Natl. Acad. Sci. USA. 106(5):1473–78

Galarza JA, Turner GF, Macpherson E, Rico C. 2009b. Patterns of genetic differentiation between two co-occurring demersal species: the red mullet (*Mullus barbatus*) and the striped red mullet (*Mullus surmuletus*). Can. J. Fish. Aquat. Sci. 66(9):1478–90

García-Ibáñez MI, Pardo PC, Carracedo LI, Mercier H, Lherminier P, et al. 2015. Structure, transports and transformations of the water masses in the Atlantic Subpolar Gyre. Prog. Oceanogr. 135:18–36

García M, Hernández-Molina FJ, Llave E, Stow DAV, León R, et al. 2009. Contourite erosive features caused by the Mediterranean Outflow Water in the Gulf of Cadiz: Quaternary tectonic and oceanographic implications. Mar. Geol. 257(1–4):24–40

Gass SE, Roberts JM. 2006. The occurrence of the cold-water coral *Lophelia pertusa* (Scleractinia) on oil and gas platforms in the North Sea: Colony growth, recruitment and environmental controls on distribution. Mar. Pollut. Bull. 52:549–59

Gebruk A V, Budaeva NE, King NJ. 2010. Bathyal benthic fauna of the Mid-Atlantic Ridge between the Azores and the Reykjanes Ridge. J. Mar. Biol. Assoc. United Kingdom. 90(1):1–14

Gehlen M, Séférian R, Jones DOB, Roy T, Roth R, et al. 2014. Projected pH reductions by 2100 might put deep North Atlantic biodiversity at risk. Biogeosciences. 11(23):6955–67

Genin A, Dower J. 2008. Seamount Plankton Dynamics. In Seamounts: Ecology, Fisheries & Conservation (eds.) Pitcher TJ, Morato T, Hart PJ, Clark MR, Haggan N, Santos RS.

Georgian SE, Dupont S, Kurman M, Butler A, Strömberg SM, et al. 2016. Biogeographic variability in the physiological response of the cold-water coral *Lophelia pertusa* to ocean acidification. Mar. Ecol. 37(6):1345–59

Georgian SE, Shedd W, Cordes EE. 2014. High-resolution ecological niche modelling of the cold-water coral *Lophelia pertusa* in the Gulf of Mexico. Mar. Ecol. Prog. Ser. 506:145–61

Gil J. 2008. Macro and mesoscale physical patterns in the Bay of Biscay. J. Mar. Biol. Assoc. United Kingdom. 88:217–25

Gil J, Sánchez R, Cervino S, Garabana D. 2004. Geostrophic circulation and heat flux across the Flemish Cap, 1988-2000. J. Northwest Atl. Fish. Sci. 34:63–83

Giorgetta MA, Jungclaus J, Reick CH, Legutke S, Bader J, et al. 2013. Climate and carbon cycle changes from 1850 to 2100 in MPI-ESM simulations for the Coupled Model Intercomparison Project phase 5. J. Adv. Model. Earth Syst. 5(3):572–97

Glover AG, Smith CR. 2003. The deep-sea floor ecosystem: Current status and prospects of anthropogenic change by the year 2025. Environ. Conserv. 30(3):219–41

Gómez CE, Wickes L, Deegan D, Etnoyer PJ, Cordes EE. 2018. Growth and feeding of deep-sea coral *Lophelia pertusa* from the California margin under simulated ocean acidification conditions. PeerJ. 6:e5671

González-García E, Rueda J, Farias C, Gil J, Bruque G, et al. 2012. Comunidades Bentónico-Demersales En Caladeros de Los Volcanes de Fango Del Golfo de Cádiz: Caracterización y Actividad Pesquera, Vol. 19

González-García E, Rueda JL, Urra J, López-González N, Palomino D, et al. 2015. Relaciones ambientales, pesqueras y bentónicas en el campo de volcanes de fango del margen español del Golfo de Cádiz. VIII Simp. Sobre El Margen Ibérico Atlántico, pp. 647–50

Gori A, Ferrier-Pages C, Hennige SJ, Murray F, Rottier C, et al. 2016. Physiological response of the cold-water coral *Desmophyllum dianthus* to thermal stress and ocean acidification. PeerJ. 4:16

Gori A, Reynaud S, Orejas C, Gili JM, Ferrier-Pages C. 2014. Physiological performance of the cold-water coral Dendrophyllia cornigera reveals its preference for temperate environments. Coral Reefs. 33:665–74

Griffin S, Druffel ERM. 1989. Sources of Carbon to Deep-Sea Corals. Radiocarbon. 31(03):533–43

Guihen D, White M, Lundälv T. 2012. Temperature shocks and ecological implications at a cold-water coral reef. Mar. Biodivers. Rec. 5:e68

Guihen D, White M, Lundälv T. 2013. Boundary layer flow dynamics at a cold-water coral reef. J. Sea Res. 78:36–44

Guijarro J, Beazley L, Lirette C, Kenchington E, Wareham V, et al. 2016. Species distribution modelling of corals and sponges from research vessel survey data in the Newfoundland and Labrador region for use in the identification of significant benthic areas. Canadian Technical Report of Fisheries and Aquatic Sciences 3167, pp. 126

Guinan J, Brown C, Dolan MFJ, Grehan AJ. 2009. Ecological niche modelling of the distribution of cold-water coral habitat using underwater remote sensing data. Ecol. Inform. 4(2):83–92

Guinotte JM, Orr J, Cairns S, Freiwald A, Morgan L, George R. 2006. Will human-induced changes in seawater chemistry alter the distribution of deep-sea Scleractinian corals? Front. Ecol. Environ. 4:141–46

H Stewart R. 2008. Introduction To Physical Oceanography. Texas A&M University.

Hansen B, Husgaro KM, Hátún H, Østerhus S. 2016. A stable Faroe Bank Channel overflow 1995-2015. Ocean Sci. 12(6):1205–20

Hátún H, Azetsu-Scott K, Somavilla R, Rey F, Johnson C, et al. 2017. The subpolar gyre regulates silicate concentrations in the North Atlantic. Sci. Rep. 7(1):14576

Hátún H, Payne MR, Beaugrand G, Reid PC, Sandø AB, et al. 2009a. Large bio-geographical shifts in the north-eastern Atlantic Ocean: From the subpolar gyre, via plankton, to blue whiting and pilot whales. Prog. Oceanogr. 80(3):149–62

Hátún H, Payne MR, Jacobsen JA. 2009b. The North Atlantic subpolar gyre regulates the spawning distribution of blue whiting (*Micromesistius poutassou*). Can. J. Fish. Aquat. Sci. 66(5):759–70

Head EJH, Harris LR, Yashayaev I. 2003. Distributions of Calanus spp. and other mesozooplankton in the Labrador Sea in relation to hydrography in spring and summer (1995–2000). Prog. Oceanogr. 59(1):1–30

Hebbeln D, Wienberg C. 2016. Good neighbours shaped by vigorous currents: Cold-water coral mounds and contourites in the North Atlantic. Mar. Geol. 378:171–85

Hebbeln D, Wienberg C, Bender M, Bergmann F, Dehning K, et al. 2017. ANNA - Cold-Water Coral Ecosystems off Angola and Namibia (Cruise No. M122). Technical Report DF & MARUM, Meteor-Berichte, pp. 191

Hebbeln D, Wienberg C, Wintersteller P, Freiwald A, Becker M, et al. 2014. Environmental forcing of the Campeche cold-water coral province, southern Gulf of Mexico. Biogeosciences. 11(7):1799–1815

Hennige SJ, Wicks LC, Kamenos NA, Bakker DCEE, Findlay HS, et al. 2014. Short-term metabolic and growth responses of the cold-water coral *Lophelia pertusa* to ocean acidification. Deep. Res. Part II Top. Stud. Oceanogr. 99:27–35

Hennige SJ, Wicks LC, Kamenos NA, Perna G, Findlay HS, Roberts JM. 2015. Hidden impacts of ocean acidification to live and dead coral framework. Proc. R. Soc. London B Biol. Sci. 282(1813):

Henry L-A, Roberts JM. 2007. Biodiversity and ecological composition of macrobenthos on cold-water coral mounds and adjacent off-mound habitat in the bathyal Porcupine Seabight, NE Atlantic. Deep. Res. Part I Oceanogr. Res. 54:654–72

Henry L-A, Roberts JM. 2008. First record of *Bedotella armata* (Cnidaria: Hydrozoa) from the Porcupine Seabight: do north-east Atlantic carbonate mound fauna have Mediterranean ancestors? Mar. Biodivers. Rec. 1:e24

Henry L-A, Roberts JM. 2017. Global biodiversity in cold-water coral reef ecosystems. In Marine Animal Forests. The Ecology of Benthic Biodiversity Hotspots, eds. S Rossi, L Bramanti, A Gori, C Orejas, p. 21. Switzerland: Springer International Publishing

Henry L-AA, Frank N, Hebbeln D, Wienberg C, Robinson L, et al. 2014. Global ocean conveyor lowers extinction risk in the deep sea. Deep. Res. Part I Oceanogr. Res. 88(1):8–16

Henry LA, Davies AJ, Roberts JM. 2010. Beta diversity of cold-water coral reef communities off western Scotland. Coral Reefs. 29(2):427–36

Henry LA, Navas JM, Hennige SJ, Wicks LC, Vad J, Murray Roberts J. 2013a. Cold-water coral reef habitats benefit recreationally valuable sharks. Biol. Conserv. 161:67–70

Henry LA, Navas JM, Roberts JM, Moreno Navas J, Roberts JM. 2013b. Multi-scale interactions between local hydrography, seabed topography, and community assembly on cold-water coral reefs. Biogeosciences. 10(4):2737–46

Hernández-Molina FJ, Nombela MA, Van Rooij D, Roson G, Ercilla G, et al. 2009. The Ortegal spur contourite depositional dystem (Bay of Biscay): the implications of the Mediterranean Outflow Waters in sedimentary processes and cold-water coral ecosystems. VI Simposio sobre el Margen Ibérico Atlántico. 281–84

Hernández-Molina FJ, Sierro FJ, Llave E, Roque C, Stow DAV, et al. 2016. Evolution of the gulf of Cadiz margin and southwest Portugal contourite depositional system: Tectonic, sedimentary and paleoceanographic implications from IODP expedition 339. Mar. Geol. 377:7–39

Herrera S, Shank TM, Sánchez JA. 2012. Spatial and temporal patterns of genetic variation in the widespread antitropical deep-sea coral *Paragorgia arborea*. Mol. Ecol. 21(24):6053–67

Hilário A, Metaxas A, Gaudron SM, Howell KL, Mercier A, et al. 2015. Estimating dispersal distance in the deep sea: challenges and applications to marine reserves. Front. Mar. Sci. 2:1–14

Hillaire-marcel C, Maccali J, Ménabréaz L, Ghaleb B, Blénet A. 2017. U-series vs 14 C ages of deep-sea corals from the southern Labrador Sea : Sporadic development of corals and geochemical processes hampering estimation of ambient water ventilation ages. 19th EGU Gen. Assem., p. 9126

Hofmann M, Schellnhuber H. 2009. Oceanic acidification affects marine carbon pump and triggers extended marine oxygen holes. Proc. Natl. Acad. Sci. USA. 106(9):3017–22

Hovland M. 2008. Deep-Water Coral Reefs. Unique Biodiversity Hot-Spots. Chichester, UK: Springer and Praxis Publishing

Hovland M, Farestveit R, Mortensen P. 1994. Large cold-water coral reefs of mid-Norway: a problem for pipe-laying? Conf. Proc. (3), Oceanol. International

Hovland M, Vasshus S, Indreeide A, Austdal L, Nilsen Ø. 2002. Mapping and imaging deep-sea coral reefs off Norway, 1982–2000. Hydrobiologia. 471(1):13–17

Howell KL, Davies JS, Narayanaswamy BE. 2010. Identifying deep-sea megafaunal epibenthic assemblages for use in habitat mapping and marine protected area network design. J. Mar. Biol. Assoc. United Kingdom. 90(1):33–68

Howell KL, Holt R, Endrino IP, Stewart H. 2011. When the species is also a habitat: Comparing the predictively modelled distributions of *Lophelia pertusa* and the reef habitat it forms. Biol. Conserv. 144(11):2656–65

Howell KL, Piechaud N, Downie AL, Kenny A. 2016. The distribution of deep-sea sponge aggregations in the North Atlantic and implications for their effective spatial management. Deep. Res. Part I Oceanogr. Res. 115:203–20

Huff DD, Yoklavich MM, Love MS, Watters DL, Chai F, Lindley ST. 2013. Environmental factors that influence the distribution, size, and biotic relationships of the Christmas tree coral *Antipathes dendrochristos* in the Southern California Bight. Mar. Ecol. Prog. Ser. 494:159–77

Husson B, Sarradin PM, Zeppilli D, Sarrazin J. 2017. Picturing thermal niches and biomass of hydrothermal vent species. Deep. Res. Part II Top. Stud. Oceanogr. 137:6–25

Huthnance JM, Van Aken HM, White M, Barton ED, Le Cann B, et al. 2002. Ocean margin exchange - Water flux estimates. J. Mar. Syst. 32(1–3):107–37

Huvenne VAI, Beyer A, de Haas H, Dekindt K, Henriet JP, et al. 2005. The seabed appearance of different coral bank provinces in the Porcupine Seabight, NE Atlantic: results from sidescan sonar and ROV seabed mapping. In Freiwald F, Roberts JM (eds.) Cold-water Corals Ecosyst. pp:535–69

Huvenne VAI, Blondel P, Henriet JP. 2002. Textural analyses of sidescan sonar imagery from two mound provinces in the Porcupine Seabight. Mar. Geol. 189:323–41

Huvenne VAI, Tyler PA, Masson DG, Fisher EH, Hauton C, et al. 2011. A Picture on the Wall: Innovative Mapping Reveals Cold-Water Coral Refuge in Submarine Canyon. PLoS One. 6(12): e28755

Iorga MC, Lozier MS. 1999. Signatures of the Mediterranean outflow from a North Atlantic climatology 1. Salinity and density fields. J. Geophys. Res. 104(11):25985–9

J.E. García-Raso. 1996. Crustacea Decapoda (excl. Sergestidae) from ibero-moroccan waters. Results of Balgim-84 expedition. Bull. Mar. Sci. 58(3):730–52

Jackson EL, Davies AJ, Howell KL, Kershaw PJ, Hall-Spencer JM. 2014. Future-proofing marine protected area networks for cold water coral reefs. ICES J. Mar. Sci. 9(1): 2621-29

James MK, Armsworth PR, Mason LB, Bode L. 2002. The structure of reef fish metapopulations: Modelling larval dispersal and retention patterns. Proc. R. Soc. London B Biol. Sci. 269(1505):2079–86

Jézéquel N, Mazé R, Pichon A. 2002. Interaction of semidiurnal tide with a continental slope in a continuously stratified ocean. Deep. Res. Part I Oceanogr. Res. 49(4):707–34

Jochumsen K, Moritz M, Nunes N, Quadfasel D, Larsen KMH, et al. 2017. Revised transport estimates of the Denmark Strait overflow. J. Geophys. Res. Ocean. 122(4):3434–50

Johanneson K, André C. 2006. Life on the margin: genetic isolation and diversity loss in a peripheral marine ecosystem, the Baltic Sea. Mol. Ecol. 15(8):2013–29

Johnson C, Inall M, Häkkinen S. 2013. Declining nutrient concentrations in the northeast Atlantic as a result of a weakening Subpolar Gyre. Deep. Res. Part I Oceanogr. Res. 82:95–107

Johnson J, Stevens I. 2000. A fine resolution model of the eastern North Atlantic between the Azores, the Canary Islands and the Gibraltar Strait. Deep. Res. Part I Oceanogr. Res. 47(5):875–99

Joint I, Groom SB, Wollast R, Chou L, Tilstone GH, et al. 2002. The response of phytoplankton production to periodic upwelling and relaxation events at the Iberian shelf break: Estimates by the14C method and by satellite remote sensing. J. Mar. Syst. 32(1–3):219–38

Jones DOB, Yool A, Wei C-L, Henson SA, Ruhl HA, et al. 2014. Global reductions in seafloor biomass in response to climate change. Glob. Chang. Biol. 20(6):1861–72

Jong MF, Steur L. 2016. Strong winter cooling over the Irminger Sea in winter 2014–2015, exceptional deep convection, and the emergence of anomalously low SST. Geophys. Res. Lett. 43(13):7106–13

Jørgensen OA, Hvingel C, Møller PR, Treble MA. 2005. Identification and mapping of bottom fish assemblages in Davis Strait and southern Baffin Bay. Can. J. Fish. Aquat. Sci. 62(8):1833–52

Jørgensen OA, Hvingel C, Treble MA. 2011. Identification and mapping of bottom fish assemblages in northern Baffin Bay. J. Northwest Atl. Fish. Sci. 43:65–79

Joubin ML. 1922. Les Coraux de Mer Profonde Nuisibles Aux Chalutiers. Paris: Blondel La Rougery

Juul-Pedersen T, Gissel Nielsen T, Michel C, Friis Møller E, Tiselius P, et al. 2006. Sedimentation following the spring bloom in Disko Bay, West Greenland, with special emphasis on the role of copepods. Mar. Ecol. Prog. Ser. 314:239–55

Kamykowski D, Zentara S-J. 1990. Hypoxia in the world ocean as recorded in the historical data set. Deep Sea Res. Part A. Oceanogr. Res. Pap. 37(12):1861–74

Kano A, Ferdelman T, Williams T, Henriet J-P, Ishikawa T, et al. 2007. Age constraints on the origin and growth history of a deep-water coral mound in the northeast Atlantic drilled during Integrated Ocean Drilling Program Expedition 307. Geology. 35(11):1051–1054

Kazanidis G, Henry L-AA, Roberts JM, Witte UFMM. 2016. Biodiversity of *Spongosorites coralliophaga* (Stephens, 1915) on coral rubble at two contrasting cold-water coral reef settings. Coral Reefs. 35(1):193–208

Kazanidis G, van Oevelen D, Veuger B, Witte UFM. 2018. Unravelling the versatile feeding and metabolic strategies of the cold-water ecosystem engineer *Spongosorites coralliophaga* (Stephens, 1915). Deep. Res. Part I Oceanogr. Res.

Kazanidis G, Witte UFM. 2016. The trophic structure of *Spongosorites coralliophaga*-coral rubble communities at two northeast Atlantic cold water coral reefs. Mar. Biol. Res. 12:932–47

Keeling RF, Körtzinger A, Gruber N. 2010. Ocean Deoxygenation in a Warming World. Ann. Rev. Mar. Sci. 2(1):199–229

Keller NB, Os'kina NS. 2008. Habitat temperature ranges of azooxantellate scleractinian corals in the World Ocean. Oceanology. 48(1):77–84

Kenchington E, Lirette C, Murillo FJ, Beazley L, Guijarro J, et al. 2016. Kernel density analyses of coral and sponge catches from research vessel survey data for use in identification of significant benthic areas. Canadian Technical Report of Fisheries and Aquatic Sciences 3167, pp. 207

Kenchington E, Murillo FJ, Lirette C, Sacau M, Koen-Alonso M, et al. 2014. Kernel density surface modelling as a means to identify significant concentrations of vulnerable marine ecosystem indicators. PLoS One. 9(10): e109365

Kenchington E, Yashayaev I, Tendal OS, Jørgensbye H. 2017. Water mass characteristics and associated fauna of a recently discovered *Lophelia pertusa* (Scleractinia: Anthozoa) reef in Greenlandic waters. Polar Biol. 40(2):321–37

Kendall VJ, Haedrich RL. 2006. Species richness in Atlantic deep-sea fishes assessed in terms of the mid-domain effect and Rapoport's rule. Deep Sea Res. Part I Oceanogr. Res. Pap. 53(3):506–15

Khélifi N, Frank M. 2014. A major change in North Atlantic deep water circulation 1.6 million years ago. Clim. Past. 10(4):1441–51

Khripounoff A, Caprais JC, Le Bruchec J, Rodier P, Noel P, Cathalot C. 2014. Deep cold-water coral ecosystems in the Brittany submarine canyons (Northeast Atlantic): Hydrodynamics, particle supply, respiration, and carbon cycling. Limnol. Oceanogr. 59(1):87–98

Klitgaard AB, Tendal OS. 2004. Distribution and species composition of mass occurrences of large-sized sponges in the northeast Atlantic. Prog. Oceanogr. 61:57–98

Klitgaard AB, Tendal OS, Westerberg H. 1997. Mass occurrences of large sponges (Porifera) in Faroe Island (NE Atlantic) shelf and slope areas: characteristics, distribution and possible causes. In Proceedings of the 30th European Marine Biology Symposium, ed. LE Hawkins, pp. 129–42

Knudby A, Kenchington E, Murillo FJ. 2013. Modeling the distribution of *Geodia* sponges and sponge grounds in the Northwest Atlantic. PLoS One. 8(12): e82306

Kröncke I, Reiss H, Eggleton JD, Aldridge J, Bergman MJN, et al. 2011. Changes in North Sea macrofauna communities and species distribution between 1986 and 2000. Estuar. Coast. Shelf Sci. 94(1):1–15

Kurihara H. 2008. Effects of CO_2-driven ocean acidification on the early developmental stages of invertebrates . Mar. Ecol. Prog. Ser. 373:275–84

Kurman MD, Gómez CE, Georgian SE, Lunden JJ, Cordes EE. 2017. Intra-specific variation reveals potential for adaptation to ocean acidification in a cold-water coral from the Gulf of Mexico. Front. Mar. Sci. 4(111):1–14

LaBella AL, Van Dover CL, Jollivet D, Cunningham CW. 2017. Gene flow between Atlantic and Pacific Ocean basins in three lineages of deep-sea clams (Bivalvia: *Vesicomyidae*: *Pliocardiinae*) and subsequent limited gene flow within the Atlantic. Deep. Res. Part II Top. Stud. Oceanogr. 137:307–17

Lambshead PJ., Tietjen J, Ferrero T, Jensenf P. 2000. Latitudinal gradients in the deep sea with special reference to North Atlantic nematodes. Mar. Ecol. Prog. Ser. 194:159–67

Larsson AI, Jarnegren J, Stromberg SM, Dahl MP, Lundalv T, Brooke S. 2014. Embryogenesis and Larval Biology of the Cold-Water Coral *Lophelia pertusa*. PLoS One. 9:e102222

Lavaleye M, Duineveld G, Lundalv T, White M, Guihen D, et al. 2009. Cold-Water Corals on the tisler reef preliminary observations on the dynamic reef environment. Oceanography. 22:76–84

Lavaleye MS., Duineveld GC., Berghuis E., Kok A, Witbaard R. 2002. A comparison between the megafauna communities on the N.W. Iberian and Celtic continental margins—effects of coastal upwelling? Prog. Oceanogr. 52(2–4):459–76

Lavelle JW, Mohn C. 2010. Motion, Commotion, and Biophysical Connections at Deep Ocean Seamounts. Oceanography. 23(01):90–103

Lavelle JW, Thurnherr AM, Ledwell JR, McGillicuddy DJ, Mullineaux LS. 2010. Deep ocean circulation and transport where the East Pacific Rise at 9–10°N meets the Lamont seamount chain. J. Geophys. Res. 115(C12):C12073

Le Goff-Vitry M, Pybus OG, Rogers AD. 2004. Genetic structure of the deep-sea coral. Mol. Ecol. 13(3):537–49

Lear WH. 1998. History of fisheries in the Northwest Atlantic: The 500-year perspective. J. Northwest Atl. Fish. Sci. 23(Table 1):41–73

Lebrato M, Iglesias-Rodríguez D, Feely RA, Greeley D, Jones DOB, et al. 2010. Global contribution of echinoderms to the marine carbon cycle: CaCO3 budget and benthic compartments. Ecol. Monogr. 80(3):441–67

León R, Somoza L, Medialdea T, González FJ, Díaz-del-Río V, et al. 2007. Sea-floor features related to hydrocarbon seeps in deepwater carbonate-mud mounds of the Gulf of Cádiz: From mud flows to carbonate precipitates. Geo-Marine Lett. 27(2–4):237–47

Levin LA. 2003. Oxygen minimum zone benthos: adaptation and community response to hypoxia. Oceanogr. Mar. Biol. an Annu. Rev. 41:1–45

Levin LA. 2018. Manifestation, Drivers, and Emergence of Open Ocean Deoxygenation. Ann. Rev. Mar. Sci. 10(1):229–60

Levin LA, Baco AR, Bowden DA, Colaco A, Cordes EE, et al. 2016. Hydrothermal Vents and Methane Seeps: Rethinking the Sphere of Influence. Front. Mar. Sci. 3(72)

Levin LA, Etter RJ, Rex M a, Gooday AJ, Smith CR, et al. 2001. Environmental influence on regional deep-sea species diversity. Annu. Rev. Ecol. Syst. 32:51–93

Levin LA, Gage JD. 1998. Relationships between oxygen, organic matter and the diversity of bathyal macrofauna. Deep. Res. Part II Top. Stud. Oceanogr. 45(1–3):129–63

Levin LA, Le Bris NL. 2015. The deep ocean under climate change. Science. 350(6262):766–68

Levin LA, Sibuet M. 2012. Understanding continental margin biodiversity: a new imperative. Ann. Rev. Mar. Sci. 4:79–112

Levitus S, Antonov JI, Boyer TP, Baranova OK, Garcia HE, et al. 2012. World ocean heat content and thermosteric sea level change (0-2000m), 1955-2010. Geophys. Res. Lett. 39(10):1–5

Lindberg B, Berndt C, Mienert J. 2007. The Fugløy Reef at 70°N; acoustic signature, geologic, geomorphologic and oceanographic setting. Int. J. Earth Sci. 96(1):201–13

Lippold J, Grützner J, Winter D, Lahaye Y, Mangini A, Christi M. 2009. Does sedimentary 231Pa/230Th from the Bermuda Rise monitor past Atlantic Meridional Overturning Circulation? Geophys. Res. Lett. 36(12):1–6

Lopez-Jamar E. 1992. Upwelling and outwelling effects on the benthic regime of the continental shelf off Galicia, NW Spain. J. Mar. Res. 50:465–88

López Correa M, Montagna P, Joseph N, Rüggeberg A, Fietzke J, et al. 2012. Preboreal onset of cold-water coral growth beyond the Arctic Circle revealed by coupled radiocarbon and U-series dating and neodymium isotopes. Quat. Sci. Rev. 34:24–43

Lozier MS, Stewart NM. 2008. On the Temporally Varying Northward Penetration of Mediterranean Overflow Water and Eastward Penetration of Labrador Sea Water. J. Phys. Oceanogr. 38(9):2097–2103

Lunden JJ, McNicholl CG, Sears CR, Morrison CL, Cordes EE. 2014. Acute survivorship of the deep-sea coral *Lophelia pertusa* from the Gulf of Mexico under acidification, warming, and deoxygenation. Front. Mar. Sci. 1:1-12

Lundsten L, Schlining KL, Frasier K, Johnson SB, Kuhnz LA, et al. 2010. Time-series analysis of six whale-fall communities in Monterey Canyon, California, USA. Deep. Res. Part I Oceanogr. Res. 57(12):1573–84

Lynch-Stieglitz J, Adkins JF, Curry WB, Dokken T, Hall IR, et al. 2007. Atlantic meridional overturning circulation during the last glacial maximum. Science (80-.). 316(5821):66–70

Maier C, Popp P, Sollfrank N, Weinbauer MG, Wild C, Gattuso JP. 2016. Effects of elevated pCO(2) and feeding on net calcification and energy budget of the Mediterranean cold-water coral *Madrepora oculata*. J. Exp. Biol. 219:3208–17

Maier C, Schubert A, Sanchez MMB, Weinbauer MG, Watremez P, Gattuso J-P. 2013. End of the century pCO_2 levels do not Impact calcification in Mediterranean cold-water corals. PLoS One. 8(4): e62655

Maier C, Watremez P, Taviani M, Weinbauer MG, Gattuso JP. 2012. Calcification rates and the effect of ocean acidification on Mediterranean cold-water corals. Proc. R. Soc. London B Biol. Sci. 279:1716–23

Martin JH, Knauer GA, Karl DM, Broenkow WW. 1987. VERTEX: carbon cycling in the northeast Pacific. Deep Sea Res. Part A. Oceanogr. Res. Pap. 34(2):267–85

Martins A, S. B. Amorim A, P. Figueiredo M, Sousa R, P. Mendonça A, et al. 2007. Sea Surface Temperature (AVHRR, MODIS) and Ocean Colour (MODIS) seasonal and interannual variability in the Macaronesian Islands of Azores, Madeira, and Canaries. Proceedings of the International Society for Optical Engineering. 6743

Masson DG, Bett BJ, Billett DSM, Jacobs CL, Wheeler AJ, Wynn RB. 2003. The origin of deep-water, coral-topped mounds in the northern Rockall Trough, Northeast Atlantic. Mar. Geol. 194(3):159–80

Matos L, Mienis F, Wienberg C, Frank N, Kwiatkowski C, et al. 2015. Interglacial occurrence of cold-water corals off Cape Lookout (NW Atlantic): First evidence of the Gulf Stream influence. Deep. Res. Part I Oceanogr. Res. 105:158–70

Matos L, Wienberg C, Titschack J, Schmiedl G, Frank N, et al. 2017. Coral mound development at the Campeche cold-water coral province, southern Gulf of Mexico: Implications of Antarctic Intermediate Water increased influence during interglacials. Mar. Geol. 392:53–65

McClain CR. 2007. Seamounts: identity crisis or split personality? J. Biogeogr. 34:2001–8

McClain CR, Allen AP, Tittensor DP, Rex MA. 2012. Energetics of life on the deep seafloor. Proc. Natl. Acad. Sci. USA. 109(38):15366

McClain CR, Barry JP. 2010. Habitat heterogeneity, disturbance, and productivity work in concert to regulate biodiversity in deep submarine canyons. Ecology. 91(4):964–76

McClain CR, Chao S-Y, Atkinson LP, Blanton JO, De Castillejo F. 1986. Wind-driven upwelling in the vicinity of Cape Finisterre, Spain. J. Geophys. Res. Ocean. 91(C7):8470–86

McClain CR, Hardy SM. 2010. The dynamics of biogeographic ranges in the deep sea. Proc. R. Soc. London B Biol. Sci. 277(1700):3533–46

McCulloch M, Falter J, Trotter J, Montagna P. 2012a. Coral resilience to ocean acidification and global warming through pH up-regulation. Nat. Clim. Chang. 2:623–27

McCulloch M, Trotter J, Montagna P, Falter J, Dunbar R, et al. 2012b. Resilience of cold-water scleractinian corals to ocean acidification: Boron isotopic systematics of pH and saturation state up-regulation. Geochim. Cosmochim. Acta. 87:21–34

McGillicuddy DJ, Lavelle JW, Thurnherr AM, Kosnyrev VK, Mullineaux LS. 2010. Larval dispersion along an axially symmetric mid-ocean ridge. Deep. Res. Part I Oceanogr. Res. 57(7):880–92

McGrath T, Nolan G, McGovern E. 2012. Chemical characteristics of water masses in the Rockall Trough. Deep. Res. Part I Oceanogr. Res. 61:57–73

McIntyre FD, Drewery J, Eerkes-Medrano D, Neat FC. 2016. Distribution and diversity of deep-sea sponge grounds on the Rosemary Bank Seamount, NE Atlantic. Mar. Biol. 163(6):1–11

McVeigh DM, Eggleston DB, Todd AC, Young CM, He RY. 2017. The influence of larval migration and dispersal depth on potential larval trajectories of a deep-sea bivalve. Deep. Res. Part I Oceanogr. Res. 127:57–64

Menezes GM, Sigler MF, Silva HM, Pinho MR. 2006. Structure and zonation of demersal fish assemblages off the Azores Archipelago (mid-Atlantic). Mar. Ecol. Prog. Ser. 324:241–60

Mienis F, de Stigter HC, de Haas H, van Weering TCE. 2009. Near-bed particle deposition and resuspension in a cold-water coral mound area at the Southwest Rockall Trough margin, NE Atlantic. Deep. Res. Part I Oceanogr. Res. 56:1026–38

Mienis F, de Stigter HC, White M, Dulneveldc G, de Haas H, van Weering TCE. 2007. Hydrodynamic controls on cold-water coral growth and carbonate-mound development at the SW and SE Rockall trough margin, NE Atlantic ocean. Deep. Res. Part I Oceanogr. Res. 54:1655–74

Mienis F, Duineveld GCA, Davies AJ, Ross SW, Seim H, et al. 2012. The influence of near-bed hydrodynamic conditions on cold-water corals in the Viosca Knoll area, Gulf of Mexico. Deep. Res. Part I Oceanogr. Res. 60:32–45

Mienis F, Duineveld GCAA, Davies AJ, Ross SW, Seim HE, et al. 2014. High-resolution ecological niche modelling of the cold-water coral *Lophelia pertusa* in the Gulf of Mexico. Deep. Res. Part I Oceanogr. Res. 93:1–32

Miller KJ, Gunasekera RM. 2017. A comparison of genetic connectivity in two deep sea corals to examine whether seamounts are isolated islands or stepping stones for dispersal. Sci. Rep. 7:46103

Mironov AN, Gebruk A, J Southward A, Mironov AN, Krylova E. 2006. Biogeography of the North Atlantic Seamounts Origin of the Fauna of the Meteor Seamounts, North-Eastern Atlantic. Moscow: KMK Scientific Press Ltd.

Moalic Y, Desbruyères D, Duarte CM, Rozenfeld AF, Bachraty C, Arnaud-Haond S. 2012. Biogeography revisited with network theory: Retracing the history of hydrothermal vent communities. Syst. Biol. 61(1):127–37

Mohn C, Rengstorf A, White M, Duineveld G, Mienis F, et al. 2014. Linking benthic hydrodynamics and cold-water coral occurrences: A high-resolution model study at three cold-water coral provinces in the NE Atlantic. Prog. Oceanogr. 122:92–104

Montero-Serrano J-C, Frank N, Colin C, Wienberg C, Eisele M. 2011. The climate influence on the mid-depth Northeast Atlantic gyres viewed by cold-water corals. Geophys. Res. Lett. 38: L19604

Mora C, Wei C-L, Rollo A, Amaro T, Baco AR, et al. 2013. Biotic and Human Vulnerability to Projected Changes in Ocean Biogeochemistry over the 21st Century. PLOS Biol. 11(10):e1001682

Morato T, Kvile K, Taranto GH, Tempera F, Narayanaswamy BE, et al. 2013. Seamount physiography and biology in the north-east Atlantic and Mediterranean Sea. Biogeosciences. 10(5):3039–54

Morato T, Machete M, Kitchingman A, Tempera F, Lai S, et al. 2008. Abundance and distribution of seamounts in the Azores. Mar. Ecol. Prog. Ser. 357:17–21

Morrison CL, Ross SW, Nizinski MS, Brooke S, Järnegren J, et al. 2011. Genetic discontinuity among regional populations of *Lophelia pertusa* in the North Atlantic Ocean. Conserv. Genet. 12:713–29

Mortensen PB, Buhl-Mortensen L. 2004. Distribution of deep-water gorgonian corals in relation to benthic habitat features in the Northeast Channel (Atlantic Canada). Mar. Biol. 144:1223–38

Mortensen PB, Buhl-Mortensen L, Jr GDC. 2006. distribution of deep-water corals in Atlantic Canada. Proc. 10th Int. Coral Reef Symp.:247–277

Mortensen PB, Fosså JH. 2006. Species diversity and spatial distribution of invertebrates on deep–water *Lophelia* reefs in Norway. Proc. 10th Int. Coral Reef Symp.:849–68.

Mortensen PB, Hovland M, Brattegard T, Farestveit R. 1995. Deep water bioherms of the scleractinian coral *Lophelia pertusa* (L.) at 64 N on the Norwegian shelf: structure and associated megafauna. Sarsia. 80:145–58

Mortensen PB, Hovland T, Fossa JH, Furevik DM, Fosså JH, Furevik DM. 2001. Distribution, abundance and size of *Lophelia pertusa* coral reefs in mid-Norway in relation to seabed characteristics. J. Mar. Biol. Assoc. United Kingdom. 81(4):581–97

Moser ML, Ross SW, Sulak KJ. 1996. Metabolic responses to hypoxia of *Lycenchelys verrillii* (wolf eelpout) and *Glyptocephalus cynoglossus* (witch flounder): Sedentary bottom fishes of the Hatteras/Virginia middle slope. Mar. Ecol. Prog. Ser. 144(1–3):57–61

Movilla J, Orejas C, Calvo E, Gori A, Lopez-Sanz A, et al. 2014. Differential response of two Mediterranean cold-water coral species to ocean acidification. Coral Reefs. 33:675–86

Mulder T, Voisset M, Lecroart P, Le Drezen E, Gonthier E, et al. 2003. The Gulf of Cadiz: An unstable giant contouritic levee. Geo-Marine Lett. 23(1):7–18

Mulder T, Zaragosi S, Garlan T, Mavel J, Cremer M, et al. 2012. Present deep-submarine canyons activity in the Bay of Biscay (NE Atlantic). Mar. Geol. 295–298:113–27

Mullineaux LS, Mills SW, Sweetman AK, Beaudreau AH, Metaxas A, Hunt HL. 2005. Vertical, lateral and temporal structure in larval distributions at hydrothermal vents. Mar. Ecol. Prog. Ser. 293:1–16

Murillo F, Kenchington E, Tompkins G, Beazley L, Baker E, et al. 2018. Sponge assemblages and predicted archetypes in the eastern Canadian Arctic. Mar. Ecol. Prog. Ser. 597:115–35

Murillo FJ, Durán Muñoz P, Altuna A, Serrano A. 2011. Distribution of deep-water corals of the Flemish Cap, Flemish Pass, and the Grand Banks of Newfoundland (Northwest Atlantic Ocean): Interaction with fishing activities. ICES J. Mar. Sci. 68(2):319–32

Murillo FJ, Kenchington E, Lawson JM, Li G, Piper DJW. 2016a. Ancient deep-sea sponge grounds on the Flemish Cap and Grand Bank, northwest Atlantic. Mar. Biol. 163(3):1–11

Murillo FJ, Muñoz PD, Cristobo J, Ríos P, González C, et al. 2012. Deep-sea sponge grounds of the Flemish Cap, Flemish Pass and the Grand Banks of Newfoundland (Northwest Atlantic Ocean): Distribution and species composition. Mar. Biol. Res. 8(9):842–54

Murillo FJ, Serrano A, Kenchington E, Mora J. 2016b. Epibenthic assemblages of the Tail of the Grand Bank and Flemish Cap (northwest Atlantic) in relation to environmental parameters and trawling intensity. Deep. Res. Part I Oceanogr. Res. 109:99–122

Naumann MS, Orejas C, Ferrier-Pagès C. 2013. High thermal tolerance of two Mediterranean cold-water coral species maintained in aquaria. Coral Reefs. 1–6

Naumann MS, Orejas C, Ferrier-Pagès C. 2014. Species-specific physiological response by the cold-water corals *Lophelia pertusa* and *Madrepora oculata* to variations within their natural temperature range. Deep. Res. Part II Top. Stud. Oceanogr. 99:36–41

Navas JM, Miller PL, Henry L-AA, Hennige SJ, Roberts JM. 2014. Ecohydrodynamics of cold-water coral reefs: A case study of the Mingulay Reef Complex (Western Scotland). PLoS One. 9(5): e98218

Nelson CH, Baraza J, Maldonado A, Rodero J, Escutia C, et al. 1999. Influence of the Atlantic inflow and Mediterranean outflow currents on late Quaternary sedimentary facies of the Gulf of Cadiz continental margin. Mar. Geol. 155(1–2):99–129

New AL, Smythe-Wright D. 2001. Aspects of the circulation in the Rockall Trough. Cont. Shelf Res. 21(8):777–810

Newton AW, Peach KJ, Coull KA, Gault M, Needle CL. 2008. Rockall and the Scottish haddock fishery. Fish. Res. 94(2):133–40

O'Hara TD, Tittensor DP. 2010. Environmental drivers of ophiuroid species richness on seamounts. Mar. Ecol. 31(Suppl. 1):26–38

Obelcz J, Brothers D, Chaytor J, Brink U ten, Ross SW, Brooke S. 2014. Geomorphic characterization of four shelf-sourced submarine canyons along the U.S. Mid-Atlantic continental margin. Deep. Res. Part II Top. Stud. Oceanogr. 104:106–19

Olabarria C, Sanders HL, Allen JA, Sanders HL. 2005. Patterns of bathymetric zonation of bivalves in the Porcupine Seabight and adjacent Abyssal plain, NE Atlantic. Deep. Res. Part I Oceanogr. Res. 52(1):15–31

Olds AD, Connolly RM, Pitt KA, Maxwell PS. 2012. Habitat connectivity improves reserve performance. Conserv. Lett. 5(1):56–63

Olu-Le Roy K, Sibuet M, Fiala-Médioni A, Gofas S, Salas C, et al. 2004. Cold seep communities in the deep eastern Mediterranean Sea: Composition, symbiosis and spatial distribution on mud volcanoes. Deep. Res. Part I Oceanogr. Res. 51(12):1915–36

Orejas C, Gori A, Rad-menéndez C, Last KS, Davies AJ, et al. 2016. The effect of flow speed and food size on the capture efficiency and feeding behaviour of the cold-water coral *Lophelia pertusa*. J. Exp. Mar. Bio. Ecol. 481:34–40

Orr JC, Fabry VJ, Aumont O, Bopp L, Doney SC, et al. 2005. Anthropogenic ocean acidification over the twenty-first century and its impact on calcifying organisms. Nature. 437:681–86

Palanques A, Durrieu de Madron X, Puig P, Fabres J, Guillén J, et al. 2006. Suspended sediment fluxes and transport processes in the Gulf of Lions submarine canyons. The role of storms and dense water cascading. Mar. Geol. 234:43–61

Pape E, Bezerra TN, Jones DOBB, Vanreusel A. 2013a. Unravelling the environmental drivers of deep-sea nematode biodiversity and its relation with carbon mineralisation along a longitudinal primary productivity gradient. Biogeosciences. 10(5):3127–43

Pape E, Jones DOB, Manini E, Bezerra TN, Vanreusel A. 2013b. Benthic-Pelagic Coupling: Effects on Nematode Communities along Southern European Continental Margins. PLoS One. 8:14

Parra HE, Pham CK, Menezes GM, Rosa A, Tempera F, Morato T. 2017. Predictive modeling of deep-sea fish distribution in the Azores. Deep Sea Res. Part II Top. Stud. Oceanogr. 145:49–60

Patarnello T, Volckaert FAMJ, Castilho R. 2007. Pillars of Hercules: Is the Atlantic-Mediterranean transition a phylogeographical break? Mol. Ecol. 16(21):4426–44

Payne MR, Egan A, Fässler SMM, Hátún H, Holst JC, et al. 2012. The rise and fall of the NE Atlantic blue whiting (*Micromesistius poutassou*). Mar. Biol. Res. 8(5–6):475–87

Pérez-Losada M, Nolte MJ, Crandall KA, Shaw PW. 2007. Testing hypotheses of population structuring in the Northeast Atlantic Ocean and Mediterranean Sea using the common cuttlefish Sepia officinalis. Mol. Ecol. 16(13):2667–79

Perez FF, Fontela M, García-Ibáñez MI, Mercier H, Velo A, et al. 2018. Meridional overturning circulation conveys fast acidification to the deep Atlantic Ocean. Nature. 554(7693):515–18

Peterson WH, Rooth CGH. 1976. Formation and exchange of deep water in the Greenland and Norwegian seas. Deep Sea Res. Oceanogr. Abstr. 23(4):273–83

Pham CK, Vandeperre F, Menezes G, Porteiro F, Isidro E, Morato T. 2015. The importance of deep-sea vulnerable marine ecosystems for demersal fish in the Azores. Deep. Res. Part I Oceanogr. Res. 96:80–88

Pickart RS, Straneo F, Moore GWK. 2003. Is Labrador Sea Water formed in the Irminger basin? Deep. Res. Part I Oceanogr. Res. 50(1):23–52

Piepenburg D, Ambrose WG, Brandt A, Renaud PE, Ahrens MJ, Jensen P. 1997. Benthic community patterns reflect water column processes in the Northeast Water polynya (Greenland). J. Mar. Syst. 10(1):467–82

Pingree R, Le Cann B. 1990. Structure, Strength and Seasonality of the Slope Currents in the Bay of Biscay Region, Vol. 70

Pinheiro LM, Ivanov MK, Sautkin A, Akhmanov G, Magalhães VH, et al. 2003. Mud volcanism in the Gulf of Cadiz: Results from the TTR-10 cruise. Mar. Geol. 195(1–4):131–51

Planes S, Jones GP, Thorrold SR. 2009. Larval dispersal connects fish populations in a network of marine protected areas. Proc. Natl. Acad. Sci. USA. 106(14):5693–97

Pollard RT, Griffttths MJ, Cunningham SA, Read JF, Pérez FF, Ríos AF. 1996. Vivaldi 1991 - A study of the formation, circulation and ventilation of Eastern North Atlantic Central Water. Prog. Oceanogr. 37(2):167–92

Pollard RT, Read JF, Holliday NP, Leach H. 2004. Water masses and circulation pathways through the Iceland Basin during Vivaldi 1996. J. Geophys. Res. Ocean. 109: C04004

Pomar L, Morsilli M, Hallock P, Bádenas B. 2012. Internal waves, an under-explored source of turbulence events in the sedimentary record. Earth-Science Rev. 111:56–81

Pörtner HO, Farrell AP. 2008. Physiology and Climate Change. Science. 322(5902):690-92

Price ARG, Keeling MJ, O'Callghan CJ. 1999. Ocean-scale patterns of 'biodiversity' of Atlantic asteroids determined from taxonomic distinctness and other measures. Biol. J. Linn. Soc. 66:187–203

Priede IG, Godbold JA, King NJ, Collins MA, Bailey DM, Gordon JDM. 2010. Deep-sea demersal fish species richness in the Porcupine Seabight, NE Atlantic Ocean: global and regional patterns. Mar. Ecol. 31:247-260

Purkey SG, Johnson GC. 2010. Warming of Global Abyssal and Deep Southern Ocean Waters between the 1990s and 2000s: Contributions to Global Heat and Sea Level Rise Budgets. J. Clim. 23(23):6336–51

Purser A, Orejas C, Gori A, Unnithan V, Thomsen L. 2013. Local variation in the distribution of benthic megafauna species associated with cold-water coral reefs on the Norwegian margin. Cont. Shelf Res. 54:37–51

Pusceddu A, Carugati L, Gambi C, Mienert J, Petani B, et al. 2016. Organic matter pools, C turnover and meiofaunal biodiversity in the sediments of the western Spitsbergen deep continental margin, Svalbard Archipelago. Deep. Res. Part I Oceanogr. Res. 107:48–58

Raddatz J, Rüggeberg A, Liebetrau V, Foubert A, Hathorne EC, et al. 2014. Environmental boundary conditions of cold-water coral mound growth over the last 3 million years in the Porcupine Seabight, Northeast Atlantic. Deep Sea Res. Part II Top. Stud. Oceanogr. 99:227–36

Radice VZ, Quattrini AM, Wareham VE, Edinger EN, Cordes EE. 2016. Vertical water mass structure in the North Atlantic influences the bathymetric distribution of species in the deep-sea coral genus *Paramuricea*. Deep. Res. Part I Oceanogr. Res. 11:253–63

Ramalho L V., López-Fé CM, Rueda JL. 2018. Three species of *Reteporella* (Bryozoa: Cheilostomata) in a diapiric and mud volcano field of the Gulf of Cádiz, with the description of *Reteporella victori n. sp*. Zootaxa. 4375(1):90–104

Ramirez-Llodra E, Ballesteros M, Company JB, Dantart L, Sarda F. 2007a. Spatio-temporal variations of biomass and abundance in bathyal non-crustacean megafauna in the Catalan Sea (North-western Mediterranean). Mar. Biol. 153:297–309

Ramirez-Llodra E, Brandt A, Danovaro R, De Mol B, Escobar E, et al. 2010. Deep, diverse and definitely different: Unique attributes of the world's largest ecosystem. Biogeosciences. 7(9):2851–99

Ramirez-Llodra E, Shank T, German C. 2007b. Biodiversity and Biogeography of Hydrothermal Vent Species: Thirty Years of Discovery and Investigations. Oceanography. 20(1):30–41

Raybaud V, Tambutté S, Ferrier-Pagès C, Reynaud S, Venn AA, et al. 2017. Computing the carbonate chemistry of the coral calcifying medium and its response to ocean acidification. J. Theor. Biol. 424:26–36

Read JF. 2000. CONVEX-91: water masses and circulation of the Northeast Atlantic subpolar gyre. Prog. Oceanogr. 48(4):461–510

Reichart GJ, Lourens LJ, Zachariasse WJ. 1998. Temporal variability in the northern Arabian Sea oxygen minimum zone (OMZ) during the last 225,000 years. Paleoceanography. 13(6):607–21

Reid JL. 1979. On the contribution of the Mediterranean Sea outflow to the Norwegian-Greenland Sea. Deep. Res. Part I Oceanogr. Res. 26(11):1199–1223

Rengstorf AM, Mohn C, Brown C, Wisz MS, Grehan AJ. 2014. Predicting the distribution of deep-sea vulnerable marine ecosystems using high-resolution data: Considerations and novel approaches. Deep. Res. Part I Oceanogr. Res. 93:72–82

Rengstorf AM, Yesson C, Brown C, Grehan AJ. 2013. High-resolution habitat suitability modelling can improve conservation of vulnerable marine ecosystems in the deep sea. J. Biogeogr. 40(9):1702–14

Reverdin G, Niiler PP, Valdimarsson H. 2003. North Atlantic Ocean surface currents. J. Geophys. Res. Ocean. 108(C1):2–21

Rex MA, Crame JA, Stuart CT, Clarke A. 2005. Large-scale biogeographic patterns in marine mollusks: a confluence of history and productivity? Ecology. 86(9):2288–97

Rex MA, Etter RJ, Morris JS, Crouse J, McClain CR, et al. 2006. Global bathymetric patterns of standing stock and body size in the deep-sea benthos . Mar. Ecol. Prog. Ser. 317:1–8

Rex MA, Stuart CT, Hessler RR, Allen JA, Sanders HL, Wilson GDF. 1993. Global-scale latitudinal patterns of species diversity in the deep-sea benthos. Nature. 365:636

Rhein M, Steinfeldt R, Kieke D, Stendardo I, Yashayaev I. 2017. Ventilation variability of Labrador Sea Water and its impact on oxygen and anthropogenic carbon: a review. Philos. Trans. R. Soc. London. Ser. A Math. Phys. Eng. Sci. 375(2102):

Rice AL, Billett DSM, Thurston MH, Lampitt RS. 1991. The institute of oceanographic sciences biology programme in the Porcupine Seabight: Background and general introduction. J. Mar. Biol. Assoc. United Kingdom. 71(2):281–310

Rice AL, Thurston MH, New AL. 1990. Dense aggregations of a hexactinellid sponge, *Pheronema carpenteri*, in the Porcupine Seabight (northeast Atlantic Ocean), and possible causes. Prog. Oceanogr. 24:179–96

Ries JB, Cohen AL, McCorkle DC. 2009. Marine calcifiers exhibit mixed responses to CO_2-induced ocean acidification. Geology. 37:1131–34

Ríos AF, Pérez FF, Fraga F. 1992. Water masses in the upper and middle North Atlantic Ocean east of the Azores. Deep. Res. Part I Oceanogr. Res. 39(3):645–58

Ritz SP, Stocker TF, Grimalt JO, Menviel L, Timmermann A. 2013. Estimated strength of the Atlantic overturning circulation during the last deglaciation. Nat. Geosci. 6:208

Rix L, De Goeij JM, Mueller CE, Struck U, Middelburg JJ, et al. 2016. Coral mucus fuels the sponge loop in warm-and cold-water coral reef ecosystems. Sci. Rep. 6:1–11

Roark EB, Guilderson TP, Dunbar RB, Fallon SJ, Mucciarone DA. 2009. Extreme longevity in proteinaceous deep-sea corals. Proc. Natl. Acad. Sci. USA. 106:5204–8

Roberts JM. 2009. Cold-Water Corals: The Biology and Geology of Deep-Sea Coral Habitats. Cambridge University Press

Roberts JM, Brown CJ, Long D, Bates CR. 2005. Acoustic mapping using a multibeam echosounder reveals cold-water coral reefs and surrounding habitats. Coral Reefs. 24:654–69

Roberts JM, Davies AJ, Henry LA, Dodds LA, Duineveld GCAA, et al. 2009. Mingulay reef complex: An interdisciplinary study of cold-water coral habitat, hydrography and biodiversity. Mar. Ecol. Prog. Ser. 397:139–51

Roberts JM, Henry LA, Long D, Hartley JP. 2008. Cold-water coral reef frameworks, megafaunal communities and evidence for coral carbonate mounds on the Hatton Bank, north east Atlantic. Facies. 54:297–316

Roberts JM, Long D, Wilson JB, Mortensen PB, Gage JD. 2003. The cold-water coral *Lophelia pertusa* (Scleractinia) and enigmatic seabed mounds along the north-east Atlantic margin: Are they related? Mar. Pollut. Bull. 46(1):7–20

Roberts JM, Roberts JM, Wheeler AJ, Freiwald A. 2006. Reefs of the deep : The biology and geology of cold-water coral ecosystems. Science. 312:543–48

Robinson LF, Adkins J, Scheirer D, Fernandez DP, Gagnon a C, Waller R. 2007. Deep-sea scleractinian coral age and depth distributions in the NW Atlantic for the last 225 thousand years. Bull. Mar. Sci. 81(3):371–91

Rodolfo-Metalpa R, Montagna P, Aliani S, Borghini M, Canese S, et al. 2015. Calcification is not the Achilles' heel of cold-water corals in an acidifying ocean. Glob. Chang. Biol. 21:2238–48

Rodrigues CF, Hilário A, Cunha MR. 2013. Chemosymbiotic species from the Gulf of Cadiz (NE Atlantic): Distribution, life styles and nutritional patterns. Biogeosciences. 10(4):2569–81

Rogers AD. 1999. The biology of *Lophelia pertusa* (Linnaeus 1758) and other deep-water reef-forming corals and impacts from human activities. Int. Rev. Hydrobiol. 84(4):315–406

Rogers AD. 2000. The role of the oceanic oxygen minima in generating biodiversity in the deep sea. Deep. Res. Part II Top. Stud. Oceanogr. 47(1–2):119–48

Rogerson M, Rohling EJ, Weaver P, Rogerson C. 2006. Promotion of Meridional Overturning by Mediterranean-Derived Salt during the Last Deglaciation, Vol. 21

Ross SW, E.F. AI, Ott. J. 2001. Literature and data inventory related to the Hatteras Middle Slope ("The Point") area off North Carolina. Occas. Pap. NC State Museum Nat. Sci. NC Biol. Surv. 13:352

Ross SW, Rhode M, Quattrini AM. 2015. Demersal fish distribution and habitat use within and near Baltimore and Norfolk Canyons, U.S. middle Atlantic slope. Deep. Res. Part I Oceanogr. Res. 103:137–54

Rowden AA, Dower JF, Schlacher TA, Consalvey M, Clark MR. 2010. Paradigms in seamount ecology: fact, fiction and future. Mar. Ecol. 31:226–41

Rowe GT, Gage JD, Tyler PA, Rowe GT. 1992. Deep-Sea Biology: A Natural History of Organisms at the Deep-Sea Floor. John D. Gage , Paul A. Tyler . Q. Rev. Biol. 67(2):224–25

Rueda JL, Gonzalez-Garcia E, Krutzky C, Lopez-Rodriguez FJ, Bruque G, et al. 2016. From chemosynthesis-based communities to cold-water corals: Vulnerable deep-sea habitats of the Gulf of Cadiz. Mar. Biodivers. 46:473–82

Ruggeberg A, Flogel S, Dullo WC, Hissmann K, Freiwald A. 2011. Water mass characteristics and sill dynamics in a subpolar cold-water coral reef setting at Stjernsund, northern Norway. Mar. Geol. 282:5–12

Rüggeberg A, Dullo C, Dorschel B, Hebbeln D. 2007. Environmental changes and growth history of a cold-water carbonate mound (Propeller Mound, Porcupine Seabight). Int. J. Earth Sci. 96(1):57–72

Ruhl HA, Smith KL. 2004. Shifts in deep-sea community structure linked to climate and food supply. Science. 305(5683):513–15

Ruiz-Villarreal M, González-Pola C, Diaz del Rio G, Lavin A, Otero P, et al. 2006. Oceanographic conditions in North and Northwest Iberia and their influence on the Prestige oil spill. Mar. Pollut. Bull. 53(5–7):220–38

Salas C. 1996. Marine Bivalves from off the Southern Iberian Peninsula collected by the Balgim and Fauna 1 expeditions. Haliotis. 25:33–100

Sameoto JA, Metaxas A. 2008. Interactive effects of haloclines and food patches on the vertical distribution of 3 species of temperate invertebrate larvae. J. Exp. Mar. Bio. Ecol. 367(2):131–41

Sampaio I, Carreiro-Silva M, Ocaña O, Stanković D. 2018. Azores as a hotspot for biodiversity of Octocorals in the Atlantic Ocean. 4th World Conf. Mar. Biodivers.

Sánchez-Leal RF, Bellanco MJ, Fernández-Salas LM, García-Lafuente J, Gasser-Rubinat M, et al. 2017. The Mediterranean Overflow in the Gulf of Cadiz: A rugged journey. Sci. Adv. 3(11):1–12

Sánchez RF, Relvas P. 2003. Spring–summer climatological circulation in the upper layer in the region of Cape St. Vincent, Southwest Portugal. ICES J. Mar. Sci. 60:1232–50

Sanders HL. 1968. Marine benthic diversity - A comparative study. Am. Nat. 102:243–82

Santana Y. 2018. Biodiversity and benthic megafaunal communities inhabiting the Formigas Bank. Msc Thesis. University of Ghent.

Santos M, Moita MT, Bashmachnikov I, Menezes GM, Carmo V, et al. 2013. Phytoplankton variability and oceanographic conditions at Condor seamount, Azores (NE Atlantic). Deep. Res. Part II Top. Stud. Oceanogr. 98:52–62

Sarafanov A, Falina A, Mercier H, Sokov A, Lherminier P, et al. 2012. Mean full-depth summer circulation and transports at the northern periphery of the Atlantic Ocean in the 2000s. J. Geophys. Res. Ocean. 117: C01014

Schaff T, Levin L, Blair N, Demaster D, Pope R, Boehme S. 1992. Spatial heterogeneity of benthos on the Carolina continental slope: large (100km)-scale variation. Mar. Ecol. Prog. Ser. 88(2–3):143–60

Schmittner A. 2005. Marine ecosystem decline caused by a reduction of the Atlantic Meridional Overturning (AMO) circulation. Lett. To Natur. 434:628–33

Schönfeld J, Zahn R. 2000. Late Glacial to Holocene history of the Mediterranean outflow. Evidence from benthic foraminiferal assemblages and stable isotopes at the Portuguese margin. Palaeogeogr. Palaeoclimatol. Palaeoecol. 159(1–2):85–111

Serrano A, Cartes JE, Papiol V, Punzón A, García-Alegre A, et al. 2017a. Epibenthic communities of sedimentary habitats in a NE Atlantic deep seamount (Galicia Bank). J. Sea Res. 130:154–65

Serrano A, González-Irusta JM, Punzón A, García-Alegre A, Lourido A, et al. 2017b. Deep-sea benthic habitats modeling and mapping in a NE Atlantic seamount (Galicia Bank). Deep. Res. Part I Oceanogr. Res. 126(June 2016):115–27

Sherwin TJ, Read JF, Holliday NP, Johnson C. 2012. The impact of changes in North Atlantic Gyre distribution on water mass characteristics in the Rockall Trough. ICES J. Mar. Sci. 69(5):751–57

Sherwood O, Heikoop JM, Scott DB, Risk M, Guilderson TP, McKinney RA. 2005. Stable Isotopic Composition of Deep-Sea Gorgonian Corals Primnoa Spp.: A New Archive of Surface Processes, Vol. 301

Sherwood OA, Edinger EN. 2009. Ages and growth rates of some deep-sea gorgonian and antipatharian corals of Newfoundland and Labrador. Can. J. Fish. Aquat. Sci. 66(1):142–52

Sherwood OA, Lehmann MF, Schubert CJ, Scott DB, McCarthy MD. 2011. Nutrient regime shift in the western North Atlantic indicated by compound-specific 15N of deep-sea gorgonian corals. Proc. Natl. Acad. Sci. USA. 108(3):1011–15

Sitjá C, Maldonado M, Farias C, Rueda JL. 2018. Deep-water sponge fauna from the mud volcanoes of the Gulf of Cadiz (North Atlantic , Spain). J. Mar. Biol. Assoc. United Kingdom. 1–25

Skarke A, Ruppel C, Kodis M, Brothers D, Lobecker E. 2014. Widespread methane leakage from the sea floor on the northern US Atlantic margin. Nat. Geosci. 7:657

Skjoldal HR. 2004. The Norwegian Sea Ecosystem. Trondheim, Norway.: Tapir Academic Press

Smith CR, De Leo FC, Bernardino AF, Sweetman AK, Arbizu PM. 2008. Abyssal food limitation, ecosystem structure and climate change. Trends Ecol. Evol. 23(9):518–28

Smith CR, Drazen J, Mincks SL. 2006a. Deep-sea Biodiversity and Biogeography: Perspectives from the Abyss. Int. Seabed Auth. Seamount Biodivers. Symp.:1–13

Smith CR, Mincks S, DeMaster DJ. 2006b. A synthesis of bentho-pelagic coupling on the Antarctic shelf: Food banks, ecosystem inertia and global climate change. Deep. Res. Part II Top. Stud. Oceanogr. 53:875–94

Smith JE, Risk MJ, Schwarcz HP, McConnaughey TA. 1997. Rapid climate change in the North Atlantic during the Younger Dryas recorded by deep-sea corals. Nature. 386(6627):818–20

Soetaert K, Mohn C, Rengstorf A, Grehan A, Van Oevelen D. 2016. Ecosystem engineering creates a direct nutritional link between 600-m deep cold-water coral mounds and surface productivity. Sci. Rep. 6:1–9

Soltwedel T. 2000. Metazoan meiobenthos along continental margins: a review. Prog. Oceanogr. 46:59–84

Somoza L, Ercilla G, Urgorri V, León R, Medialdea T, et al. 2014. Detection and mapping of cold-water coral mounds and living *Lophelia reefs* in the Galicia Bank, Atlantic NW Iberia margin. Mar. Geol. 349:73–90

Sorbe JC. 1999. Deep-sea macrofaunal assemblages within the Benthic Boundary Layer of the Cap-Ferret Canyon (Bay of Biscay, NE Atlantic). Deep Sea Res. Part II Top. Stud. Oceanogr. 46(10):2309–29

Souto J, Berning B, Ostrovsky AN. 2016. Systematics and diversity of deep-water Cheilostomata (Bryozoa) from Galicia Bank (NE Atlantic). Zootaxa. 4067(4):401–59

Spezzaferri S, Rüggeberg A, Stalder C, Margreth S. 2013. Benthic foraminifer assemblages from Norwegian cold-water coral reefs. J. Foraminifer. Res. 43(1):21–39

Stendardo I, Gruber N. 2012. Oxygen trends over five decades in the North Atlantic. J. Geophys. Res. Ocean. 117:C11004

Stramma L, Schmidtko S, Levin LA, Johnson GC. 2010. Ocean oxygen minima expansions and their biological impacts. Deep. Res. Part I Oceanogr. Res. 57(4):587–95

Strand R, Whalan S, Webster NS, Kutti T, Fang JKH, et al. 2017. The response of a boreal deep-sea sponge holobiont to acute thermal stress. Sci. Rep. 7(1):1660

Strömberg SM, Larsson AI. 2017. Larval behavior and longevity in the cold-water coral *Lophelia pertusa* indicate potential for long distance dispersal. Front. Mar. Sci. 4(411)

Stuart CT, Rex MA. 2009. Bathymetric patterns of deep-sea gastropod species diversity in 10 basins of the Atlantic Ocean and Norwegian Sea. Mar. Ecol. Evol. Perspect. 30:164–80

Sulak K, Ross S. 2006. Lilliputian Bottom Fish Fauna of the Hatteras Upper Middle Continental Slope. J. Fish. Biol. 49:91-113

Svanson A. 1975. Physical and chemical oceanography of the Skagerrak and the Kattegat. I. Open Sea Conditions. Technical Report of Fishery Board of Sweden. Institute of Marine Research, pp. 88

Sweetman AK, Thurber AR, Smith CR, Levin LA, Mora C, et al. 2017. Major impacts of climate change on deep-sea benthic ecosystems. Elem. Sci. Anth. 5(4)

Taboada S, Pérez-Portela R. 2016. Contrasted phylogeographic patterns on mitochondrial DNA of shallow and deep brittle stars across the Atlantic-Mediterranean area. Sci. Rep. 6:1–13

Tempera F, Atchoi E, Amorim P, Gomes-Pereira J, Gonçalves J. 2013. Atlantic Area Marine Habitats: Adding new Macaronesian habitat types from the Azores to the EUNIS Habitat Classification. Horta

Tempera F, Gomes-Pereira JN, Braga-Henriques A, Porteiro F, Morato T, et al. 2012. Cataloguing deep-sea biological facies of the Azores. In Using EUNIS Habitat Classification for Benthic Mapping in European Seas. Revista de Investigación Marina, AZTI-Tecnalia. 19: 21–70

Teske PR, Sandoval-Castillo J, Van Sebille E, Waters J, Beheregaray LB. 2016. Oceanography promotes self-recruitment in a planktonic larval disperser. Sci. Rep. 6(1):34205

Thiagarajan N, Gerlach D, Roberts ML, Burke A, McNichol A, et al. 2013. Movement of deep-sea coral populations on climatic timescales. Paleoceanography. 28(2):227–36

Thiede J. 1979. History of the North Atlantic Ocean; evolution of an asymmetric zonal paleo-environment in a latitudinal ocean basin.; Deep drilling results in the Atlantic Ocean; continental margins and paleoenvironment. Maurice Ewing Ser. 3:275–96

Thiem O, Ravagnan E, Fosså JH, Berntsen J. 2006. Food supply mechanisms for cold-water corals along a continental shelf edge. J. Mar. Syst. 60:207–19

Thoma JN, Pante E, Brugler MR, France SC. 2009. Deep-sea octocorals and antipatharians show no evidence of seamount-scale endemism in the NW Atlantic. Mar. Ecol. Prog. Ser. 397:25–35

Thornalley DJR, Oppo DW, Ortega P, Robson JI, Brierley CM, et al. 2018. Anomalously weak Labrador Sea convection and Atlantic overturning during the past 150 years. Nature. 556(7700):227–30

Tittensor DP, Baco AR, Hall-Spencer JM, Orr JC, Rogers AD. 2010. Seamounts as refugia from ocean acidification for cold-water stony corals. Mar. Ecol. 31:212–25

Tittensor DP, Rex MA, Stuart CT, McClain CR, Smith CR. 2011. Species-energy relationships in deep-sea molluscs. Biol. Lett. 7(5):718–22

Tong R, Purser A, Guinan J, Unnithan V, Yu J, Zhang C. 2016. Quantifying relationships between abundances of cold-water coral *Lophelia pertusa* and terrain features: A case study on the Norwegian margin. Cont. Shelf Res. 116:13–26

Tong R, Purser A, Unnithan V, Guinan J. 2012. Multivariate statistical analysis of distribution of deep-water gorgonian corals in relation to seabed topography on the Norwegian Margin. PLoS One. 7(8): e43534

Truelove NK, Kough AS, Behringer DC, Paris CB, Box SJ, et al. 2017. Biophysical connectivity explains population genetic structure in a highly dispersive marine species. Coral Reefs. 36(1):233–44

Tsuchiya M. 1989. Circulation of the Antarctic Intermediate Water in the North Atlantic Ocean. J. Mar. Res. 47(4):747–55

Tunnicliffe V, Davies KTA, Butterfield DA, Embley RW, Rose JM, Chadwick WW. 2009. Survival of mussels in extremely acidic waters on a submarine volcano. Nat. Geosci. 2(5):344–48

Turner JT. 2002. Zooplankton fecal pellets, marine snow and sinking phytoplankton blooms. Aquat. Microb. Ecol. 27:57–102

Tursi A, Mastrototaro F, Matarrese A, Maiorano P, D'onghia G. 2004. Biodiversity of the white coral reefs in the Ionian Sea (Central Mediterranean). Chem. Ecol. 20:107–16

Ullgren JE, White M. 2010. Water mass interaction at intermediate depths in the southern Rockall Trough, northeastern North Atlantic. Deep Sea Res. Part I Oceanogr. Res. Pap. 57(2):248–57

Vad J. 2013. *Lophelia pertusa* and associated species spatial distribution patterns and density at Mingulay Reef Complex. Msc Thesis. University of Edinburgh.

van Aken HM. 2000a. The hydrography of the mid-latitude Northeast Atlantic Ocean: II: The intermediate water masses. Deep. Res. Part I Oceanogr. Res. 47(5):789–824

van Aken HM. 2000b. The hydrography of the mid-latitude northeast Atlantic Ocean: I: The deep water masses. Deep. Res. Part I Oceanogr. Res. 47(5):757–88

Van Aken HM. 2002. Surface currents in the Bay of Biscay as observed with drifters between 1995 and 1999. Deep. Res. Part I Oceanogr. Res. 49(6):1071–86

Van Aken HM, De Boer CJ. 1995. On the synoptic hydrography of intermediate and deep water masses in the Iceland Basin. Deep. Res. Part I Oceanogr. Res. 42(2):165–89

van den Beld IMJ, Bourillet J-F, Arnaud-Haond S, de Chambure L, Davies JS, et al. 2017. Cold-Water Coral Habitats in Submarine Canyons of the Bay of Biscay. Front. Mar. Sci. 4(118)

Van Dover CL, German CR, Speer KG, Parson LM, Vrijenhoek RC. 2002. Evolution and biogeography of deep-sea vent and seep invertebrates. Science. 295:1253–57

van Haren H, Mienis F, Duineveld GCA, Lavaleye MSS. 2014. High-resolution temperature observations of a trapped nonlinear diurnal tide influencing cold-water corals on the Logachev mounds. Prog. Oceanogr. 125:16–25

Van Haren H, Mienis F, Duineveld GCA, Lavaleye MSS. 2014. High-resolution temperature observations of a trapped nonlinear diurnal tide influencing cold-water corals on the Logachev mounds. Prog. Oceanogr. 125:16–25

van Oevelen D, Duineveld G, Lavaleye M, Mienis F, Soetaert K, Heip CHR. 2009. The cold-water coral community as hotspot of carbon cycling on continental margins: A food-web analysis from Rockall Bank (northeast Atlantic). Limnol. Oceanogr. 54(6):1829–44

Van Oevelen D, Mueller CE, Lundälv T, Van Duyl FC, De Goeij JM, Middelburg JJ. 2018. Niche overlap between a cold-water coral and an associated sponge for isotopically enriched particulate food sources. PLoS One. 13(3): e0194659

Van Rooij D, Blamart D, De Mol L, Mienis F, Pirlet H, et al. 2011. Cold-water coral mounds on the Pen Duick Escarpment, Gulf of Cadiz: The MiCROSYSTEMS project approach. Mar. Geol. 282(1–2):102–17

Van Rooij D, Blamart D, Kozachenko M, Henriet J-P. 2007a. Small mounded contourite drifts associated with deep-water coral banks, Porcupine Seabight, NE Atlantic Ocean. Geol. Soc. London, Spec. Publ. 276(1):225-244

Van Rooij D, Blamart D, Richter T, Wheeler A, Kozachenko M, Henriet JP. 2007b. Quaternary sediment dynamics in the Belgica mound province, Porcupine Seabight: ice-rafting events and contour current processes. Int. J. Earth Sci. 96:121–40

Van Rooij D, De Mol L, Le Guilloux E, Wisshak M, Huvenne VAI, et al. 2010. Environmental setting of deep-water oysters in the Bay of Biscay. Deep. Res. Part I Oceanogr. Res. 57(12):1561–72

Van Soest RWM, De Voogd NJ. 2015. Sponge species composition of north-east Atlantic cold-water coral reefs compared in a bathyal to inshore gradient. J. Mar. Biol. Assoc. United Kingdom. 95(7):1461–74

Vazquez-Rodriguez M, Perez FF, Velo A, Rios AF, Mercier H. 2012. Observed acidification trends in North Atlantic water masses. Biogeosciences. 9(12):5217–30

Vázquez JT, Medialdea T, Ercilla G, Somoza L, Estrada F, et al. 2008. Cenozoic deformational structures on the Galicia Bank Region (NW Iberian continental margin). Mar. Geol. 249(1–2):128–49

Verkaik K, Hamel JF, Mercier A. 2017. Impact of ocean acidification on reproductive output in the deep-sea annelid Ophryotrocha sp. (Polychaeta: *Dorvilleidae*). Deep. Res. Part II Top. Stud. Oceanogr. 137:368–76

Vetter EW, Dayton PK. 1998. Macrofaunal communities within and adjacent to a detritus-rich submarine canyon system. Deep. Res. Part II Top. Stud. Oceanogr. 45:25–54

Wade IP, Ellett DJ, Heywood KJ. 1997. The influence of intermediate waters on the stability of the eastern North Atlantic. Deep. Res. Part I Oceanogr. Res. 44(8):1405–26

Wagner H, Purser A, Thomsen L, Jesus CC, Lundälv T, Lundalv T. 2011. Particulate organic matter fluxes and hydrodynamics at the Tisler cold-water coral reef. J. Mar. Syst. 85(1–2):19–29

Wall M, Ragazzola F, Foster LC, Form A, Schmidt DN. 2015. pH up-regulation as a potential mechanism for the cold-water coral *Lophelia pertusa* to sustain growth in aragonite undersaturated conditions. Biogeosciences. 12(23):6869–80

Wang XT, Prokopenko MG, Sigman DM, Adkins JF, Robinson LF, et al. 2014. Isotopic composition of carbonate-bound organic nitrogen in deep-sea scleractinian corals: A new window into past biogeochemical change. Earth Planet. Sci. Lett. 400:243–50

Wangensteen OS, Turon X, Pérez-Portela R, Palacín C. 2012. Natural or Naturalized? Phylogeography Suggests That the Abundant Sea Urchin *Arbacia lixula* Is a Recent Colonizer of the Mediterranean. PLoS One. 7(9): e45067

Watling L, Guinotte J, Clark MR, Smith CR. 2013. A proposed biogeography of the deep ocean floor. Prog. Oceanogr. 111:91–112

Wheeler AJ, Beyer A, Freiwald A, de Haas H, Huvenne VAI, et al. 2007. Morphology and environment of cold-water coral carbonate mounds on the NW European margin. Int. J. Earth Sci. 96(1):37–56

White M. 2003. Comparison of near seabed currents at two locations in the Porcupine Sea Bight - Implications for benthic fauna. J. Mar. Biol. Assoc. United Kingdom. 83(4):683–86

White M, Bashmachnikov I, Arístegui J, Martins A. 2007a. Physical Processes and Seamount Productivity. In Seamounts: Ecology, Fisheries & Conservation, eds. TJ Pitcher, T Morato, PJB Hart, MR Clark, N Haggan, RS Santos, pp. 65–84. Oxford: Blackwell Publishing

White M, Dorschel B. 2010. The importance of the permanent thermocline to the cold water coral carbonate mound distribution in the NE Atlantic. Earth Planet. Sci. Lett. 296:395–402

White M, Mohn C, de Stigter H, Mottram G. 2005. Deep-water coral development as a function of hydrodynamics and surface productivity around the submarine banks of the Rockall Trough, NE Atlantic. Cold-Water Corals Ecosyst. 503–14

White M, Roberts JM, van Weering T. 2007b. Do bottom-intensified diurnal tidal currents shape the alignment of carbonate mounds in the NE Atlantic? Geo-Marine Lett. 27:391–97

White M, Wolff GA, Lundälv T, Guihen D, Kiriakoulakis K, et al. 2012. Cold-water coral ecosystem (Tisler Reef, Norwegian shelf) may be a hotspot for carbon cycling. Mar. Ecol. Prog. Ser. 465:11–23

Wienberg C, Beuck L, Heidkamp S, Hebbeln D, Freiwald A, et al. 2008. Franken Mound: facies and biocoenoses on a newly-discovered “carbonate mound” on the western Rockall Bank, NE Atlantic. Facies. 54(1):1–24

Wienberg C, Hebbeln D, Fink HG, Mienis F, Dorschel B, et al. 2009. Scleractinian cold-water corals in the Gulf of Cádiz-First clues about their spatial and temporal distribution. Deep. Res. Part I Oceanogr. Res. 56(10):1873–93

Wienberg C, Titschack J, Freiwald A, Frank N, Lundälv T, et al. 2018. The giant Mauritanian cold-water coral mound province: Oxygen control on coral mound formation. Quat. Sci. Rev. 185:135–52

Wienberg C, Witschack J. 2017. Framework-forming scleractinian cold-water corals through space and time: a late Quaternary North Atlantic perspective. In Marine Animal Forests: The Ecology of Benthic Biodiversity Hotspots, eds. S Rossi, L Bramanti, A Gori, C Orejas, pp. 1–34. Switzerland: Springer International Publishing

Wild C, LM W, Mayr C, SI S, Allers E, Lundälv T. 2009. Microbial degradation of cold-water coral-derived organic matter: potential implication for organic C cycling in the water column above Tisler Reef . Aquat. Biol. 7(1–2):71–80

Willig MR, Kaufman DM, Stevens RD. 2003. Latitudinal Gradients of Biodiversity: Pattern, Process, Scale, and Synthesis. Annu. Rev. Ecol. Evol. Syst. 34(1):273–309

Wilson AM, Raine R, Mohn C, White M. 2015. Nepheloid layer distribution in the Whittard Canyon, NE Atlantic Margin. Mar. Geol. 367:130–42

Wilson RP, Mcmahon CR. 2015. Dispersal and population connectivity in the deep North Atlantic estimated from physical transport processes. Deep. Res. 4(3):147–54

Wilson SK, Graham NAJ, Polunin NVC. 2007. Appraisal of visual assessments of habitat complexity and benthic composition on coral reefs. Mar. Biol. 151:1069–76

Wisshak M, Freiwald A, Lundalv T, Gektidis M. 2005. The physical niche of the bathyal Lophelia pertusa in a non-bathyal setting: environmental controls and palaeoecological implications. In Cold-Water Corals and Ecosystems, eds. A Freiwald, J Roberts, pp. 979–1001

Wisshak M, Schönberg CHL, Form A, Freiwald A. 2012. Ocean Acidification Accelerates Reef Bioerosion. PLoS One. 7(9):e45124

Wisshak M, Schönberg CHL, Form A, Freiwald A. 2014. Sponge bioerosion accelerated by ocean acidification across species and latitudes? Helgol. Mar. Res. 68(2):253–62

Wlodarska-Kowalczuk M, Kendall MA, Marcin Weslawski J, Klages M, Soltwedel T. 2004. Depth gradients of benthic standing stock and diversity on the continental margin at a high-latitude ice-free site (off Spitsbergen, 79°N). Deep. Res. Part I Oceanogr. Res. 51(12):1903–14

Woolsey ES, Byrne M, Baird AH. 2013. The effects of temperature on embryonic development and larval survival in two scleractinian corals. Mar. Ecol. Prog. Ser. 493:179–84

Woulds C, Cowie G. 2007. Oxygen as a control on sea floor biological communities and their roles in sedimentary carbon cycling. Limnol. Oceanogr. 52(4):1698–1709

Xavier J, Van Soest R. 2007. Demosponge fauna of Ormonde and Gettysburg Seamounts (Gorringe Bank, north-east Atlantic): Diversity and zoogeographical affinities. J. Mar. Biol. Assoc. United Kingdom. 87(6):1643–53

Xie RC, Marcantonio F, Schmidt MW. 2012. Deglacial variability of Antarctic Intermediate Water penetration into the North Atlantic from authigenic neodymium isotope ratios. Paleoceanography. 27(3):1–12

Yashayaev I. 2007. Hydrographic changes in the Labrador Sea, 1960–2005. Prog. Oceanogr. 73(3):242–76

Yashayaev I, Loder JW. 2016. Recurrent replenishment of Labrador Sea Water and associated decadal-scale variability. J. Geophys. Res. Ocean. 121(11):8095–8114

Yashayaev I, Loder JW. 2017. Further intensification of deep convection in the Labrador Sea in 2016. Geophys. Res. Lett. 44(3):1429–38

Yashayaev I, Seidov D, Demirov E. 2015. A new collective view of oceanography of the Arctic and North Atlantic basins. Prog. Oceanogr. 132:1–21

Yasuhara M, Danovaro R. 2014. Temperature impacts on deep-sea biodiversity. Biol. Rev. 91(2):275–87

Yearsley JM, Sigwart JD. 2011. Larval transport modeling of deep-sea invertebrates can aid the search for undiscovered populations. PLoS One. 6(8):e23063

Yesson C, Taylor ML, Tittensor DP, Davies AJ, Guinotte J, et al. 2012. Global habitat suitability of cold-water octocorals. J. Biogeogr. 39(7):1278–92

Young CM, He R, Emlet RB, Li Y, Qian H, et al. 2012. Dispersal of deep-sea larvae from the intra-American seas: Simulations of trajectories using ocean models. Integr. Comp. Biol. 52(4):483–96

Zardus JD, Etter RJ, Chase MR, Rex MA, Boyle EE. 2006. Bathymetric and geographic population structure in the pan-Atlantic deep-sea bivalve *Deminucula atacellana* (Schenck, 1939). Mol. Ecol. 15(3):639–51

Zenk W, Armi L. 1990. The complex spreading pattern of Mediterranean Water off the Portuguese continental slope. Deep Sea Res. Part A. Oceanogr. Res. Pap. 37(12):1805–23

Zheng M Di, Cao L. 2014. Simulation of global ocean acidification and chemical habitats of shallow- and cold-water coral reefs. Adv. Clim. Chang. Res. 5(4):189–96

3. Case Studies on Effects of Hydrography and Oceanography on North Atlantic VME Biodiversity and Biogeography

Summary

The comprehensive synthesis provided by Section 2 of Deliverable 3.2 identified several hydrograhic and oceanographic variables that could exert strong control of biodiversity and biogeography of VMEs and their biological communities in ATLAS Case Studies. Six of these Case Studies were selected for more in-depth empirical studies.

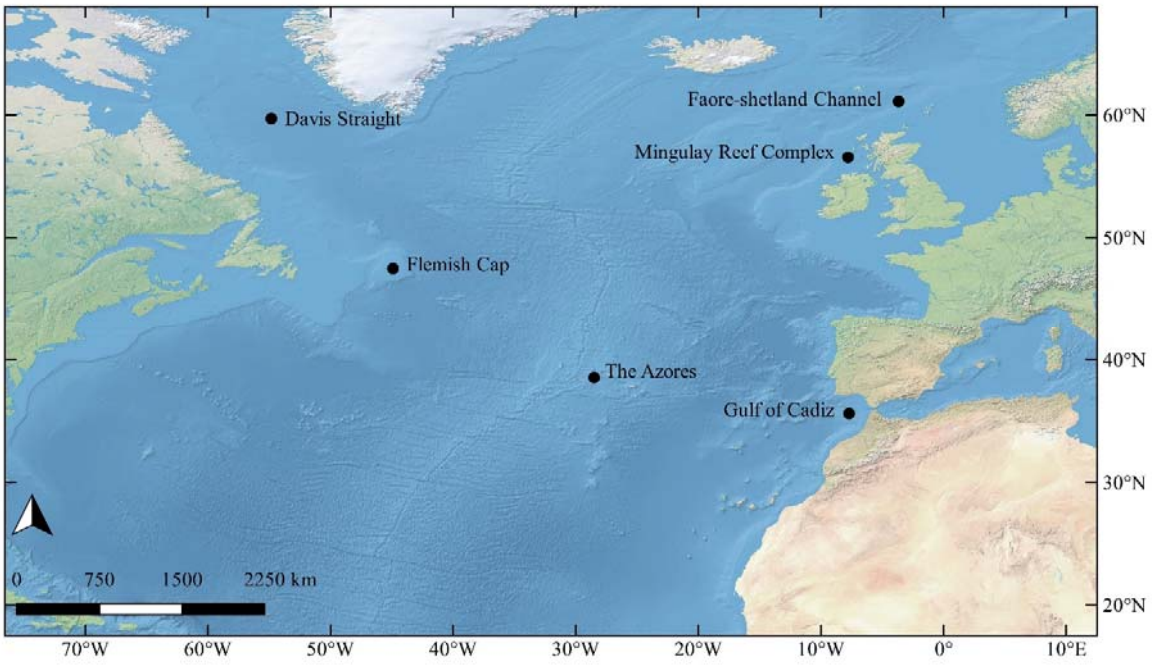

In this second half of Deliverable 3.2 we performed in-depth analyses regarding effects of:

- 3.1 and 3.2: North Atlantic gyre dynamics (Mingulay Reef Complex) and effects of water mass properties including temperature, salinity and oxygen relative to anthropogenic pressures (Faroe Shetland Channel);
- 3.3: sea water temperature in relation to interspecific competition, VME habitat-structuring, and antropogenic pressures (Flemish Cap and the continental slope);
- 3.4: export of Mediterranean Outflow Water into the North Atlantic and effects of water mass properties (Alboran Sea to the Azores);
- 3.5: effects of organic matter supply (Davis Strait, Azores, Rockall Bank).

3.1 Faroe-Shetland Channel (northeast Atlantic, UK): Biodiversity of deep-sea sponge grounds in relation to oceanographic and anthropogenic activities

Authors: Georgios Kazanidis, Johanne Vad, Lea-Anne Henry, Francis Neat, Barbara Berx, Konstantinos Georgoulas, J Murray Roberts

Abstract

The synthesis in Part 1 of Deliverable 3.2 identified critical changes in pH in the Faroe Shetland Channel by 2100. However, decadal changes in water temperatures and salinity profiles of the channel's water masses are already being recorded. Thus, we set out to quantify effects of these other variables as well as effects of human activities on the richness and composition of sponges using existing and new data collected during ATLAS inside and outside the Faroe Shetland Channel Nature Conservation marine protected area (MPA). Analyses of 465 high-resolution images from 13 towed-camera transects found that sponge ground VMEs occurred within a narrow depth zone between 450 and 530 m depth, within relatively warm and saline water masses along the continental slope. Multiple size cohorts were recorded inside the MPA, in contrast to a single cohort outside. Distance-based linear modelling showed that a combination of demersal fisheries effort, substratum, salinity and temperature explained a statistically significant amount of variation in morphotype composition (R^2=48%, $p<0.001$) across the study area. This study ground-truths the sensitivity of sponge ground VMEs to fisheries activities and to decadal shifts in water mass properties, possibly on shorter time scales than any effects of critical changes in pH predicted by the synthesis in Part 2 of Deliverable 3.2.

Introduction

The Faroe-Shetland Chanel in the northeast Atlantic hosts complex hydrographic and sedimentary features (Bett, 2003). Interestingly, multisectoral collaborations between industry, government and academia have allowed detailed investigations of how the ecology of deep-sea benthic communities is shaped by the hydrography and sedimentary regimes in FSC (Bett, 2001; Henry and

Roberts, 2004; Jones et al., 2006; Narayanaswamy et al., 2010). These studies helped document the presence of sponge aggregations within a narrow bathymetric zone (i.e. the "sponge belt") (Bett, 2001; Axelsson, 2003). The area hosting these deep-sea sponge aggregations was designated in 2014 as the Faroe-Shetland Channel Nature Conservation Marine Protected Area. Mixed sponge assemblages are recorded there including boreal "ostur" communities (Klitgaard and Tendal, 2004) a mixture of geodiid sponges such as *Geodia barretti*, *G. macandrewi*, *G. atlantica*, *G. phlegraei* (as *Isops phlegraei*) and several other flabellate, lobose, stipitate and encrusting species (Bett, 2001; Howell et al., 2010; Henry and Roberts, 2014a). Sponge density ranged from 0.001 to 0.818 sponges/m^2 (Axelsson 2003; Henry and Roberts, 2014a). More detailed information on density, bathymetric distribution and body size of different species is currently missing.

Hátún et al. (2017) showed a decline over the last 25 years in silicate in North Atlantic including the Faroe Shetland Channel, while changes in the temperature and salinity profiles of regional water masses over the last two decades have also been shown (Turrell et al., 1999; Sherwin et al., 2006; Berx et al., 2013; Broadbridge and Toumi, 2015; McKenna et al., 2016). Reduction in concentration of silicate especially can have detrimental effects on deep-sea sponges, as silicate contributes to primary production (and thus the food supply to sponges and is incorporated as part of sponges' skeletons (Maldonado et al. 2011). On top of changes in silicate concentration, long-term measurements (1994-2011) in the Faroe Shetland Channel have also shown that surface layers (NAW and MNAW) have become warmer and more saline over the past two decades: temperatures have been increasing by 0.5^{o}C per decade and salinities by approximately 0.07 (Berx et al., 2013). The role of these water mass properties on deep-sea sponge grounds elsewhere suggest important roles of hydrography and temperature (Rice et al., 1990; Bett, 2001; Murillo et al., 2012), ocean chemistry (e.g. salinity and silicate) (Beazley et al., 2015; Howell et al., 2016), and biological parameters such as the concentration of particulate organic carbon (Barthel et al., 1996; Howell et al., 2016).

How anthropogenic activities in the channel (fisheries, oil and gas, telecommunications) interact with environmental parameters to shape the richness and composition of these sponge grounds has also not been examined in the Faroe Shetland Channel, but extractive industries have exploited the area for decades (Vad et al., 2018). Investigations on the physical disturbance caused from drilling on the megafaunal communities have been shown to smother fauna within a radius of 50-120 m from the drill

site (Jones et al., 2006), causing significant reduction in abundance, diversity and species richness of fauna including deep-sea sponges (Jones et al., 2006, 2007, 2012). Previous visual surveys confirmed disturbance to sponges likely from trawling (Bett, 2000) for Greenland halibut *(Reinhardtius hippoglossoides)* and roughhead grenadier *(Macrourus berglax)*. Currently, there the MPA has no specific management measures in place, and the statutory agency Marine Scotland is in the process of developing a joint recommendation to implement measures under the Common Fisheries Policy (Marine Scotland, 2017).

In the present study, we analysed video and stills imagery collected from the UK sector of the Faroe Shetland Channel to investigate how the richness, composition, density, and body-size distribution varied in relation to water mass properties, bottom substrate type, and demersal fisheries effort.

Methods

The Faroe-Shetland Channel (FSC) is characterised by complex hydrography as five water masses flow through it: North Atlantic Water (NAW), Modified North Atlantic Water (MNAW), Modified East Icelandic Water (MEIW), Norwegian Sea Arctic Intermediate Water (NSAIW) and Norwegian Sea Deep Water (NSDW) (Hansen and Østerhus, 2000). The distribution of these five water masses in the FSC is indicated by their characteristic temperature and salinity values, which are accompanied by a specific spectrum of chemical and biological characteristics. In the channel, water masses >400 m water depth comprise NAW (9.5-10.5^{o}C; 35.35-35.45psu) or MNAW (7-8.5^{o}C; 35.10-35.30 psu). At depths 400-800 m, water masses comprise MEIW (2-4.5^{o}C; 34.76-34.99 psu) and NSAIW (-0.5-0.5^{o}C; 34.89-34.91 psu). Its bottom water mass is the NSDW (<-0.5^{o}C; 34.91-34.92 psu), which has the greatest contribution in the southwards overflow through the Faroe Bank Channel and across the Wyville Thomson Ridge (Berx, 2012; McKenna et al., 2016; Broadbridge and Toumi, 2015). The boundary area occurring between the warm and cold-waters (found between ~ 350-650 m) experiences rapid changes in seawater temperature (decreases up to 7^{o}C within 1 h have been recorded, Bett, 2001), thought to be created by internal waves created by water flow across the Wyville Thomson Ridge that propagate at the boundary between warm and cold-water masses (Sherwin, 1991). Apart from the unusual temperature profile, the channel is also interesting in terms of sedimentary habitat types that include areas of iceberg

ploughmarks and North Sea Fan among others (Masson, 2001 for details; see also Bett, 2003; Narayanaswamy et al., 2010).

In September 2014, an underwater camera survey was conducted by Marine Scotland on board the MRV Scotia ("MoreDeep" cruise) to investigate the deep-sea sponge aggregations. The survey was conducted using a Seatronics (www.seatrnics-group.com) towed body hosting a Kongsberg Maritime OE14-366 PAL colour zoom camera (www.km.kongsberg.com). The system was also equipped with 6 high-intensity lights and sensors that measured at 1 second intervals, the altitude (the distance between the camera system and the seabed), depth (± 0.1 m), and pitch and roll of the system (see McIntyre et al., 2013, 2016 for details). Seawater temperature was recorded (± 0.01°C) through the sensor attached to the camera system.

In total, 13 camera tows were conducted, which were grouped into one area inside and three areas outside the MPA (Figure 1). The average duration of each transect was ~1 h 21 min at a speed of 1.5 m/sec. The altitude was 2-6 m.

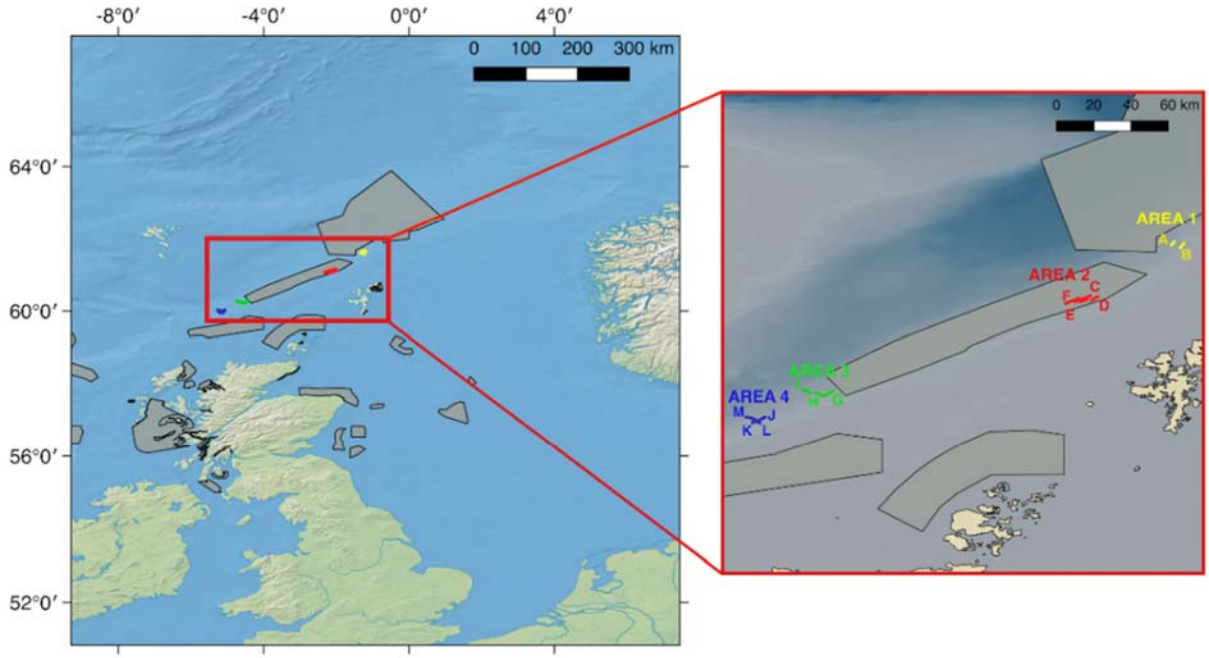

Figure 1. *Faroe-Shetland Chanel highlighting the Nature Conservation Marine Protected Area (red rectangle) (left panel) and camera tows inside (Area 2) and outside the MPA (Areas 1, Area 3 and Area 4) (right panel).*

The camera recorded continuous high definition (HD) video from which individual image frames were extracted every 20 sec. Extraction was carried out with the open-access software VLC. Frames were subjected to quality check with low-visibility frames been discarded. In total, 465 high quality image frames were subjected to further analysis.

Numbers of each individual sponge was recorded and categorised into morphotype categories (Figure 2), based on the "Thesaurus of Sponge Morphology" (Boury-Esnault and Rützler, 1997) and accompanied by studies on the distribution and structure of deep-sea sponge aggregations in the North Atlantic (Bett, 2001; Axelsson, 2003; Klitgaard and Tendal, 2004; Cárdenas et al., 2013; Henry and Roberts, 2014; McIntyre et al., 2016).

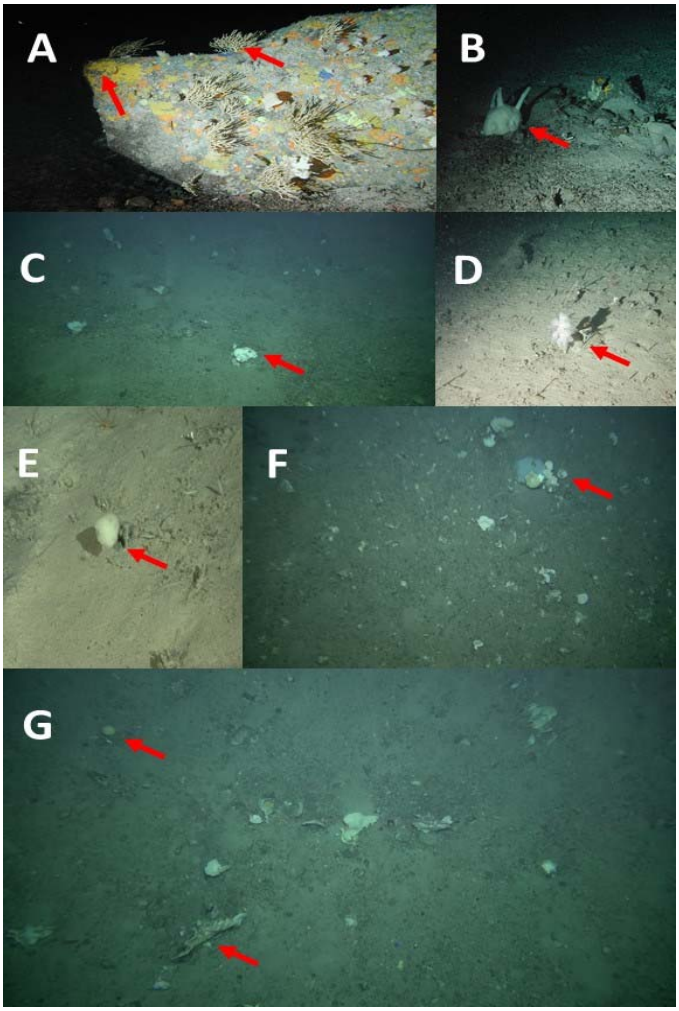

Figure 2. Categories of sponge morphotypes. Category 1: encrusting (seen in A). Category 2: arborescent or "tree-like" (also seen in (A). Category 3: massive (seen in C), spherical (seen in G), or papillate (seen in B). Category 4: flabellate or "fan-shaped" (seen in G) or caliculate/"cup-shaped"(seen in F). Category 5: stipitate or "stalked"(seen in E) or clavate/"club-shaped")(seen in D).

The surface of the seabed seen in each of the HD image frames (field of view) was quantified (in m^2) by matching the time point that a frame was captured with the relevant data (altitude and pitch angle of the towed camera system) provided by the sensor attached to the system. A detailed description of the methodology followed for measuring the field of view (in m^2) is given in McIntyre et al. (2013). In brief, altitude and pitch of the towed body were used in the survey area calculations using trigonometric equations. To correct for the

effect of the distance on the visibility of the seabed, image analysis techniques in MATLAB Image Processing Toolbox were used to construct a correction factor. The latter was a proportion of visible seabed of camera distance from the bottom for each transect.

Using the number of sponge specimens from each morphotype category recorded in each image and the surface of the seabed, values of sponge density were measured in sponge individuals per category/m^2), except for Category 1 ("encrusting"), which were logged in terms of presence/absence. Furthermore, using the camera's laser points as a reference (7.5 cm), we measured the width of flabellate sponges and the average value between "length" and "width" for the massive/spherical/papillate and the caliculate sponges. Body size measurements were grouped into 5 cm size classes following Bo et al. (2012).

Data on depth, type of substratum and temperature were available for each of the images collected during the visual survey of the present study. Substratum in each of the 465 images was grouped into one of four categories (following Bett, 2003): 1) cobble, 2) cobble with boulder, 3) sand, and 4) sand with boulder. Data on salinity, water density and oxygen saturation (derived from equivalent temperature and salinity using a MATLAB routine from the channel) were supplied from Marine Scotland. These data came from locations inside the transects of the visual survey at similar depths.

Preliminary investigation of environmental parameters showed high correlations between salinity-density and between salinity-oxygen saturation and thus density and oxygen saturation data were not used further. However, it is noted that these are also key water mass properties that explain differences in richness and composition, they were simply removed to avoid statistical Type I errors. Data on demersal fishing activity were extracted using Quantum GIS from the Marine Scotland MAPS NMPI (National Marine Plan Interactive) website using the layer entitled "Fishing statistics – Demersal landings (tonnes) from Scottish waters [per International Council for the Exploration of the Sea (ICES) statistical rectangle]". Data for this layer were available only for five years (2012-2016), enabling an assessment of recent demersal fishing impact on the sponge communities. For each of the ICES rectangles taken into account (i.e., rectangle 52E8 for Area 1; 51E7 for Area 2; 49E5 for Area 3; 48E4 for Area 4), an average value was calculated over the time period 2012-2016. The average value for the

annual demersal landings were: 113 tonnes in Area 1, 64 tonnes in Area 2, 2836 tonnes in Area 3 and 3011 tonnes in Area 4.

Numbers of morphotypes (S) and Shannon's diversity index (H) were calculated using Primer-7 (Clarke et al., 2014) and compared inside and outside the MPA. Density was compared 1) inside versus outside the MPA, 2) across the four Areas, and 3) across all transects. Sponge sizes were compared inside versus outside the MPA. These comparisons were carried out in the software R (R Core Team, 2018). The Shapiro-Wilk test was applied to test for normality, followed by the Bartlett-test or the F-test to verify the equality of variances (for two or three groups, respectively). If the distributions were normal and the variances were equal, then the hypothesis that the groups have the same mean was tested using the two-sample t-test or the one-way ANOVA (for two or three groups, respectively). If distributions were normal but variances were not equal, the hypothesis that the means of the groups were the same was examined through the Welch's two sample t-test or one-way analysis of means (not assuming equal variances) (for two groups or three groups, respectively). If distributions were not normal, the hypothesis that the groups have the same median was tested through a Wilcoxon rank sum test or a Kruskal-Wallis rank sum test (for two or three groups, respectively). All values in the text are presented as mean ± standard error (SE).

Size-frequency distributions were analyzed applying the Bhattacharya analysis using the FISAT software package (Gayanilo and Pauly, 1997; Kazanidis et al., 2010). Size-frequency distributions were compared between inside and outside the MPA.

Non-transformed data on the density (individuals/m^2) of each sponge morphotype were used in the calculation of Bray–Curtis similarities and similarity matrices to conduct clustering analyses, and the role of oceanic variables, substrate and fisheries effort on sponge densities analysed through distance-based linear modeling ("Dist-LM" routine) in Primer 7.

Results

Richness of sponge morphotypes

Richness of sponge morphotypes (S) was significantly higher inside than outside the MPA (Wilcoxon rank sum test=46716, $p<0.0001$; $n=465$). Similarly, Shannon's diversity (H) was also significantly higher inside the MPA (Wilcoxon rank sum test=36628, $p<0.0001$, $n=465$).

Density of sponge morphotypes

Density of sponge morphotypes was significantly higher inside than outside the MPA, and significant differences were also detected across the four Areas. Clustering analysis revealed a higher level of similarity (~50%) for transects in Area 2 (i.e., inside the MPA) than outside. Significant differences in density were recorded across all transects, the highest density for Category 3 was found in transect F, for Category 4 in transect C and for all sponge morphotypes in transect F.

Density of sponge morphotypes across depth

Densities of Categories 3 and 4 sponges peaked within a narrow depth zone of about ~80 m in ~450-530 m water depth. Maximum density for Category 3 was 0.79 individuals/m^2, and 1.93 individuals/m^2 for Category 4.

Sponge mean sizes and size spectra

Mean size of Category 3 sponges was significantly higher inside the MPA than outside (Wilcoxon rank sum test=944.5, $p<0.05$, $n=145$), but no trend was detected for Category 4 (Wilcoxon rank sum test=2713.5, $p>0.05$, $n=469$). However, taking all sponge morphotypes together, average size inside the MPA did not statistically differ from that outside (Wilcoxon rank sum test=7621.5, $p>0.05$, $n=614$).

Besides mean sponge size, the Bhattacharya method revealed clear differences in the size spectrum of sponges inside versus outside the MPA. Taking all sponge morphotypes together showed four size cohorts inside the MPA but only one cohort outside.

Effects of fisheries, bottom substrate and oceanographic variability

Fisheries, substrate and oceanographic variables explained 48% of the variation in the density of sponge morphotypes broken down as: fisheries effort (29.75%), occurrence of cobble with boulder (12.02%), salinity (4.89%) and water temperature (1.07%) (Table 1). Temperature and salinity in transects with highest sponge densities ranged from 6.52°C to 8.98°C, and 34.91 to 35.13 psu, respectively, indicating that the sponge aggregations were mainly sitting within the relatively warm and saline NAW, MNAW and MEIW water masses.

Table 1. Outcome of distance-based linear modelling on the role of environmental parameters in the variation of density of sponge morphotypes.

Sequential tests					
Variable	**R^2**	**Pseudo-F**	***p***	**Individual proportion**	**Cumulative**
+Depth	0.00022201	0.10281	0.82	0.00022201	0.00022201
+Temperature	0.01089	4.9827	0.012	0.010668	0.01089
+Cobble	0.011417	0.24591	0.717	0.00052733	0.011417
+Cobble with boulder	0.13158	63.65	0.001	0.12016	0.13158
+Sand	0.13292	0.70859	0.465	0.0013386	0.13292
+Sand with boulder	0.13342	0.26302	0.771	0.00049766	0.13342
+Salinity	0.1511	9.5174	0.001	0.017679	0.1511

Discussion

The present study showed significant differences in sponge ground VMEs inside versus outside the designated MPA. Richness, diversity, densities, and morphotype composition were all different, the MPA enclosing the richest most varied sponge ground VMEs. Variation in density was mostly explained by fisheries pressure, not oceanographic variability. However, water temperature and salinity still explained a significant amount of variation, with highest densities corresponding to water masses with temperature and salinity ranging from 6.52°C to 8.98°C and 34.91 to 35.13 psu respectively, approximately the zone characterized by the relatively warmer and saline mixture of NAW, MNAW and MEIW water masses.

Although the available timeseries on demersal fisheries were time-limited, our findings indicate that fisheries exert the strongest control over deep-sea sponge ground biodiversity in the Faroe Shetland

Channel. Notably, we did not observe trawl marks in any of the 465 images analysed, however with the hydrographical conditions being so dynamic in the area (Sherwin et al., 2006), trawl marks could have been erased. In addition, fishermen may now actively avoid sponge grounds to limit damage to fishing gear, or due to relatively little fish biomass present in sponge aggregations (e.g. see Munoz et al., 2012; Kenchington et al., 2013; Kutti et al., 2014).

Present findings on sponge richness/diversity and body-size distribution are a strong indication of favourable conditions for reproduction, recruitment and growth of sponges in the Faroe Shetland Channel MPA. Data on these very important parameters, however, and their role in shaping deep-sea sponge aggregations are extremely limited (Witte, 1996; Fallon et al., 2010). Existing studies typically show unimodal distributions with long tails e.g., in *Pachastrella monilifera* and *Poecillastra compressa* (Bo et al., 2012); in *Isops phlegraei pyriformis* (Klitgaard and Tendal, 2004); and across various other taxa (Rooper et al., 2016), while other species exhibit multimodal distributions e.g., in *Pheronema carpenteri* (Rice et al., 1990); or in *Geodia mesotriaena* (Klitgaard and Tendal, 2004).

Apart from fisheries pressure and substratum, it was actually a suite of oceanographic variables that control sponge grounds in the Faroe Shetland Channel. Oxygen and water mass density were omitted from analyses to avoid over-fitting the model and reduce our Type 1 error rate, but these too are part of the signature of each water mass and thus we can preliminarily conclude that future changes to oxygen and density in this region could likewise affect sponge grounds. As noted in the synthesis in Part 1 of Deliverable 3.2, key variables include water temperature, salinity and silicate concentrations (Murillo et al., 2012; Knudby et al., 2013; Beazley et al., 2015; Howell et al., 2016), topography, internal waves, current speeds, food supply (Rice et al., 1990; Klitgaard and Tendal, 2004; Knudby et al., 2013; Howell et al., 2016). Establishing a precise relationship between the contribution of each of the environmental parameters mentioned above and the distribution of deep-sea sponges/deep-sea sponge aggregations is still an open question given the limited availability of data on a) species' physiological tolerances, b) geographical/bathymetric distribution of these organisms and c) measurements of environmental data at appropriate spatial scales (Tjensvoll et al., 2013; Beazley et al., 2015; Strand et al., 2017). In the present study, the values of temperature and salinity per transect inside the FSC NCMPA ranged from 6.5^{o}C/35.00 psu (transect F) to ~8.7^{o}C/35.00 psu (transects C, D, E), which fall within the temperature and salinity range reported up to now for *Geodia* sponges in the North East Atlantic

(Klitgaard and Tendal, 2004; Bett, 2012). Despite this agreement, it is not clear to what extent the high density of sponge aggregations recorded inside the MPA was due to the physical/chemical parameters of the water masses *per se* and/or due to the outcome of the interaction of these water masses (i.e. NAW, MNAW, MEIW, NSAIW, NSDW) with the continental slope, which would create internal waves supplying food particles to deep-sea benthos (Mienis et al., 2009; Mohn et al., 2014). Taking into account, however, that a) rapid changes in temperature have been recorded at the Faroe-Shetland Channel (up to 7^{o}C within 1 h) at a depth of 550 m (Bett, 2001) and that deep-sea sponges feed mainly on particulate organic matter (e.g. Kazanidis et al., 2018), it is likely that the hydrographic conditions (i.e. internal waves) play a role at least equal to that of temperature and salinity themselves in promoting the proliferation of sponges within the MPA (Rice et al., 1990; Klitgaard and Tendal, 2004; Beazley et al., 2015).

Suggestions made above about the role of water mass characteristics and hydrography in promoting the proliferation of sponge aggregations within the FSC NCMPA gain further interest considering long-term changes in major chemical features in North Atlantic including the FSC NCMPA (Hátún et al., 2017). On top of changes in silicate concentration, long-term measurements (1994-2011) in the Faroe Shetland Channel have also shown that surface layers (NAW and MNAW) have become warmer and more saline over the past two decades: temperatures have been increasing by 0.5^{o}C per decade and salinities by approximately 0.07 (Berx et al., 2013).

Datasets used in the present manuscript have been deposited to PANGAEA (doi:10.1594/PANGAEA.897604).

References

Ackers, R.G., Moss, D., Picton, B.E., Stone, S.M.K., Morrow, C.C. (2007). Sponges of the British Isles ("Sponge V"). A Colour Guide and Working Document. Marine Conservation Society. 165 pp.

Arnaud-Haond, S., Van den Beld, I.M.J., Becheler, R., Orejas, C., Menot, L., Frank N. et al. (2017). Two "pillars" of cold-water coral reefs along Atlantic European margins: Prevalent association of *Madrepora oculata* with *Lophelia pertusa*, from reef to colony scale. Deep-Sea Res. II 145, 110-119. https://doi.org/10.1016/j.dsr2.2015.07.013.

Asch, R.G., and Collie, J.S. (2008). Changes in a benthic megafaunal community due to disturbance from bottom fishing and the establishment of a fishery closure. Fish. Bull. 106, 438-456.

Austin, J.A., Cannon, S.J.C., Ellis, D. (2014). Hydrocarbon exploration and exploitation West of Shetlands. Geol. Soc. Lond. Spec. Pub. 397, 1–10.

Axelsson, M.B. (2003). The deep-seabed environment of the UK continental margin – integration and interpretation of geological and biological data. [PhD thesis]. [Southampton]: University of Southampton.

Barthel, D., Tendal, O.S., Thiel, H. (1996). A Wandering Population of the Hexactinellid Sponge *Pheronema carpenteri* on the Continental Slope off Morocco, Northwest Africa. P.S.Z.N. I: Mar. Ecol. 17, 603-616. https://doi.org/10.1111/j.1439-0485.1996.tb00420.x.

Beazley, L., Kenchington, E., Yashayaev, I., Murillo, F.J. (2015). Drivers of epibenthic megafaunal composition in the sponge grounds of the Sackville Spur, northwest Atlantic. Deep-Sea Res. I 98, 102–14. https://doi.org/10.1016/j.dsr.2014.11.016.

Bell, J.J. (2008). The functional roles of marine sponges. Est. Coast. Shelf Sci. 79, 341-353. https://doi.org/10.1016/j.ecss.2008.05.002.

Bell, J.J., and Barnes, D.K.A. (2000). The influences of bathymetry and flow regime upon the morphology of sublittoral sponge communities. J. Mar. Biol. Assoc. UK 80, 707-718.

Bell, J.J., Barnes, D.K.A., Shaw, C. (2002). Branching dynamics of two species of arborescent demosponge: the effect of flow regime and bathymetry. J. Mar. Biol. Assoc. UK 82, 279-294. https://doi.org/10.1017/S0025315402005465.

Berx, B. (2012). The hydrography and circulation of the Faroe-Shetland Channel. Ocean Chall. 19, 15-19.

Berx, B., Hansen, B., Osterhus, S., Larsen, K.M., Sherwin, T., Jochumsen, K. (2013). Combining in situ measurements and altimetry to estimate volume, heat and salt transport variability through the Faroe–Shetland Channel. Ocean Sci. 9, 639-654. https://doi.org/10.5194/os-9-639-2013.

Bett, B.J. (2000) Signs and symptoms of deepwater trawling on the Atlantic Margin. Man-made objects on the seafloor, 107-118. Society for Underwater Technology, London.

Bett, B. (2001). UK Atlantic Margin Environmental Survey: Introduction and overview of bathyal benthic ecology. Cont. Shelf Res. 21, 917-956. https://doi.org/10.1016/S0278-4343(00)00119-9.

Bett, B. (2003). An introduction to the benthic ecology of the Faroe-Shetland Channel (SEA4). 84 pp.

Bett, B. (2012). Seafloor biotope analysis of the deep waters of the SEA4 region of Scotland's seas. JNCC Report No. 472. 104 pp.

Bo, M., Bertolino, M., Bavestrello, G., Canese, S., Giusti, M., Angiolillo, M. et al. (2012). Role of deep sponge grounds in the Mediterranean Sea: a case study in southern Italy. Hydrobiol. 687, 163–177.

Boury-Esnault, N., Rützler, K. (1997). Thesaurus of sponge morphology. Smithsonian Contributions in Zoology 596, 55 pages. https://doi.org/10.5479/si.00810282.596

Broadbridge, M.B., and Toumi, R. (2015). The deep circulation of the Faroe-Shetland Channel: Opposing flows and topographic eddies. J. Geophys. Res. Oceans: 120, 5983–5996. https://doi.org/10.1002/2015JC010833.

Buhl-Mortensen, P., Hovland, M., Brattegard, T., Farestveit, R. (1995). Deepwater bioherms of the scleractinian coral *Lophelia pertusa* (L.) at 64°N on the Norwegian shelf: structure and associated megafauna. Sarsia 80, 145-158. https://doi.org/10.1080/00364827.1995.10413586.

Bullough, L.W., Turrell, W.R., Buchan, P., Priede, I.G. (1998). Commercial deep water trawling at sub-zero temperatures - Observations from the Faroe-Shetland channel. Fish. Res. 39, 33–41. doi:10.1016/S0165-7836(98)00170-2.

Cárdenas, P., and Moore, J.A. (2017). First records of *Geodia* demosponges from the New England seamounts, an opportunity to test the use of DNA mini-barcodes on museum specimens. Mar. Biodivers. doi: 10.1007/s12526-017-0775-3.

Cárdenas, P., and Rapp, H.T. (2015). Demosponges from the Northern Mid-Atlantic Ridge shed more light on the diversity and biogeography of North Atlantic deep-sea sponges. J. Mar. Biol. Assoc. UK 95, 1475-1516. https://doi.org/10.1017/S0025315415000983.

Cárdenas, P., Perez, T., Boury-Esnault, N. (2012). Sponge systematics facing new challenges. Adv. Mar. Biol. 61. 79-209. doi: 10.1016/B978-0-12-387787-1.00010-6.

Cárdenas, P., Rapp, H.T., Klitgaard, A.B., Best, M., Thollesson, M., Tendal, O.S. (2013). Taxonomy, biogeography and DNA barcodes of *Geodia* species (Porifera, Demospongiae, Tetractinellida) in the Atlantic boreo-arctic region. Zool. J. Linn. Soc. 169, 251–311. https://doi.org/10.1111/zoj.12056.

Cathalot, C., van Oevelen, D., Cox, T.J.S., Kutti, T., Lavaleye, M., Duineveld, G. et al. (2015). Cold-water coral reefs and adjacent sponge grounds: hot spots of benthic respiration and organic carbon cycling in the deep sea. Front. Mar. Sci. 2:37. doi: 10.3389/fmars.2015.00037.

Clarke, K.R., Gorley, R.N., Somerfield, P.J., Warwick, R.M. (2014). Change in marine communities: an approach to statistical analysis and interpretation, 3nd edition. PRIMER-E: Plymouth.

Danovaro, R., Corinaldesi, C., Dell'Anno, A., Snelgrove, P.V.R. (2017). The deep-sea under global change. Curr. Biol. 27, R461-R465. https://doi.org/10.1016/j.cub.2017.02.046.

de Goeij, J.M., van Oevelen, D., Vermeij, M.J.A., Osinga, R., Middelburg, J.J., de Goeij, A.F.P.M. et al. (2013). Surviving in a marine desert: the sponge loop retains resources within coral reefs. Sci. 342, 108–110. https://doi.org/10.1126/science. 1241981.

Fallon, S.J., James, K., Norman, R., Kelly, M., Ellwood, M.J. (2010). A simple radiocarbon dating method for determining the age and growth rate of deep-sea sponges. Nucl. Instrum. Method. Phys. Res. B 268, 1241-1243. https://doi.org/10.1016/j.nimb.2009.10.143.

Gates, A.R., and Jones, D.O.B. (2012). Recovery of Benthic Megafauna from Anthropogenic Disturbance at a Hydrocarbon Drilling Well (380 m Depth in the Norwegian Sea). PLoS ONE 7(10): e44114. doi:10.1371/journal.pone.0044114.

Gayanilo, F.C.J., and Pauly, D. (1997). The FAO–ICLARM Stock Assessment Tools (FiSAT) Reference Manual. Rome: FAO Computerized Information Series (Fisheries). No. 8.

George, A.M., Brodie, J., Daniell, J., Capper, A., Jonker, M. (2018). Can the sponge morphologies act as environmental proxies to biophysical factors in the Great Barrier Reef, Australia? Ecol. Indic. 93: 1152-1162. https://doi.org/10.1016/j.ecolind.2018.06.016.

Ginn, B.K., Logan, A., Thomas, M.L.H. (2000). Sponge ecology on sublittoral hard substrates in a high current velocity area. Est. Coast. Shelf Sci. 50, 403-414. https://doi.org/10.1006/ecss.1999.0563.

Guijarro, J., Beazley, L., Lirette, C., Kenchington, E., Wareham, V., Gilkinson, K. et al. (2016). Species distribution modelling of corals and sponges from research vessel survey data in the Newfoundland and Labrador region for use in the Identification of significant benthic areas. Canadian Technical Report of Fisheries and Aquatic Sciences 3171: vi+126p. doi: 10.13140/RG.2.1.2441.8800.

Hansen, B., and Østerhus, S. (2000). North Atlantic–Nordic Seas exchanges. Prog. Oceanogr. 45, 109-208. https://doi.org/10.1016/S0079-6611(99)00052-X.

Hátún, H., Azetsu-Scott, K., Somavilla, R., Rey, F., Johnson, C., Mathis, M. et al. (2017). The subpolar gyre regulates silicate concentrations in the North Atlantic. Sci. Rep. 7:14576. doi:10.1038/s41598-017-14837-4.

Henry, L-A., and Roberts, J.M. (2004). The biodiversity, characteristics and distinguishing features of deep-water epifaunal communities from the Wyville-Thomson Ridge, Darwin Mounds and Faeroes Plateau. Report to the Atlantic Frontier Environment Network, 44p.
Henry, L.-A., and Roberts, J.M. (2014a). Applying the OSPAR habitat definition of deep-sea sponge aggregations to verify suspected records of the habitat in UK waters, JNCC Report No 508, 41pp.

Henry, L-A., and Roberts, J.M. (2014b). Recommendations for best practice in deep-sea habitat classification: Bullimore et al. as a case study. ICES J. Mar. Sci. 71, 895-898. https://doi.org/10.1093/icesjms/fst175.

Hentschel, U., Piel, J., Degnan, S.M., Taylor, M.W. (2012). Genomic insights into the marine sponge microbiome. Nat. Rev. Microbiol. 10, 641-654. doi: 10.1038/nrmicro2839.

Hoffmann, F., Radax, R., Woebken, D., Holtappels, M., Lavik, G., Rapp, H.T. et al. (2009). Complex nitrogen cycling in the sponge *Geodia barretti*. Environ. Microbiol. 11, 2228–2243. doi: 10.1111/j.1462-2920.2009.01944.x.

Hoffmann, F., Rapp, H.T., Zöller, T., Reitner, J. (2003). Growth and regeneration in cultivated fragments of the boreal deep water sponge *Geodia barretti* bowerbank, 1858 (Geodiidae, Tetractinellida, Demospongiae). J. Biotechnol. 100, 109-118. https://doi.org/10.1016/S0168-1656(02)00258-4.

Hogg, M.M., Tendal, O.S., Conway, K.W., Pomponi, S.A., van Soest, R.W.M., Gutt, J. et al. (2010). Deep-sea Sponge Grounds: Reservoirs of Biodiversity. UNEP-WCMC Biodiversity Series No. 32, UNEP-WCMC, Cambridge.

Howell, K., Davies, J. S., Narayanaswamy, B.E. (2010). Identifying deep-sea megafaunal epibenthic assemblages for use in habitat mapping and marine protected area network design. J Mar. Biol. Assoc. UK 90, 33-68. https://doi.org/10.1017/S0025315409991299.

Howell K.L., Piechaud N, Downie A.L., Kenny A. (2016). The distribution of deep-sea sponge aggregations in the North Atlantic and implications for their effective spatial management. Deep-Sea Res. I 115, 309-320. https://doi.org/10.1016/j.dsr.2016.07.005.

Howell, K.L. 2017. International Workshop on the Development of a Standardised Deep-Sea Species Image Catalogue/NEADS morphospecies catalogue. 04/12/17-05/12/17, Plymouth University, UK.

Jiménez, E., and Ribes, M. (2007). Sponges as a source of dissolved inorganic nitrogen: nitrification mediated by temperate sponges. Limnol. Oceanogr. 52, 948–958. https:// doi.org/10.4319/lo.2007.52.3.0948.

Johnson, D., Ferreira, M.F., Kenchington, E. (2018). Climate change is likely to severely limit the effectiveness of deep-sea ABMTs in the North Atlantic. Mar. Policy 87:111-122. https://doi.org/10.1016/j.marpol.2017.09.034.

Jones, D.O.B., Hudson, I.A., Bett, B.J. (2006). Effects of physical disturbance on the cold-water megafaunal communities of the Faroe–Shetland Channel. Mar. Ecol. Prog. Ser. 319, 43-54.

Jones, D.O.B., Wigham, B.D., Hudson, I.R., Bett, B.J. (2007). Anthropogenic disturbance of deep-sea megabenthic assemblages: a study with remotely operated vehicles in the Faroe-Shetland Channel, NE Atlantic. Mar. Biol. 151, 1731–1741.

Jones, D.O.B., Gates, A.R., Lausen, B. (2012). Recovery of deep-water megafaunal assemblages from hydrocarbon drilling disturbance in the Faroe−Shetland Channel. Mar. Ecol. Prog. Ser. 461, 71-82.

Kahn, A.S., Chu, J.W.F., Leys, S.P. (2018). Trophic ecology of glass sponge reefs in the Strait of Georgia, British Columbia. Sci. Rep. 8:756. doi:10.1038/s41598-017-19107-x.

Kazanidis, G., Antoniadou, C., Lolas, A.P., Neofitou, N., Vafidis, D., Chintiroglou, C. et al. (2010). Population dynamics and reproduction of *Holothuria tubulosa* (Holothuroidea: Echinodermata) in the Aegean Sea J. Mar. Biol. Assoc. UK 90, 895-901. https://doi.org/10.1017/S0025315410000251.

Kazanidis, G., Henry, L-A., Roberts, J.M., Witte, U.F.M. (2016). Biodiversity of *Spongosorites coralliophaga* (Stephens, 1915) on coral rubble at two contrasting cold-water coral reef settings. Coral Reefs 35, 193–208. doi:10.1007/s00338-015-1355-2.

Kazanidis, G., van oevelen, D., Veuger, B., Witte, U.F.M. (2018). Unravelling the versatile feeding and metabolic strategies of the cold-water ecosystem engineer *Spongosorites coralliophaga* (Stephens, 1915). Deep-Sea Res Part I 141, 71-82. https://doi.org/10.1016/j.dsr.2018.07.009.

Kenchington, E., F.J. Murillo, C. Lirette, M. Sacau, M. Koen-Alonso, A. Kenny, N. et al. (2014). Kernel density surface modelling as a means to identify significant concentrations of vulnerable marine ecosystem indicators. PLoS ONE 9:e109365. doi:10.1371/journal.pone.0109365.

Kenchington, E., Power, D., Koen-Alonso, M. (2013). Associations of demersal fish with sponge grounds on the continental slopes of the northwest Atlantic. Mar. Ecol. Prog. Ser. 477, 217-230. doi: https://doi.org/10.3354/meps1012.

Klitgaard, A.B. (1995). The fauna associated with outer shelf and upper slope sponges (Porifera, Demospongiae) at the Faroe Islands, northeastern Atlantic. Sarsia 80, 1–22. https://doi.org/10.1080/00364827.1995.10413574.

Klitgaard, A.B., and Tendal, O.S. (2004). Distribution and species composition of mass occurrences of large-sized sponges in the northeast Atlantic. Prog. Oceanogr. 61, 57–98. https://doi.org/10.1016/j.pocean.2004.06.002.

Knudby, A., Kenchington, E., Murillo, F.J. (2013). Modeling the distribution of *Geodia* sponges and sponge grounds in the Northwest Atlantic. PLoS One 8:e82306. https://doi.org/10.1371/journal.pone.0082306.

Kutti, T., Bannister, R.J., Fossa, J.H. (2013). Community structure and ecological function of deep-water sponge grounds in the Traenadypet MPA—Northern Norwegian continental shelf. Cont. Shelf Res. 69, 21-30. https://doi.org/10.1016/j.csr.2013.09.011.

Kutti, T., Bergstad, O.A., Fosså, J.H., Helle, K. (2014). Cold-water coral mounds and sponge-beds as habitats for demersal fish on the Norwegian shelf. Deep-Sea Res. II 99, 122-133. https://doi.org/10.1016/j.dsr2.2013.07.021.

Leach, H., Herbert, N., Los, A., Smith, R. (1999). The Schiehallion development. in Petroleum Geology of Northwest Europe: Proceedings of the 5th Conference, 683–692. doi: 10.1144/0050683.

Leghorn, J., Brookes, D., Shearman, M. (1996). The Foinaven and Schiehallion Developments. in Offshore Technology Conference, 41–56. doi: 10.4043/8033-MS.

Leys, S.P., Kahn, A.S., Fang, J.K.H., Kutti, T., Bannister, R.J. (2018). Phagocytosis of microbial symbionts balances the carbon and nitrogen budget for the deep-water boreal sponge *Geodia barretti.* Limnol. Oceanogr. 63, 187-202. https://doi.org/10.1002/lno.10623.

Maldonado, M., Aguilar, R., Bannister, R.J., James, J., Conway, K.W., Dayton, P.K., et al. (2017). "Sponge grounds as key marine habitats: a synthetic review of types, structure, functional roles and conservation concerns", in Marine Animal Forests, eds. S. Rossi, L. Bramanti, A. Gori, C. Orejas (Springer), 145- 183. doi: 10.1007/978-3-319-17001-5_24-1.

Maldonado, M., Navarro, L., Grasa, A., Gonzalez, A., Vaquerizo, I. (2011). Silicon uptake by sponges: a twist to understanding nutrient cycling on continental margins. Sci. Rep. 1:30, DOI: 10.1038/srep00030.

Maldonado, M., Ribes, M., van Duyl, F.C. (2012). "Nutrient fluxes through sponges: biology, budgets, and ecological implications", in Advances in Sponge Science: Physiology, Chemical and Microbial Diversity, Biotechnology, eds. M.A. Becerro, M.J. Uriz, M. Maldonado, X. Turon (Oxford, Academic Press), 113–182. doi: 10.1016/B978-0-12-394283-8.00003-5.

Marine Scotland (2017). Northern North Sea Proposals. JNCC feedback on proposed fisheries management measures. 99 p.

Masson, D.G. (2001). Sedimentary processes shaping the eastern slope of the Faeroe-Shetland Channel. Cont. Shelf Res. 21, 825–857. https://doi.org/10.1016/S0278-4343(00)00115-1.

McIntyre, F.D., Collie, N., Stewart, M., Scala, L., Fernandes, P.G. (2013). A visual survey technique for deep-water fishes: estimating anglerfish *Lophius* spp. abundance in closed areas. J. Fish Biol. 83, 739-753. doi: 10.1111/jfb.12114.

McIntyre, F.D., Drewery, J., Eerkes-Medrano, D., Neat, F. C. (2016). Distribution and diversity of deep-sea sponge grounds on the Rosemary Bank Seamount, NE Atlantic. Mar. Bio1. 63, 142-152. doi: 10.1007/s00227-016-2913-z.

McKenna, C., Berx, B., Austin, W.E.N. (2016). The decomposition of the Faroe-Shetland Channel water masses using Parametric Optimum Multi-Parameter analysis. Deep-Sea Res. I 107, 9-21. https://doi.org/10.1016/j.dsr.2015.10.013.

Mienis, F., de Stigter, H.C., de Haas, H., van Weering, T.C.E. (2009). Near-bed particle deposition and resuspension in a cold-water coral mound area at the Southwest Rockall Trough margin, NE. Atlantic. Deep-Sea Res. I 56, 1026-1038. https://doi.org/10.1016/j.dsr.2009.01.006.

Mohn, C., Rengstorf, A., White, M., Duineveld, G., Mienis, F., Soetaert, K. et al. (2014). Linking benthic hydrodynamics and cold-water coral occurrences: A high-resolution model study at three cold-water coral provinces in the NE Atlantic. Prog. Oceanogr. 122, 92–104. https://doi.org/10.1016/j.pocean.2013.12.003.

Munoz, P.D., Sayago-Gil, M., Patrocinio, T., González-Porto, M., Murillo, F.J., Sacau, M. et al. (2012). Distribution patterns of deep-sea fish and benthic invertebrates from trawlable grounds of the Hatton Bank, north-east Atlantic: Effects of deep-sea bottom trawling. J. Mar. Biol. Assoc. UK 92, 1509-1524. https://doi.org/10.1017/S002531541200015X.

Murillo, F.J., Muñoz, P.D., Cristobo, J., Ríos, P., González, C., Kenchington, E. et al. (2012). Deep-sea sponge grounds of the Flemish Cap, Flemish Pass and the Grand Banks of Newfoundland (Northwest Atlantic Ocean): distribution and species composition. Mar. Biol. Res. 8, 8842–8854. https://doi.org/10.1080/17451000.2012.682583.

Murillo, F.J., Kenchington, E., Lawson, J.M., Li, G., Piper, D.J.W. (2016). Ancient deep-sea sponge grounds on the Flemish Cap and Grand Bank, northwest Atlantic. Mar. Biol. 163, 63-73. doi:10.1007/s00227-016-2839-5.

Narayanaswamy, B.E., Bett, B.J., Hughes, D.J. (2010). Deep-water macrofaunal diversity in the Faroe-Shetland region (NE Atlantic): a margin subject to an unusual thermal regime. Mar. Ecol. 31, 237-246. https://doi.org/10.1111/j.1439-0485.2010.00360.x.

Orejas, C., Gori, A., Iacono, C.L., Puig, P., Gili, J-M., Dale, M.R.T. (2009). Cold-water corals in the Cap de Creus canyon, northwestern Mediterranean: spatial distribution, density and anthropogenic impact. Mar. Ecol. Prog. Ser. 397, 37-51. doi: https://doi.org/10.3354/meps08314.

OSPAR (2008). OSPAR List of Threatened and/or Declining Species and Habitats. Reference Number: 2008-6.

Plotkin, A., Voigt, O., Willassen, E., Rapp, H.T. (2017). Molecular phylogenies challenge the classification of Polymastiidae (Porifera, Demospongiae) based on morphology. Org. Divers. Evol. 17, 45-66. doi: 10.1007/s13127-016-0301-7.

Purser, A., Orejas, C., Gori, A., Tong, R., Unnithan, V., Thomsen, L. (2013). Local variation in the distribution of benthic megafauna species associated with cold-water coral reefs on the Norwegian margin. Cont. Shelf Res. 54, 37–51. https://doi.org/10.1016/j.csr.2012.12.013.

Pusceddu A, Bianchelli S, Martín J, Puig P, Palanques A, Masqué P. et al. (2014). Chronic and intensive bottom trawling impairs deep-sea biodiversity and ecosystem functioning. Proc. Natl. Acad. Sci. 111, 8861–8866. doi:10.1073/pnas.140545411.

R Core Team (2018) R: A Language and Environment for Statistical Computing. R Foundation for Statistical Computing, Vienna. https://www.R-project.org.

Ramirez-Llodra, E., Tyler, P.A., Baker, M.C., Bergstad, O.A., Clark, M.R., Escobar, E., et al., (2011). Man and the last great wilderness: human impact on the deep sea. PLoS One 6:e22588. https://doi.org/10.1371/journal.pone.0022588.

Rice, A.L., Thurston, M.H., New, A.L. (1990). Dense aggregations of a hexactinellid sponge, *Pheronema carpenteri,* in the Porcupine Seabight (northeast Atlantic Ocean), and possible causes. Prog. Oceanogr. 24, 179-196. https://doi.org/10.1016/0079-6611(90)90029-2.

Roberts, J.M., Harvey, S.M., Lamont, P.A., Gage, J.D., Humphery, J.D. (2000). Seabed photography, environmental assessment and evidence for deep-water trawling on the continental margin west of the Hebrides. Hydrobiol. 441, 173-183.

Rooper, C.N., Sigler, M.F., Goddard, P., Malecha, P., Towler, R., Williams, K. et al. (2016). Validation and improvement of species distribution models for structure-forming invertebrates in the eastern Bering Sea with an independent survey. Mar. Ecol. Prog. Ser. 551, 117-130. doi: https://doi.org/10.3354/meps11703.

Sherwin, T.J. (1991). “Evidence of a deep internal tide in the Faroe-Shetland Channel”, in Tidal Hydrodynamics, eds. B.B. Parker B.B. (New York, John Wiley & Sons), 469–488.

Sherwin, T.J., Williams, M.O., Turrell, W.R., Hughes, S.L., Miller, P. (2006). A description and analysis of mesoscale variability in the Faroe-Shetland Channel. J. Geophys. Res. 111, C03003, doi:10.1029/2005JC002867.

Strand, R., Whalan, S., Webster, N.S., Kutti, T., Fang, J.K.H., Luter, H.M. et al. (2017). The response of a boreal deep-sea sponge holobiont to acute thermal stress. Sci. Rep. 7:1660. https://doi.org/10.1038/s41598-017-01091-x.

Sweetman, A.K., Thurber, A.R., Smith, C.R., Levin, L.A., Mora, C., Wei, C-L. et al. (2017). Major impacts of climate change on deep-sea benthic ecosystems. Elem. Sci. Anthr. 5:4. doi: https://doi.org/10.1525/elementa.203.

Thomas, T.R.A., Kavlekar, D.P., LokaBharathi, P.A. (2010). Marine Drugs from Sponge-Microbe Association—A Review. Mar. Drugs 8, 1417-1468. doi:[10.3390/md8041417].

Tjensvoll, I., Kutti, T., Fosså, J.H., Bannister, R.J. (2013). Rapid respiratory responses of the deep-water sponge *Geodia barretti* exposed to suspended sediments. Aquat. Biol. 19, 65-73. https://doi.org/10.3354/ab00522.

Turrell, W.R., Slesser, G., Adams, R.D., Payne, R., Gillibrand, P.A. (1999). Decadal variability in the composition of Faroe Shetland Channel bottom water. Deep-Sea Res. Part I 46, 1-25. https://doi.org/10.1016/S0967-0637(98)00067-3.

Vad J., Kazanidis G., Henry L-A., Jones D.O.B., Tendal O.S., Christiansen S. et al. (2018). Potential impacts of offshore oil and gas activities on deep-sea sponges and the habitats they form. Adv. Mar. Biol. 79, 33-60. https://doi.org/10.1016/bs.amb.2018.01.001.

van Soest, R.W.M., and Lavaleye, M.S.S. (2005). Diversity and abundance of sponges in bathyal coral reefs of Rockall Bank, NE Atlantic, from boxcore samples. Mar. Biol. Res. 1, 338–349. https://doi.org/10.1080/17451000500380322.

van Soest, R.W.M., Cleary, D.F.R., de Kluijver, M.J., Lavaleye, M.S.S., Maier, C., van Duyl, F.C. (2007). Sponge diversity and community composition in Irish bathyal coral reefs. Contrib. Zool. 76:121–142.

Victorero, L., Watling, L., Deng Palomares, M.L., Nouvian, C. (2018). Out of Sight, But Within Reach: A Global History of Bottom-Trawled Deep-Sea Fisheries From >400 m Depth. Front. Mar. Sci. 5:98. doi: 10.3389/fmars.2018.00098.

Witte, U. (1996). Seasonal reproduction in deep-sea sponges – triggered by vertical particle flux? Mar. Biol. 124, 571-581.

Yahel, G., Whitney, F., Reiswig, H.M., Eerkes-Medrano, D.I, Leys, S.P. (2007). In situ feeding and metabolism of glass sponges (Hexactinellida, Porifera) studied in a deep temperate fjord with a remotely operated submersible. Limnol. Oceanogr. 52, 428–440. https://doi.org/10.4319/lo.2007.52.1.0428.

3.2 Mingulay Reef Complex (northeast Atlantic, UK): Impacts of the North Atlantic Oscillation and gyre dynamics on cold-water coral reef biodiversity and biogeography

Authors: Georgios Kazanidis, Lea-Anne Henry, Johanne Vad, Laurence H. De Clippele, J Murray Roberts

Acknowledgements: Sam Jones, Clare Johnson, Mark Inall

Abstract

The present study quantified effects of the North Atlantic Oscillation (the major mode of atmospheric variability in the North Atlantic) and changing gyre dynamics relative to spatial variability in seafloor terrain on cold-water coral reef communities in Scotland. Benthic sampling took place in 78 stations over 2003-2011 at the Mingulay Reef Complex, an inshore cold-water coral reef off western Scotland (northeast Atlantic). Spatial patterns of bathymetry, topography, macrohabitat type and hydrography were examined vs. the interannual variability of the North Atlantic Oscillation Index (NAOI) and associated changes in the intensity of the subpolar gyre (SPG), temperature, salinity and kinetic energy. Statistical analysis based on partial redundancy analyses (pRDAs) revealed that both spatial (macrohabitat, maximum speed current, fine-scale bathymetric position index, eastness, ruggedness and slope; 10.53%, $p<0.001$) and temporal variability (previous- and same year NAOI; 4.31%, $p<0.001$) exerted a significant impact on shaping Mingulay macrobenthos composition (total variance explained 16.91%, $p<0.001$). Suspension feeders of a transatlantic distribution were associated with high NAOI, probably due to increased seawater temperature and kinetic energy in Mingulay during high NAOI years (2003-2005). On the contrary, low NAOI supported the expansion of suspension/filter feeders with a North-Atlantic and Arctic distribution; it is highly likely that this was due to a sharp decrease in Mingulay seawater temperature in 2009-2010 and 2011. Interestingly, most of the taxa associated with NAOI shifts were sessile suspension feeders indicating the higher susceptibility of this group to changing oceanic conditions. In addition, large-sized predator polychaetes (Eunicidae) were associated with low NAOI, implying substantial changes in the Mingulay food web structure and reef strengthening in low NAOI

years. In conclusion, all the taxa associated with NAOI shifts belong to the most common species of Mingulay Reef Complex in terms of distribution, density and biomass. This suggests that the interannual variability of the North Atlantic Oscillation and longer term gyre dynamics can induce substantial shifts in the core of the macrobenthic community alternating thus ecosystem structure and functioning in this VME.

Introduction

Unraveling atmosphere-ocean interactions is of major importance in our efforts to understand the structure and functioning of marine ecosystems as these interactions can have an impact on the hydrography (i.e. direction and magnitude of ocean fluxes) (Furevik and Nilsen 2013; Seyfried et al. 2017; Gastineau et al. 2018) as well as on the physical, chemical and biological properties of water masses (Naqvi et al. 2005; Patara et al. 2011; Döös et al. 2017; Simpson et al. 2018). In the North Atlantic, the major mode of atmospheric variability is the North Atlantic Oscillation (NAO), usually expressed through the normalized Sea-Level Pressure (SLP) difference between Iceland and the Azores or as the dominant Principle Component (PC) of the SLP over the North Atlantic. This mode incorporates several climatic variables (e.g., water temperature, prevailing wind direction and speed, precipitation) (Jones et al. 1997; Hurrell et al. 2003). A large difference in SLP, mentioned as a high North Atlantic Oscillation Index (NAOI, hereafter), is associated with stronger than normal westerlies and with a higher intensity and frequency of storms over the subpolar North Atlantic Ocean. On the contrary, low NAOI is associated with warmer than normal weather and relatively fewer storms (Yashayaev et al. 2015). This NAOI-related atmospheric variability is a major driving force for long term variability in the Subpolar North Atlantic Ocean water mass characteristics and circulation. Specifically, NAOI has been related -among others- with the weakening in the extent and intensity of the subpolar gyre (SPG) after the mid-90's (changing from strong high to low NAOI values, in the winter 1995/96; Lohmann et al. 2009), a gradual decrease in the transport of the North Atlantic Current during the low NAOI period of the 1960s followed by an increase during the subsequent 25 years of high NAOI (Curry and McCartney 2001; Breckenfelder et al. 2017). NAO is also linked to the interannual variability of the eddie kinetic energy in the west Greenland current (Zhang and Yan 2018), more (less) vigorous Iceland-Scotland Overflow Water flow during low (high) phases of the NAOI (Boessenkool et al. 2007), and a quick response of dense water outflow into the deep layers of the North Atlantic through the Denmark Strait on monthly scale (Moshonkin et al. 2017). Furthermore,

the NAOI variability has been connected to local sea surface heat fluxes in the Labrador Sea (Ortega et al. 2017), the creation of negative salinity anomalies in the north Atlantic's eastern SPG (transport of fresh, cold water in eastern SPG in high NAOI; Herbaut and Houssais 2009; see also above), changes in the thermohaline features across most of the intermediate levels in the northwestern Iberian deep ocean (with the most notable event being the warming and increasing salinity that followed the large NAOI drop of 2010; Prieto et al. 2015), increase in the salinity of the Iceland–Scotland Overflow Water due to the retraction of the SPG (Sarafanov et al. 2010; see also above) and raised salinity of western Europe shelf waters following prolonged periods of high NAOI (Inall et al. 2009).

On top of changes in seawater hydrology/physical/chemical parameters, NAOI has also been investigated for its impact across a plethora of organisms and their associations. In the pelagic zone, studies have shown changes in the timing of algae bloom in Greenland (Qu et al. 2016), Mediterranean chlorophyll biomass (Basterretxea et al. 2018 *Calanus finmarchicus* abundance (Turner et al. 2006; Heath et al. 2008; see also Kimmel and Hameed 2008) and populations dynamics of carnivorous zooplankton, fish and top predators (e.g. Báez 2016; D'Ambrosio et al. 2016; Alheit et al. 2018). Long-term studies on benthos have shown a positive association between NAOI and total abundance, species richness and total biomass in coastal macrofaunal communities in southern North Sea, and sea surface temperature (SST) was suggested as the link between climate variability and benthos (Kröncke et al. 1998, 2001; see also Beuchel et al. 2006 for analogous findings on hard-bottom communities). Furthermore, positive association was found between Swedish coastal soft-bottom macrobenthos's abundance/biomass and stream flow, which in turn was negatively correlated with NAOI; based on that Tunberg and Nelson (1998) suggested that climate variability results in bottom-up control of benthic communities through shaping primary production.

Despite these findings, the relationship between NAOI and benthic communities is not consistent across regions, not homogenous across all the faunal groups of a community and may be influenced by local environmental conditions (e.g. hydrography, food supply, extreme events), faunal community composition and species' autoecology (Birchenough et al. 2015). For example, species diversity has shown a positive (Dippner and Kröncke 2003), negative (Rees et al. 2006) and no association to NAOI (Frid et al. 2009). In addition, extreme events linked with NAOI did not have the same impact across all groups of a community, e.g. the severe winter of 1979 linked to low NAOI values caused the greatest

reductions in biomass and species richness in areas low in the intertidal zone of the Wadden Sea (Beukema 1979). Furthermore, the epibenthic communities in the German Bight were severely affected by the cold winter in 1995-1996 (linked also to a low NAOI), which also resulted in high abundance and biomass of the opportunistic brittle star *Ophiura albida* (Neumann et al. 2008).

In contrast to the information available for the effects of NAOI-related processes to shallow-water communities, there is a lack of times series for deep-sea benthic ecosystems including studies on NAOI-related effects (Glover et al. 2010). Interestingly, existing studies have shown that dramatic changes in the community composition, biomass and ecosystem functioning in the abyssal zone of North-East Atlantic (i.e. the "*Amperima* Event"; Billett et al. 2001, 2010) may have been caused by changes in quantity and quality of food supplied to benthos (Kiriakoulakis et al. 2001; Lampitt et al. 2001, 2010) caused in turn by low winter NAOI values inducing shifts in upper ocean biogeochemistry (Smith et al. 2009). Furthermore, NAOI-related impacts have also been shown in deep slope off Catalonia. There, the increase in the abundance of benthic feeders and the deepening of the decapod crustacean assemblages were linked to low NAOI-related increased rainfall and increased river discharges in western Mediterranean leading to an enhanced food supply for the macrobenthos (Cartes et al. 2009, 2015).

Information presented above provides evidence that apart from shallow water, deep-water ecosystems can also be affected severely by changes in atmosphere-ocean interactions. Filling this gap is of uttermost importance not only for advancing our understanding about the processes that shape structure and functioning of deep-sea ecosystems but also for implementing effective conservation and environmental monitoring strategies in deep-water ecosystems because we need to be able to disentangle impacts of human activities from other drivers of change. Cold-water coral reefs are ideal systems for advancing our understanding about the possible impacts of NAOI in the deep sea as they are hotspots of biodiversity (Henry and Roberts 2017) facilitating thus the investigation of NAOI-related impacts across a wide spectrum of taxonomic and functional groups. On top of that, the reefs are structurally-complex systems providing the opportunity to unravel the relative importance of temporal vs spatial gradients of environmental parameters in shaping ecosystem structure and functioning.

Taking into account the above, we investigated changes in cold-water coral reef communities in order to disentangle natural spatial variability from effects of inter-annual climate change at the Mingulay Reef Complex, an inshore cold-water coral reef in the North-East Atlantic. The Mingulay Reef

Complex (MRC, hereafter) is one of the most-studied cold-water coral reefs in terms of acoustic seabed mapping, hydrographic circulation and biodiversity (Roberts et al. 2005, 2009, Henry et al. 2010, 2013; Findlay et al. 2013; Navas et al. 2014; De Clippele et al. 2017). It is found in a topographically complex deep-water channel connecting south to the Scottish continental shelf and Atlantic Ocean and is restricted to areas of full salinity Atlantic water (35 psu). MRC hosts high biodiversity (both in terms of taxonomic and functional traits composition) (Roberts et al. 2009) which changes across broad- and fine-scale spatial gradients (Henry et al. 2010, 2013; Kazanidis et al. 2016). Recent findings have shown a strong positive association between NAOI and temporal variability in MRC salinity and kinetic energy (Jonson et al. 2018; see also Inall et al. 2009); however, the role of this temporal variability in shaping the composition of Mingulay macrobenthos is unknown.

In the present study, we have investigated changes in Mingulay Reef Complex macrobenthos composition across spatial and temporal gradients, focusing on the role of NAOI. Unravelling the impacts of inter-annual variability in NAOI on cold-water coral reef biodiversity will advance our knowledge about deep-sea ecosystems in the North Atlantic. This knowledge will, in turn, facilitate the prediction of their status under future climate scenarios and guide the adaptive management of these vulnerable marine ecosystems.

Methods

Study Area

The Mingulay Reef Complex is an inshore seascape of reef mounds in east Mingulay (Outer Hebrides Sea) in western Scotland. Surveys carried out in 2003 using multibeam echosounder accompanied by seabed video surveys revealed mounds of *L. pertusa* in three sites 14 km east of Mingulay and at depths ranging from 120 to 190 m water depth [i.e. in Mingulay Area 1 (MRC1; 72-215m water depth), Mingulay Area 5 northern (MRC 5N; 109-240m) and Mingulay Area 5 southern (MRC 5S; 148-254m)] (Roberts et al. 2005, 2009). Subsequent studies in 2006 using also acoustic and seabed video techniques revealed two new reef areas in Mingulay, i.e. the elongated “Banana Reef” and a series of mounds called the “Four Mounds” (Maier 2006).

Mingulay Area 1 is ~4 km long and ~500 m wide east-west ridge rising 40 to 80 m above seafloor. It has a steep southern slope and a gentler slope to the north (Davies et al. 2009; Roberts et al. 2009). MRC 5N is another ridge about 2 km long, oriented SW–NE. It slopes gently down from 109 to 240 m

depth. Extraction of data took place for 78 stations, where benthic sampling took place (Figure 1; Table 1; see also below). The extraction of bathymetric (i.e. depth) and topographic (slope, aspect, ruggedness, broad-scale bathymetric position index (BPI), fine-scale BPI)) was based on multibeam echosounder data (see above), using the Spatial Analyst and Benthic Terrain Modeler toolboxes (Walbridge et al. 2018) in ArcGIS (10.6). Only standardized BPIs were considered here in order to avoid any bias due to the shift in scale between broad and fine indices (Walbridge et al. 2018). Aspect was subsequently converted into eastness and northness as explained in Wilson et al. (2017). Bathymetric and topographic variables were available for 78 stations, where benthic sampling took place (Table 1; Figure 1).

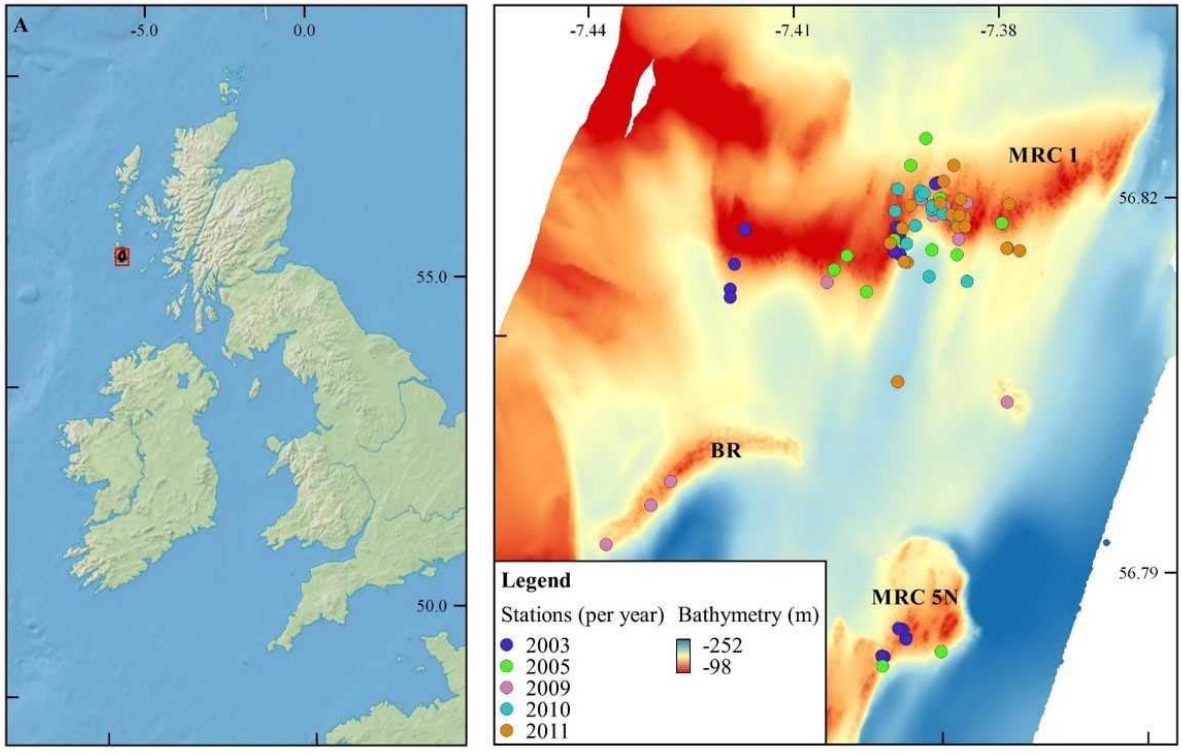

Figure 1. *Left panel: Mingulay Reef Complex in the Outer Hebrides Sea (North-East Atlantic). Right panel: Sampling stations (per year) in Mingulay Reef Complex 1 (MRC 1), Mingulay Reef Complex 5 North (MRC 5N) and Bana Reef (BR).*

The currents on the summit of the Mingulay Area 1 have a SSW-NNE direction with average current speed being higher at the easternmost part than the westernmost (Davies et al. 2009). Near the base of the southern flank of Mingulay Area 1, the main current direction is SW-NE as a response to the local topography. Local hydrography data was extracted from a high-resolution 3D ocean model described by Moreno Navas et al. (2014). From this model, both average current speed and maximum current speed

(m/s) were extracted at the location of each station using the Spatial Analyst toolbox in ArcGIS (10.6) (Table 1).

The North-Atlantic Oscillation (NAOI) and Subpolar Gyre (SPG)

Winter North Atlantic Oscillation Index (NAOI, hereafter) values ((both for Principal Component (PC) and Station Based (ST)) were extracted from the NCAR UCAR Climate Data Guide online platform (climatedataguide.ucar.edu) (Hurrell et al. 2003), both for same- and previous year of macrobenthos sampling (Table 2) (Zettler et al. 2017). Intensity of the Subpolar Gyre (SPG), temperature and salinity values in Mingulay were provided by the Scottish Association for Marine Science (Table 2).

Macrobenthos sampling

Benthic samples were collected in June/July 2003 (Research Vessel "*Lough Foyle";* Roberts et al. 2005; Henry et al. 2010), May 2005 (RV "*Esperanza*"; Henry et al. 2013), June/July 2009 (Royal Research Ship "*Discovery*"; Inall and shipboard party 2009), Feb/May 2010 (RV "Calanus"; Last et al. 2010a, b) and June/July 2011 (RRS "*Discovery*"; Achterberg and shipboard party 2011). The collection of benthic samples was carried using a Day Grab in 2003, and a modified Van Veen Grab in 2005, 2009, 2010 and 2011; both grans sampled an area of approximately 0.1 m^2 each time it was deployed. Type of macrohabitat was grouped in one of the following categories: muddy sand, rubble, rock, live coral, dead framework, live and dead framework. Samples were sieved at 1 mm, stored in 4% borax-buffered seawater and transferred to 70% industrial methylated spirit. These were identified to the lowest possible taxonomic level using available taxonomic keys and guidance from expert taxonomists (see Acknowledgements). A list of 344 taxonomic groups was produced (excluding sponges/nematodes due to a lack of taxonomic resolution and hydroids due to time constraints; Table S1 in the Supplementary Material). Each species was classified into a) a feeding guild (suspension/filter feeders, deposit feeder/grazer, predator, omnivore) based on predominant feeding traits (Henry et al. 2013; Kazanidis et al. 2016) and b) mobility status (sessile, mobile).

Statistical analysis

In order to eliminate any statistical bias in our analysis, correlations between environmental variables were determined, using the R package corrplot (Wei and Simko 2017). As regards the topographic variables, there was high (>0.60) positive correlation between a) fine-scale and broad-scale BPI leading

to the exclusion of the broad-scale BPI. As regards the NAOI, there was high (>0.60) positive correlation between the PC-based and the Station-Based NAOIs leading to the exclusion of the Station-Based.

In order to unravel the impact of temporal and spatial variables, a set of redundancy analyses (RDA) and partial redundancy analyses (pRDA) were performed. First, a Hellinger transformation was applied to the benthic community presence/absence matrix to reduce the weight of rare species (Legendre and Gallagher, 2001). Then, a full RDA was conducted to estimate the total proportion of variation in the benthic community, which could be explained by all the available environmental variables. Finally, pRDAs considering either spatial or temporal variables were performed to determine the proportions of variation in the benthic community explained by each variable subgroup. All models were run with R package vegan (Oksanen et al. 2017). Biplots for the full RDA model and for each pRDAs were also constructed with R (R Core Team, 2018). To extract the members of the benthic community that were the most influenced by fluctuations in the NAOI, the sum of the squared score values for each species points on the temporal pRDA biplot were first calculated. The sums were then ranked the fifteen highest scores corresponding to the fifteen most external species points on the temporal pRDA biplot were selected.

Table 1. *Principal Component-based North Atlantic Oscillation Index (NAOI) for previous and same year of benthic sampling (source: www.climatedataguide.ucar.edu); Subpolar Gyre (SPG) intensity, temperature and salinity values in Mingulay Reef Complex over the years of benthic sampling.*

Variable / Year	**2003**	**2005**	**2009**	**2010**	**2011**
PC-based same-year NAOI	0.06	0.36	0.05	-2.56	-0.67
PC-based previous- year NAOI	0.63	-0.11	1.07	0.05	-2.56
SPG	High	High	Low	Low	Low
Temp (^{o}C)	11.336	12.436	9.498	9.1395	9.7006
Salinity (psu)	35.338	35.27	35.358	35.287	35.252

Results

The total RDA model -a combination of depth, slope, northness, eastness, ruggedness, fine-scale BPI, macrohabitat, average current speed (C_{AVE}), maximum current speed (C_{MAX}), same- and previous-year NAOI- explained 16.91% (p<0.001) of the variation in macrobenthos community composition (Table

3). Excluding the effects of temporal variability in the pRDA, it was shown that spatial variability had a significant impact in shaping the community composition and explained 10.53% (p<0.001) of the variability. Variables that had a significant contribution in explaining variability in the composition of the macrobenthos were macrohabitat, maximum current speed (C_{MAX}), fine BPI, eastness, ruggedness and slope (Table 2; Figures 2 and 3). Excluding the effects of spatial variability, it was shown that the same-year and the previous-year NAOI explained also a significant amount of variation in community composition (4.31%, p<0.001) (Table 2; Figure 4).

Out of the fifteen taxa mostly affected by topographic and hydrographic variables, six were bryozoans (*Reteporella beaniana*, *Annectocyma major*, *Pencilletta penicillata*, *Plagioecia patina*, *Buskia* sp., *Diplosolen obelium*), two were polychaetes (*Lumbrineris* spp., *Glycera* sp.), two arthropods (*Munida sarsi*), two bivalves (*Modiolula phaseolina,* Bivalvia sp.*,*), two echinoderms (*Amphiura chiajei*, *Ophiothrix fragilis*) and one anthozoan (*Parazoanthus anguicomus*) (Figure 5). In terms of feeding types most of these taxa were suspension/filter feeders (66.7%), followed by predators (20%) and deposit feeders/grazers (13.3%). Most of the taxa were sessile organisms (60%).

Out of the fifteen species most affected by NAOI, five were bryozoans (*Disporella hispida*, *Schizomavella* (*Schizomavella*) *linearis*, *Plagioecia patina*, *Buskia* sp., *Tubulipora* spp.), four polychaetes (Syllidae spp., Eunicidae spp., *Serpula vermicularis*, *Brachiomma bombyx*), two echinoderms (*Amphiura chiajei*, *Ophiactis balli*), two bivalves (*Modiolula phaseolina, Heteranomia squamula*), one Tunicate (*Polycarpa pomaria*) and one anthozoan (*Parazoanthus anguicomus*) (Table 3; Figure 6). In terms of feeding types, most of the taxa were suspension/filter feeders (73.3%), followed by predators (13.3%), deposit feeders/grazers and omnivores (13.3%, in total). Most of the taxa were sessile (73.3%).

Table 2. *Results from the RDA and pRDA analysis.*

	RDA1	RDA2	R^2	*p*
Spatial RDA				
Macrohabitat	0.84103	-0.54099	0.4040	0.001
Depth	-0.85790	0.51381	0.0383	0.241
Slope	-0.22708	-0.97388	0.0783	0.037
Northness	-0.05088	0.99870	0.0786	0.057
Eastness	-0.36233	0.93205	0.1210	0.009
Ruggedness	-0.68882	-0.72494	0.0994	0.025
Fine BPI	0.27646	-0.96103	0.1716	0.002
Average Current Speed (C_{AVE})	-0.14102	-0.99001	0.0081	0.747
Maximum Current Speed (C_{MAX})	0.99600	-0.08933	0.2181	0.001
Variance explained by Spatial RDA: 10.53% ($p<0.001$)				
Temporal RDA				
Same year-NAOI	0.92346	0.38369	0.6240	0.001
Previous year-NAOI	0.70973	-0.70448	0.3814	0.001
Variance explained by Temporal RDA: 4.31% ($p<0.001$)				
Total RDA Variance explained by Total RDA: 16.91% ($p<0.001$)				

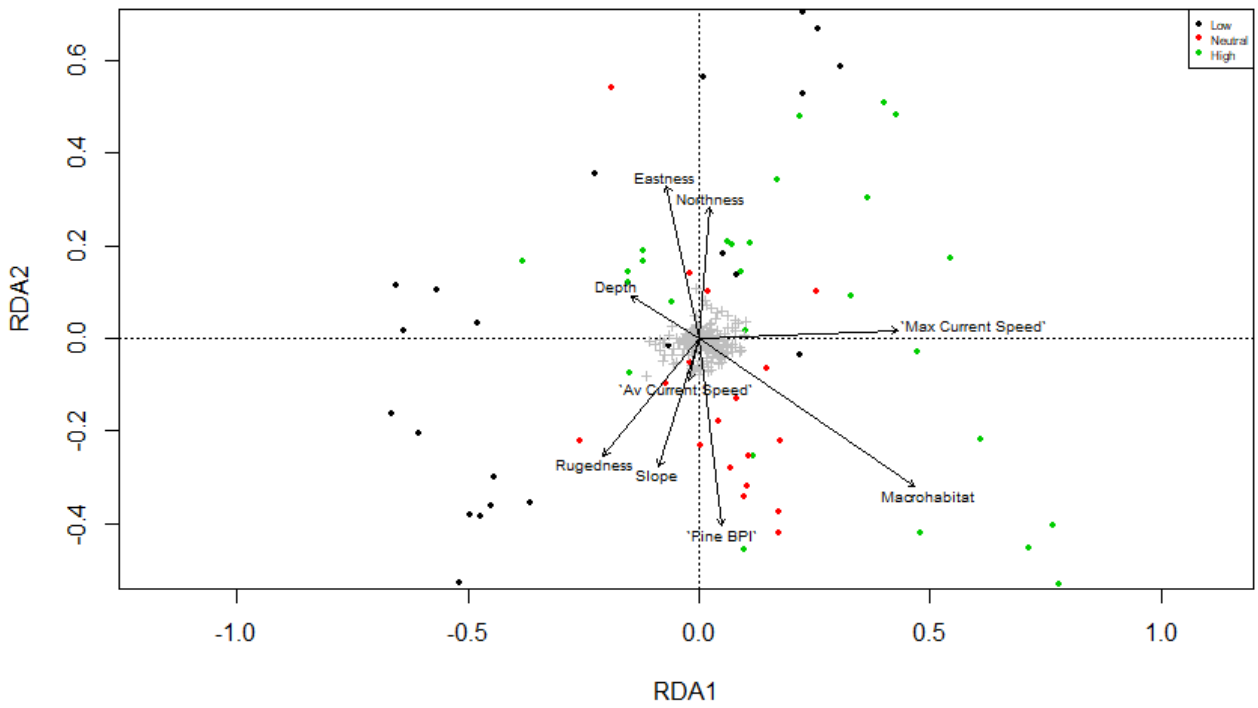

Figure 2. *Biplot of pRDA showing the impact of spatial variability in bathymetric, topographic and hydrographic variables in the composition of macrobenthos in Mingulay Reef Complex. Each circle represents a station. Each grey cross represents a species. Legend: "Low": low intensity of Subpolar Gyre (SPG); "Medium": medium intensity of SPG; "High": high intensity of SPG.*

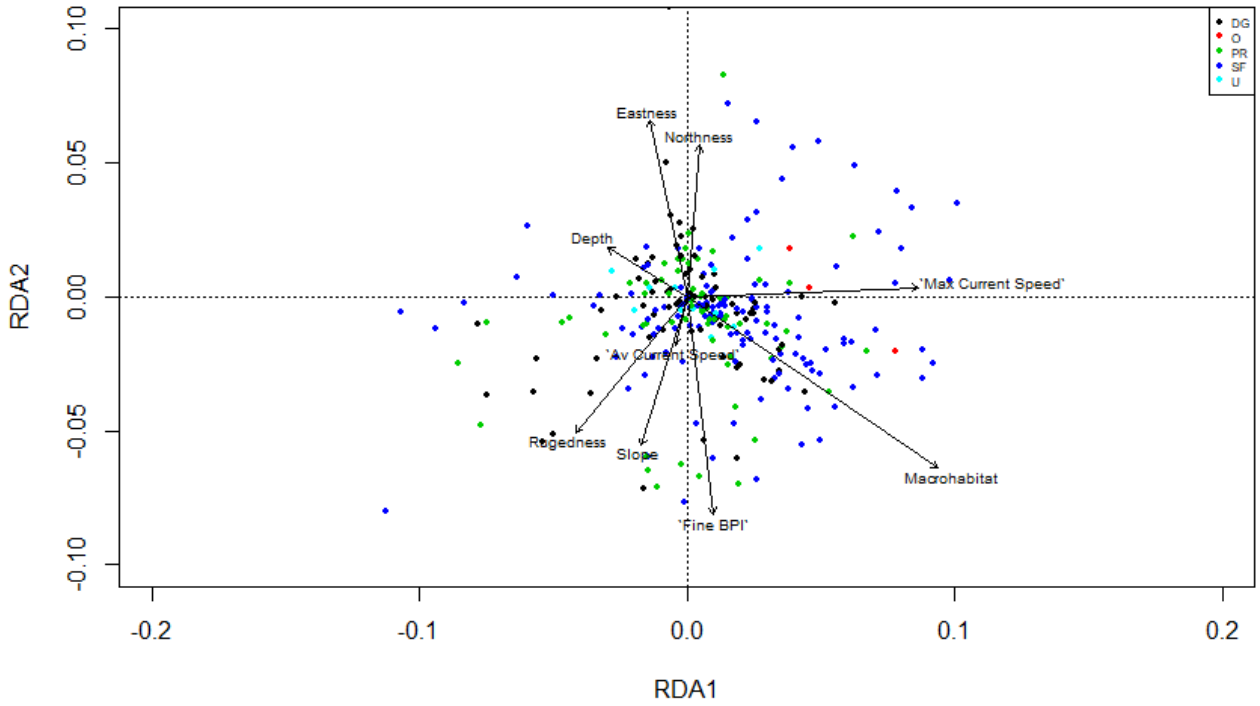

Figure 3. *Biplot of pRDA showing the impact of spatial variability in bathymetric, topographic and hydrographic variables in the composition of feeding types of macrobenthos in Mingulay Reef Complex. Each circle represents a feeding type (see legend for details).*

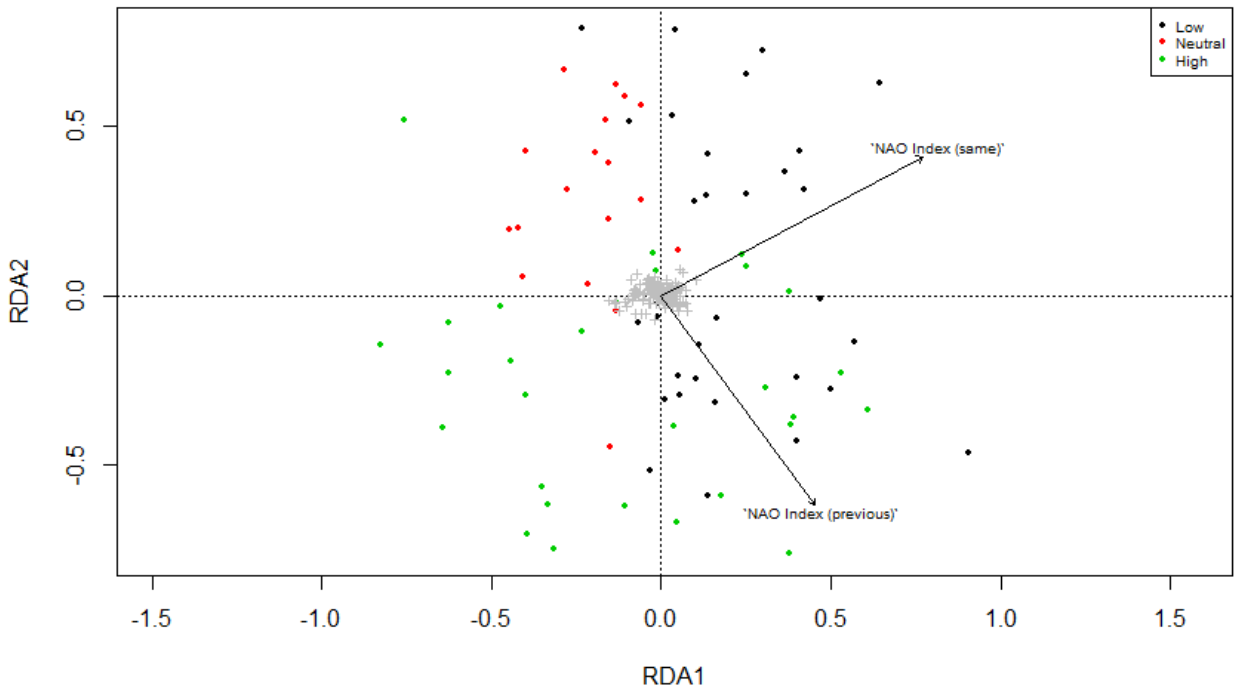

Figure 4. *Biplot of pRDA showing the impact of previous- and same-year North Atlantic Oscillation Index (NAOI) in the composition of macrobenthos in Mingulay Reef Complex. Each circle represents a station. Each grey cross represents a species. Legend: "Low": low intensity of Subpolar Gyre (SPG); "Medium": medium intensity of SPG; "High": high intensity of SPG.*

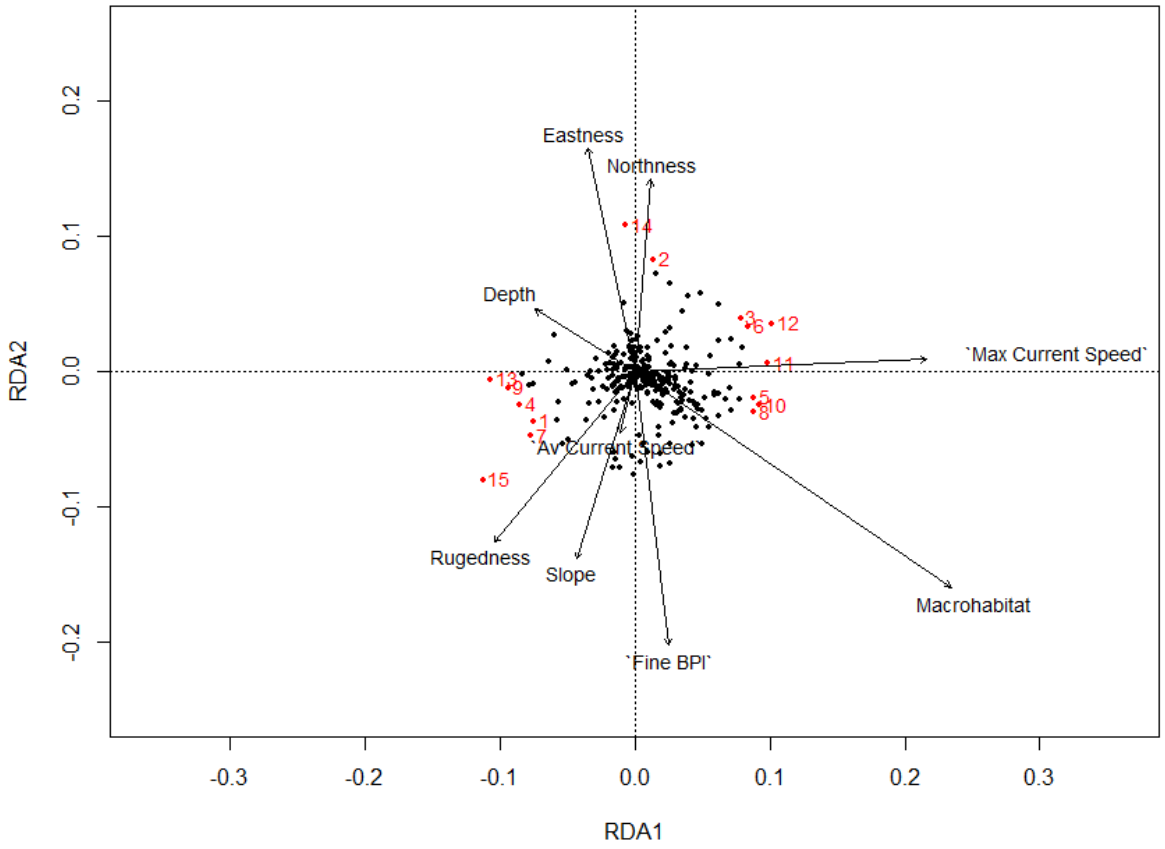

Figure 5. *Biplot of pRDA showing the impact of bathymetric, topographic and hydrographic variables on Mingulay Reef Complex macrobenthic species. The fifteen mostly NAOI-associated species are highlighted in red.* ***1:*** Lumbrineris *spp.,* ***2*****:** Munida sarsi*,* ***3:*** Reteporella beaniana*,* ***4:*** Munida rugosa*,* ***5:*** Annectocyma major*,* ***6:*** Pencilletta penicillata ***7:*** Glycera *sp.,* ***8*****:** Plagioecia patina*,* ***9:*** *Bivalvia spp.,* ***10:*** Buskia *sp.,* ***11:*** Diplosolen obelium*,* ***12:*** Modiolula phaseolina*,* ***13:*** Parazoanthus anguicomus*,* ***14:*** Amphiura chiajei*,* ***15*****:** Ophiothrix fragilis*.*

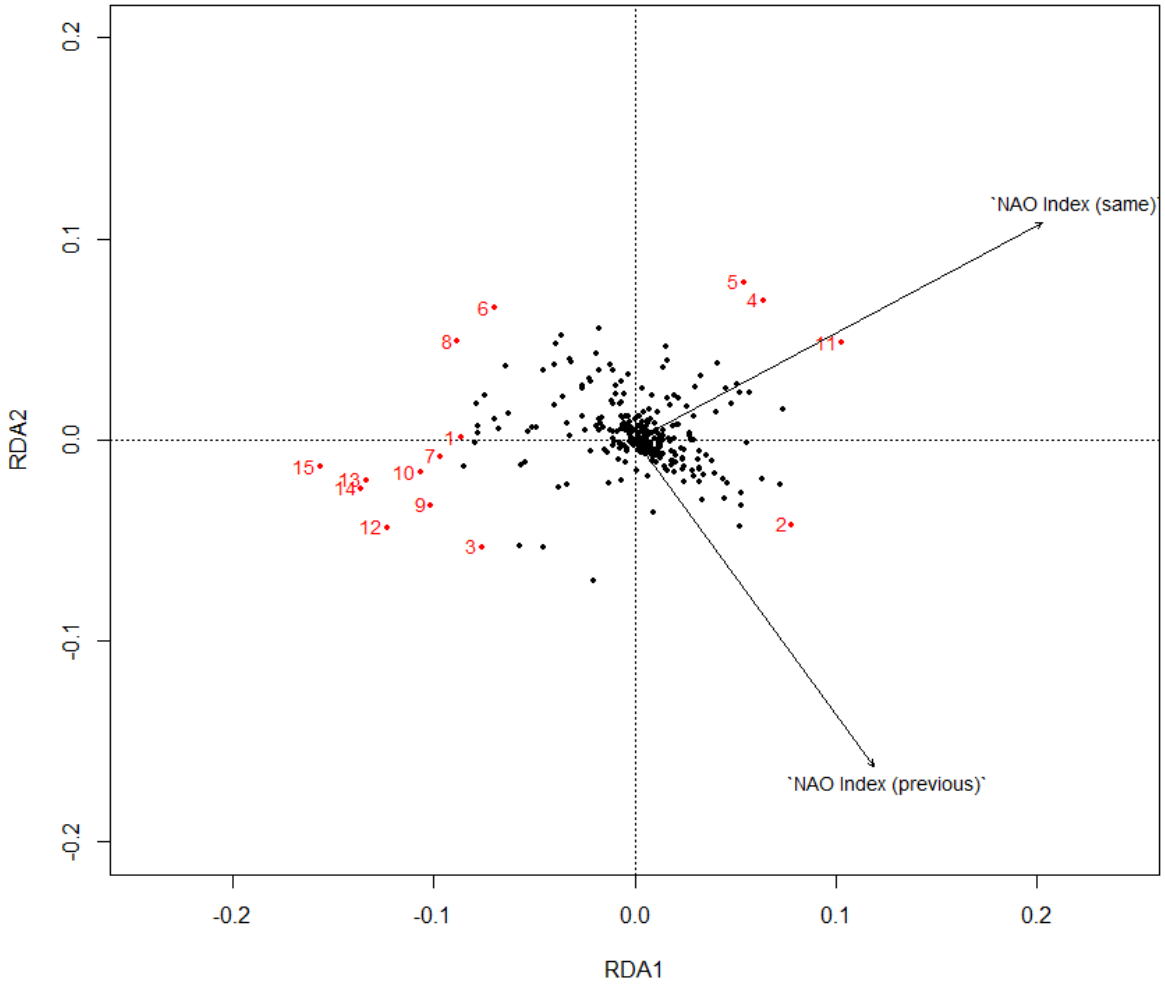

Figure 6. *Biplot of pRDA showing the impact of previous- and same-year North Atlantic Oscillation Index (NAOI) on Mingulay Reef Complex macrobenthic species. The fifteen mostly NAOI-associated species are highlighted in red.* ***1:*** Disporella hispida*,* ***2:*** *Syllidae spp.,* ***3:*** *Eunicidae spp.,* ***4:*** Amphiura chiajei*,* ***5:*** Serpula vermicularis*,* ***6:*** Branchiomma bombyx*,* ***7:*** Modiolula phaseolina*,* ***8:*** Polycarpa pomaria*,* ***9:*** Heteranomia squamula*,* ***10:*** Schizomavella (Schizomavella) linearis*,* ***11:*** Parazoanthus anguicomus*,* ***12:*** Plagioecia patina*,* ***13:*** Buskia *sp.,* ***14:*** *Tubulipora spp.,* ***15:*** *Ophiactis balli****.*** *Top left quartile: low previous-year North Atlantic Oscillation Index (NAOI); top right quartile: high same-year NAOI; bottom right quartile: high previous-year NAOI; bottom left quartile: low same-year quartile NAOI.*

Table 3. *PC-based NAOI values, feeding type (SF: suspension/filter feeder; DG: deposit feeder/grazer; O:omnivore;), mobility (SE: sessile; MB: mobile) and geographic distribution (extracted from World Register of Marine Species website - http://www.marinespecies.org/). Abbreviations: ANT: Anthozoans; POL: Polychaetes; ECHIN: Echinoderms; MOL: Molluscs; BRY: Bryozoans; TUN: Tunicates; FT: Feeding Type; SF: Suspension/filter feeders; DG: Deposit feeder/Grazers; PR: Predators; O: omnivores; MOB: Mobility; SE: Sessile; MB: Mobile. NE: North-East; NW: North-West; SW: South-West.*

	Species	GROUP	FT	MOB	Geographic distribution
High same-year NAOI	*Parazoanthus anguicomus*	ANT	SF	SE	NE ATLANTIC, MEDITERRANEAN SEA
	Serpula vermicularis	POL	SF	SE	NE/NW ATLANTIC, MEDITERRANEAN, RED SEA, SW INDIAN, NEW ZEALAND
	Amphiura chiajei	ECHIN	DG	MB	NE ATLANTIC, ARCTIC, MEDITERRANEAN SEA
High previous-year NAOI	Syllidae spp.	POL	PR	MB	-
Low same-year NAOI	*Modiolula phaseolina*	MOL	SF	SE	NE ATLANTIC, MEDITERRANEAN SEA, BLACK SEA, ARCTIC
	Ophiactis balli	ECHIN	O	MB	NE ATLANTIC, ARCTIC
	Schizomavella linearis	BRY	SF	SE	NE & NW ATLANTIC, MEDITERRANEAN SEA
	Heteranomia squamula	MOL	SF	SE	ALL ATLANTIC, MEDITERRANEAN SEA, ARCTIC, NE PACIFIC
	Plagioecia patina	BRY	SF	SE	NE & NW ATLANTIC, MEDITERRANEAN SEA
	Buskia sp.	BRY	SF	SE	-
	Tubulipora spp.	BRY	SF	SE	-
	Eunicidae spp.	POL	PR	MB	-
Low previous-year NAOI	*Branchiomma bombyx*	POL	SF	SE	NE ATLANTIC, MEDITERRANEAN SEA, ARCTIC
	Polycarpa pomaria	TUN	SF	SE	NE ATLANTIC, MEDITERRANEAN SEA, ARCTIC
	Disporella hispida	BRY	SF	SE	NE & NW ATLANTIC, MEDITERRANEAN SEA

Discussion

The present work examined the role of spatial and temporal gradients of major environmental parameters in shaping a diverse both in terms of taxonomic and functional traits composition-community in the North-East Atlantic. Both the spatial patterns of topography and hydrography, as well as the interannual variability in the North Atlantic Oscillation Index (and the accompanying changes in water mass characteristics), played a significant role in shaping Mingulay Reef Complex macrobenthos. In agreement with previous studies on Mingulay Reef Complex macrobenthos (Henry et al. 2010, 2013;

Kazanidis et al. 2016), the present study has provided evidence about the significant role of macrohabitat, topographic (e.g. ruggedness) and hydrographic (e.g. maximum current speed) variables in shaping Mingulay macrobenthos. In addition, we have now advanced our knowledge for the dynamics of biodiversity in this inshore cold-water coral reef by unravelling the impact of interannual changes in the major mode of atmospheric variability in the North Atlantic. Sessile suspension/filter feeders seem to be the most impacted group by NAOI-induced changes in temperature, salinity and kinetic energy. Also, we have provided evidence that large-sized predators are also associated with NAOI-interannual changes which may cause cascading changes in Mingulay food-web structure and reef strengthening. Interestingly, all species associated with NAOI (either with high or low values) are among the commonest species of Mingulay Reef Complex (Henry et al. 2010, 2013; Kazanidis et al. 2016). This finding suggests that interannual changes in NAOI can induce substantial shifts in the core of the macrobenthic community of this inshore cold-water coral reef

Impacts of seafloor topography and local currents on Mingulay macrobenthos

Macrohabitat, eastness, maximum current speed (C_{MAX}), fine-scale BPI, ruggedness and slope exerted a significant impact on shaping Mingulay macrobenthos by creating different benthic environmental conditions which in turn hosted distinct communities both in taxonomic composition and functional traits (Figure 3). The type of macrohabitat had a positive association with suspension/filter feeders. Live and dead framework create complex 3-D structures hosting a species-rich fauna of suspension and filter feeders (e.g. anthozoans, hydrozoans, tunicates) (Henry et al. 2013), which often also has high density and biomass (Kazanidis et al. 2016). A relatively small number of suspension/filter feeders were strongly associated with maximum speed currents. These organisms were encrusting or adhered to solid surfaces which enabled them to capture food particles efficiently and proliferate under these fast-flow regimes. The community associated with maximum speed current included the encrusting bryozoans *Annectocyma major*, *Plagioecia patina*, *Diplosolen obelium* and the soft-bodied bryozoan *Buskia* sp. As it was expected, deposit-feeders/grazers and predators were not associated with high-flow regimes as under these conditions the food capture would be limited; indeed, the predator *Munida sarsi* which uses ambush tactics to capture prey from burrows (Hudson and Wigham 2003) was associated with low-speed currents (Figure 5).

Impacts of the NAO and SPG on Mingulay macrobenthos

The interannual variability of NAOI had a significant impact on shaping the temporal changes of macrobenthos community composition in Mingulay Reef Complex. To the best of our knowledge, this is the first time where evidence is provided about the impact of NAOI on cold-water coral reef communities. NAOI is the major mode of atmospheric variability in the North Atlantic, and its interannual variability causes shifts in the dynamics of oceanic systems (e.g. the SPG) and water mass features (e.g. temperature, salinity, kinetic energy), from year to year (Hátún et al. 2005; Lohmann et al. 2009). In Mingulay Reef Complex over the period 2003-2011, there were major changes in water mass characteristics, e.g. a decrease in seawater temperature (up to 3^{o}C) between the 2003/2005 and 2009/2010/2011 time periods (Table 1). These NAOI/SPG-induced changes in water mass characteristics had a clear impact to temporal changes detected in the community composition of Mingulay Reef Complex macrobenthos.

Same-year high NAOI showed a strong association with the anthozoan *Parazoanthus anguicomus* and the sedentary polychaete *Serpula vermicularis*. These two are among the most common macrobenthic species in Mingulay Reef Complex having a wide distribution, high density and high biomass (Henry et al. 2010, 2013; Kazanidis et al. 2016; Kazanidis and Witte 2016; present study). These two species feed mainly on fresh microalgae (Kazanidis and Witte 2016; Kazanidis et al. 2018), transported from the surface to the seabed through rapid downwelling (Davies et al. 2009). It is highly likely that the high kinetic energy in Mingulay Reef Complex associated with high NAOI (Johnson et al. 2018) promotes the extended suspension of food particles, which in turn benefits the proliferation of these two suspension feeders. This suggestion is in agreement with previous findings for sublittoral and deep-slope benthos where high NAOI induced the expansion or even the dominance of suspension feeders through an increase in suspended food particles, along with increase in seawater temperature and stronger hydrodynamic conditions (Kröncke et al. 2001, 2006; Cartes et al. 2009). The high kinetic energy recorded in Mingulay Reef Complex during high NAOI, may support even further the proliferation of *P. anguicomus* and *S. vermicularis* by facilitating their gametes' and larvae dispersal (Orton 1914; Ryland 2000).

Apart from the high kinetic energy, the expansion of *S. vermicularis* maybe further supported through the higher seawater temperature observed in Mingulay Reef Complex during high NAOI years.

Indeed, this species has a wide geographic distribution (see Table 3) including the Mediterranean Sea, New Zealand and the Red Sea; in the latter area the winter seawater temperature is ~21^{o}C (Gertman and Brenner 2004), i.e. much higher than ~9^{o}C in Mingulay Reef Complex (Findlay et al. 2013). Previous studies on the English Channel benthos have also revealed the extension of the geographic range of 2 warm water molluscs, i.e. *Ocenebra erinacea* and the introduced American slipper limpet *Crepidula fornicata* as well as the presence of warm water species absent in historic surveys; these biogeographic changes were possibly due to increased seawater temperature (Hinz et al. 2011).

In contrast to the suspension/filter feeders mentioned above linked to high NAOI, a group of suspension/filter feeders was associated with low NAOI (Table 3). Interestingly, half of these suspension/filter feeders have been recorded in Arctic regions (Table 3); thus, it seems that the NAOI/SPG-induced sharp decrease in seawater temperature in Mingulay over the years 2009-2010-2011 (Johnson et al. 2018) facilitated the expansion of these species. It is highly likely, also, that the low NAOI has supported the proliferation of the omnivorous ophiuroid *Ophiactis balli.* This species, which has also been recorded in Arctic areas, had not been found in Mingulay before 2009 (Henry et al. 2010; 2013). Interestingly, an increase in the abundance and biomass of the opportunistic brittle star *Ophiura albida* in German Bight was linked to the cold winter of 1995/1996 associated with low NAOI (Neumann et al. 2008). The proliferation and expansion of species associated with the low-NAOI may have also been supported through lower kinetic energy. This could be true for the small-sized bivalves *Modiolula phaseolina* and *Heteranomia squamula*. Although direct evidence is not available, these delicate-structured organisms probably prefer relatively slow currents while thick-walled *P. anguicomu*s and the sedentary *S. vermicularis* perform better under high kinetic-energy conditions (Henry et al. 2013; see also above).

Most species being associated with NAOI shifts (i.e. eleven out of fifteen, Table 3) are sessile suspension/filter feeders. This finding indicates the higher susceptibility of this functional group to changing oceanic conditions as they are unable to migrate in areas of more suitable environmental conditions. On the contrary, there were only four mobile species affected by a low or high NAOI (Table 4). The case of the Eunicidae polychaetes is perhaps, the most intriguing of them, both in terms of the parameters driving their proliferation in low NAOI years as well as the implications of such a shift for ecosystem functioning. The Eunicidae usually found in Mingulay Reef Complex is the large-sized predator

Eunice norvegica (Henry et al. 2010; present study). Although direct evidence is not available, increased availability of small-sized invertebrates that eunicids feed on (Table 4; Fauchald and Jumars 1979; Kazanidis and Witte 2016) may have triggered their proliferation. In turn, Eunicidae expansion may have induced changes in ecosystem functioning, e.g. higher predation, altered food-web structure and strengthened reef structure (Roberts 2005; Mueller et al. 2013).

In overall, the present investigation about the impact of NAOI interannual variability in Mingulay macrobenthos have shown that fifteen species had a strong association with NAOI. Interestingly, the fifteen species depicted from our analysis are among the most common macrobenthic species in Mingulay in terms of distribution, density and biomass (Henry et al. 2010, 2013; Kazanidis et al. 2016; Kazanidis and Witte 2016; present study). This finding indicates clearly the strong impact that interannual variability in NAOI and accompanying changes in water mass characteristics can have on Mingulay Reef Complex biodiversity by alternating the core of the macrobenthic community.

Acknowledgements

We would like to acknowledge captains, crews and scientists participated in the cruises where data used in the present study were collected (Research Vessel "*Lough Foyle"* - June/July 2003; RV "*Esperanza*" - May 2005; D340b cruise, Royal Research Ship "*Discovery*" - June/July 2009; RV "*Calanus*" - Feb/May 2010; D366/367 cruise, RRS "*Discovery*", June/July 2011). Also, we would like to thank the expert taxonomists for providing guidance on species identification: Meg Daly, Daphne Fautin (Anthozoa), Tammy Horton (Arthropoda), Jennifer Loxton (Bryozoa), Andrew Campbell, Chris Mah, Eve Southward (Echinodermata), Anna Holmes, Graham Oliver (Mollusca), Fabio Badalamenti, Ruth Barnich, Susan Chambers, Adriana Giangrande, Tim Worsfold (Polychaeta), Gretchen Lambert (Tunicata).

References

Achterberg E and shipboard party (2011) Cruise Report D366/367, RRS Discovery 366/367 6th June to 12th July 2011. University of Southampton, School of Ocean and Earth Science, National Oceanography Centre Southampton, 153 pages

Alheit J, Gröger J, Licandro P, McQuinn IH, Pohlmann T, Tsikliras AC (2019) What happened in the mid-1990s? The coupled ocean-atmosphere processes behind climate-induced ecosystem changes in the Northeast Atlantic and the Mediterranean. Deep-Sea Res II 159:130-142

Báez JC (2016) Assessing the influence of the North Atlantic Oscillation on a migratory demersal predator in the Alboran Sea. J Mar Biol Assoc UK 96:1499-1505

Basterretxea G, Font-Munoz JS, Salgado Hernanz PM, Arrieta J, Hernández-Carrasco I (2018) Patterns of chlorophyll interannual variability in Mediterranean biogeographical regions. Remote Sens Environ 215:7 17

Beuchel F, Gulliksen B, Carroll ML (2006) Long-term patterns of rocky bottom macrobenthic community structure in an Arctic fjord (Kongsfjorden, Svalbard) in relation to climate variability (1980–2003). J Mar Syst 63:35-48

Beukema JJ (1979) Biomass and species richness of the microbenthic animals living on a tidal flat area in the Dutch Wadden Sea: effects of a severe winter. Neth J Sea Res 13:203-223

Billett DSM, Bett BJ, Rice AL, Thurston ML, Galéron J, Sibuet M, Wolff GA (2001) Long-term change in the megabenthos of the Porcupine Abyssal Plain (NE Atlantic). Prog Oceanogr 50:325-348

Billett DSM, Bett BJ, Reid WDK, Boorman B, Priede IG (2010) Long-term change in the abyssal NE Atlantic: The 'Amperima Event' revisited. Deep-Sea Res II 57:1406-1417

Birchenough SNR, Reiss H, Degraer S, Mieszkowska N, Borja A, Buhl-Mortensen L, Braeckman U, Craeymeersch J, De Mesel I, Kerckhof F, Kröncke I, Parra S, Rabaut M, Schröder A, van Colen C, Van Hoey G, Vincx M, Wätjen K (2015) Climate change and marine benthos: a review of existing research and future directions in the North Atlantic. WIREs Clim Change 6:203–223

Boessenkool KP, Hall IR, Elderfield H, Yashayaev I (2007) North Atlantic climate and deep-ocean flow speed changes during the last 230 years. Geophys Res Lett 34: L13614, doi:10.1029/2007GL030285

Breckenfelder T, Rhein M, Roessler A, Boning CW, Biastoch A, Behrens E, Mertens C (2017) Flow paths and variability of the North Atlantic Current: A comparison of observations and a high-resolution model. J Geophys Res Oceans 122:2686-2708

Cartes JE, Maynou F, Fanelli E, Papiol V, Lloris D (2009) Long-term changes in the composition and diversity of deep-slope megabenthos and trophic webs off Catalonia (western Mediterranean): Are trends related to climatic oscillations? Prog Oceanogr 82:32-46

Cartes JE, Maynou F, Fanelli E, López-Pérez C, Papiol V (2015) Changes in deep-sea fish and crustacean communities at 1000–2200 m in the Western Mediterranean after 25 years: Relation to hydro-climatic conditions. J Mar Syst 143:138-153

Curry RG, McCartney MS (2001) Ocean Gyre Circulation Changes Associated with the North Atlantic Oscillation. J Phys Oceanogr 31:3374-3400

Davies AJ, Duineveld GCA, Lavaleye MSS, Bergman MJN, van Haren H, Roberts JM (2009) Downwelling and deep-water bottom currents as food supply mechanisms to the cold-water coral Lophelia pertusa (Scleractinia) at the Mingulay Reef complex. Limnol Oceanogr 54:620-629

D'Ambrosio M, Molinero JC, Azeiteiro UM, Pardal MA, Primo AL, Nyitrai D, Marques SC (2016) Interannual abundance changes of gelatinous carnivore zooplankton unveil climate-driven hydrographic variations in the Iberian Peninsula, Portugal. Mar Environ Res 120:103-110

De Clippele LH, Gafeira J, Robert K, Hennige S, Lavaleye MS, Duineveld GCA., Huvenne VAI, Roberts JM (2017) Using novel acoustic and visual mapping tools to predict the small-scale spatial distribution of live biogenic reef framework in cold-water coral habitats. Coral Reefs 36:255-268

Dippner JW, Kröncke I (2003) Forecast of climate-induced change in macrozoobenthos in the southern North Sea in spring. Clim Res 25:179-182

Döös K, Kjellsson J, Zika J, Laliberté F, Brodeau L, Campino AA (2017) The coupled ocean–atmosphere hydrothermohaline circulation. J Clim 30:631-647

Duineveld GCA, Jeffreys RM, Lavaleye MSS, Davies AJ, Bergman MJN, Watmough T, Witbaard R (2012) Spatial and tidal variation in food supply to shallow cold-water coral reefs of the Mingulay Reef complex (Outer Hebrides, Scotland). Mar Ecol Prog Ser 444:97-115

Fauchald K, Jumars PA (1979) The diet of worms: a study of polychaete feeding guilds. Oceanogr Mar Biol Ann Rev 17:193-284

Findlay H, Artioli Y, Moreno Navas J, Hennige SJ, Wicks LC, Huvenne VAI, Woodward EMS, Roberts JM (2013) Tidal downwelling and implications for the carbon biogeochemistry of cold-water corals in relation to future ocean acidification and warming. Global Change Biol 19, 2708-2719
Frid CLJ, Garwood PR, Robinson LA (2009) Observing change in a North Sea benthic system: A 33 year time series. J Mar Syst 77:227-236

Furevik T, Nilsen JEO (2013) Large-scale atmospheric circulation variability and its impacts on the Nordic seas ocean climate—a review. In: Drange H, Dokken T, Furevik T, Gerdes R, Berger W (eds). The Nordic Seas: An Integrated Perspective. Geophysical Monograph Series, 105-136

Gastineau G, Mignot J, Arzel O, Huck T (2018) North Atlantic ocean internal decadal variability: role of the mean state and ocean-atmosphere coupling. J Geophys Res, DOI: 10.1029/2018JC01407

Gertman I, Brenner S (2004) Analysis of water temperature variability in the Gulf of Eilat. Israel Oceanogr Limnol Res, 13 pages

Glover AG, Gooday AJ, Bailey DM, Billett DSM, Chevaldonné P, Colaco A, Copley J, Cuvelier D, Desbruyères D, Kalogeropoulou V, Klages M, Lampadariou N, Lejeusne C, Mestre NC, Paterson GLJ, Perez T, Ruhl H, Sarrazin J, Soltwedel T, Soto EH, Thatje S, Tselepides A, Van Gaever S, Vanreusel A (2010) Temporal Change in Deep-Sea Benthic Ecosystems: A Review of the Evidence From Recent Time-Series Studies. Adv Mar Biol 58:1-95

Hátún H, Sandø AB, Drange H, Hansen B, Valdimarsson H (2005) Influence of the Atlantic subpolar gyre on the thermohaline circulation. Science 309:1841–1844

Hurrell JW, Kushnir Y, Ottersen G, Visbeck M (2003) An overview of the North Atlantic Oscillation. The North Atlantic Oscillation: Climatic Significance and Environmental Impact, vol. 134. AGU, Washington, DC, pp. 1–35

Inall ME and shipboard party (2009) D340b Cruise Report, RRS "Discovery", Dunstaffnage to Govan via Barra Head and the Surrounding Shelf, 26th June to 4th July 2009, Scottish Association for Marine Science, 124 pages

Heath MR, Rsamussen J, Ahmed Y, Allen J, Anderson CIH, Brierley As, Brown L, Bunker A, Cook K, Davidson R, Fielding S, Gurney WSC, Harris R, Hay S, Henson S, Hirst AG, Holliday NP, Ingvarsdottir A, Irigoien X, Lindeque P, Mayor DJ, Montagnes D, Moffat C, Pollard R, Richards S, Saunders RA, Sidey J, Smerdon G, Speirs D, Walsham P, Waniek J, Webster L, Wilson D (2008) Spatial demography of *Calanus finmarchicus* in the Irminger Sea. Prog Oceanogr 76:39-88

Henry LA, Roberts JM (2017) Global biodiversity in cold-water coral reef ecosystems. In Marine Animal Forests, eds. Rossi S, Bramanti L, Gori A, Orejas C (Springer), pp. 235-256

Henry L, Davies AJ, Roberts JM (2010) Beta diversity of cold-water coral reef communities off western Scotland. Coral Reefs 29:427-436
Henry L, Moreno Navas J, Roberts JM (2013) Multi-scale interactions between local hydrography, seabed topography, and community assembly on cold-water coral reefs. Biogeosciences 10:2737-2746

Herbaut C, Houssais M-N (2009) Response of the eastern North Atlantic subpolar gyre to the North Atlantic Oscillation. Geophys Res Lett 36, L17607, doi:10.1029/2009GL039090

Hinz H, Capasso E, Lilley M, Frost M, Jenkins SR (2011) Temporal differences across a bio-geographical boundary reveal slow response of sub-littoral benthos to climate change. Mar Ecol Prog Ser 423:69-82

Hudson IR, Wigham BD (2003) In situ observations of predatory feeding behaviour of the galatheid squat lobster Munida sarsi using a remotely operated vehicle. J Mar Biol Assoc UK 83:463–463, 2003

Johnson D, Adelaide Ferreira M, Kenchington E (2018) Climate change is likely to severely limit the effectiveness of deep-sea ABMTs in the North Atlantic. Mar Pol 87:111-122

Jones P, Jonsson T, Wheeler D (1997), Extension to the North Atlantic Oscillation using early instrumental pressure observations from Gibraltar and south-west Iceland. Int J Climatol 17:1433– 1450

Inall M, Gillibrand P, Griffiths C, MacDougal N, Blackwell K (2009) On the oceanographic variability of the North-West European Shelf to the West of Scotland. J Mar Syst 77:210-226

Kazanidis G, Henry L-A, Roberts JM, Witte UFM (2016) Biodiversity of *Spongosorites coralliophaga* (Stephens, 1915) on coral rubble at two contrasting cold-water coral reef settings. Coral Reefs 35:193-208

Kazanidis G, Witte UFM (2016) The trophic structure of *Spongosorites coralliophaga* coral rubble communities at two northeast Atlantic cold water coral reefs. Mar Biol Res 12:932-947

Kazanidis G, Van Oevelen D, Veuger B, Witte UFM (2018) Unravelling the versatile feeding and metabolic strategies of the cold-water ecosystem engineer *Spongosorites coralliophaga* (Stephens, 1915). Deep-Sea Res 141:71-82

Kimmel DG, Hameed S (2008) Update on the relationship between the North Atlantic Oscillation and *Calanus finmarchicus*. Mar Ecol Prog Ser 366:111-117

Kiriakoulakis K, Stutt E, Rowland SJ, Vangriesheim A, Lampitt RS, Wolff GA. (2001) Controls on the organic chemical composition of settling particles in the Northeast Atlantic Ocean. Prog Oceanogr 50:65-87

Kröncke I (2006) Structure and function of macrofaunal communities influenced by hydrodynamically controlled food availability in the Wadden Sea, the open North Sea, and the Deep-sea. A synopsis. Senckenbergiana maritima 36:123-164

Kröncke I, Dippner JW, Heyen H, Zeiss B (1998) Long-term changes in macrofaunal communities off Norderney (East Frisia, Germany) in relation to climate variability. Mar Ecol Prog Ser 167:25-36

Kröncke I, Zeiss B, Rensing C (2001) Long-term variability in macrofauna species composition off the island of Norderney (East Frisia, Germany) in relation to changes in climatic and environmental conditions. Senckenbergiana maritima 31:65-82

Lampitt RS, Bett BJ, Kiriakoulakis K, Popova EE, Ragueneau O, Vangreisheim A, Wolff GA (2001) Material supply to the abyssal seafloor in the Northeast Atlantic. Prog Oceanogr 50:27-63

Lampitt RS, Salter I, de Cuevas BA, Hartman S, Larkin KE, Pebody CA (2010) Long-term variability of downward particle flux in the deep northeast Atlantic: Causes and trends. Deep-Sea Res II 57:1346-1361

Last K, Roberts JM, Wicks L, Hogg M (2010) Report of the RV Calanus cold-water coral research cruise to the Mingulay reef complex, 22-24th February 2010. Scottish Association of Marine Science / Heriot-Watt University, 7 pages

Last K, Wicks L, de Francisco B, Douarin M (2010) Report of the RV Calanus cold-water coral research cruise to the Mingulay reef complex, 3rd- 6th May 2010. Scottish Association of Marine Science / Heriot-Watt University, CSIC, 8 pages

Legendre PD, Gallagher ED (2001) Ecologically meaningful transformations for ordination of species data, Oecologia 129:271–280

Lohmann K, Drange H, Bentsen M (2009) A possible mechanism for the strong weakening of the North Atlantic subpolar gyre in the mid-1990s. Geophys Res Lett 36: L15602, doi:10.1029/2009GL039166

Maier C (2006) Biology and ecosystem functioning of cold water coral bioherms at Mingulay (Hebrides), NE Atlantic. Cruise Report, BIOSYS 2006 Cruise 64PE250 on R/V Pelagia, Oban–Oban, 7–23 July 2006. Royal Netherlands Institute for Sea Research, Texel

Martins FA, Neves RJ, Leitão PC (1998) A three-dimensional hydrodynamic model with generic vertical coordinate, in: Proceedings of Hidroinformatics, edited by: Babovic V, Larsen LC., 98, 2, Balkerna/Rotterdam, Copenhague, Denmark, August 1998, 1403–1410

Martins FA, Leitao PC, Silva A, Neves RJ (2001) 3D modelling in the Sado estuary using a new generic vertical discretization approach. Oceanol Acta 24:51–62

Moreno Navas J, Miller PL, Henry L-A, Hennige SJ, Roberts JM (2014) Ecohydrodynamics of cold-water coral reefs: a case study of the Mingulay Reef Complex (Western Scotland). PLoS ONE 9 [doi: 10.1371/journal.pone.0098218]

Moshonkin SN, Bagno AV, Gusev AV, Filyushkin BN, Zalesny VB (2017) Physical properties of the formation of water exchange between Atlantic and Arctic ocean. Atmos Ocean Phys 53:213-223

Mueller CE, Lundälv T., Middelburg JJ, van Oevelen D (2013) The symbiosis between *Lophelia pertusa* and *Eunice norvegica* stimulates coral calcification and worm assimilation. PLoS ONE 8(3): e58660. doi:10.1371/journal.pone.0058660

Naqvi SWA, Bange HW, Gibb SW, Goyet C, Hatton AD, Upstill-Goddard R (2005) Biogeochemical ocean-atmosphere transfers in the Arabian Sea. Prog Oceanogr 65:116-144

Navas JM, Miller PL, Henry L.A, Hennige SJ, Roberts JM (2014) Ecohydrodynamics of cold-water coral reefs: a case study of the Mingulay Reef Complex (Western Scotland). PloS ONE 9:p.e98218

Neumann H, Ehrich S, Kröncke I (2008) Effects of cold winters and climate on the temporal variability of an epibenthic community in the German Bight. Clim Res 37:241-251

Oksanen JF, Blanchet FG, Friendly M, Kindt R, Legendre P, McGlinn D, Minchin PR, O'Hara RB, Simpson GL, Solymos P, Steven MHH, Szoecs E, Wagner H (2017) vegan: Community Ecology Package. R package version 2.4-5

Ortega P, Robson J, Sutton RT, Andrews MB (2017) Mechanisms of decadal variability in the Labrador Sea and the wider North Atlantic in a high-resolution climate model. Clim Dyn 49:2625-2647

Orton J (1914) Preliminary account of a contribution to an evaluation of the sea. J Mar Biol Assoc UK 10:312–326

Patara L, Visbeck M, Masina S, Krahmann G, Vichi M (2011) Marine biogeochemical responses to the North Atlantic Oscillation in a coupled climate model. J Geophys Res 116, doi:10.1029/2010JC006785

Prieto E, González-Pola C, Lavín A, Holliday NP (2015) Interannual variability of the northwestern Iberia deep ocean: Response to large-scale North Atlantic forcing. J Geophys Res Oceans 120:832-847

Qu B, Gabric A, Lu Z, Li H, Zhao L (2016) Unusual phytoplankton bloom phenology in the northern Greenland Sea during 2010. J Mar Syst 164:144-150

R Core Team (2018). R: A language and environment for statistical computing. R Foundation for Statistical Computing, Vienna, Austria. URL https://www.R-project.org/

Rees HL, Pendle MA, Limpenny DS, Mason CE, Boyd SE, Birchenough S, Vivian CMG (2006) Benthic responses to organic enrichment and climatic events in the western North Sea. J Mar Biol Assoc UK 86: 5108/1-18

Roberts JM (2005) Reef-aggregating behaviour by symbiotic eunicid polychaetes from cold-water corals: do worms assemble reefs? J Mar Biol Assoc UK 85:813–819

Roberts JM, Brown CJ, Long D, Bates CR (2005) Acoustic mapping using a multibeam echosounder reveals cold-water coral reefs and surrounding habitats. Coral Reefs 24:654-669

Roberts JM, Davies AJ, Henry L, Dodds LA, Duineveld GCA, Lavaleye MSS, Maier C, van Soest RWM, Bergman MJN, Huhnerbach V, Huvenne VAI, Sinclair DJ, Watmough T, Long D, Green SL, van Haren H (2009) Mingulay reef complex: an interdisciplinary study of cold-water coral habitat, hydrography and biodiversity. Mar Ecol Prog Ser 397:139-151

Ryland JS (2000) Reproduction in British zoanthids, and an unusual process in *Parazoanthus anguicomus*. J Mar Biol Assoc UK 80:943-944

Santos AP (1995) Modelo hidrodinámico de circulacáo oceaánica e estuarina, PhD Thesis, IST, Lisbon, 1995 (in Portuguese)

Sarafanov A, Mercier H, Falina A, Sokov A (2010) Cessation and partial reversal of deep water freshening in the northern North Atlantic: observation-based estimates and attribution. Tellus 62A:80-90

Seyfried L, Marsaleix P, Richard E, Estournel C (2017) Modelling deep-water formation in the north-west Mediterranean Sea with a new air–sea coupled model: sensitivity to turbulent flux parameterizations. Ocean Sci 13:1093-1112

Simpson IR, Deser C, McKinnon KA, Barnes E (2018) Modeled and observed multidecadal variability in the North Atlantic jet stream and its connection to sea surface temperatures. J Clim 31:8313-8338

Smith Jr KL, Ruhl HA, Bett BJ, Billett DSM, Lampitt RS, Kaufmann RS (2009) Climate, carbon cycling, and deep-ocean ecosystems. Proc Natl Acad Sci USA 106:19211-19218

Tunberg BG, Nelson WG (1998) Do climatic oscillations influence cyclical patterns of soft bottom microbenthic communities on the Swedish west coast? Mar Ecol Prog Ser 170:85-94

Turner JT, Borkman DG, Hunt CD (2006) Zooplankton of Massachusetts Bay, USA, 1992-2003: Relationships between the copepod *Calanus finmarchicus* and the North Atlantic Oscillation. Mar Ecol Prog Ser 311:115-124

Walbridge S, Slocum N, Pobuda M, Wright DJ (2018) Unified geomorphological analysis workflows with benthic terrain modeler. Geosci 8:94, https://doi.org/10.3390/geosciences8030094

Zettler ML, Friedland R, Gogina M, Darr A (2017) Variation in benthic long-term data of transitional waters: Is interpretation more than speculation? PLoS ONE 12(4): e0175746. https:// doi.org/10.1371/journal.pone.0175746

Wilson MFJ, O'Connell B, Brown C, Guinan J, Grehan AJ (2007) Multiscale terrain analysis of multibeam bathymetry data for habitat mapping on the continental slope. Mar Geod 30:3-35

Wright DJ, Lundblad ER, Larkin EM, Rinehart RW, Murphy J, Cary-Kothera L, Draganov K (2005) ArcGIS Benthic Terrain Modeler, Corvallis, Oregon, Oregon State University, Davey Jones Locker Seafloor Mapping/Marine GIS Laboratory and NOAA Coastal Services Center, available at: http://csc. noaa.gov/digitalcoast/tools/btm/index.html

Yashayaev I, Seidov D, Demirov E (2015) A new collective view of oceanography of the Arctic and North Atlantic basins. Prog Oceanogr 132:1-21

Zhang W, Yan X-H (2018) Variability of the Labrador sea surface eddy kinetic energy observed by altimeter from 1993 to 2012. J Geophys Res: Oceans 123:601-612

3.3 Flemish Cap and continental slope (northwest Atlantic, High Seas): Effects of sea temperature, food availability, and currents on macrofaunal species and phylogenetic diversity relative to fishing pressure

Author: Alex Rogers

Contributors: Oliver Ashford, Andrew Kenny, Christopher Barrio Froján, Michael Bonsall, Tammy Horton, Angelika Brandt, Graham Bird, Sarah Gerken

Abstract

The NEREIDA project, NAFO PotEntial VulneRable Marine Ecosystems-impacts of Deep-sea Fisheries (https://www.nafo.int/About-us/International-Cooperation), provided an excellent opportunity to investigate the physical and anthropogenic (fishing) factors driving the structure of deep-sea benthic communities in an area of the High Seas. The investigations undertaken on 312 sediment samples from box cores yielded benthic macrofauna that resulted in an improved understanding of the anthropogenic, physical and biological factors influencing benthic community structure in an area of the NW Atlantic with a variety of VMEs, including sponge grounds. Key results were:

(i) That environmental parameters rather than interspecific interactions largely drive the biodiversity and structure of macrofaunal communities at bathyal depths on the NW Atlantic slope;

(ii) Seabed trawling has a complex effect on sediment macrofaunal communities, potentially increasing abundance and biomass but reducing the phylogenetic and functional diversity of communities;

(iii) Benthic community structure may be extremely sensitive to changes in sea temperature.

Introduction

Competition between species has long been recognised as an important factor determining the ecological diversity and structure of organismal communities. Intense interspecific competition for scarce resources can result in the exclusion of certain taxa (Gause, 1934; Elton, 1946; Hardin, 1960), shaping species' realized niches and distributions, and influencing ecosystem functioning (Riginos, 2009; Leduc et al., 2015). Numerous studies have investigated the role of competition in

structuring terrestrial (such as plant; Goldberg & Barton, 1992) and shallow-water (such as coral reef; McCook et al., 2001) assemblages, but the importance of interspecific competition in structuring the expansive and functionally important communities of the deep ocean has been a matter of debate because the discovery of high alpha diversity in deep-water sediments (Hessler & Sanders, 1967; Sanders, 1968; McClain & Schlacher, 2015). Some researchers have emphasised an important role of biological interactions in structuring deep-seafloor communities, theorising a dynamic balance between competitive forces and predation. Others have argued that extensive niche differentiation, coupled with typically low organismal densities and the availability of space, mean that competitive interactions are unlikely to be significant in structuring modern-day deep-ocean communities (Hessler & Sanders, 1967; Sanders, 1968; Wilson, 1990; Grant, 2000).

The NEREIDA project, NAFO PotEntial VulneRable Marine Ecosystems-impacts of Deep-sea Fisheries (https://www.nafo.int/About-us/International-Cooperation), provided a unique opportunity to investigate the importance of such biological forces amongst the backdrop of natural environmental gradients in ocean temperature, food supply and currents, as well as anthropogenic (fishing) pressures on the biodiversity of deep-sea benthic communities.

Methods

A total of 312 sediment samples, forming the largest macrofaunal sample set yet were collected from the deep ocean of the Northwest Atlantic (Figure 1). Samples were collected with a box corer (area 0.25 m^2) from the continental slope across a depth range of 582–2294 m (Figure 1) between May-August 2009 and June–August 2010. It should be noted that these samples are no longer available for study as they were accidently destroyed when attempting to relocate them from Lowestoft, UK.

Sediment subsamples were taken for geochemical and particle size analyses and remaining sediment was washed over a 1 mm mesh sieve for faunal analyses. As well as biological samples the following environmental parameters were measured or generated as part of the project: bathymetry (depth, slope, aspect, seafloor rugosity, bathymetric position index (BPI)); fishing intensity (vessel monitoring system (VMS) signal density and total trawl length per km^2); geological context; seafloor sediment particle size (percentage clay/silt/sand); carbon availability (percentage inorganic, organic and total carbon, surface chlorophyll a and particulate organic carbon (POC) concentrations, modelled transport of POC to depth); physical oceanographic variables (temperature, salinity and current speed); and month and year of sample collection just to investigate the potentially confounding effects of natural variability over space and time. Of note was that there was no

temporal replication in this study and that temporal samples arose through the sampling of different areas at slightly different times in the different years; the whole area was not sampled in a single year. All samples were taken in the summer months and so the important temporal component of variability in these short-lived high turnover species was not addressed in this study.

To investigate the role of these potentially important (biological) interspecific interactions versus environmental and anthropogenic drivers in structuring communities of peracarids on the northwest Atlantic margin, a community phylogenetic analysis was undertaken. Peracarids are a large group of malacostracan crustaceans and include amphipods, isopods, mysids and tanaids amongst others. This estimated the dispersion of sampled taxa across a phylogeny and a functional trait dendrogram compared with the dispersion that would be expected by chance. If taxa within samples are found, on average, to be less similar to one another than would be expected by random draw from the available taxa pool, assemblages are described as 'over-dispersed'; this is typically considered evidence of a dominance of competitive exclusion in shaping assemblage structure, because phylogenetically / functionally similar taxa are assumed to be ecologically similar (Elton, 1946; Webb et al., 2002; Helmus et al., 2007). Conversely, if taxa within samples are found, on average, to be more similar to one another than would be expected by chance, assemblages are described as 'under-dispersed'; this is typically considered evidence of a dominance of the physical environment (i.e., ocean currents, sea temperature, food supply) in determining assemblage structure, because phylogenetically / functionally similar taxa are assumed to share the particular traits that are necessary for survival under the prevailing environmental conditions (Elton, 1946; Webb et al., 2002; Helmus et al., 2007).

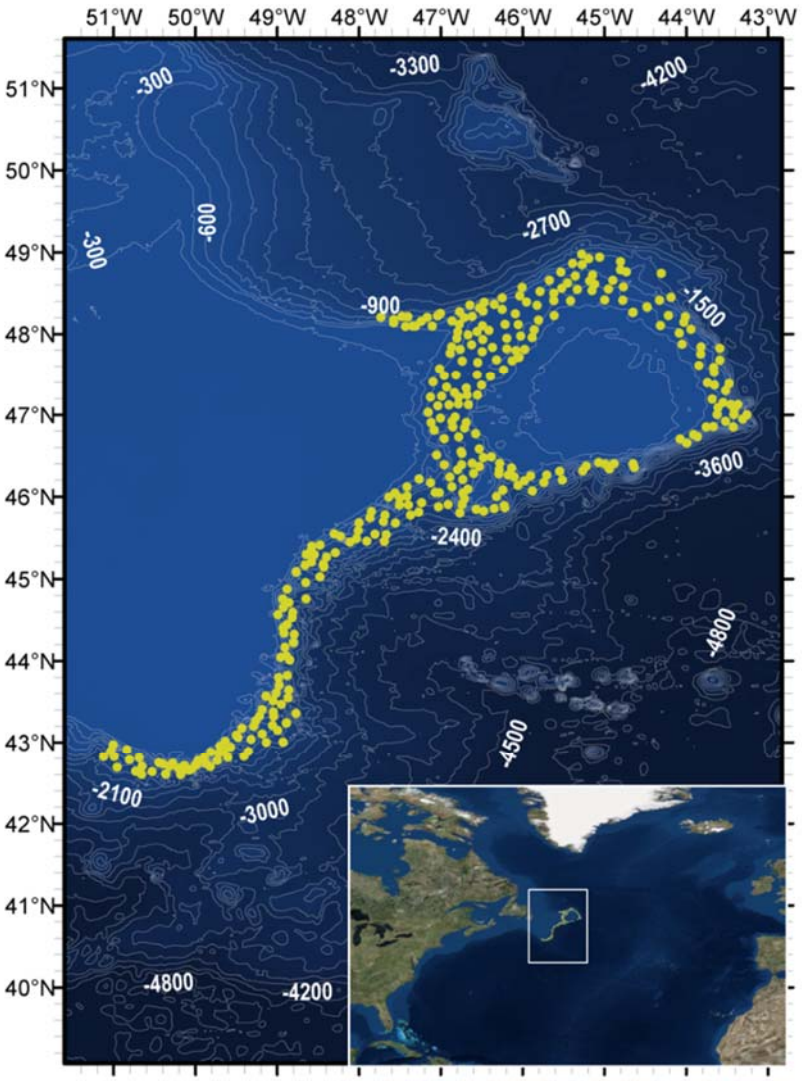

Figure 1*. Box corer deployment locations (yellow dots,* n *= 312) and bathymetry (darker areas = greater water depth) of the sampling area in the Northwest Atlantic Ocean (300 m depth contours; SRTM30 bathymetric data).*

An alternative approach to analysing the influence of physical and anthropogenic drivers on community structure is the use of Structural Equation Modelling (SEM). The complexity of natural systems, where the biological community can influence the environment and vice versa, can make it difficult to disentangle relationships between biodiversity and ecosystem functioning in natural systems. Network models, like SEM, allow for the incorporation of the influences of environmental feedback on both biodiversity and ecosystem functioning and their multivariate relationship, as well as allowing for the incorporation of anthropogenic effects in one framework. SEM takes together multiple relationships observed in previous studies via *a priori* specification, and then allows for the testing of these relationships together in a larger framework. In particular, it tests whether the previously obtained relationships might still hold true when taken all together based on the model specified. SEMs allows for the incorporation of latent variables, which are constructs of theoretical

entities that may not be measurable in reality but exist as concepts, and indicator variables, which are observed quantities and are used to characterise the latent variables.

SEM was undertaken for peracarid crustaceans to investigate the specific nature of biodiversity – ecosystem function relationships. The exact shape of such relationships are important in understanding the impacts of biodiversity loss on ecosystem function and consequently ecosystem service provision. Relationships can be positive and accelerating, linear or saturating. Accelerating relationships between biodiversity and ecosystem function imply a significant impact on ecosystem function or even small reductions in biodiversity whilst a saturating relationship implies some redundancy among species, buffering the effects of biodiversity loss. A description of full Methods including characterising of the deep-sea environmental variables are provided in the published paper by Ashford et al. (2018).

Results

Both for phylogenetic and functional trait analyses (Figure 2), the peracarids were under-dispersed, strongly suggestive of a process of environmental filtering of the taxa present on the northwest Atlantic Slope. The under-dispersion can be seen as many of the taxa sharing phylogenetic histories but also shared functional traits, suggesting that particular traits have been favoured and selected for in the prevailing environmental conditions.

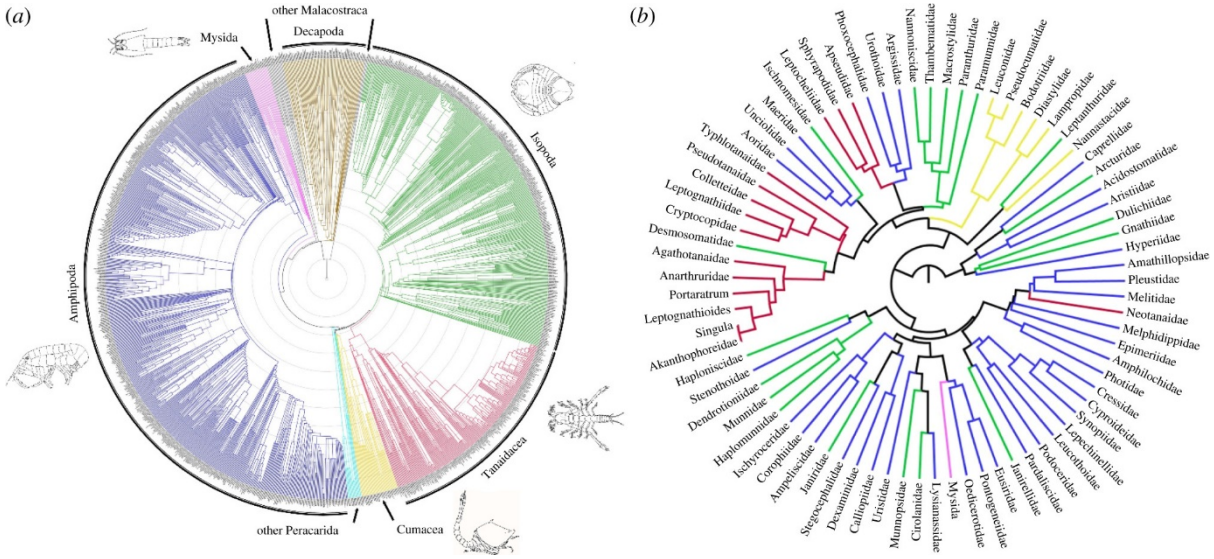

Figure 2*. (a) Supertree chronogram of Peracarida (Crustacea), including other malacostracan taxa as outgroups; 1487 terminal taxa; produced from 129 source trees using MULTILEVELSUPERTREE 1.0 (Berry et al., 2013). Root at 600 Ma, concentric circles representing 50 Ma steps to present day (tips). Examples of taxa—Amphipoda (blue branches):* Leucothoe rudicola *(modified from White & Thomas, 2009); Cumacea (yellow branches):* Procampylaspis chathamensis *(image from Sarah Gerken); Tanaidacea (red branches):* Pseudosphyrapus anomalus *(image from Graham J. Bird); Isopoda (green branches):* Atlantoserolis vemae *(modified from Brandt et al., 2014); Mysida (pink branches):* Heteromysis modlini *(modified from Price & Heard, 2011). (b) Functional dendrogram of 77 peracarid taxa sampled by box corer from the NW Atlantic Ocean. Produced by the clustering (UPGMA, Euclidean distance) of a database of 38 functional traits in 10 trait groupings. Branches coloured by higher taxonomic identity of terminal taxa using same palette as the supertree. 'Newick' format files for both the supertree and functional dendrogram are available in the electronic supplementary material to enable detailed examination of their topology.*

The results from the pericarid SEM are shown in Figure 3. Positive influences on ecosystem functioning (measured here as secondary biomass production) were obtained for fishing intensity, habitat heterogeneity, biogenic habitat, and a small positive effect of family richness, while there is a negative influence of functional evenness on ecosystem functioning. Polychaete density was positively influenced by temperature, biogenic habitat, habitat heterogeneity and fishing intensity, while it is negatively influenced by food availability, current speed and sediment characteristics, although the latter two have very small effects. Density itself negatively influences functional evenness, as well as family evenness, and functional dispersion, while it positively influences family richness. The latent variable fishing intensity shows complex interplay between other latent variables: as stated before, it positively influences polychaete density and ecosystem functioning, while it negatively affects family evenness and functional evenness, as well as reducing biogenic habitats.

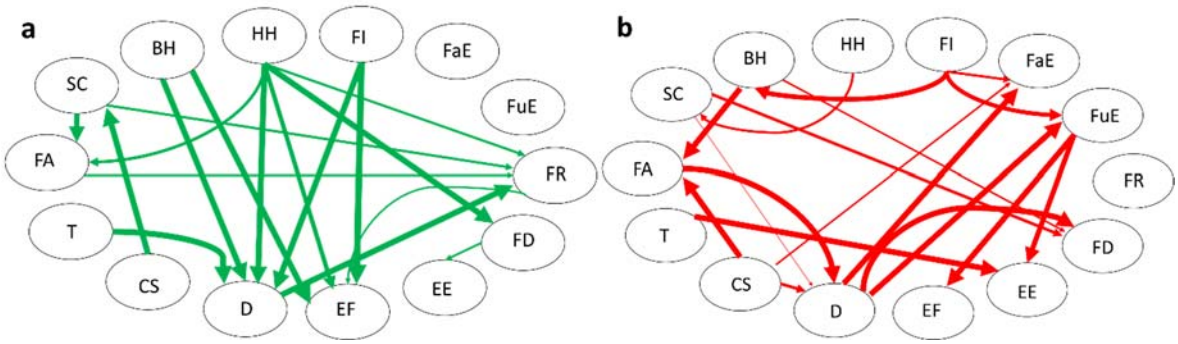

***Figure 3**. The significant, standardized relationships between the latent variables constructed in the structural equation model, showing (a) the positive relationships, and (b) the negative relationships. The thickness of the arrows is proportional to significance levels. D = Abundance, EF = ecosystem functioning, EE = ecosystem efficiency, FD = functional dispersion, FR = family richness, FuE = functional evenness, FaE = family evenness, FI = fishing intensity, HH = habitat heterogeneity, BH = biogenic habitats, SC = sediment characteristics, FA = food availability, CS = current speed.*

The SEM for peracarids is shown in Figure 4. In agreement with the conclusions of BEF studies conducted in terrestrial and shallow water environments (Hooper et al., 2005, Balvanera et al., 2006, Cardinale et al., 2006, Worm et al., 2006; Zeppilli et al., 2016), the biodiversity of continental slope macrobenthic peracarids was found to significantly influence the magnitude of a selection of proxies for ecosystem functioning. However, the extent of variation explained for each ecosystem functioning proxy by biodiversity metrics (i.e. the strength of BEF relationships) was found to be highly variable. For example, variation in 'standing stock' and 'ecosystem efficiency' was found to be relatively well explained by the structural equation model (R^2 = 0.72 and 0.47, respectively), but a high level of unexplained variance in 'carbon cycling efficiency' remained following model fitting (R^2 = 0.075). The directionality and absolute form of the recovered BEF relationships was also found to vary depending on the biodiversity and ecosystem functioning metrics under analysis. For example, all significant relationships between biodiversity metrics and 'carbon cycling efficiency' were found to be positive and saturating in form. In contrast, 'diversity' was found to relate to 'ecosystem efficiency' in a linear manner, whilst only the relationships between 'diversity' and 'standing stock', and 'richness' and 'standing stock' were found to have an accelerating form across the spectrum of biodiversity values encountered in this study.

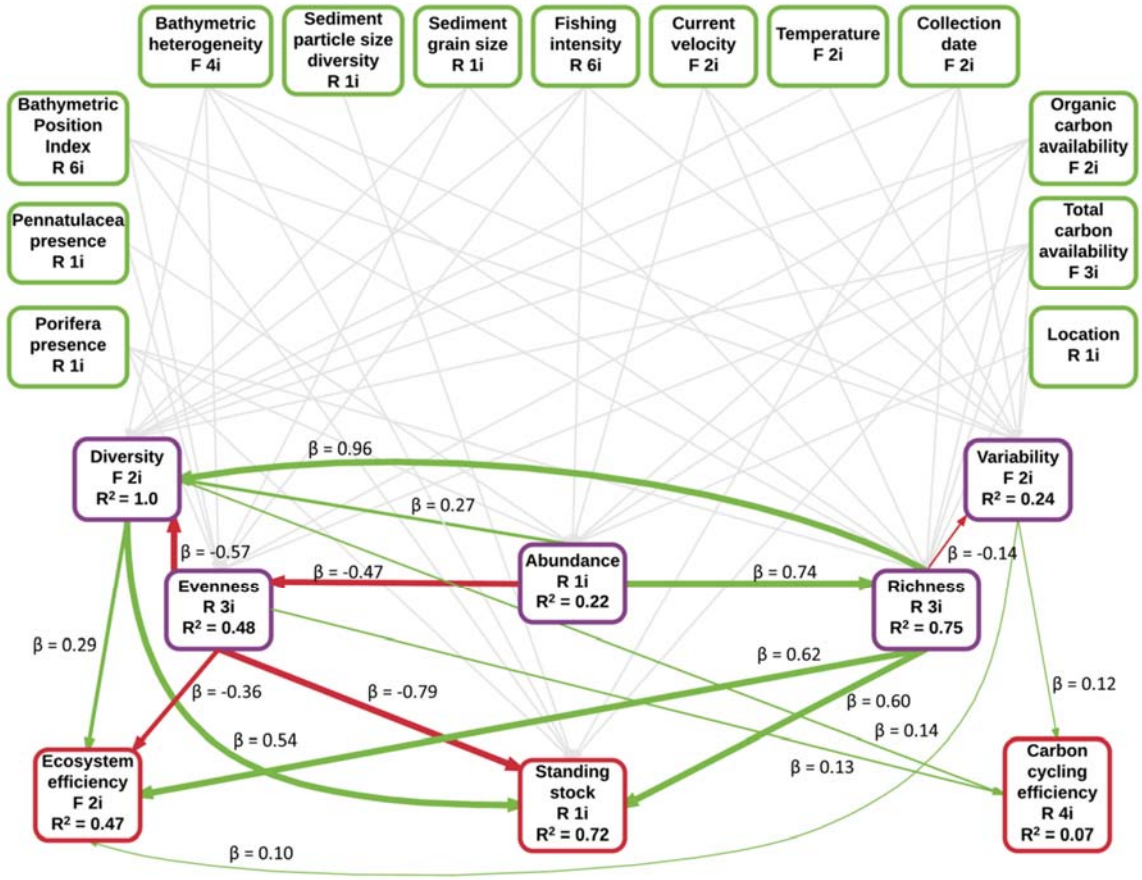

Figure 4*. Structural equation model results. Only significant links between biodiversity and ecosystem functioning latent variables are detailed for simplicity. Of these, positive relationships are highlighted in green and negative relationships in red. The width of each significant link is directly proportional to its β coefficient. R^2 values are displayed for endogenous variables.*

Analyses of the possible environmental drivers of assemblage variability demonstrated that both natural and anthropogenic factors may influence the structure of the deep-sea assemblages, and revealed in particular a negative relationship between bottom trawling intensity and assemblage functional trait variability (Figure 5).

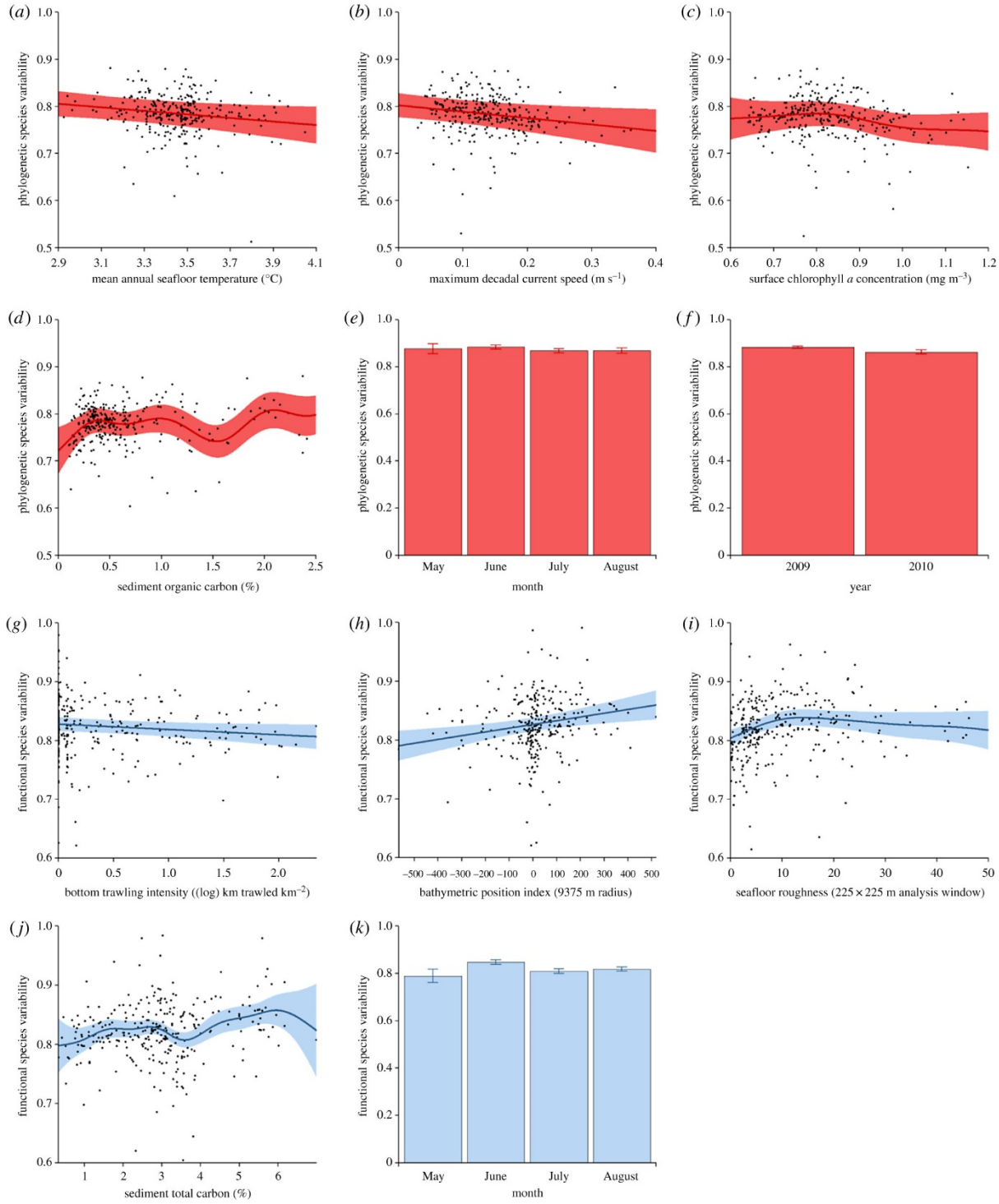

***Figure 5**: Relationships between the phylogenetic species variability (PSV, in red)/functional species variability (FSV, in blue) of sampled peracarid assemblages (n ¼ 299) and environmental parameters: (a) PSV/mean annual seafloor temperature, (b) PSV/maximal decadal current speed, (c) PSV/surface chlorophyll a concentration, (d) PSV/sediment organic carbon content, (e) PSV/month, (f) PSV/year, (g) FSV/bottom trawling intensity, (h) FSV/BPI, (i) FSV/seafloor roughness, (j) FSV/sediment total carbon content, (k) FSV/month. Error around best-fit lines/bar values represent ¼ 95% confidence intervals.*

Notably for ATLAS and the role that seafloor temperatures and climate change may play in driving biodiversity patterns in the deep North Atlantic, these analyses demonstrated a negative relationship between seafloor temperature and the phylogenetic diversity of the sampled peracarid assemblages (Figure 5), indicating that the physiological tolerances of peracarid taxa to temperature change are preserved within evolutionary lineages. This relationship is apparent across a narrow sea temperature range of only approximately 1.28^{o}C. Of important note here, is that the review in Part 2 identified critical changes in seafloor temperatures at the Flemish Cap of at least 1 ^{o}C; thus, one might conclude that significant shifts in the phylogenetic and functional trait signatures of the macrobenthic communities will occur in the future too.

Discussion

The importance of environmental filtering over other (biological) processes on the Flemish Cap and continental slope revealed by the present study challenges those studies that hypothesise an importance of competition and character displacement as a significant ecological structuring agent in the deep sea (Rex, 1976, 1981), and conflict with investigations that have examined the morphological or trophic characteristics of deep-sea assemblages (McClain, 2005; Laakmann et al., 2009). Instead, they substantiate the hypothesis that competitive interactions between species in the deep ocean are weak and unlikely to be significant in structuring communities at the spatial scales investigated (Wilson, 1990; Grant, 2000). Further, they support the results of previous analyses of lesser spatial scope that have investigated the taxonomic and phylogenetic structure of deep-sea assemblages (Rex & Waren, 1981; Quattrini et al., 2017).

The negative relationship between trawling and functional trait diversity suggests that physical disturbance by bottom trawling reduces soft-sediment functional diversity, with the resulting assemblages exhibiting a reduced subset of the functional traits that would otherwise be present in an undisturbed assemblage. While generally concordant with the small number of studies that have investigated trawling impacts on deep-sea macrofauna and meiofauna (Koslow et al., 2001; Clark & Rowden, 2009; Pusceddu et al., 2014; Clark et al. 2016; Román et al., 2016), this finding adds a new facet to our understanding of the impacts of bottom trawling in the deep ocean. It is important to note, however, that impacts of bottom trawling in the northwest Atlantic may be obscured by the rapid turnover and natural temporal variability of macrobenthic taxa such as polychaetes and peracarids such as amphipods (Kenchington et al., 2001). Future studies will be needed to further disentangle effects of bottom trawling on microbenthic biodiversity from the naturally high variability

over space and time in these communities and consider the rapid recovery of such species in the face of disturbance (Kenchington et al., 2001).

The negative relationship between sea temperature and phylogenetic diversity suggests that even the superficially small increases in deep-ocean temperature that are predicted to occur over this century as a result of climate change (Balmaseda et al., 2013; Somavilla et al., 2013), particularly in the High Seas of the North Atlantic will significantly reduce the phylogenetic diversity of the communities found there, potentially impacting deep-ocean ecosystem functioning (Danavaro et al., 2008). An altered phylogenetic profile of deep-sea ecosystems may eventually lead to a change in the cycling, storage and sequestration pathways of nutrients and chemicals, such as carbon. These results were all published in Ashford et al (2018).

As noted earlier, of great relevance to ATLAS is that critical changes in seafloor temperatures at the Flemish Cap are predicted to be on the order of at least 1 ^{o}C (see Part 2 of Deliverable 3.4); this could translate into significant shifts in the phylogenetic and functional trait signatures of the macrobenthic communities (as represented by the components studied) in the region as well.

An increase in abundance and biomass is generally perceived as a beneficial aspect for a community when measuring ecosystem functioning. However, as fishing intensity also reduces family and functional evenness, a higher ecosystem functioning would implicitly also indicate a less diverse system. This effect of bottom trawling has been hypothesised in the theoretical model of van Denderen et al. (2013), which showed that, under certain conditions, trawling intensity can have a positive effect on benthic abundance, and in turn potentially on biomass. Our model, informed by extensive deep-sea observational data, agrees with this hypothesis, and adds to it by showing that cumulative trawling influences evenness. Empirical data collected on grab-sampled macrobenthos in a three-year trawling impact experiment on the adjacent Grand Banks on a sandy bottom similar to some areas of Flemish Cap noted that when trawling disturbance was indicated, it appeared to mimic natural disturbance, shifting the community in the same direction in multi-dimensional scaling (MDS) ordination; no distinctive trawling signature was observed (Kenchington et al., 2001). Trawling disturbance was observed immediately after trawling in some instances but recovered within a year.

The change in evenness is an important notion as it potentially indicates by what mechanism the pattern between biodiversity and ecosystem function is established. There are two potential mechanisms, the selection effect for dominant groups and the complementarity effect of niches (Loreau & Hector, 2001). It is generally assumed that the complementarity effect is stronger than the selection effect, especially in the deep sea (Cardinale et al., 2007; Danavaro et al., 2008). However,

results published by Ashford et al. that also arose from the present study (Ashford et al., 2018) suggested that the selection effect plays a stronger role: high relative abundances of Capitellidae, a family of polychaetes known to be opportunistic and used as indicators of local organic enrichment (Gage & Tyler, 1991) were found in samples with high total abundances. At least some polychaete taxa are known to be not significantly affected by trawling, and these could increase in abundance under such disturbance conditions, although the finer mechanisms of what allows this increase are not fully understood – for example, competitive release, predatory release, or locally-enriched carbon supply could all play an important role (Rijnsdorp & Vingerhoed, 2001). Bottom trawling can change carbon (food) availability as a result of increased (epi)benthos mortality (Puig et al., 2012) or resuspension of buried organic material. It is possible that opportunistic groups might become more numerous following an increase in food availability and/or if competition for food is weaker (Thrush & Dayton, 2002). It is possible that trawling creates conditions that favour high relative abundances of capitellids, thereby influencing functional and taxonomic evenness in the whole community. Since capitellids are a group known to be early colonizers after a disturbance, it further suggests the system is highly disturbed. The community response to trawling observed in this study is similar to benthic community responses close to and under fish farms, where organic carbon fluxes are higher compared to background fluxes (Kutti et al., 2008). High abundances of capitellids were also found in deep-sea colonization experiments in treatments with high organic enrichment, where capitellids have been shown to be pioneering species and early colonisers of a newly available patch of habitat (Grassle & Morse-Porteous, 1987). While food availability and fishing intensity were not found to be significantly correlated in this model presented by Ashford et al. (2018), the positive effect of fishing intensity on abundances is higher than the negative effect of food availability on abundances.

The results of this study suggest that the form of deep-sea BEF relationships are more variable than previously reported (Danovaro et al., 2008, Leduc et al., 2013, Narayanaswamy et al., 2013, Pape et al., 2013, Baldrighi et al., 2017) or hypothesised, and that they cannot be classified into discreet categories of saturating/linear/accelerating. The form of BEF relationships is instead found to be dependent on the type and generality of biodiversity and ecosystem functioning metrics analysed. Based on the evidence outlined above, it is proposed here that all positive BEF relationships contain portions that are accelerating, linear and saturating, and that these portions are always exhibited in that sequence with increasing diversity (Figure 6).

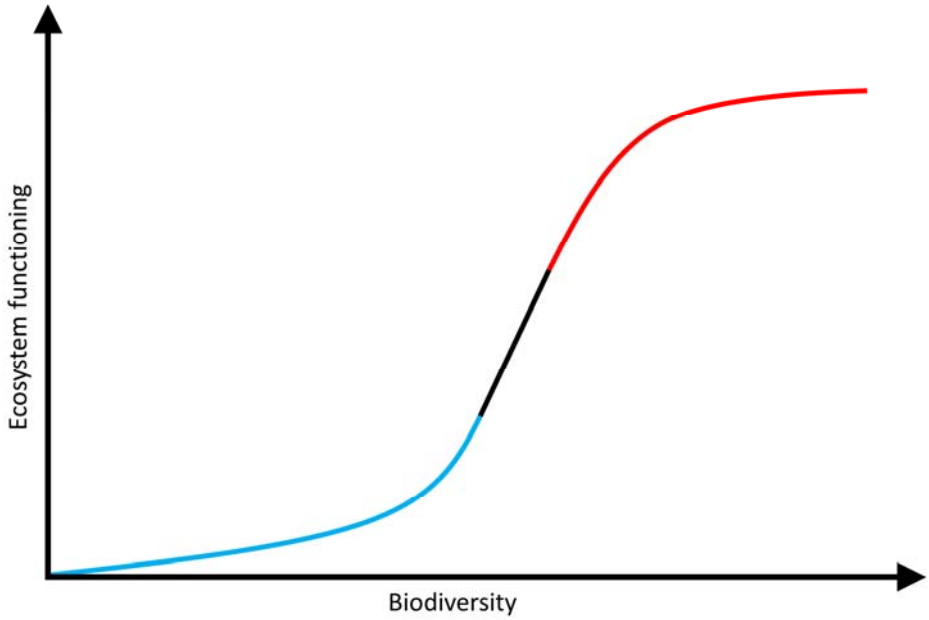

Figure 6: *Hypothesised form of biodiversity ecosystem functioning relationships. All relationships are composed of three portions: accelerating portion (blue), linear portion (black), and saturating portion (red). The relative dominance of each of these three components of the relationship (accelerating/linear/saturating) in natural communities is dependent on the average 'interaction frequency' of organisms contributing towards the ecosystem function in question.*

Such a progression in the form of BEF relationships with increasing diversity has been briefly discussed by Leduc et al. (2013), however, here it is developed further by hypothesising that the relative dominance of each of these three portions of the BEF relationship (accelerating → linear → saturating) in natural communities is dependent on the average 'interaction frequency' of organisms in an assemblage that are contributing towards an ecosystem function in question. 'Interaction frequency' is here defined as *the number of individuals per unit area contributing towards a particular ecosystem function, divided by the reciprocal of the average body size of the individuals in question* (i.e. density / (1 / average body size)). At a high average 'interaction frequency' of organisms, the saturating portion of the BEF relationship will be relatively expanded, with competitive interactions and functional redundancy setting a limit to further increases in ecosystem functioning with increasing biodiversity. In contrast, at a low average 'interaction frequency' of organisms, the accelerating portion of the BEF relationship will be relatively magnified, with facilitation and low levels of redundancy and competition promoting accelerating ecosystem functioning with increasing biodiversity.

References

Ashford OS, Kenny AJ, Barrio Froján CR, Bonsall MB, Horton T, Brandt A, Bird GJ, Gerken S, & Rogers AD. 2018. Phylogenetic and functional evidence suggests that deep-ocean ecosystems are highly sensitive to environmental change and direct human disturbance. *Proc. Roy. Soc. B* 285: 20180923.

Baldrighi E, Giovannelli D, D'errico G, Lavaleye M. & Manini, E. 2017. Exploring the relationship between macrofaunal biodiversity and ecosystem functioning in the deep sea. *Front. Mar. Sci.* 4: 198.

Balmaseda MA, Trenberth KE, Kallen E (2013) Distinctive climate signals in reanalysis of global ocean heat content. *Geophys. Res. Lett.* 40: 1754–1759.

Balvanera P, Pfisterer AB, Buchmann N, He, J-S, Nakashizuka T, Raffaelli D, Schmid B (2006) Quantifying the evidence for biodiversity effects on ecosystem functioning and services. *Ecol. Lett.* 9**:** 1146-1156.

Berry V, Bininda-Emonds ORP, Semple C (2013) Amalgamating source trees with different taxonomic levels. *Syst. Biol.* 62: 231–249.

Brandt A, Brix S, Held C, Kihara TC. 2014 Molecular differentiation in sympatry despite morphological stasis: deep-sea *Atlantoserolis* Wägele, 1994 and *Glabroserolis* Menzies, 1962 from the south-west Atlantic (Crustacea: Isopoda: Serolidae). *Zool. J. Linn. Soc.* 172: 318–359.

Cardinale BJ, et al. (2007) Impacts of plant diversity on biomass production increase through time because of species complementarity. *Proc Natl Acad Sci USA* 104: 18123-18128.

Cardinale BJ, Srivastava DS, Duffy JE, Wright JP, Downing AL, Sankaran M, Jouseau C (2006) Effects of biodiversity on the functioning of trophic groups and ecosystems. *Nature* 443**:** 989-992.

Clark MR, Althaus F, Schlacher TA, Williams A, Bowden DA, Rowden AA (2016) The impacts of deep-sea fisheries on benthic communities: a review. ICES J. Mar. Sci. 73: i51–i69.

Clark MR, Rowden AA (2009) Effect of deep-water trawling on the macro-invertebrate assemblages of seamounts on the Chatham Rise, New Zealand. *Deep Sea Res. I* 56: 1540–1554.

Danovaro R, Gambi C, Dell'Anno A, Corinaldesi C, Fraschetti S, Vanreusel A, Vincx M, Gooday AJ (2008) Exponential decline of deep-sea ecosystem functioning linked to benthic biodiversity loss. *Curr. Biol*. 18: 1–8.

van Denderen PD, van Kooten T, Rijnsdorp AD (2013) When does fishing lead to more fish? Community consequences of bottom trawl fisheries in demersal food webs. *Proc. Roy. Soc. B: Biol. Sci* 280: 20131883.

Elton C (1946) Competition and the structure of ecological communities. *J. Anim. Ecol*. 15: 54–68.

Gage JD, Tyler PA (1991) *Deep-sea Biology: a natural history of organisms at the deep-sea floor*. (Cambridge University Press, Cambridge, United Kingdom).

Gause GF (1934) The struggle for existence. Baltimore, MD: The Williams and Wilkins Company.

Goldberg DE, Barton AM (1992) Patterns and consequences of interspecific competition in natural communities: a review of field experiments with plants. *Am. Nat.* 139: 771–801.

Grant A. 2000 Deep-sea diversity: overlooked messages from shallow-water sediments. *Mar. Ecol.* 21, 97–112.

Grassle JF, Morse-Porteous LS (1987) Macrofaunal colonization of disturbed deep-sea environments and the structure of deep-sea benthic communities. *Deep Sea Res Part I* 34: 1911-1950.

Hardin G (1960) The competitive exclusion principle. *Science* 131: 1292–1297.

Helmus MR, Savage K, Diebel MW, Maxted JT, Ives AR. 2007 Separating the determinants of phylogenetic community structure. *Ecol. Lett*. 10, 917–925.

Hessler RR, Sanders HL (1967) Faunal diversity in the deep-sea. *Deep Sea Res. Oceanogr*. Abstr. 14: 65–78.

Hooper DU, et al. (2005) Effects of biodiversity on ecosystem functioning: a consensus of current knowledge. *Ecol. Monogr.* 75**:** 3-35.

Kenchington ELR, Prena J, Gilkinson KD, Gordon Jr DC, MacIsaac KG, Bourbonnais-Boyce C, Schwinghamer PJ, Rowell TW, McKeown DL, Vass WP (2001) Effects of experimental otter trawling on the macrofauna of a sandy bottom ecosystem on the Grand Banks of Newfoundland. *Can. J. Fish. Aquat. Sci.* 58: 1043–1057 .

Koslow JA, Gowlett-Holmes K, Lowry JK, O'Hara T, Poore GCB, Williams A (2001) Seamount benthic macrofauna off southern Tasmania: community structure and impacts of trawling. *Mar. Ecol. Prog. Ser.* 213: 111–125.

Kutti T, Ervik A, Høisæter T (2008) Effects of organic effluents from a salmon farm on a fjord system. III. Linking deposition rates of organic matter and benthic productivity. *Aquaculture* 282: 47-53.

Laakmann S, Kochzius M, Auel H (2009) Ecological niches of Arctic deep-sea copepods: vertical partitioning, dietary preferences and different trophic levels minimize inter-specific competition. *Deep Sea Res. I* 56: 741–756.

Leduc AOHC, da Silva EM, Rosenfeld JS (2015) Effects of species vs. functional diversity: understanding the roles of complementarity and competition on ecosystem function in a tropical stream fish assemblage. *Ecol. Indic.* 48, 627–635.

Loreau M, Hector A (2001) Partitioning selection and complementarity in biodiversity experiments. *Nature* 412: 72-76.

McClain CR (2005) Bathymetric patterns of morphological disparity in deep-sea gastropods from the western north Atlantic basin. *Evolution* 59: 1492–1499.

McClain CR, Schlacher TA (2015) On some hypotheses of diversity of animal life at great depths on the sea floor. *Mar. Ecol*. 36: 849–872.

McCook L, Jompa J, Diaz-Pulido G (2001) Competition between corals and algae on coral reefs: a review of evidence and mechanisms. *Coral Reefs* 19: 400–417.

Narayanaswamy BE, Coll M, Danovaro R, Davidson K, Ojaveer H, Renaud PE (2013) Synthesis of knowledge on marine biodiversity in European seas: from census to sustainable management. *PLoS One* 8**:** e58909

Pape E, Bezerra TN, Jones DOB, Vanreusel A (2013) Unravelling the environmental drivers of deep-sea nematode biodiversity and its relation with carbon mineralisation along a longitudinal primary productivity gradient. *Biogeosciences* 10**:** 3127-3143.

Price WW, Heard RW (2011) Two new species of *Heteromysis* (*Olivemysis*) (Mysida, Mysidae, Heteromysinae) from the tropical northwest Atlantic with diagnostics on the subgenus *Olivemysis* Băcescu, 1968. *Zootaxa* 2823: 32–46.

Puig P, et al. (2012). Ploughing the deep sea floor. *Nature* 489: 286-289.

Pusceddu A, Bianchelli S, Martin J, Puig P, Palanques A, Masqué P, Danovaro R (2014) Chronic and intensive bottom trawling impairs deep-sea biodiversity and ecosystem functioning*. Proc. Natl Acad. Sci. USA* 111: 8861–8866.

Quattrini AM, Gomez CE, Cordes EE (2017) Environmental filtering and neutral processes shape octocoral communities in the deep sea. *Oecologia* 183: 221–236.

Rex MA (1976) Biological accomodation in the deepsea benthos: comparative evidence on the importance of predation and productivity. *Deep Sea Res. Oceanogr*. Abstr. 23: 975–987.

Rex MA (1981) Community structure in the deep-sea benthos. *Annu. Rev. Ecol. Syst*. 12: 331–353.

Rex MA, Waren A (eds) (1981) Evolution in the deep sea: taxonomic diversity of gastropod assemblages. In Proc. of the XIV Pacific Science Congress, 1981. Vladivostock, Russia: Academy of Sciences of the USSR, Far East Science Center, Institute of Marine Biology.

Riginos C (2009) Grass competition suppresses savanna tree growth across multiple demographic stages. *Ecology* 90: 335–340.

Rijnsdorp AD, Vingerhoed B (2001) Feeding of plaice *Pleuronectes platessa* L. and sole *Solea solea* (L.) in relation to the effects of bottom trawling. *J Sea Res* 45: 219-229.

Román S, Vanreusel A, Romano C, Ingels J, Puig P, Company, JB, Martin D. 2016 High spatiotemporal variability in meiofaunal assemblages in Blanes Canyon (NW Mediterranean) subject to anthropogenic and natural disturbances. *Deep Sea Res*. I 117: 70–83.

Sanders HL (1968) Marine benthic diversity: a comparative study. *Am. Nat*. 102: 243–282.

Somavilla R, Schauer U, Budéus G. 2013 Increasing amount of Arctic Ocean deep waters in the Greenland Sea. *Geophys. Res. Lett*. 40: 4361–4366.

Thrush SF, Dayton PK (2002) Disturbance to marine benthic habitats by trawling and dredging: implications for marine biodiversity. *Annu. Rev. Ecol. Evol. Sys.* 33: 449-473.

Webb CO, Ackerly DD, McPeek MA, Donoghue MJ (2002) Phylogenies and community ecology. *Annu. Rev. Ecol. Syst*. 33: 475–505.

Wilson WH (1990) Competition and predation in marine soft-sediment communities. *Annu. Rev. Ecol. Syst*. 21: 221–241.

White KN, Thomas JD (2009) Leucothoidae. *Zootaxa*. 2260: 494–555.

Worm B, Barbier EB, Beaumont N, Duffy JE, Folke C, Halpern BS, Jackson JB, Lotze HK, Micheli F, Palumbi SR, Sala E, Selkoe KA, Stachowicz JJ, Watson R (2006) Impacts of biodiversity loss on ocean ecosystem services. *Science* 314**:** 787-790.

Zeppilli D, Pusceddu A, Trincardi F, Danovaro R (2016) Seafloor heterogeneity influences the biodiversity–ecosystem functioning relationships in the deep sea. *Scientific Reports* 6**:** 26352.

3.4 Alborán Sea to the Azores: influence of water mass properties on VME biodiversity and biogeography

Authors: Covadonga Orejas, Patricia Puerta, Ángela Mosquera, Olga Reñones, Carlos Domínguez-Carrió, Jordi Blasco, Albert Fuster, Marina Carreiro-Silva, Jose Luis Rueda, Javier Urra

Contributors: Cristina Gutiérrez-Zárate, Guillem Mateu, Telmo Morato, Jesús Rivera, Yaiza Santana, Pedro Vélez-Belchí

Acknowledgements: Ricardo Aguilar, Álvaro Altuna, Manuela Ramos, Íris Sampaio

Abstract

One of the main questions of the MEDWAVES cruise was to what degree oceanographic parameters shape the distribution patterns of species, as ambient seawater conditions vary depending on the properties of a given water mass, including temperature, salinity, density and chemical parameters (e.g. nutrients, pH, oxygen). Water mass structure varies temporally and spatially and can affect the distribution of benthic organisms. During MEDWAVES, sampling was conducted along a belt spanning the Gulf of Cádiz-Strait of Gibraltar-Alboran Sea to the Azores. Four geomorphological features have been targeted: The Seco de los Olivos seamount in the Alborán Sea, the Gazul mud volcano in the Gulf of Cádiz, the Ormonde seamount in the Portuguese continental shelf and the Formigas seamount, close to the Açores. Some interesting effects of water properties were observed, notably that the VME communities at Seco de los Olivos and at the Gazul Mud Volcano, most of the recorded taxa inhabited areas bathed entirely by MOW, indicating an important link between species biodiversity and biogeography and the export of this water mass from the Mediterranean into the Atlantic. Here, the presence of species such as *Flabellum* sp. and *Acanthogorgia* spp. varied with only small variations in O_2, and this seemed also to affect their presence. At the Formigas Seamount, high VME diversity was noted in areas bathed by MOW. Effects of O_2 were also very pronounced for *Lophelia pertusa* and *Acanthogorgia hirsuta* in this area, while salinity had strong effects on abundances of *Acanthogorgia hirsuta*, *Narella bellissima* and *N. versluyi*, indicating close links to the more saline upper MOW layer. Notably, the soft coral genus *Narella*, which has a strong Atlantic affinity, was also found in the areas highly influenced by MOW. The foraminiferal communities have been revealed as a good indicator of the different water masses. Specifically, relative abundances of the levorotatory form of the planktonic species *Globorotalia*

truncatulinoides raeched maximum values in the Mediterranean Sea (94% in Seco de los Olivos), decreasing progressively towards the most distant location in the Atlantic (36% in the Formigas seamounts); therefore, this species is an adequate indicator of the Mediterranean influence in the Atlantic.

Introduction

The MEDWAVES (MEDiterranean out flow WAter and Vulnerable EcosystemS) cruise targeted areas under the potential influence of the Mediterranean Outflow Water (MOW) within the Atlantic realm, including also the study of a Mediterranean geomorphological feature in the Alborán Sea. The targeted areas include seamounts where cold-water corals (CWCs) have been reported but that are still poorly known, and which may act as essential "stepping stones" connecting fauna of seamounts in the Mediterranean with those of the continental shelf of Portugal, the Azores and the Mid-Atlantic Ridge.

The Strait of Gibraltar (SG) and the surrounding areas, Gulf of Cádiz (GoC) in the Atlantic, and Alborán sea (AS) in the Mediterranean, are key areas to understand the distribution and connectivity of marine communities (Patarnello et al. 2007), as the SG and the encounter of water masses at the Almeria Oran front represent an oceanographic transition area, connecting the Atlantic Ocean and the Mediterranean Sea (Lacombe and Richez 1982).

The Mediterranean water flows out from Gibraltar (MOW), extends towards the East of the Atlantic, building a warm and salty water mass which propagates in North West direction from Portugal originating the "Mediterranean Water" (MW) in the Atlantic. This warm and salty water mass becomes characteristic of the North Atlantic in mid waters (around 1100 m) (Candela 2001). The occurrence of CWC communities in the NE Atlantic has been related to the pathway of the MOW, whereby this current system would have an historical influence on the migration of coral larvae and (re)colonization of the Atlantic in the post-glacial era (De Mol et al. 2005, Henry et al. 2014).

Even at scales of several hundred meters, it has been already demonstrated that the presence of distinct water mass layers affects the distribution of deep-water coral species (Long and Baco 2014) and populations (Quattrini et al. 2015). With the possibility of warm salty MOW having a strong influence on VME biodiversity and biogeography, this study aimed at determining whether effects of MOW and water mass properties in general are discernible in VME indicator taxa. Thus, in this section of Deliverable 3.2, results of the video analyses, interpreted on the light of the oceanographic data, are presented here for three of the four targeted features. Further, for all four features (The Seco de los Olivos seamount in the Alborán Sea, the Gazul mud volcano in the Gulf of Cádiz, the Ormonde

seamount in the Portuguese continental shelf and the Formigas seamount, close to the Açores), results of the analyses of the foraminiferans collected are also presented.

Methods

Oceanography

To achieve the planned specific objectives, in each one of the sub regions (Fig. 1), a set of hydrographic stations were carried out to determinate the hydrographic conditions, the geostrophic circulation and to identify the water masses in the area. The number of stations, and its distribution was designed as the minimum to determine the geostrophic circulation for each one of the regions sampled.

The water column was sampled from the surface to 5 metres to the bottom, by means of a CTD-Rosette. Water samples were taken at different levels along the cast and at the bottom, to determine pH, alkalinity, dissolved oxygen and nutrient concentration (see Orejas et al. 2017 for more details), and to calibrate the conductivity sensors. Special attention was given to sampling the layer of Mediterranean Outflow Water (MOW, maximum salinity and minimum oxygen). Additionally, in each of the stations, LADCP measurements were carried out to reference the geostrophic estimation of the circulation with a known reference level.

Hydrographic data were acquired with CTD SBE911+ using the acquisition software Seasave V7 of SEA BIRD. Seasave V7 acquires, converts, and displays real-time or archived raw data from Sea-Bird profiling CTDs and thermosalinographs. Seasave V7 is part of Seasoft V2 software suite of Sea Bird. The raw data was processed with a set of routines from the SBE Data processing package of SEA BIRD. This routine allowed us to transform the data to ascii format (*.cnv), correct for the cell thermal mass effect, the alignment between the conductivity and temperature sensors, and average in pressure bins. A first visualization of these data was obtained by mean software packed named Ocean Data View. Ocean Data View (ODV) is a software package for the interactive exploration, analysis and visualization of oceanographic and other geo-referenced profile, time-series, trajectory or sequence data. On a second step, MATLAB (matrix laboratory) multi-paradigm numerical computing environment and fourth-generation programming language, was used to analyse the data. LADCP data was processed using the LDEO Software (Version IX.7). VADCP data was acquired with an RDI Ocean Surveyor 75 khz using the acquisition software VmDas (Version 1.46.5) and the raw data was processed with CODAS software. After that, MATLAB was used to plot, and analyses the results.

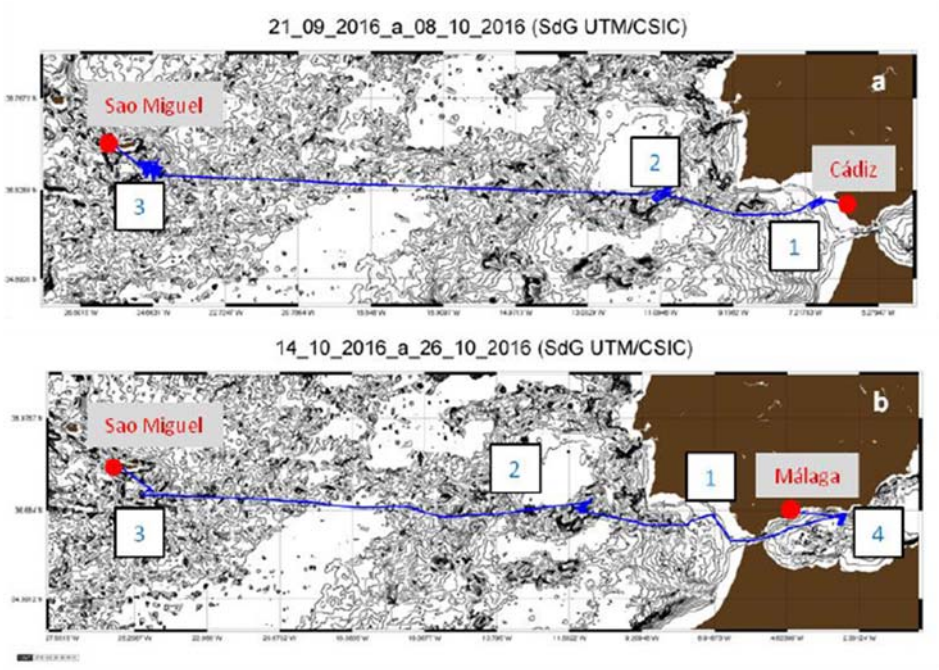

Fig. 1 *MEDWAVES itinerary. a) first leg, starting in Cádiz (Spain) and finishing in São Miguel (Azores); numbers correspond to the research areas 1: Gazul mud volcano, 2: Ormonde seamount, 3: Formigas seamount. b) second leg, starting in São Miguel and finishing in Málaga (Spain); numbers correspond to the research areas 3: Formigas seamount, 2: Ormonde seamount, 1: Gazul mud volcano, 4: Seco de los Olivos.*

Geomorphology

Multibeam echo sounders (MBES) are the most important tool for geomorphological studies in the marine environment. Thanks to this acoustic technique, we can build a Digital Elevation Model (DEM) of the seabed. The DEM is the first step in the geomorphological description of the study area and the base map for the sampling activity. The primary task of the Geomorphology team in MEDWAVES cruise was the collection of MBES data (Gazul mud volcano, Ormonde and Formigas seamounts). The Seco de los Olivos seamount MBES was already available, hence no MBES acquisition took place during MEDWAVES. Swath bathymetry in conjunction with video footage, sediment sampling, and a close-up to the local hydrodynamics let to interpret the seascape in order to have a first impression of the benthic environment. Based on that first quick geomorphological interpretation the geology and nature of the seabed could be approached in order to help in the ROV dive planning, suggesting dive locations in accordance to cruise objectives and providing geomorphometric parameters useful for ROV dives; as depth, slope, and the orientation of the geomorphological features. All these outputs were crucial to guide the ROV operations during the performance of the dives, which was one of the main tasks within MEDWAVES.

The used MBES was a Hydrosweep DS-3 model from ATLAS. Each beam width is 1º along track by 1º across track. Position records from GPS and vessel attitude is controlled by a POS MV unit from Applanix. Sound refraction is corrected by real time measurements of the sound velocity at the transducer depth in addition to sound velocity profiles of the water column gathered from different CTD casts taken before and after each survey. Navisuite software package from EIVA was used for the management of the navigation planning lines and for the control of the swath coverage in real time. MBES settings and acquisition parameters were controlled by ATLAS software running under Linux OS.

The topographic calibration of the sensors (DGPS antennas, transducers and Motion reference unit) was performed when the vessel was stranded for maintenance and the calibration offsets were set afterwards navigating calibration lines following the ATLAS calibration procedure. Vessel configuration file containing calibration offsets was used for TPE calculation and data processing using CUBE.

DEM from swath bathymetry was analysed and inspected using GIS software (ArcGis 10.2) and advance 3D viewers (Fledermaus 7.6) in order to select the best locations for the ROV dives in accordance to main cruise objectives.

Benthic Community Surveys

ROV videos represent a powerful tool to characterize deep-sea habitats and biotopes and quantitatively describe benthic communities *in situ.* Vulnerable marine ecosystems (VMEs) and ecologically or biologically significant areas (EBSAs) identified through video analyses can inform management strategies and ultimately guide the formation of marine reserves. Moreover, videos collected through ROV footage help assess the extent of human impacts in deep basins (Pham et al. 2014). Finally, the coupled biological and environmental information obtained through ROV dives is crucial to construct and validate habitat suitability models which can then be used to predict the behaviour of deep-sea communities under different scenarios of climate change and human pressure.

During MEDWAVES the video transects were performed by means of the ROV Liropus in the four targeted areas we were able to explore. Transects were conducted in different locations of the target areas in order to characterize in a comprehensive way the benthic communities inhabiting areas with different geographical orientations and influence of water masses and currents (ATLAS Task 1.3).

Positioning of the ROV *Liropus* was achieved using the HYPACK software. The multibeam bathymetry data available and the new data acquired during the cruise were used to locate the transects, with the aim of surveying hard bottom areas as far as possible. Throughout the dives, a pair of parallel laser beams mounted 10 cm apart allowed to have a scale which will help to determine the wide of the transects to be analysed later in the home lab. The Liropus was equipped with a Kongsber HDTW colour zoom video camera oe14-502, a colour zoom camera Kongsberg oe14-366/367, a LCC – 600 video monochrome video camera and a Kongsberg minicamera oe14-376/377and a Kongsber low light underwater navigation camera oe13-124/125. The illumination was provided by a Sealite Spheres. A Kongsberg underwater photo still camera OE14-408 / 408E, was also mounted in the ROV, as well as Kongsberg flash OE11-442.

During MEDWAVES, more than 115 hours of videos were recorded in 25 different ROV dives (see for more details MEDWAVES cruise report by Orejas et al. 2017).

Video Processing

Previous to video analysis, the selected ROV transects were visualized in order to assess: (1) the quality of the sequences and (2) determine which video fragments were suitable for quantitative analyses. Based on the characteristic of the video transects, a methodology of analysis was selected based on still images captured from the video footage. Still images were taken at regular length intervals based on the positioning of the ROV using the software OFOP. A distance of 5 meters was the best length interval to be used based on the largest area covered that at the same time avoided images to overlap. Once all still images were generated, those with bad quality (silt clouds obscuring the image, out of focus or too distant from the bottom) were disregarded for the following analyses. The area observed in each photograph, differed among still images due to the variable distance of the ROV to the seafloor along the transect. In order to select images covering a similar area, the width of the images was measured using the distance between the two laser pointers (10 cm) as a reference using the software PAPARA(ZZ)I (Marcon and Purser 2017). The image width selected was 1.5 to 2.5 m for Gazul mud vocano and Formigas seamount and, 1.0 to 2.0 m for Seco de los Olivos. The number of usable images varies among transects. In Table 1 a summary of the total number of processed images is presented.

Still Image Analysis

The following substrate categories have been defined: Mud, Sand, Soft – detritic, Soft – flagstone, Hard – flagstone, Pebbles and Rock. Substrate type was determined and quantified for every still image by overlapping a grid of 20 points, using again the PAPARA(ZZ)I software. A substrate

type was assigned to each point, which allows to objectively assign the percentage of substrate type for further analysis.

A species/taxa/morphotypes list, previously prepared and uploaded in the PAPARA(ZZ)I software, was used to annotate the benthic fauna. Specimens were annotated only in the usable area of each still image, only species/morphotypes occurring in the selected width of the images and presenting at least 10 records per video transect have been considered in the analyses. A separated list of taxa/morphotypes has been prepared for each underwater feature. This was mandatory at this stage of the analyses due to: 1) the video material from the four features has been processed by different individuals in Açores and Palma; and 2) the morphotypes found in each feature are different. Forthcoming analyses will allow examining all obtained images and agreed in potential common morphotypes among all areas. For these first analyses, each feature has been analysed separately.

Table 1. *Number of still images extracted from the video transects for each feature. Dive number, width of the analysed images, total number of useful images and total number of useful images with the selected width are included in the table.*

Feature	**Dive number**	**Still image width (m)**	**Total number of useful still images**	**Total number of useful still images with selected width**
Gazul		1.5 – 2.5	601	355
	1		268	139
	2		333	216
Formigas		1.5 – 2.5	1173	801
	4		161	129 *
	5		215	200 *
	6		321	149
	7		166	66
	8		97	53
	9		138	134 *
	10		75	70 *
Seco de los Olivos		1 – 2	660	477
	22		211	165
	23		75	27
	24		223	204
	25		151	81

* dives where images of a specific width were selected "*a priori*". This is the reason why number of useful images with the selected width is similar to the number of images with the selected width.

Statistical Analyses

To analyse community structure within each of the studied features, the non-metric multidimensional scaling (NMDS) technique was used. This method is superior than other ordination techniques when datasets contains different gradients of variance (Paliy and Shankar, 2016). It can handle non-linear species responses, it is robust with respect to zero-zero species density pairs and effective finding the underlying gradients. The NMDS finds the best configuration of the data, explaining all the variability, in (a priori selected) reduced number of ordination axes. The configuration of the data (sites x species) used a Bray-Curtis dissimilarity matrix. NMDS algorithm tries and provides multiple solutions for the configuration of the data. In every try a 'stress' parameter is calculated as a measurement of lack of fit. Best configuration is selected when the algorithm converges, and the stress value is ≤ 0.05. The NMDS is represented in a biplot of the pairwise dissimilarities in species composition among sampled sites. However, the ordination axes do not correspond to any particular gradient in the original data. To explain the NMDS ordination, the vectors of environmental variables (including percentage of substrate, temperature, salinity, dissolved oxygen or water density) were fitted onto the ordination axes of the NMDS. The vector fitting was tested for significance by means of 1000 permutations. Environmental gradients are represented by arrows that point the direction of change in the corresponding environmental variable and its length is proportional to the linear correlation between the ordination axes and the environmental variable. These gradients can be represented as contours (fitted using a generalized additive models) when a non-linear relationship between variable and axes was observed. Different number of dimensions, random starting points and a maximum of 400 tries of configurations were tested in the NMDS analyses. In cases of small sample size, metric or ordinary MDS (also known as principal coordinates analysis) was applied instead. Each principal component (PCO) is a linear combination of original variables (species) that produce the largest dispersion of values along this component and they are calculated as orthogonal to the preceding components (Paily and Shankar 2016). Thus, MDS goodness of fit is provided by the percentage of explained variance in this case. Vector fitting method and contour were also used to identify the associated environmental gradients. All analyses were performed in R software, version 3.4.4 (R Core Team, 2018) using the package vegan (Oksanen et al 2018).

We also aimed to disentangle potential effects environmental variables at species-specific level and define more accurately how water masses characteristics influence presence, abundance and distribution of target species (e.g. structuring species, key functional species, VME indicator taxa). For this purpose, univariate methods were also applied on the same data used for community analysis for 5 species and one morphotype in Gazul and for 5 species in Formigas. Sample size of still images in each feature and ROV transect independently was, in some cases, large enough to perform univariate models. However, the high number of zeros (records of species absence) and consequently, the low number of positive (presence or abundance) records for most of the species have been a considerable handicap and led to some limitations in the performance of quantitative analyses. Different model approaches were used to deal with zero-inflated distributions (see details below) since data contains more zeros than might be predicted or specified from commonly known distributions. For this reason, the univariate modelling has been reduced to the more frequent and abundant taxa/morphotypes found in the corresponding studied feature.

Regression-based models are widely used for modelling variation in species occurrence or abundance related to environmental gradients, and selecting predictors (explanatory variables) according to their observed importance (Elith and Leathwick, 2009). Three main model formulation were tested here:

- Generalised Additive Models (GAMs) are a widely used non-parametric regression technique which can describe non-linear relationship between the response and the explanatory variable (Hastie and Tibshirani 1990). The main assumptions of this model are that functions, i.e. the effects of explanatory variables, are smooth (i.e. non-linear) and independent, and therefore, additively affecting the response. When the output of GAM indicated a linear relationship, a Generalised Linear Model (GLM) was performed instead. In the GLM explanatory variables are simply added as combinations of linear terms. They are based on an assumed relationship between the mean of the response variable and the linear combination of the explanatory variables.

- An observed zero-inflated distribution was overcome by fitting two completely independent models to find relationships between environmental variables and the presence or abundance of a particular species / morphotype. Thus, two GAM (or GLM) were parameterized either on presence/absence data, using a binomial distribution, or abundances (excluding zero data), using a negative binomial distribution and a log link function. Thus, a completely different combination of explanatory variables can be included for each type of model. GAMs were applied using the R package mgcv (Wood 2017).

A particular formulation of GAM was tested by using a zero-inflated family term, which accounts for a zero inflated Poisson and an identity link. This approach combines presence/absence and abundance data within the same model and it is usually appropriate when none of the explanatory variables help to explain the zeros in the data (Wood et al. 2016). However, it cannot disentangle what variables affects presence from those affecting abundances. Zero-inflated models assumes a) different sources for the zero data: true negative observations (i.e. unsuitable habitat or unoccupied habitat because species does not saturate its environment) and false negatives attributable to experimental design (i.e. survey site is utilized by the species, but not during the survey period) or observer error (i.e. species is present but not detected (Potts and Elith 2006); and b) the data come from a mixture of two populations: one where the counts are always zero, and another where the counts has a Poisson distribution (i.e. zeros or positive values).

- Hurdle Models are a type of two-component model: a model of the zero versus the non-zero counts, and a truncated negative binomial count component applied for the non-zero counts; both using a logistic link. Indeed, it is equivalent to a combination of a GLM on presence/absence data using a binomial distribution and a GLM performed on the abundance data under a negative binomial distribution. Model predictions results from multiplying the predictions of the two model components. In this case, a completely different combination of explanatory variables can be also included in each model component. In contrast to the zero-inflated models, the hurdle model assumes that the zero observations are all true negatives. That is, a zero observation is observed because the species can never occur there (i.e. unsuitable habitat, (Potts and Elith 2006). This approach removes effect of zero-inflation in the presence/absence model and over-dispersion in the non-zero observations. The second component accommodates zero observations, permitting the stochastic process resulting in unoccupied sites, even when habitat is suitable (Potts and Elith 2006). Hurdle models were applied using the R package pscl (Loeys et al. 2012, Jackman 2017).
- In GAMs, the knots for splines (i.e. smooth functions) were kept to a maximum of 4 to avoid overfitting. Model inspection of residuals was performed in all cases for checking common model assumptions (Zuur et al. 2009). An assumed significance level of 5% was used in all statistical analyses.

Regardless the type of model formulation used, selection of environmental variables with effects on a particular species / morphotype data, was perform by comparing models that include all possible combinations of the environmental variables. Only variables with significant effects ($p \leq 0.05$) were retained and models with different configuration of environmental variables were

compared and selected based on the lowest Akaike Information Criterion (AIC) as a measure of goodness of fit and the percentage of explained variability. In addition, every variable retained in final models was also checked for significant effect when included as the unique explanatory. Collinearity among explanatory variables was check prior variable and model selection. The degree of collinearity between explanatory variables was tested with plots of paired variables (pair-plots), a matrix of scatter plots that show the bivariate relationships of variables, and variance inflation factor (VIF) values (Zuur et al. 2009). Variables with Pearson's correlation coefficient >0.6 (absolute value) and VIF value >5 were considered correlated, and one of the pairs was not included in the variable selection.

Planktonic and benthic foraminifera sampling

During the MEDWAVES cruise, 33 sediment samples were collected in the four targeted features by means of a Van Veen Grab, taking a small quantity of the sediment surface using a 6 cc syringe; each sample was placed and labelled in plastic bags with the sample code, date and expedition for further analyses of foraminifera at the University of the Balearic Islands (UIB). In the three Atlantic features: Formigas seamount, Ormonde seamount and the Gazul mud volcano, thirteen six and three samples were respectively collected, whereas 11 samples were taken in Seco de los Olivos. In the home laboratory sampled were washed using a 65 µm sieve in order to remove nanoparticles and allow the processing of the samples. Number of specimens for each sample has been determined using rarefaction curves and the taxonomical classification was performed. Further the growth direction of the helix was also noted.

Individuals were clustered following several criteria as for instance the latitudinal and longitudinal distribution, following the literature. The percentage of each species or species clusters was also annotated for each geomorphological feature.

Results & Discussion

Seco de los Olivos

Seco de los Olivos also called Chella Bank (Fig. 2) is placed in a very active tectonic area. Its origin is related with a distensive regime resulting from two transpressive fault zones (Ballesteros et al. 2008). One is located to the north: Alpujaras fault zone, and the other one extends 90 km from land at north east side of the Bank to 1000 m depth to the south from Seco de los Olivos; The Serrata Carboneras Fault Zone, a sinistral strike slip fault. Due to the flat top summit of the seamount we can infer it was emerged in the past. The rocky outcrops around and on top denote the volcanic nature

of the edifice. Thank to hard substrata that represents the wide area of exposed rock sessile organisms are abundant including cold water coral colonies (Pardo et al. 2011, Lo Iacono et al.2012).

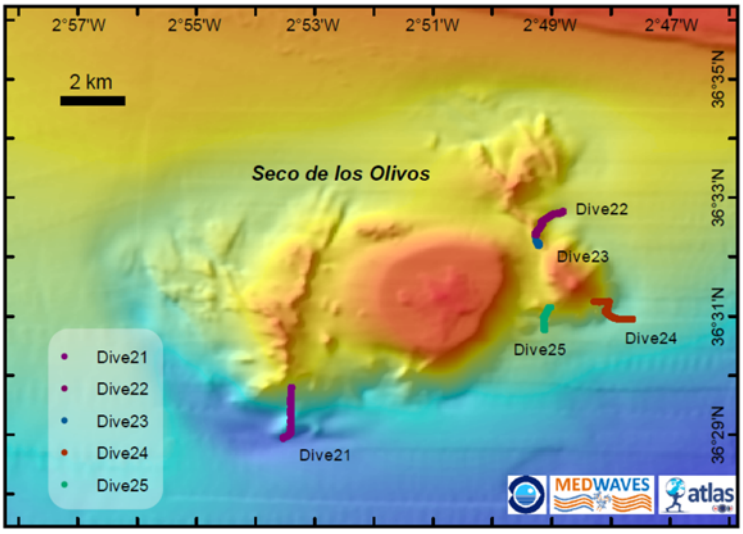

***Figure 2**: Swath bathymetry for Seco de los Olivos and video transects (ROV dives) conducted during the MEDWAVES cruise (Source: IEO, ISBN:84-491-0620-6).*

The CTD survey performed at Seco de los Olivos comprises 21 CTD casts distributed in three across-slope hydrographic sections over the bank (Fig. 3).

The general structure of the water column was uniform, with Atlantic-origin warmer and fresher surface waters overlying cooler, saltier deeper waters, with a salinity maximum about 400-500 m depth corresponding to the core of the Levantine Intermediate Water (LIW), the main contributor to the characteristics of the MOW. Beneath the LIW, a smooth halocline/thermocline over the $\sigma\theta$= 29.1 kg m^{-3}isopycnal leads to the Western Mediterranean Deep Water (WMDW) (Fig. 4).

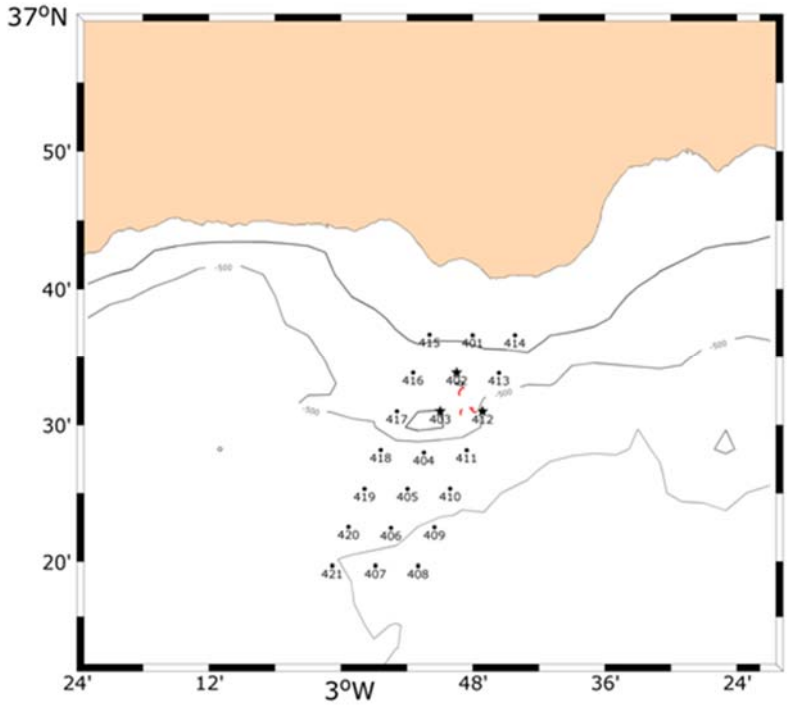

Figure 3. *Distribution of the oceanographic stations at the Seco de los Olivos. The red dots / lines show the locations of the ROV video transects.*

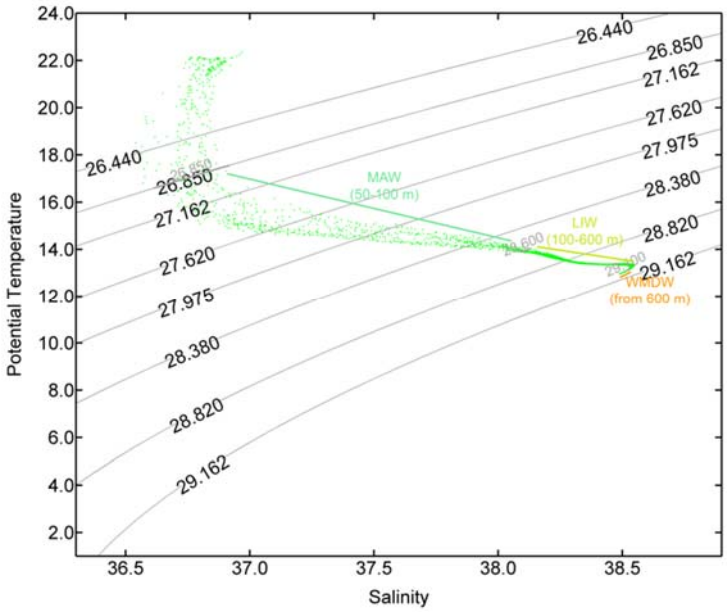

Figure 4*. T/S Diagram of all the stations sampled in the Seco de los Olivos. The modified Atlantic Water (MAW) is depicted in green, Levantine Intermediate Water (LIW) in pale green and Western Mediterranean Deep Water (WMDW) in orange. The depth range where these three water masses have been detected is indicated.*

The depleted oxygen levels associated with the LIW are the source of the low oxygen signal in MOW in the Atlantic (Fig. 5). The slightly differences in temperature and salinity across-slope suggest the presence of modified Atlantic Water (MAW) over the shelf (Fig. 5). Sloping isotherms and isohalines suggest also some circulation associated with the seamount (Fig. 5). The final water mass structure is depicted in Fig. 6.

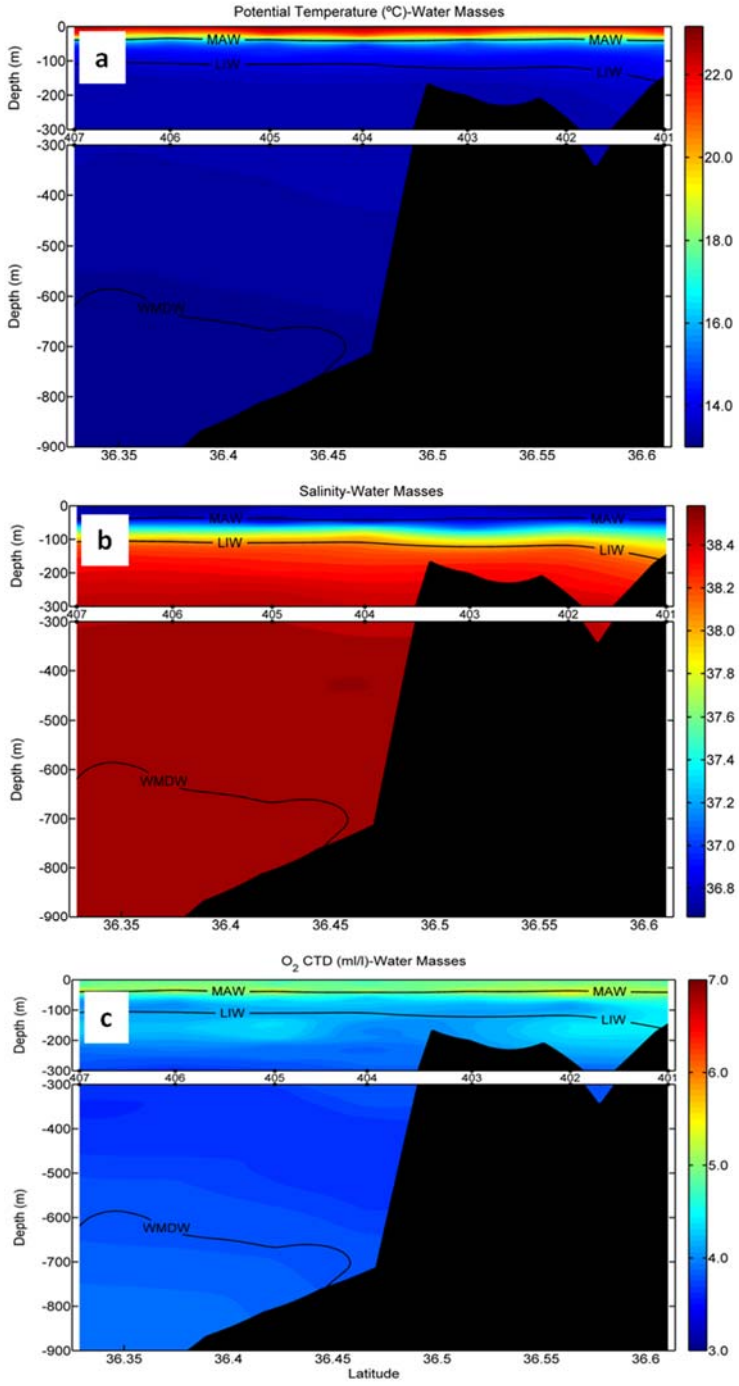

Figure 5. *Vertical section of (a) temperature, (b) salinity and (c) oxygen in the Seco de los Olivos. MAW: Modified Atlantic Water, LIW: Levantine Intermediate Water, WMDW: Western Mediterranean Deep Water.*

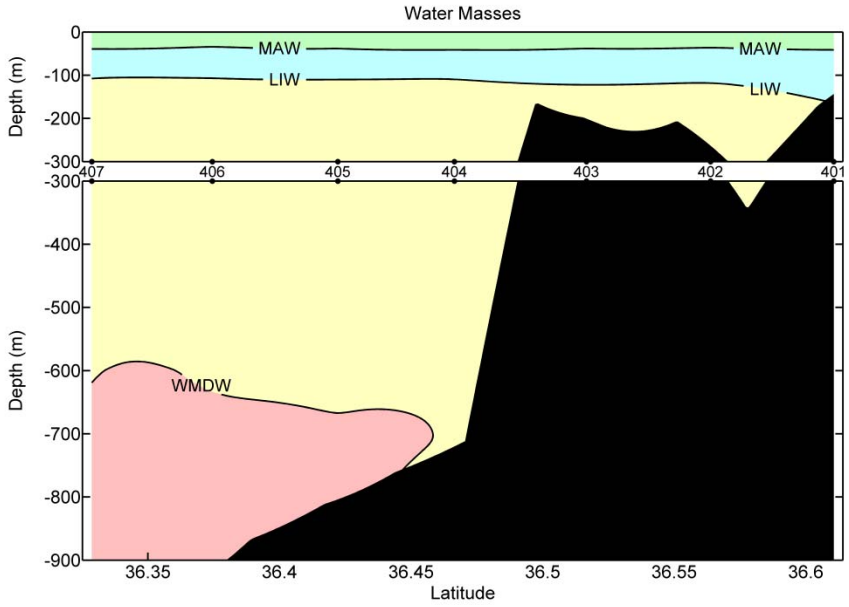

Figure 6. *Water masses detected in Seco de los Olivos: from 50 to ca. 100 m the modified Atlantic Water (MAW), from 100 to 600/700 the Levantine Intermediate Water (LIW) and from 600/900 the Western Mediterranean Deep water (WMDW).*

Benthic communities

The characterization of the benthic fauna in the Seco de los Olivos seamount has been done by analysing 4 (Dives 22, 23, 24, 25) of a total of 6 ROV video transects conducted in the area covering a depth range from 560 to 220 meters depth. All analysed dives were conducted in the East side of the Seco de los Olivos seamount.

Two main habitat types have been identified: 1) Muddy bottoms characterised by the occurrence of *Gadiculus argenteus* and 2) Soft detritic with patched occurrence of rocky substrates. Both habitat types occurred across the bathymetric gradient of the four video transects (from 560 to 220 meters depth). Some images to illustrate some of the benthic habitats of Seco de los Olivos are displayed in Fig. 7.

The muddy bottoms show slightly low occurrence of megabenthic organisms, with exception of some isolated sponges (Dive 25). However, it is worthy to mention the presence of some seapens as *Kophobelemon* sp., different species of *ceriantharians* and the holothuroidea *Parantichopus* sp. This substrate type harbours an abundant population of the fish species *Gadiculus argenteus;* this was previously documented for Seco de los Olivos by Abad et al. (2007) who found high abundances of this species (around 10 times higher) in El Seco de los Olivos compared to other sampled areas in the Alborán Sea.

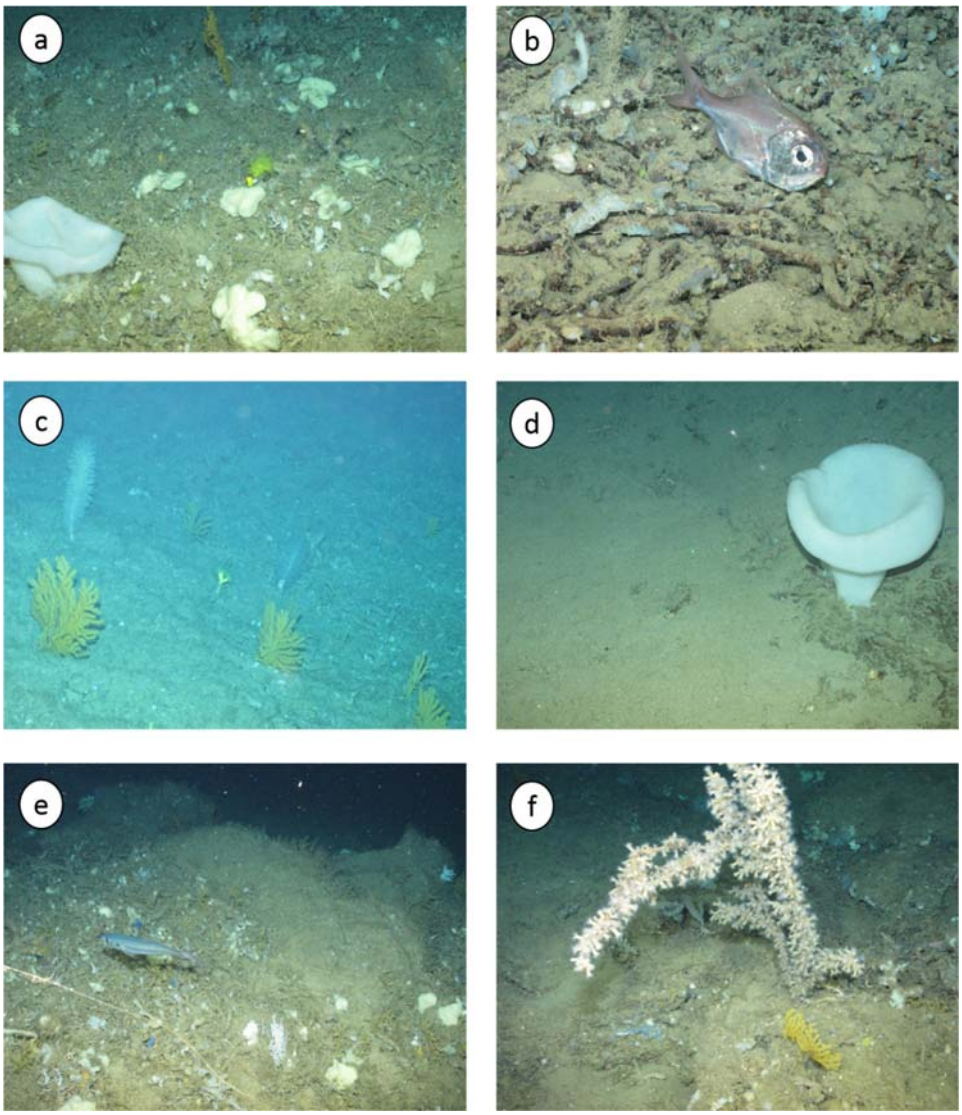

Figure 7. *Some of the benthic habitats of Seco de los Olivos seamount. a) sponge field (200-250 m depth), b) specimen of* Gadiculus argenteus *lying in the seafloor covered by coral rubble (690 m depth), c) coral garden dominated by* Acanthogorgia s*p. (200-250 m depth), d) large specimen of the dee-sea sponge* Asconema setubalense *in an area dominated by soft substrate (ca. 600 m depth), e) a promontory covered by sponges, with presence of cnidarians, a well as an specimen of* Trachurus trachurus *and long-line gear (200-250 m depth), f) a zoanthid and a colony of* Acanthogorgia *sp. (200-250 m depth).*

Regarding the soft detritic areas, spotted with some rocks, the megabenthic fauna was characterised by different types of sponges, displaying many different morphotypes: encrusting pedunculate, massive and lamellate. The scarce current knowledge on sponge taxonomy prevents to obtain at this stage a more precise classification of the documented specimens. Only four have been identified at genus level*: Cladocroce, Rhizaxinella, Asconema* and *Phakellia,* the last two with low frequency of occurrence*. Cladocroce*, together with encrusting sponges, dominated in Dive 22,

however it is worthy to remark that registered abundances in all the analysed dives were low. In this same Dive (22), sporadic occurrence of different cnidarians species (i.e. alcyonaceans and some specimens of the black coral *Paranthipathes*) was observed in areas where hard substrates where present, as well as specimens of the fish *Helicolenus dactylopterus* present in all substrate types of this dive; this species, as *G. argenteus*, has been also referred by Abad et al. (2007) as a common and abundant species in the Seco de los Olivos, indeed very high abundances (around 20 times higher) have been registered in Seco de los Olivos compared to other sampled areas in the Alborán Sea. Cnidarians are represented mostly by *Acanthogorgia* spp. which present in some cases (Dive 23) relatively dense patches, as well as spotted specimens of *Dendrophyllia cornigera* and *Parantipathes* spp. This same Dive (23) was dominated by the occurrence of sponges (mostly encrusting species). The Dive 24 was conducted in muddy substrate and few megabenthic organisms (with exception of encrusting sponges) have been identified, being *G. argenteus* the most conspicuous and abundant species present. A mixture of muddy bottoms and soft detritic substrates characterised Dive 25 where *G. argenteus* was again the dominant species in the muddy locations whereas different morphotypes of sponges (mostly dominated by encrusting sponges) and some spotted cnidarians, formed this community. In general, the fauna documented across these four transects was similar with slightly higher dominances of the different morphotypes along the transects.

Effects of environmental factors on benthic communities at Seco de los Olivos

The non-metric multidimensional scaling analyses (NMDS) performed for the 4 dives displayed a spatial configuration reducing data to 3 dimensions (only 2 dimensions are shown for graphical purposes) with a very low stress value (0.028). The environmental variables fitted to the resulted NMDS showed that substrate was the most important factor defining the composition of the benthic communities. The four analysed dives are depicted considering the taxa/morphotypes described in the previous section, as well as all environmental factors analysed (e.g. depth, substrate types, temperature, salinity, oxygen; Fig. 8).

It is worthy to consider that due to the narrow bathymetric range of the four video transects (deepest location: 560 m and shallowest 220 m), all video transects are under the influence of the LIW and remarkable differences due to changes in environmental factors are not expected and indeed, only relatively small changes in these factors have been recorded. For instance, temperature varied from 13.31 to 13.73 ºC along the four video transects, the range of values for dissolved oxygen (DO) were however more remarkable: from 3.67 to 4.32 ml L^{-1}. Nevertheless, the most remarkable environmental change detected across the four analysed transects was the substrate type. However

further analyses need to be conducted analysing the potential role of the slope in the occurrence and distribution of benthic communities as this has been documented, together with depth, as a main factor defining the characteristics of the benthos in Seco de los Olivos (de la Torriente et al. 2018), but these same authors also identify a specific substrate type for each of the 13 habitats they describe in Seco de los Olivos. Although de la Torriente et al. (2018) identified slope and depth as the main drivers for the occurrence of the different benthic communities, it is worthy to mention that in their study water column factors have not been analysed. Due to the narrow depth range analysed and the fact that all analysed communities where under the influence of the same water masses and therefore, univariate models have been not performed for Seco de los Olivos species.

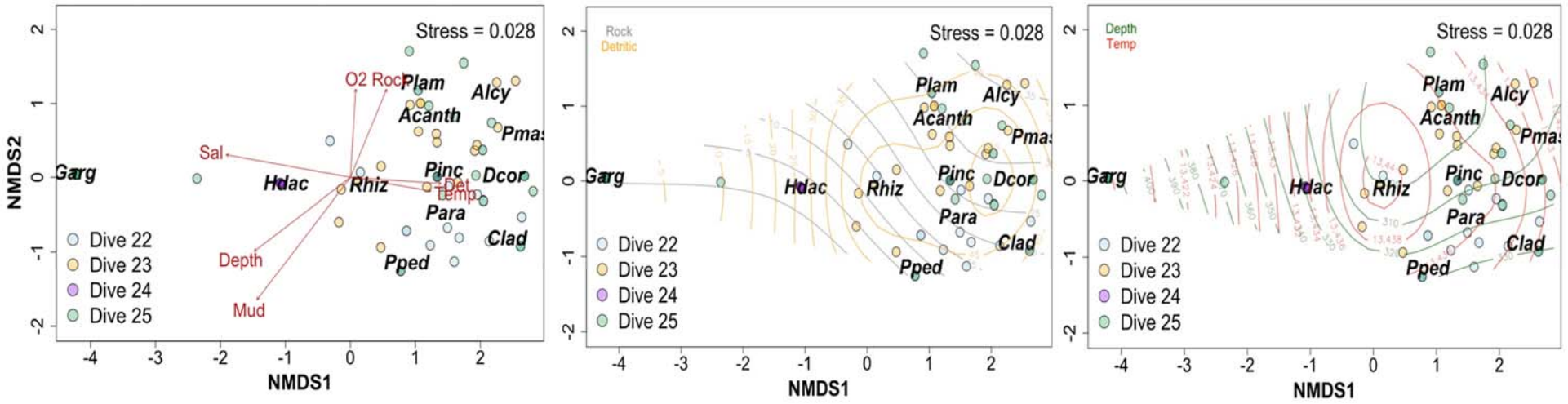

Figure 8. *Multiple nMDS plots performed on Seco de los Olivos data with significant environmental factors fitted. The left panel display vectors for all significant variables, whereas the central and right panel present contour fit for a selection of individual variables, rock-detritic and depth-temperature respectively (abbreviations for species and morphotypes are included in the species/morphotype lists compiled for each dive in the Annex 1).*

Gazul Mud Volcano

Gazul is a mud volcano located in the Gulf of Cádiz whose shape is sculpted by the Mediterranean Outflow Water (MOW). The intense bottom current has carved two depressions at both sides of the volcano cone downstream. Those depressions suggest erosion due to the increase of the flow velocity at both sides of the apron facing the flow, whereas at the rear sector, a velocity waning enable sedimentation and models a peculiar saddle shape (Rueda et al. 2012, Palomino et al. 2016). Two factors are responsible of the rough appearance of the Digital Elevation Model (DEM) inside the depressions (Fig. 9). One is the more intense flow that rinses away sediment particles exposing hard substrata. The other one is the presence of methane-derived authigenic carbonates such as large chimneys and slabs, as we could corroborate from ROV video records (Orejas et al. 2017).

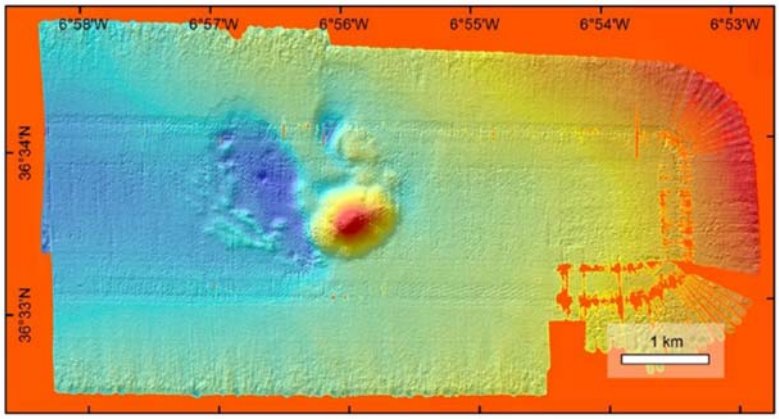

Figure 9. *Swath bathymetry for Gazul mud vocano acquired during the MEDWAVES cruise.*

The sampling design in the mud volcano of Gazul was composed of 3 hydrographic sections perpendicular to the slope, one over the volcano, one 5 nm north of it, and the last one 5 nm south of it (Fig. 10).

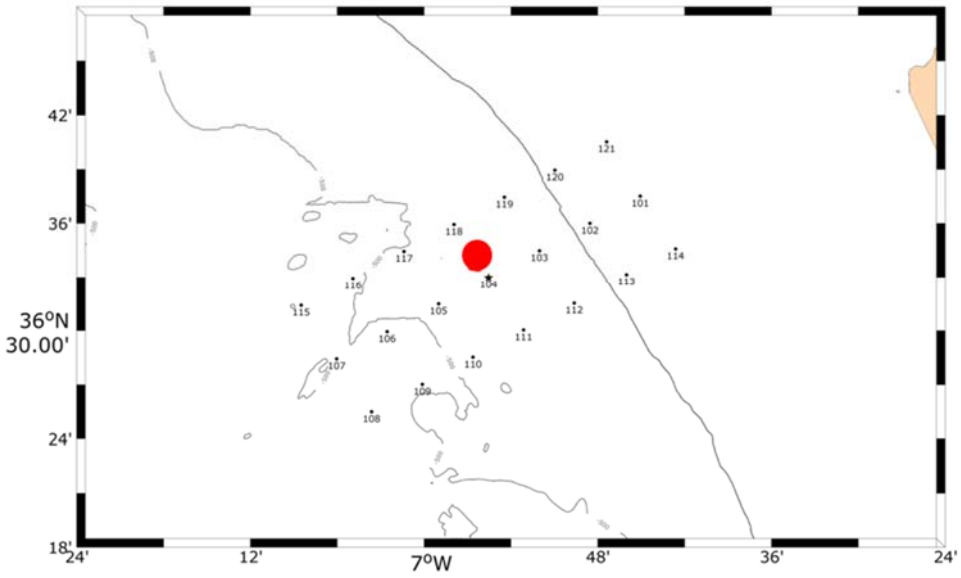

Figure 10. *Distribution of the oceanographic stations at Gazul Mud Volcano. The mud volcano location is highlighted with the red dot.*

The ocean circulation is characterized by a two-layer flow, with Atlantic waters on the upper layer and waters of Mediterranean influence near the bottom. The □/S diagram (Fig. 11) shows these two different waters masses, the colder and fresher North Atlantic Central Water (NACW), lighter than the γn=27.1 kg/m3 isopycnal and the relative warmer and saltier Mediterranean Outflow water (MOW), closer to the bottom.

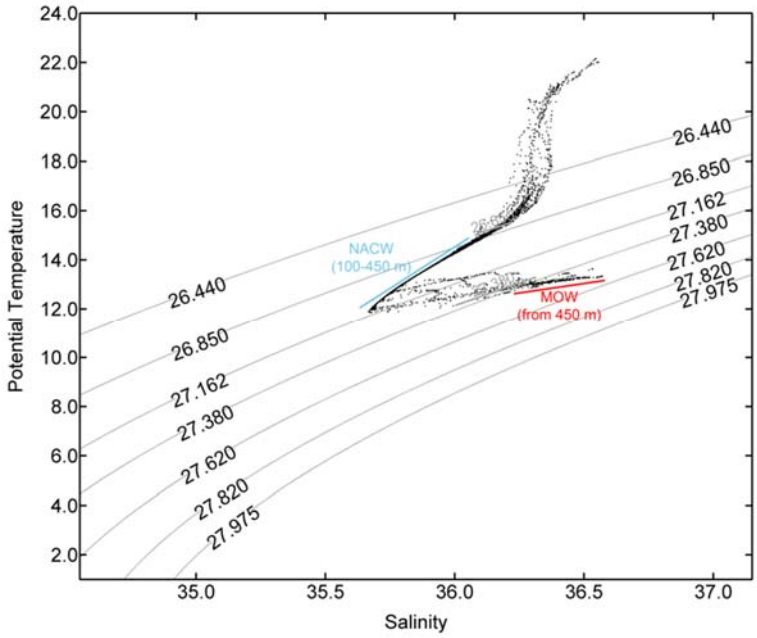

Figure 11. *T/S Diagram of all the stations sampled in the Gazul Mud Volcano. North Atlantic Central Water (NACW) is depicted in blue and Mediterranean Outflow Water (MOW) in red. In both cases the depth range where these two water masses have been detected is indicated.*

The two waters masses are separated by the isohaline of 35.75, at approximately 150 m above the bottom, and deeper than 350 m (Fig. 12). The signal of the Mediterranean waters is also observed in the vertical distribution of temperature, with a relative maximum in temperature below the 350 m, and in the 150 m above the bottom. In the case of the temperature, the 12.5°C isotherm divide the waters from Atlantic and Mediterranean origin. This two-layer structure, with light NACW on top of heavier MOW, is also observed in the schematic image (Fig. 13)**.**

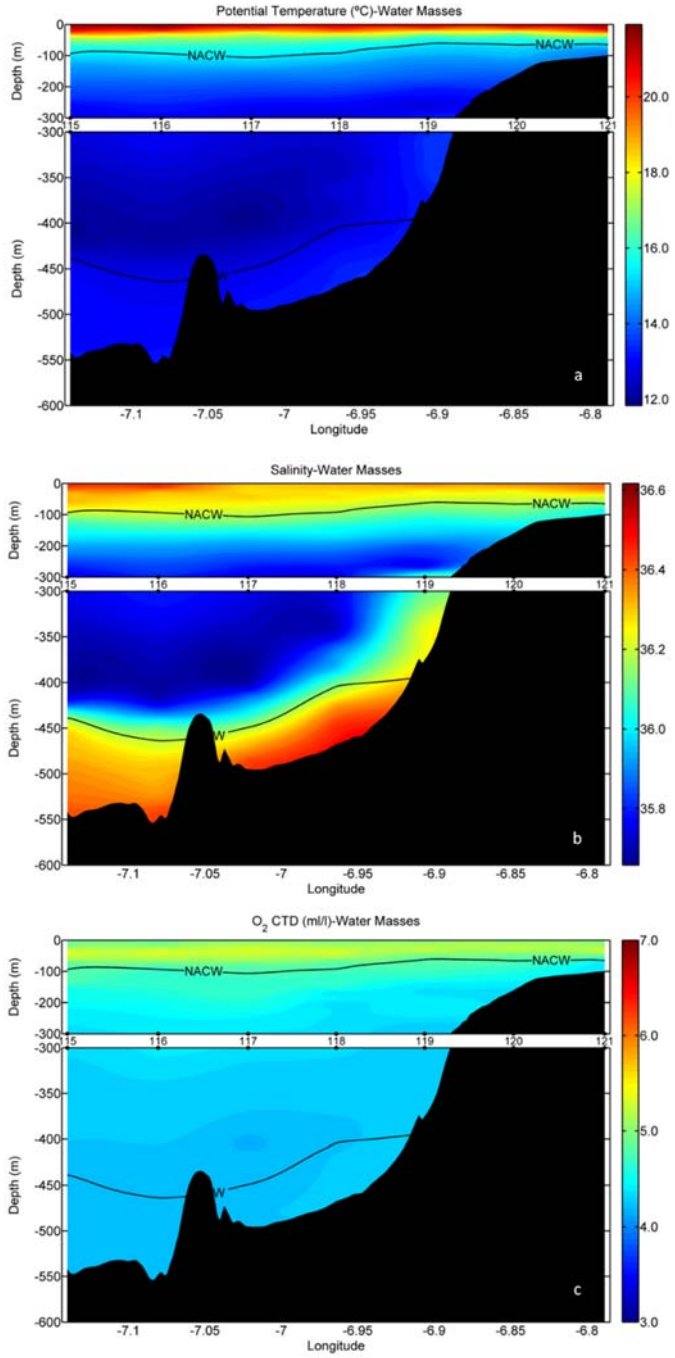

Figure 12. *Vertical section of (a) temperature, (b) salinity and (c) oxygen in the Gazul region. NACW: North Atlantic Central Water, MOW: Mediterranean Outflow Water.*

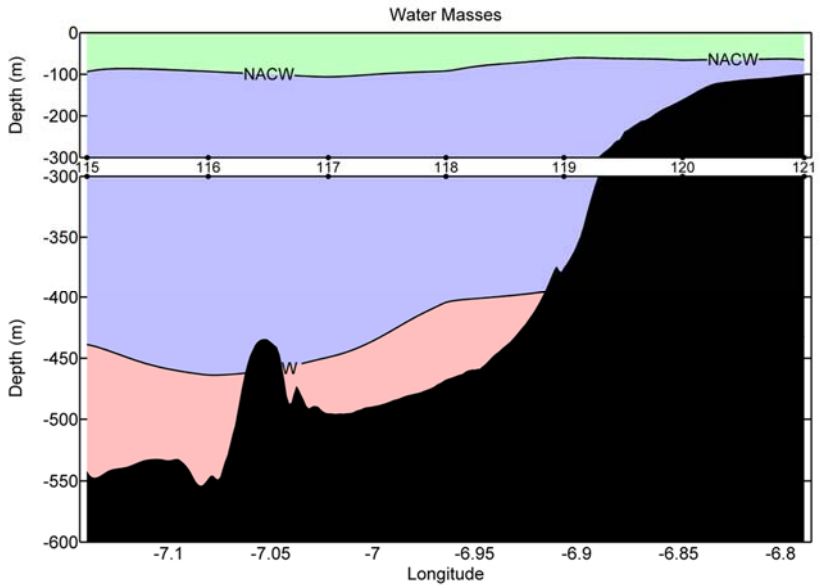

Figure 13. *Water masses detected in the Gazul Mud Volcano: from 100 to 400 m the NACW (North Atlantic Central Water), from 400 to the seafloor the MOW (Mediterranean Outflow Water).*

Benthic Communities

The characterization of the benthic fauna in Gazul has been done by analysing the two ROV video transects conducted in the area. Both transects presented clearly distinct communities Figure 14 shows some examples of the benthic habitats documented in Gazul mud volcano during the MEDWAVES cruise.

In Dive 1, three main sections were observed. The deeper part of the transect, from ca 460 to ca 448 m depth (transect distance 0 to ca. 745 m) is dominated by a community characterized by gorgonians (*Acanthogorgia*-like) mixed with different poriferans morphotypes and patchy occurrence of crinoids where hard substrate was present. This part of the transect was dominated by sandy substrate and scattered presence of different type of rocky substrates as well as detritic. In the transect section comprised from ca. 448 to ca. 443 m depth (from 745 to ca. 1250 m transect distance), *Flabellum chunii* dominated with low abundances, being one of the most abundant species group in the soft substrate. In the shallower parts, from 443 to 385 m depth (from 1250 to 1800 m transect distance) different morphotypes of Porifera dominated with scattered presence of *Acanthogorgia*-like colonies and the white corals, largely dominated by *Madrepora oculata*, but also mixed with a few colonies of *Lophelia pertusa*.

Regarding Dive 2, soft substrates dominated in the first and deepest part of the transect, from ca 473 to 464 m depth, (from 0 to 1030 m transect distance) with a quasi-monospecific community

of the actinia *Actinauge richardi* dominating the soft substrate and scattered occurrence of *Flabellum chunii*. A change in substrate type from sandy bottom to an almost complete dominance of detritic bottom, defined a change in the community composition. The area where substrate types mixed, at 464 m depth (from 1030 to 1340 m transect distance) displays an also mixed community of *Actinauge richardi* and *Acanthogorgia*-like, as well as different morphotypes of poriferans. The detritic bottom was dominated by different Porifera morphotypes mixed with low abundances *of Acanthogorgia*-like morphotype in the last part of the transect that covered depths from 482 to 408 m (from 2550 to 3125 m transect distance. White corals are also present in this second part of the transect linked to patches of rocky substrate.

Abundances are in general low, but higher in Dive 1 than in Dive 2, except for *Actinauge richardi* who present very high abundances in several parts of Dive 2.

Effects of environmental factors on benthic communities at Gazul

The performance of the non-metric multidimensional scaling analyses (nMDS) resulted in a reduction of data to 3 dimensions (only 2 dimensions are shown for graphical purposes) and non-converge model. We inspected the possible data configurations and concluded that due to the high sample size, the low stress values in all configurations tested (stress$<$ 0.055, 0.085 and 0.042 for both, Dive 1 and Dive 2, respectively) and consistency in the fitted environmental variables to the axes, we can assume any NMDS produced showed a data configuration very close to the real one. The NMDS reveals that substrate was the most important factor defining the different composition of the benthic communities. In Figure 15**,** the biplot of both Gazul Dives are depicted considering the taxa/morphotypes described in the previous section and a selection of the significant environmental variables (i.e. depth, sandy and detritic substrates and temperature with $p < 0.01$) fitted to the NMDS axes. The NMDS clearly showed that sand is the factor that explains the dominance of a taxa/morphotype across the transects, which is strongly linked to the very high abundances (compared to other taxa/morphotypes) of *Actinauge richardi*. It is worthy to consider that due to the narrow bathymetric range of the two video transects (deepest location: 475 m and shallowest 400 m), remarkable differences due to changes in environmental factors are not expected and indeed, slight changes in these factors have been recorded. For instance, temperature varied from 12.8 to 13.5 °C along the two video transects, whereas concentrations of dissolved oxygen (DO) only ranged from 4.26 to 4.29 ml L^{-1}. Consequently, the most remarkable environmental change across the two transects was the substrate type. In addition, depth and temperature seem to play a role in the community composition, although their effects cannot be clearly associated with any taxa or location.

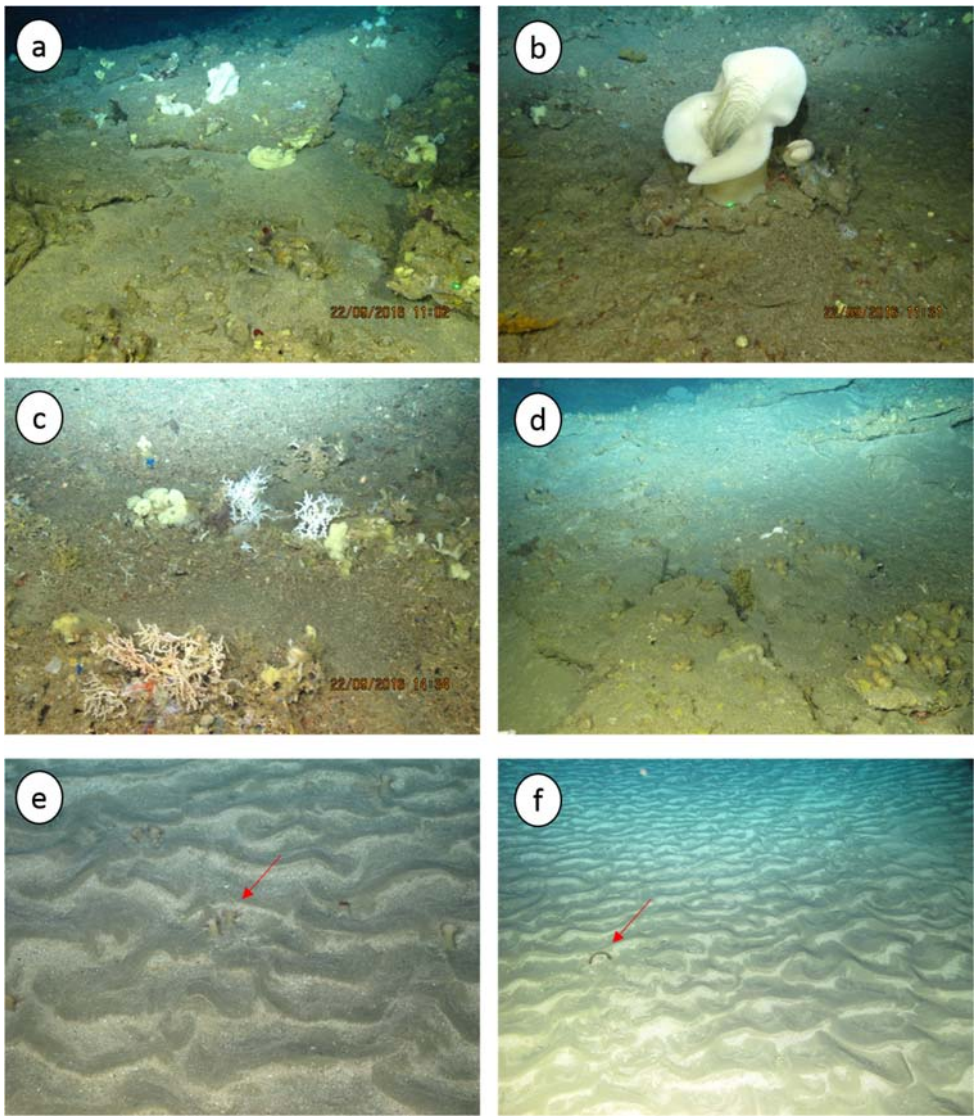

Figure 14. *Some of the benthic habitats of Gaul mud volcano (470-400 m depth). a) sponge field colonising areas of flag-stone substrate, b) specimen of the sponge* Asconema setubalense*, c) patch of some small colonies of scleractinian corals (*Madrepora oculata*) with sponges, d) specimens of an ascidia in flag-stone substrate, e) sandy substrate with presence of* Actinauge richardi *(indicated by the red arrows) f) sandy substrate with presence of* Flabellum chunii *(indicated by the red arrows).*

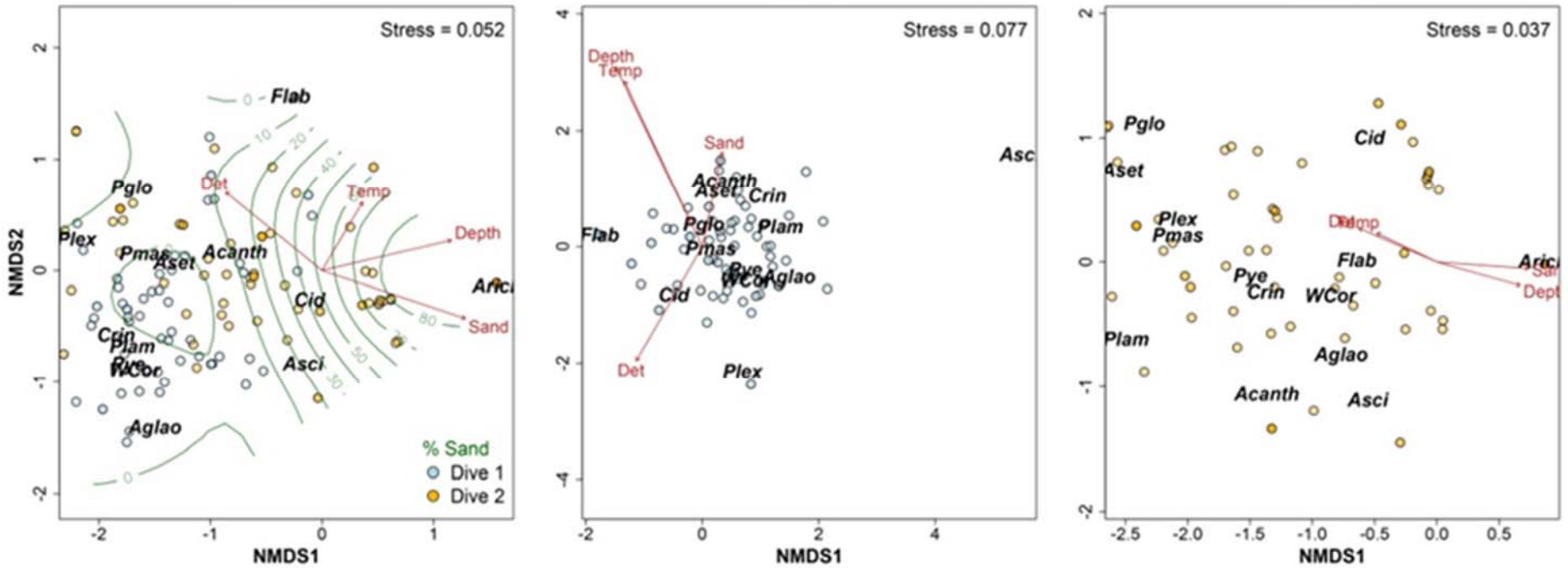

Figure 15. *Multiple nMDS plots performed on Gazul data using both transects together (left panel) and independently (middle and right panel), with significant environmental factors fitted. Still images of Dive 1 are in blue and those of Dive 2 in orange. Contour lines for sand were added in green.*

For Gazul, we also aimed to disentangle potential effects of different environmental factors in the benthic fauna of Gazul at species/morphotype level. From the results of community composition we know that the most frequent and abundant taxa/morphotypes where the following: the colonial scleractinian white corals (*Lophelia pertusa* and *Madrepora oculata*), gorgonians that were *Acanthogorgia*-like, the actinarian *Actinauge richardii,* the solitary scleractinian *Flabellum chunii* and Porifera morphotypes. In order to explore which environmental factors, in particular beyond substrate type, could potentially drive the occurrence and the abundance of these taxa/morphtypes, several univariate models have been tested for all four groups.

White corals

The results of the different model formulations tested for white corals presence/absence and abundance data were, in general, in agreement. Despite of the type of response might vary from linear to non-linear depending on the model performed, the selection of significant explanatory variables affecting white corals were similar in all models (Fig. 16). Thus, temperature, dissolved oxygen (DO) and depth seem to be determinant for the distribution of this morphotype. It is worth noticing that all models provided a quite reasonable data fit (explaining between 30 and 70% of the variance) and were able to capture significant effects of the environmental factors considering the very low variation in the values of the explanatory variables.

Effects of Sea Temperature

Although the temperature range is, as already mention, very narrow, all models (regardless presence or abundance was fitted) consistently detect a significant effect of temperature (Fig. 16, Temperature). In general, presence and abundances of white corals decreased as the temperature increase, but this effect was particularly enhanced when the temperature reached 13.4°C and beyond. This is an interesting result as it is known from previous studies that the white corals, especially *Lophelia pertusa*, seems to live in the Mediterranean at its upper thermal limit (Freiwald 2002). The white corals documented in Gazul mud volcano occur in the depth range (400 to 465 m depth), these depths are partially under the influence of the MOW and this can be the reason for this sensitivity to the higher temperatures of the registered range. Indeed, results displayed higher abundances in relatively shallower areas of the transect (420-430 m) close to the depth where both water masses NACW and MOW encounter (Fig. 16; see details below). Aquaria experiments conducted with Mediterranean *Lophelia* and *Madrepora* have demonstrated different accommodation capabilities of these two species to temperature (Naumann et al. 2014), hence it

would be interesting to disentangle the presence and abundance of the two species, however the scarce number of samples with positive presence/abundance values as well as the difficulties to distinguish both species in many images hamper to analyse the two species separately.

Effects of oxygen

The outputs of the models for oxygen were less clear and provide more variable results than those observed for temperature (Fig. 16). In general, a threshold point can be observed in all model outputs, where a detrimental effect for white corals presence and abundances occur at around a value of dissolved oxygen of 4.28 mL L^{-1}. However, this result should be taken with caution due to the low range of oxygen variability, the low number of data used and a possible entangle effect oxygen-depth. The oxygen concentrations documented in Gazul are above the values documented for other areas where *Lophelia pertusa* has been documented. Overall DO levels of 4.8–6.7mL L^{-1}have been documented from *L. pertusa* occurrences at 100 m depth in the Swedish Kosterfjord (Wisshak et al. 2005), however according to Freiwald (2002), most *L. pertusa* records in the NE Atlantic coincide with zones of relatively low oxygen cc of around 3–5 mL L^{-1}. Indeed, for the NE Atlantic (including the Mediterranean Sea) values of ~3.7 mL L^{-1} have been recorded (Dullo et al. 2008, Freiwald et al. 2009)whereas lower values have been registered in the NW Atlantic (~2 mL L^{-1}; including the Gulf of Mexico, Brooke and Ross 2014, Georgian et al. 2016, Hebbeln et al. 2014) as well as in the SE Atlantic (1.1 ml L^{-1} which are the lower values ever recorded for a *Lophelia* reef, Hebbeln et al. 2016). Regarding *Madrepora oculata* there is no in situ information on DO specific for this white coral species. Consequently, considering the currently available information the *L. pertusa* specimens in the GoC seems to be within the oxygen ranges natural for the species.

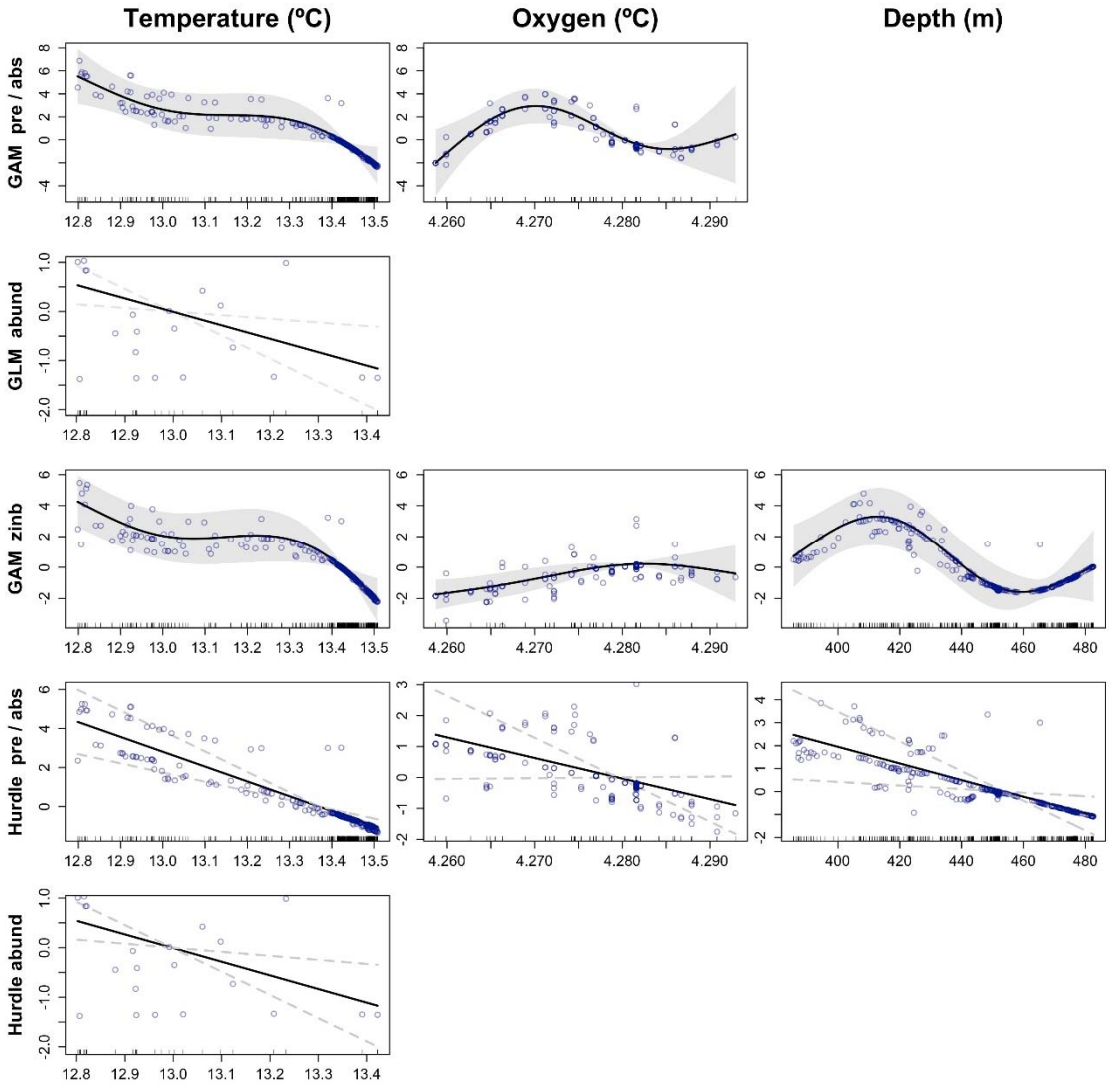

Figure 16*. Models outputs for white corals in Gazul Mud Volcano. Outputs of the 5 models tested, from the upper to the lower part of the image: GAM for presence/absence, GLM for abundance, zero-inflated GAM (presence/absence and abundance combined), Hurdle model (presence/absence and abundance independently). From the left to the right the tested variables: temperature, oxygen and depth.*

Effects of Water Depth

The zero-inflated GAM and the Hurdle model found significant effect of depth for white corals. An optimal depth range can be extracted from the zero-inflated GAM varying from 400 to 430 m. Although the depth range we are analysing is quite narrow, it is worthy to remark that the limit between the MOC and NACW has been detected by 450 m depth. This optimal depth range might be related with any water characteristic, as can be elucidate from the results of DO described above.

Considering the records of *Madrepora* and *Lophelia* from Gazul mud volcano, is worthy to stress that most records correspond to *Madrepora* (a total of 10 *Lophelia* colonies have been properly identified *vs*. 119 *Madrepora* colonies); *Madrepora* has been documented from 402 to 465 m depth, being however more abundant at depths shallower than 450, whereas the *Lophelia* specimens were detected from 394 to 431, always well above the MOW influence. Indeed, in previous extensive sampling events at deeper areas in Gazul and its vicinity, *Madrepora* and *Lophelia* have never been documented at deeper areas with strong MOW influence (Palomino et al. 2016, Rueda et al. 2016). The number of samples is reduced and the depth where the MOW and the NACW occur varies among localities. However, we consider worthy to highlight these findings. Forthcoming results on the chemical parameters of the water column will be included in these analyses in the next months in order to explore other potential factors influencing the occurrence and abundances of the white coral species.

Model predictions for cold-water coral occurrence and abundance

To further test the different models' capabilities performed for white corals, we have compared the predictions of the 4 models along the Dive 1 transect, where most of the white corals' colonies were observed (Fig. 17). As expected, due to the good fitting observed in the models, predictions were quite reasonable and precise in terms of the location along the transect. Thus, in this case, any of the model formulation tested would be a good choice for habitat suitability models and predictions. However, the range of the predicted value might differ considerably depending on the model selection. While independent presence/absence and abundance models returned predictions closer to real values, the model formulations that combine these two data within same model (zero-inflated and hurdle models) provided lower abundances since they are 'weighted' by the probability of presence. However, when combing independent presence/absence and abundance models by multiplying their predictions (also known as Delta model approach), we found similar results as in previous models (results not shown).

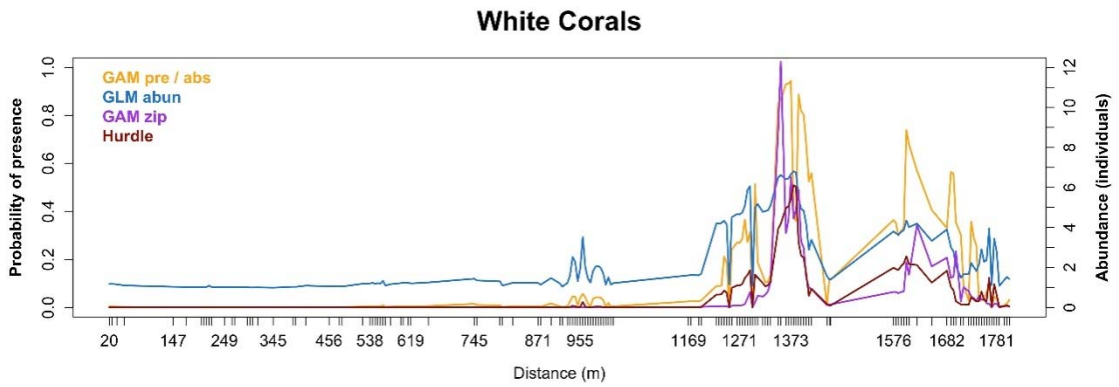

Figure 17. *Comparison of the predictions of the 4 tested models along the Dive 1 transect for white corals (*Lophelia pertusa *and* Madrepora oculata*).*

Acanthogorgia-*like and* Porifera *morphotypes*

For these morphotypes, none of the model formulations resulted in good fits. In general, models selected a large number of significant variables but explained very low variability (< 30 %), indicating that none of the available environmental factors were goods predictor for these morphotypes.

The clearest results were found for the presence of *Acanthogorgia*-like morphotype (Fig. 18), where multiple environmental factors can be responsible for its occurrence. It seems that when detritic substrates dominate the occurrence of *Acanthogorgia*-like morphotype decreases. Regarding temperature, even if the recorded range across the transects is very small (12.8 to 13.5ºC), similarly as it was the case for the white corals, it appear that between 13.2-13.3 ºC the occurrence of the species experience a change, being *Acanthogorgia*-like more frequent when the temperature is higher, this is an opposite result to the trend observed by the white corals. Species occurrence decrease in the deepest depth range (ca 440-480 m), this led us to speculate about a possible link of this species to the NACW masses more than to the MOW. However, with the current data there is not a clear explanation for this trend, as the *Acanthogorgia*-like category include most probably different species with potential different features regarding thermal tolerance and depth range distribution. Moreover, to our knowledge nothing is known regarding the biology of the species belonging to this genus, hampering any correct interpretation of these results.

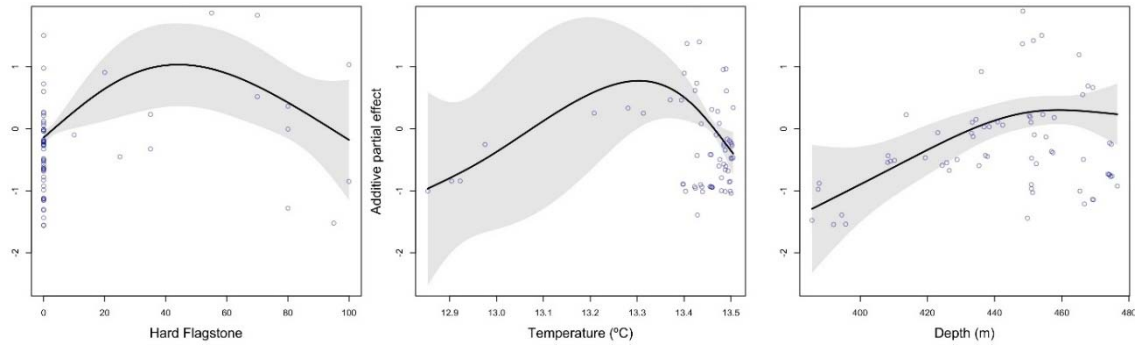

Figure 18. *GAM outputs for* Acanthogorgia*-like in Gazul mud volcano displaying partial effects of the significant environmental variables for presence/absence data.*

The model also displays a higher occurrence of the *Acanthogorgia*-like morphotype at higher concentrations of DO, but again the variation range for Oxygen CC values is very narrow and the absence of information on the biology of this species make it difficult to interpret the observed trend. Forthcoming ATLAS results on biogeography will contribute to enlarge our knowledge on the biogeography of the species allowing identifying the degree of Mediterranean-Atlantic distribution for the species and hence contributing to better interpret the results obtained here. For instance, *Acanthogorgia hirsuta*, which is most probably included in the *Acanthogorgia*-like category here analysed, present a Mediterranean-Atlantic distribution and seems to be (at least in the Mediterranean) a more common species than *Acanthogorgia armata*. *A. hirsuta* bathymetric range has been documented as from 70 to 470 meters and it is frequent in the Mediterranean as well as in the Atlantic (see Otero et al. 2017 and references therein, IUCN Mediterranean Red list). *Acanathogorgia armata* is a more Atlantic species which occur in the Mediterranean only in the Alborán Sea (Otero et al. 2017 and references therein, IUCN Mediterranean Red list); The upper depth limit in the Mediterranean has been documented at 150 m, whereas in the Atlantic it is found deeper than 200 meters and it has been registered below 2,000 m (Bachman et al. 2012). *Acanthogorgia armata* has been found together with crinoids' assemblages of *Leptometra celtica* (Fonseca et al. 2013), in this study the co-occurrence of *Acanthogorgia* spp. with crinoids has been also documented.

Actinauge richardi *and* Flabellum chunii

For *A. richardi* and *Flabellum chunii* the main factor explaining presence was substrate, being *A. richardi* dominant in sandy substrates and *Flabellum chunii* in substrates with high percentage of detritic. The abundance of both taxa seemed to be related to temperature, but as aforementioned, the model fits in these cases were quite poor to extract any reasonably conclusions. Sand and detritic

substrate were highly and negatively correlated (Pearsons correlation = -0.083, $p<0.01$), and thus, these taxa describe an opposite probability of presence depending on the substrate type selected (Fig. 19). For *F. chunii*, the GLM captured a significant signature of the effect of oxygen (dissolved oxygen, DO) concentration (Fig. 19) Thus, the probability of presence in the detritic substrate increases with higher values of DO concentrations (figure shows predictions for minimum and maximum values of DO recorded).

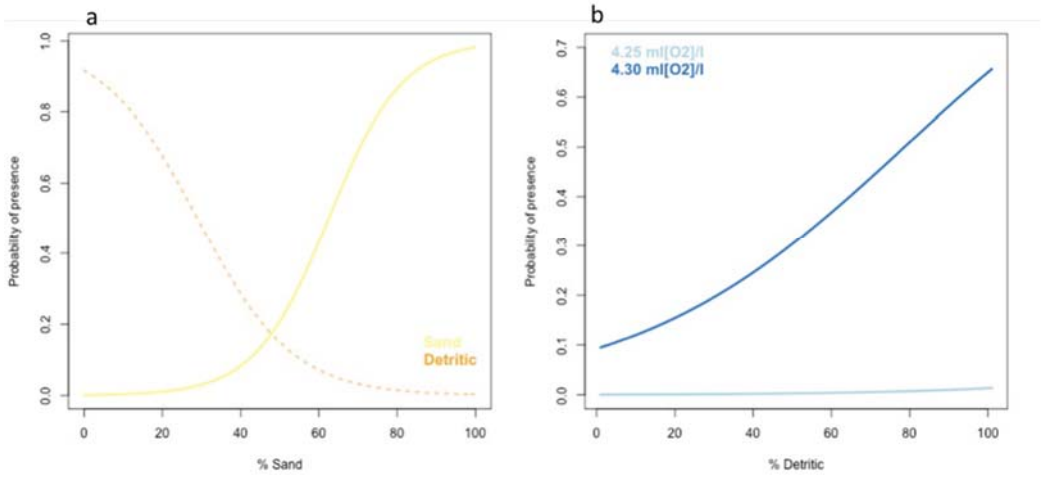

Figure 19. *a) Probability of presence of* Actinauge richardi *in Gazul Mud Volcano depending on the substrate type; b) Probability of presence of* Flabellum chunii *in Gazul Mud Volcano depending on the DO.*

Actinauge richardi is a species widely distributed in the north-east Atlantic Ocean (from Norway to the Bay of Biscay) and the Mediterranean Sea. In the Mediterranean, it is only known to occur around the Western basin, the Alborán Sea, the western Ionian Sea and Eastern Aegean Sea (see Otero et al. 2017 and references therein, IUCN Mediterranean Red list). The species has been detected in Gazul in the deepest range of the explored area (ca 480-460 m depth), in the Atlantic greater abundance have been detected for the species below 730 meters depth (see Otero et al. 2017 and references therein, IUCN Mediterranean Red list), whereas in the Mediterranean the species have been mostly recorded at 150-450m depth (see Otero et al. 2017 and references therein, UICN Mediterranean Red list). As the investigated depth range is narrow, with the current level of information any pattern can be explain for the species in relation to the bathymetric range or other factor except the substrate which clearly define the occurrence of the species. Regarding *Flabellum chunii* with the current available information, the obtained results cannot be discussed on the light of the current literature as the species have not been yet determined. We expect to have a better

taxonomical description of the organisms detected in the video records in order to better interpret the results.

Formigas Seamount

Formigas Islets are part of a promontory named Formigas Bank (Abdel-Monem et al. 1975). This promontory is located next to the junction of East Atlantic Fracture Zone (EAFZ) and Terceira Rift (Tempera et al. 2013). A rift belt that extends from Mid Atlantic Ridge (MAR) to EAFZ crossing through Graciosa, Terceira and São Miguel Islands (Machado 1959). Although EAFZ is formally a transform fault close to the MAR, is defined as a dextral strike-slip fault system at the eastern side of Sta. Maria Island. On the contrary, Terceira Rift is dominated by tensional and/or transtensional forces depending on the authors (Madeira and Ribeiro 1990), (Fig. 20). Digital Elevation Model (DEM) evidence this high tectonic activity in the area with two main fracture directions NNE to SWS (more perceptible in the eastern and southeastern sectors), and a WNW to ESE direction predominating in the Northern sector. On the western sector an 1,800 m depth flat abyssal plain extends. No remarkable morphological features are present at this side of the bank but a few incipient gullies on its flank. At the northeastern side of the surveyed area at least twenty knolls are spread on an area of 130 km2. They probably are part of a volcanic field extending to the northeast beyond the limits of the DEM. Formigas was the most intensive surveyed area, with ten ROV dives and more than two thousand square kilometers surveyed (Fig. 21).

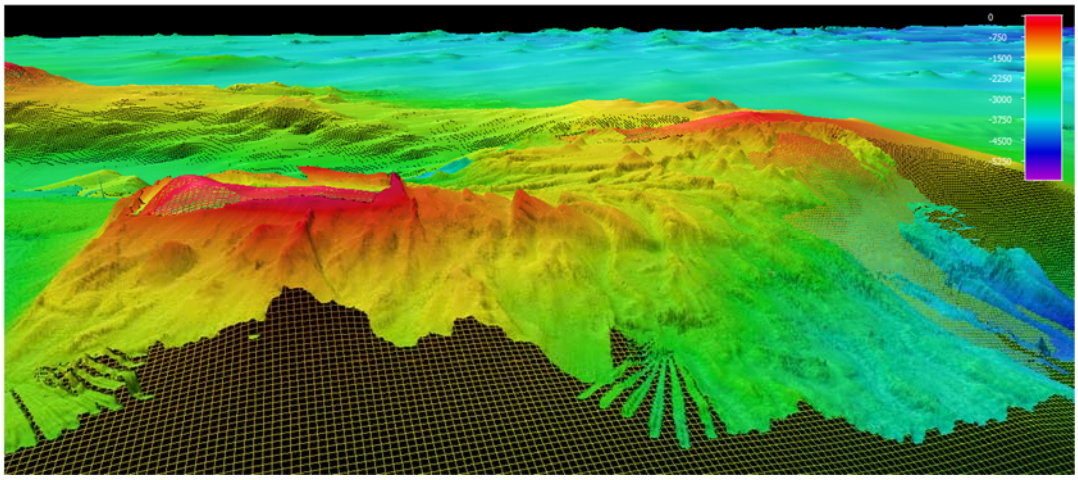

Figure 20. *Swath bathymetry for the Formigas bank acquired during the MEDWAVES cruise.*

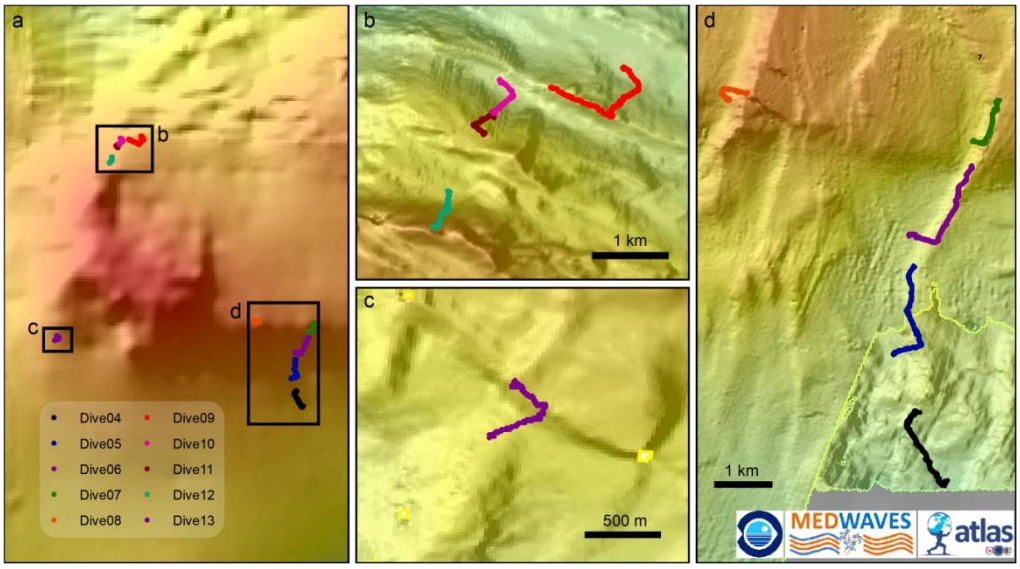

Figure 21. *Location of the ROV video transects conducted in Formigas seamount. a) overview of the location of the transects, b-d) detail on the transect locations in the different flanks of the seamount.*

The sampling design in the Formigas seamount was composed of 5 hydrographic sections perpendicular to the slope and crossing the summit of the seamount (Fig. 22). The Formigas seamount shows the vertical distribution of water masses characteristic of the central subtropical Atlantic. The waters above the seasonal thermocline (Fig. 23), γn < 26.850 kg m-3, are characterized on the θ/S diagram by relative low scattering in the temperature and salinity values, as opposed to other areas where the seasonal heating and evaporation produces large scattering. This is a consequence of the proximity of the Formigas seamount to the center of the subtropical gyre, characterized by subduction and therefore homogeneity at the surface levels. Below the seasonal thermocline and through the permanent thermocline is the NACW, roughly delimited by 26.850 <γn< 27.200 kg m-3. These waters are characterized in the θ/S diagram by an approximately straight-line relationship between potential temperature (11.40ºC<θ<14.03ºC) and salinity (35.60<S<35.85). Below the NACW there is a slight decrease in salinity that indicates the presence of diluted Antarctic Intermediate Waters (AAIW), due to the proximity of the seamount to the MAR. Below the AAIW, there is an increase in salinity that corresponds to the influence of the MOW, diluted due to the distance of Formigas seamount to the Strait of Gibraltar (approx. 900 nm). This diluted MOW, between 27.380 <γn < 27.720 kg m-3, has salinity values up to 35.82. Below the MOW, the constant increase in salinity and temperature indicates the presence of upper North Atlantic Deep Waters (uNADW). The vertical distribution of temperature, salinity and γn (Fig. 24) shows the distribution of waters masses (see also Fig. 25). In the top 50 m there is a relatively weak gradient in temperature,

salinity and γn that corresponds to the seasonal thermocline. Between 200 and 400 m, salinity and temperature decrease linearly, a characteristic of the NACW. Below 500 m, salinity decreases slightly, mostly in the western side of the seamount, to reach a relative minimum of 35.56, characteristic of the AAIW, at 600 m. The presence of this diluted Antarctic AAIW is due to the proximity of the seamount to the MAR; this is also coherent as the Formigas seamount blocks the eastern propagation of the AAIW, and the presence of this water mass is mostly observed in the western side of the seamount. Below the AAIW, there is a linear increase in salinity to reach the maximum value of 36.70 at 1000 m, at the core of the MOW. Temperature then decreases linearly with depth, with the core of the MOW with a value of 11ºC. Waters with Mediterranean influence reach 1400 m, as denoted by the 35.58 isohaline and the γn= 27.820 kg m-3 isoline.

The vertical distribution of density and temperature shows the upward doming of the isopycnal, and isotherms, that characterizes the cyclonic circulation on top of seamounts. Mediterranean waters (MOW) present in the area are well mixed with the surrounding NACW, and possibly with the AAIW, with maximum salinity values close to 35.75. This maximum in salinity is slightly lower in the eastern side of the seamount as a consequence of the mixing associated with the topography. This change in the properties of the Mediterranean waters across the seamount was also observed in the mean depth of the core of maximum of salinity, which was shallower in the eastern side of the seamount.

The presence of the MOW has also a signature in the squared Brunt-Väisälä frequency (Fig. 26), with a relative maximum around the core of the MOW and therefore suggests internal wave breaking in the slope of the seamount.

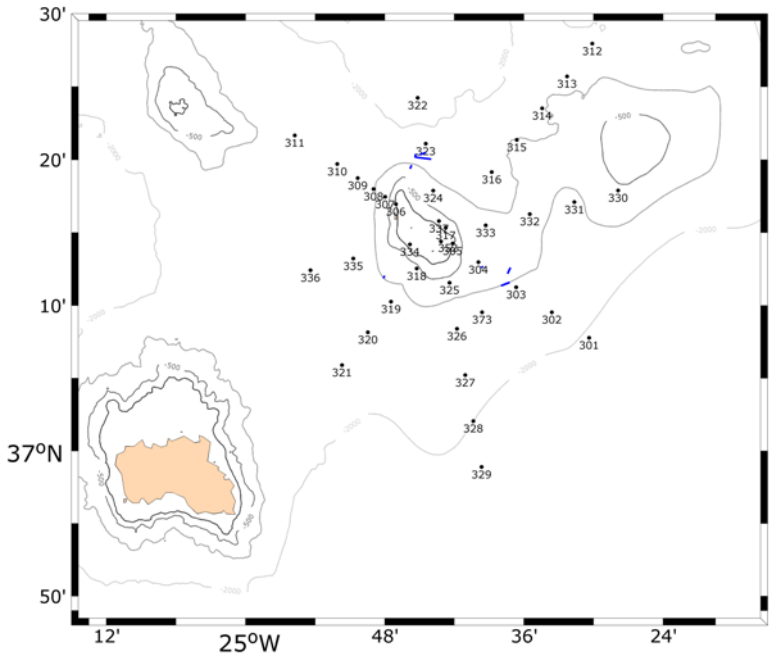

Figure 22. *Distribution of sampling stations in Formigas seamount for the MEDWAVES cruise. Blue lines show the location of the ROV deployments.*

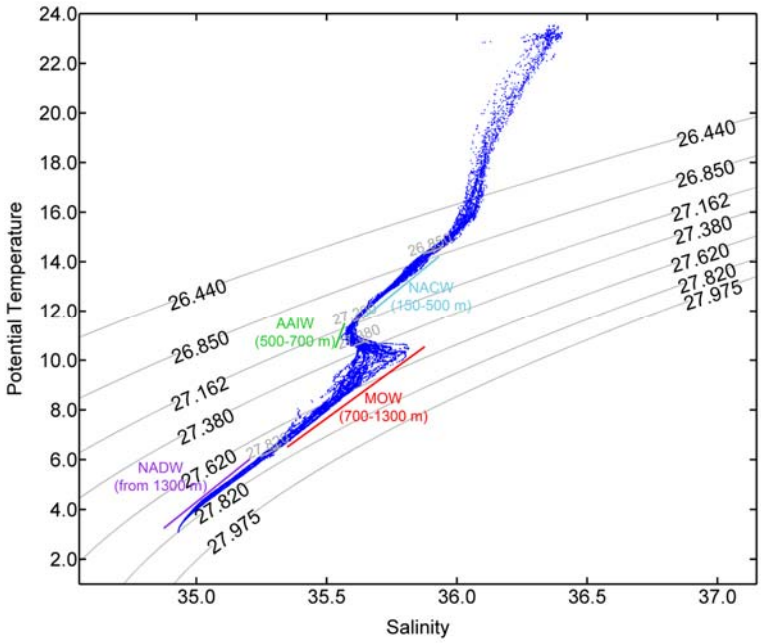

Figure 23. *T/S diagram of all stations sampled in Formigas Seamount. North Atlantic Central Water (NACW) is depicted in light blue, Mediterranean Outflow Water (MOW) in red, North Atlantic Deep water (NADW) in purple and Antarctic Intermediate Waters (AAIW) in green. The depth range where these four water masses were detected is indicated.*

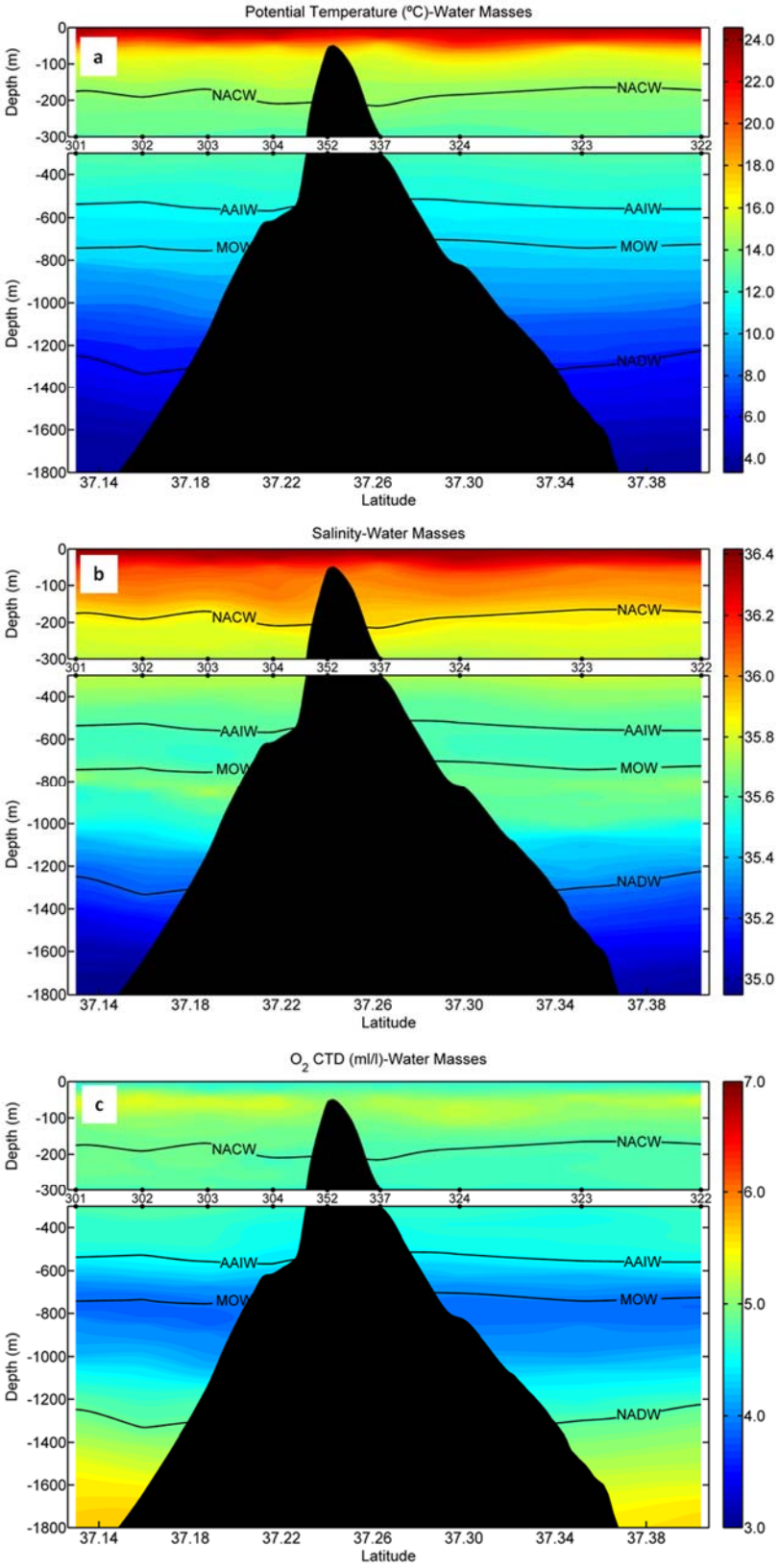

Figure 24. *Vertical section of (a) temperature, (b) salinity and (c) oxygen in the Formigas seamount. NACW: North Atlantic Central Water, MOW: Mediterranean Outflow Water, NADW: North Atlantic Deep water, AAIW: Antarctic Intermediate Waters.*

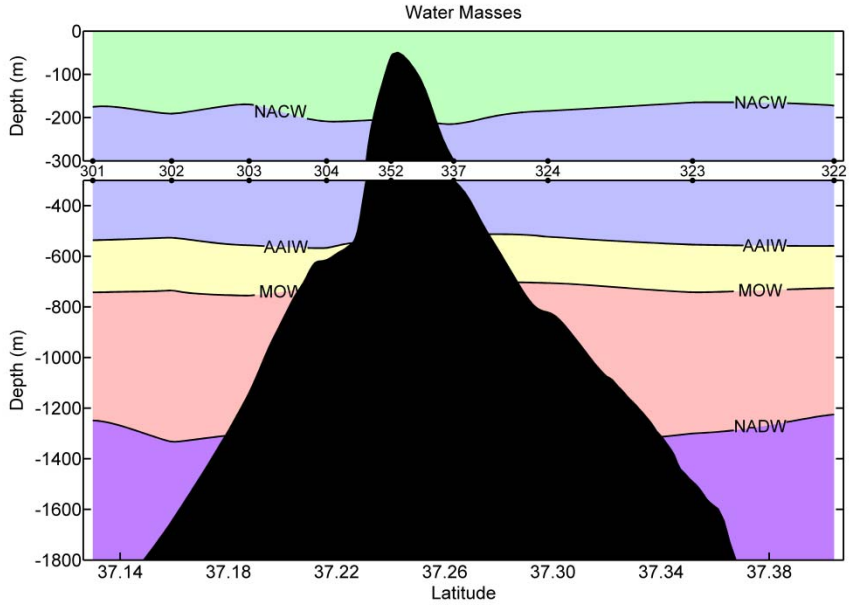

Figure 25. *Water masses detected in Formigas seamount. NACW: from ca. 180 m to ca. 550 m depth; AAIW: from ca. 550 to ca. 780; MOW: from ca. 780 m to 1250-1300 m; NADW: from ca. 1250 m to the bottom of the seamount.*

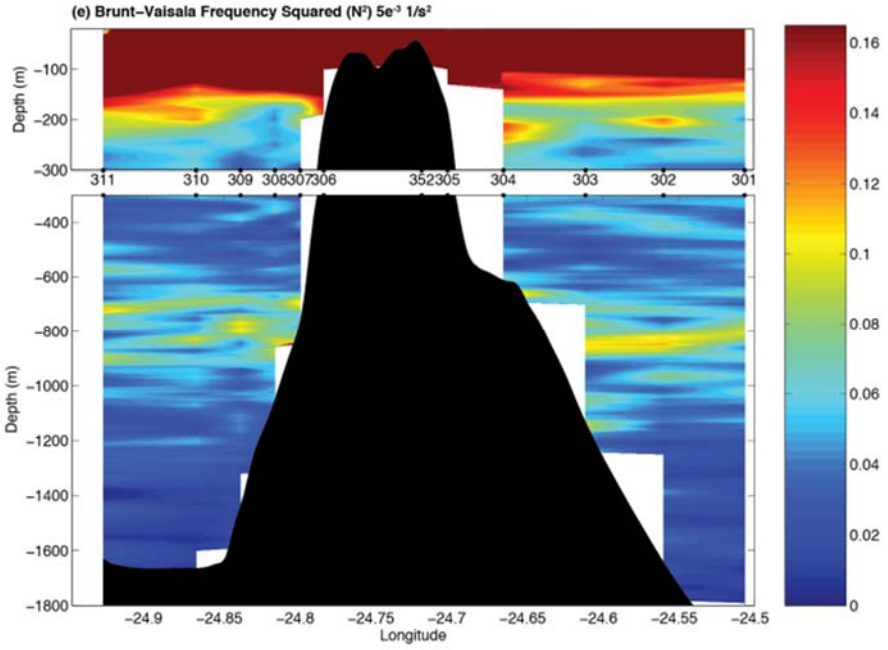

Figure 26. *Brunt-Väisälä Frequency Squared in Formigas seamount.*

Benthic Communities

Ten ROV dives were conducted in Formigas seamount. Here we present the analyses of 8 dives, which covered a depth range between 500-1,575 m water depth. The images analysed show

that Formigas is highly diverse geomorphologically, with a great variety of substrate types and with a high number of species/morphotypes identified, especially if compared to the other areas evaluated (Gazul Mud Volcano and Seco de los Olivos). A brief description of the benthic megafauna observed in the images is provided in the coming paragraphs, starting from the deepest areas and finishing in the shallower ones. Dives 4 to 8 were conducted in the South East (SE) Flank of the seamount, whereas Dives 9 and 10 were conducted in the North West (NW) Flank.

Dive 4 covered a depth range between ca. 1350-1600 m water depth. Substrate was mostly dominated by sand with some patches of rocky outcrops. Sandy areas were characterised by a very scarce presence of benthic megafauna, represented by isolated specimens of the burrowing anemone *Cerianthus* sp. and the bamboo coral *Acanella arbuscula*, together with some gorgonians of the family Plexauridae, such as Swiftia and *Iridogorgia* (family Chrysogorgiidae). The presence of gorgonians as well as some scleractinians (*Desmophyllum dianthus*) and black corals (*Parantipathes* cf. *hirondelle*) seems to be associated with the patchy distribution of some pebbles and rocks along the sand-dominated areas. Areas dominated by rocky substrates (shallower part of the dive, from ca. 1430 to 1340 m depth) presented a highly diverse community dominated by cnidarian species, mostly gorgonians of the family Plexauridae, together with the gorgonians *Radicipes* cf. *gracilis* and *Swiftia pallida*, the bamboo coral *Acanella arbuscula* and other species of cnidarians that appeared scattered along the transect, as for instance the black coral *Antipathes dichotoma*. Some representatives of Porifera species also occurred in this community, the most abundant morphotype being “Encrusting transparent porifera” together with isolated specimens of other species such as cf. *Farrea occa* and the stylasterid *Crypthelia* sp. (see Annex I for a more comprehensive list of the taxa identified).

Dive 5 covered a depth range between ca. 1200-1350 m. Substrate was also dominated by sand, with some patches of detritic material and rocky substrates, especially at the beginning of the transect, in the deepest zones (1350-1250 m depth) and also towards the end, in the shallower areas (ca. 1180 m depth). Overall, sandy areas were characterised by low densities of benthic megafauna species, although the bamboo coral *Acanella arbuscula* was detected with some high frequencies, together with the sea urchin *Cidaris cidaris* and the anemone *Cerianthus* sp. Some Plexauridae specimens, the black coral *Leiopathes glaberrima* and the scleractinian *Caryophyllia* sp. were also documented in some patches of rocks and soft detritic sediment in areas characterised by sandy substrates. Large rocky outcrops presented a highly diverse community, dominated by a mixture of cnidarian and sponge species. Among the diverse number of cnidarians, a small and white Plexauridae species was characteristic (named “Plexauridae white sp.1” for now since identification

to species level has not been possible yet, although progress is being made). The other most abundant species was the porifera morphotype “Encrusting transparent porifera”, very difficult to be identified into a lower taxonomic level. In lower abundances but also relevant to the community composition, specimens belonging to the gorgonians cf. *Swiftia* sp. and *Chrysogorgia agassizi*, the scleractinian *Caryophyllia* sp., as well as some specimens of other Plexauridae (“Plexauridae purple sp. 1”) or *Iridigorgia* cf *pourtalesii*. Large colonies of the black coral *Leiopathes glaberrima* were also observed, although in low numbers (Annex I).

Dive 6 covered a depth range between ca. 920-1260 m water depth. Substrate along this dive varied between patches of outcropping rocks, areas dominated by sand and areas with a mixture of soft detritic, rocks and pebbles. Sandy areas were characterised by patches of *Acanella arbuscula* and Porifera species belonging to different morphotypes, with the small “Porifera digitate sp. 1” the most abundant in terms of number of individuals. Sponges were the more frequent and abundant group in areas where some patches of rocky substrates occurred within the sandy areas. Beside these two dominant taxa, several other species belonging to Cnidaria and Porifera also were observed in lower abundances.

Some areas of this transect were characterized by a mixture of sediments, with hard and soft substrates equally present. In this situation, a high abundance of the pedunculate sponge *Stylocordila pellita* was recorded, in a depth range from ca 1180 to ca 1130 m. This species was accompanied by other Porifera morphotypes, mostly digitate morphotypes, as well as some cnidarians such as *Acanella arbuscula*.

At depths between ca. 1070 to 920 m, areas dominated by hard substrates presented a diverse community, as already observed in the other transects, with a mixed dominance between Porifera and Cnidaria. The dominant species were the sponge cf. *Farrea occa* and the gorgonian *Candidella imbricata*. Other abundant organisms growing over the rocks were Plexauridae White sp. 1, the gorgonian *Narella versluysi*, the black coral *Leiopathes glaberrima* and the sponges “Porifera digitate sp. 2” and cf. *Polymastia* sp.1. Many other species occurred in the rocky outcrops in lower abundances, providing an idea of the high diversity that this habiats sustains (see Annex I).

Dive 7 covered a depth range between ca. 750-1000 m water depth. Substrate along this dive was dominated by hard flagstone and rocks with some patches of mud, sand and soft detritic materials. Hard substrate areas displayed a mixed community of cnidarians and poriferans, with a dominance of different species along the transect. In some areas *Narella verluysi* dominated together with the morphotypes “Porifera digitate sp.1” and “Porifera encrusting transparent”. In others,

Narella bellisima dominated together with the morphotype "Porifera encrusting transparent". The gorgonian cf. *Acanthogorgia armata* was also present, but with lower abundances than the morphotypes previously mentioned. Variations in depth across the transect as well as across substrates did not produced significant changes in species composition.

Dive 8 covered a depth range from ca. 400 -740 m water depth. Hard substrates (mostly rocks and pebbles) were the most common, with some patches of soft detritic materials. In the deepest part, *Narella verluysi* was dominant, forming areas of great densities, with *Narella bellissima* taking over in some other. The shallower parts of the transect (560 to 478 m depth) were characterized by large rocks, with high abundances of different morphotypes of Porifera, together with some dense patches of the gorgonian "Plexauridae White sp. 1". The occurrence of specimens belonging to the family Nidaliidae was also reported. Some specimens of gorgonian *Corallium tricolor* also occurred in the shallower areas together with some black corals of the genera *Stichopathes*. Transects 9 and 10 were conducted in the NW flank of Formigas bank. The megabenthic fauna encountered in these two dives is shortly described in the following paragraphs, starting from the deepest areas.

Dive 9 covered a depth range between ca. 1200-1420 m water depth. High densities of megafauna species were always associated to the presence of hard substrates. In the deepest areas of the transect (ca. 1370 m), the morphotype "Encrusting porifera" was the most abundant, followed by the corals *Acanella arbuscula* and *Lophelia pertusa*. Interestingly, from all analysed transects, *L. pertusa* was only recorded in Dive 9. In the shallower parts of this dive (around 1200 m water depth), the number of Porifera decreased and the most abundant species where *L. pertusa*, as well as the white gorgonian "Plexauridae white sp. 1", followed by *Chrysogorgia agassizi*, *Madrepora oculata* and *Leiopathes glaberrima*. Other species and morphotypes occurred in much lower abundances (see Annex 1). In the areas dominated by soft bottoms (sand), Anemone sp. 3 and *Cerianthus* sp. 1 occurred with relatively high frequencies, but always with low abundances.

Dive 10 covered a depth range between 1170-1330 m depth. Overall, the occurrence of megabenthic organisms was very low. The deepest part of the transect was dominated by soft substrates, where Anemone sp. 3, *Cerianthus* sp. 1 and *Acanella arbuscular* were registered. The shallower areas (1270-1170 m depth) displayed hard substrates colonised by encrusting Porifera with almost no other benthic organisms (see Annex 1).

Figure 27 displays some of the benthic habitats documented in Formigas seamount.

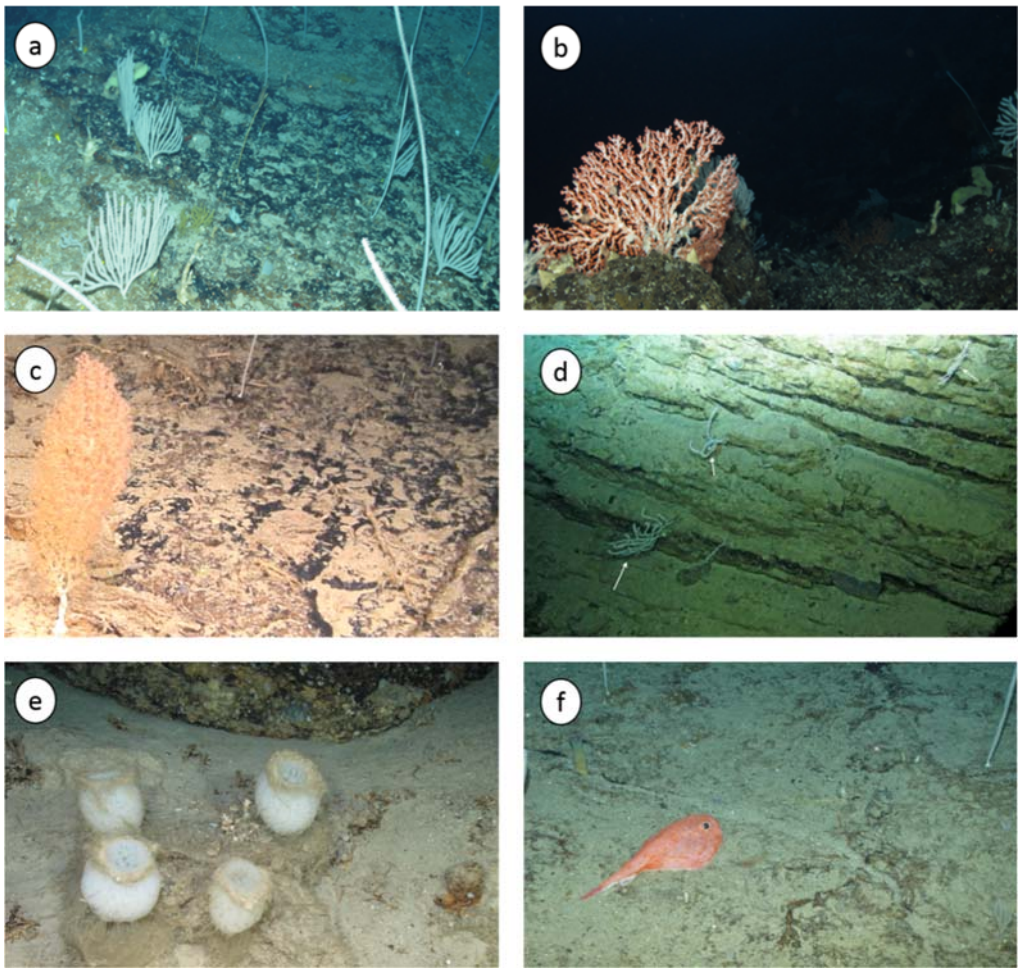

Figure 27. *Some of the benthic habitats of Formigas seamount. a) coral garden dominated* by Narella bellissima *(740-780 m depth), b) specimen of* Corallium tricolor *at ca. 1230 m depth, c) specimen of the bamboo coral* Acanella arbuscula *at ca. 1300 m depth, d) specimens of the "Pleaxauridae white species 1" in a vertical rocky wall at ca. 1400 m depth, e)* Pheronema carpentieri *in a mixed substrate od sand and rocks at ca.1200 m depth, f) specimen of* Chaunax *sp. at ca. 900 m depth.*

Effects of environmental factors on benthic communities at Formigas

A non-metric MDS was performed using data from all 7 dives analysed in Formigas. The resulting bidimensional ordination is displayed in Fig. 28. The model did not converge, but the aforementioned assumptions for a good fit were all met. In the case of Formigas, the ROV footage was more abundant and covered a wider area than in the previous study areas and should provide a more complex view of the benthic environment. Indeed, dives performed in Formigas were carried out along a great depth range and going through different water masses across the water column, which provided invaluable information to understand the influence of water characteristics on the composition of deep benthic assemblages. To visualize differences in community structure each

sample (i.e. every still image) was colour coded according to the water mass where it was found. All significant environmental variables were fitted as vectors over the ordination. Both substrate type and water mass properties seemed to be important in defining the composition of the benthic communities in Formigas bank.

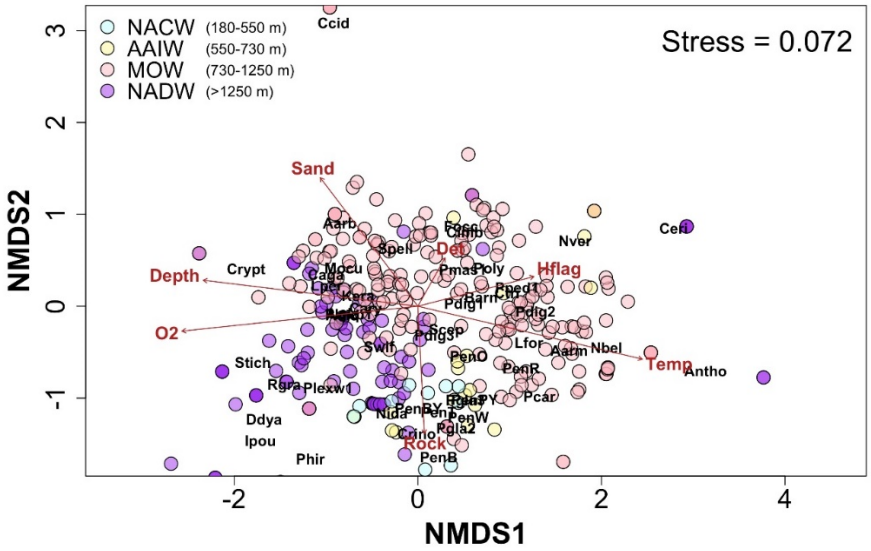

Figure 28. *nMDS performed on Formigas data with the significant environmental factors fitted. NACW: North Atlantic Central Water, AAIW: Antarctic Intermediate Water, MOW: Mediterranean Outflow Water and NADW: North Atlantic Deep Water. (Abbreviations for species and morphotypes are included in the species lists compiled for each dive in the Annex 1)*

Fauna occurring in areas under the influence of the MOW and the NADW appeared separated in the nMDS plot. To better understand the influence of water masses in the composition of the benthic community, ordination analyses were performed independently for data collected in the South East and the North West flank.

The NW flank of Formigas includes Dive 9 corresponding to areas under the influence of the NADW and Dive 10 under the NADW/MOW boundary. The SE side of the Formigas seamount encompasses Dives 4-5 which corresponded to areas under the influence of the NADW, Dives 6-7 mainly influenced by the MOW and dive 8 in the mixed zone MOW and NACW/AAIW. To disentangle the strong influence of substrate type, the analyses were also carried out separately for “hard” and “soft” substrates, within the SE flank. Hard substrates included those where pebbles, rocks or hard flagstone occupied more than 40 % of the image, whereas soft sediments included at least 50% of sands. An nMDS for all substrates together is not display as no differences were detected compared to the nMDS perform for all dives conducted in Formigas analysed together.

The two dives conducted in the NW flank were also analysed using a metric MDS due to the low sample size. These data only covered depths below 1170 m. In this case, the variance explained in the first two axes was slightly higher (39%). The fitted environmental vectors showed a strong linear gradient in temperature and salinity, with most of the species preferring intermediate values. The deeper dive (Dive 9) was carried out in an area under the influence of the NADW and the shallower one (Dive 10) in an area under the mixed influence of NADW-MOW boundary; the mixture of water masses and the low number of usable images limited the possibility of finding a clear trend associated to the characteristics of the water masses s (Fig. 29).

The nMDS performed on data located in the SE flank using samples of hard substrates is shown in Fig. 30. The model did not converge, but the aforementioned assumptions for a good fit were all met. Dismissing the effect of the substrate type, the environmental variables fitted to the nMDS showed that temperature and salinity were mainly associated with communities under the MOW influence, which also presented the lowest oxygen values. Higher depths, which have higher oxygen values as well as lower temperatures and salinities, are associated with the communities under the NADW influence whereas intermediate values of oxygen, salinity and temperature are related with communities under the mixed influence of the AAIW and NACW. The analysis of SE flank data only using samples on soft sediments was performed using a metric MDS, which explained 34% of the variance in community composition in the first two axes (Fig. 31). In this case, no data was recorded above the MOW bathymetric range, and the high dispersion of the data prevents from identifying clear trends related to the water mass properties (Fig. 31).

The deep benthic communities of Formigas are dominated by 1) coral gardens, 2) sponge fields and 3) mixed communities of gorgonians and sponges. Beside the fundamental role played by substrate type in defining the benthic communities, the first results of the video analyses reveal a potential effect of the water masses in species composition, mostly referring to the areas under the influence of the NADW and the MOW. Previous studies already highlighted that the distribution of deep-water octocorals depends on the adequacy of the habitat, which is based on several determinant environmental factors including substrate, temperature, salinity, slope, oxygen levels, and productivity, among others (Bryan and Metaxas 2006, 2007, Yesson et al. 2012). Other works also revealed that depth-related factors, including water masses (Arantes et al. 2009 and references therein, Radice et al. 2016), substrate (Messing et al. 1990) seafloor characteristics (Edinger et al. 2011, Baker et al. 2012), and other environmental factors (Quattrini et al. 2013, Doughty et al. 2014), play a role in controlling the global and local distribution of octocorals.

In Formigas, the areas under the influence of the NADW (from ca. 1200 to ca. 1600 m depth) seem to be characterized by a mixed community of sponges and corals, where a species of Plexauridae was dominant in terms of number of individuals and frequency of appearance. This species was called “Plexauridae White sp. 1”, but it possibly relates to a species of the genus *Muriceides*. Biodiversity values seem to be lower in areas under influence of the NADW (see Table 2), although these results are still preliminary and should be considered with caution. In this sense, the taxonomical identifications are still ongoing and will require further work. The abundance of this Plexauridae species decreased when the area of influence of the MOW started to occur, at around 1100-meter depth. At these depths, a mixed community of sponges (with a high diversity of species) and gorgonians was dominant. The most frequent gorgonians were two species of the genus *Narella*: *Narella bellissima* and *Narella verluysi*. These two species have been historically been reported in the North Atlantic, both having amphi-Atlantic distributions (Cairns and Bayer 2008) with depth ranges from 225 to 1968 m for *N. bellissima*, and from 550 to 3100 m water depth for *N. verluysi* (Cairns and Bayer 2008). Despite the growing knowledge of their distributional ranges (spatial and bathymetrical) and habitat preferences (Braga-Henriques et al. 2011, 2013, van den Beld et al. 2017, Sampaio et al. 2019), baseline information (e.g. dispersal strategy, reproductive mode and population genetics) is still lacking for those species (but see the recently published work by Yesson et al. 2018). *Narella versluysi* is found across the central North Atlantic including observations from Bermuda, Straits of Florida, Azores, W Ireland, and Bay of Biscay at depths of 550–3100 m (Cairns and Bayer 2003). The species occur associated with *Lophelia / Madrepora* reefs and mixed coral habitats in Bay of Biscay (van den Beld et al. 2017) and is a commonly found in mixed coral gardens in the Azores (Tempera et al. 2013). It is reported in the Bay of Biscay at depths of 678–1734 m, where it is the most abundant gorgonian coral (van den Beld et al. 2017). The northern most records of *Narella bellissima* have been documented for the Gulf of Biscay and the species has been cited in Antilles and Bahamas for the West Atlantic (Cairns and Bayer 2003). Although in the investigated areas of Formigas that the occurrence of the two species coincides with the MOW, no records of these two species exist in the Mediterranean. The lack of knowledge on the biology and ecology of these two species, and the wide bathymetric range they display in other areas, prevent any clear explanation for this observed distribution pattern. The occurrence of the two *Narella* species in this specific depth range could be linked to many different parameters besides the analysed here. Further environmental parameters will be investigated in the near future (e.g. pH, nutrients, POC among others) to increase our understanding of the observed patterns and to disentangle the occurrence and distribution of the

benthic organisms in the area. The case of POC as a proxy for food supply might be a key parameter to better understand the occurrence and distribution of benthic communities. Biological aspects could also be playing a role, including competition for space with other species, but the lack of information prevents, at that time, any conclusions to be made.

Unfortunately, the currently poor taxonomical identification, especially for poriferans, limit our capacity to extract more conclusions. However, taxonomical advances in the identification of specimens from images is currently ongoing and in the coming months we anticipate a more detailed analyses of the influence of water masses in the composition of benthic communities. This is more so in the case of Formigas, as it is the area where a larger depth range was covered, which should provide information of how the community composition is influenced by four different water masses.

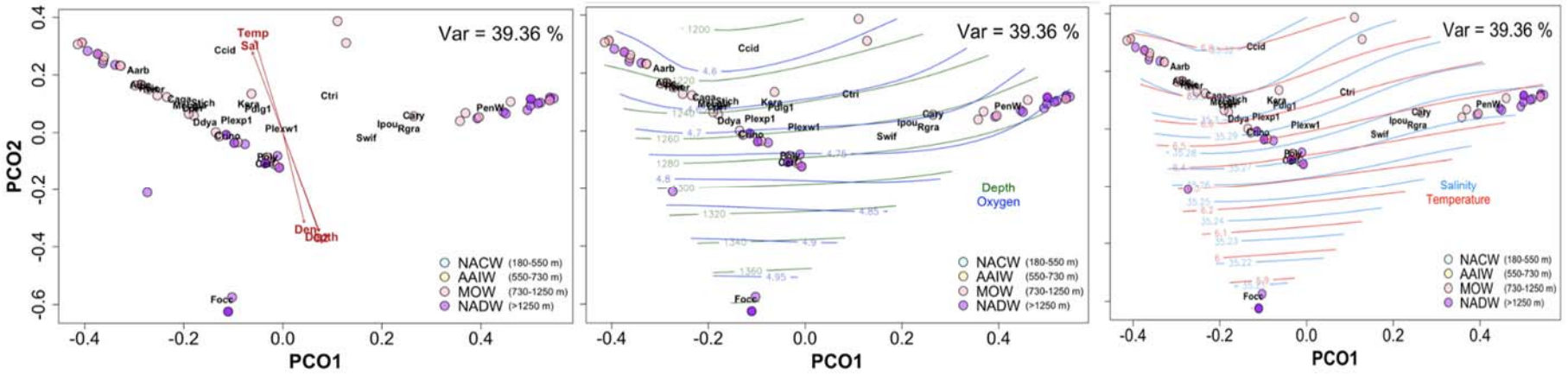

Figure 29. *Multiple MDS plots performed on the data from NW flank of Formigas seamount with significant environmental factors fitted. Vector fitting (left panel) and contour fits of individual variables (middle and right panel) are shown. NACW: North Atlantic Central Water, AAIW: Antarctic Intermediate Water, MOW: Mediterranean Outflow Water and NADW: North Atlantic Deep Water (abbreviations for species and morphotypes are included in the species/morphotype lists compiled for each dive in the Annex 1).*

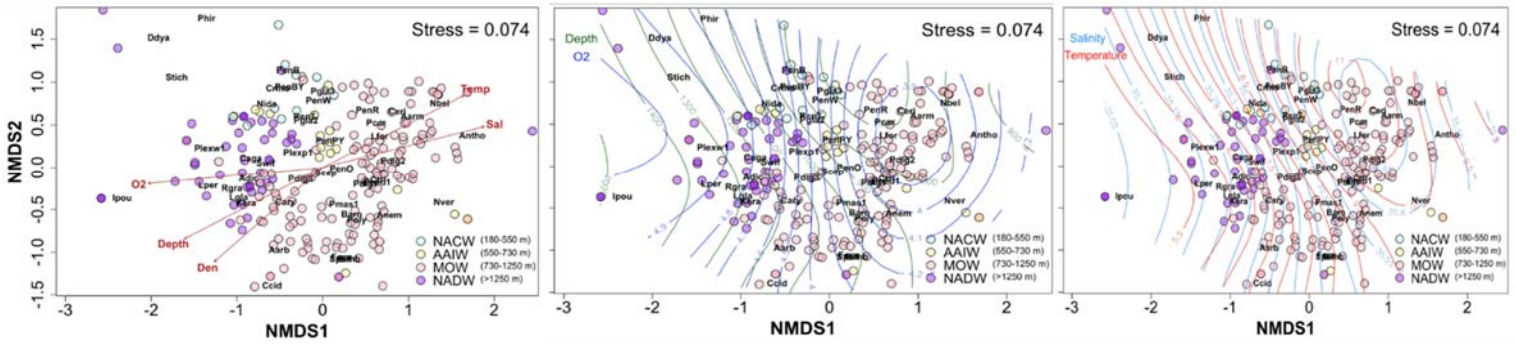

Figure 30. *NMDS performed on the data from SE flank and hard substrate of Formigas seamount with significant environmental factors fitted. Vector fitting (left panel) and contour fits of individual variables (middle and right panel) are shown. NACW: North Atlantic Central Water, AAIW: Antarctic Intermediate Water, MOW: Mediterranean Outflow Water and NADW: North Atlantic Deep Water (abbreviations for species and morphotypes are included in the species/morphotype lists compiled for each dive in the Annex 1).*

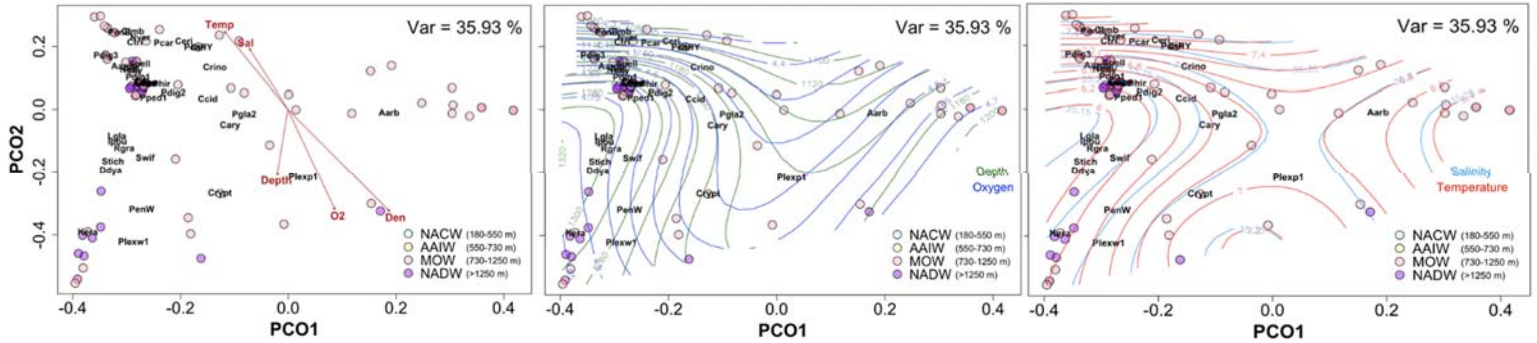

Figure 31. MDS performed on the data from SE flank and soft substrate of Formigas seamount with significant environmental factors fitted. Vector fitting (left panel) and contour fits of individual variables (middle and right panel) are shown. NACW: North Atlantic Central Water, AAIW: Antartic Intermediate Water, MOW: Mediterranean Outflow Water and NADW: North Atlantic Deep Water (abbreviations for species and morphotypes are included in the species/morphotype lists compiled for each dive in the Annex 1).

We explored the potential differences in Formigas biodiversity considering the depth ranges defined by the convergence of the four main water masses: NACW, AAIW, MOW and NADW. The Shannon-Wiener diversity index has been calculated for images gathered within the depth ranges of the different water masses identified in Formigas and including all species found. The analysis has been performed considering a) all images regardless quality, b) all usable images and c) usable images within the selected width range (1.5-2.5 meters; i.e. those used for multivariate and univariate analyses). In all cases the results were similar, being the Shannon-Wiener index higher for the communities under the influence of the MOW, followed by the deeper NADW (Table 2). However, it is worthy to consider these results with caution as the number of analysed images for the different depth ranges varies widely. The value of the index varied considerably depending on the data used. As expected, sample size might remarkably affect the diversity index results, but also pointed out the potential bias of the results when some data are removed for standardization processes. It is however informative the comparison between the index for the images corresponding to the MOW and NADW, since with comparable sample sizes, MOW showed higher diversity regardless the data selected. Further analyses need to be carried out in more detail and considering the different taxonomical groups to better understand the potential influence of water masses in species diversity.

Table 2. *Shannon index calculated for species and for all usable images (independently of the width) and images in width range (1.5-2.5 m) for the depth ranges of the different identified water masses.*

	Categories	**NACW (≤ 550 m)**		**AAIW (550-730 m)**		**MOW (730-1250 m)**		**NADW (> 1250 m)**	
		H	**n**	**H**	**n**	**H**	**n**	**H**	**n**
all images	spp	1,938227	17	2,636329	42	2,808122	1126	2,41468	679
all usable images	spp	1,921207	15	2,636329	42	2,8065	719	2,41468	392
images in width range	spp	1,868128	11	2,555534	19	3,042503	440	2,342036	385

We aimed, as in the previous areas included in this report, to disentangle potential effects of different environmental factors in the benthic fauna of Formigas at species level. From the results of

community composition presented in section 5.3 we select a pool of species establishing according the following criteria: 1) species present in other areas, and 2) species which appear to be related to a specific depth range/water mass also taking into consideration that the number of records would be enough to allow the performance of the analyses (see figures 5.8 to 5.12). Therefore, the species selected for univariate analysis (see mat & met section for model specifications) were: the Scleractinia *Lophelia pertusa*, the gorgonians *Acanthogorgia armata*, *Narella versluysi*, *Narella bellissima* and the bamboo coral *Acanella arbuscula*. It is worth noticing that the results of the analyses revealed that the oceanographic variables are particular highly correlated in Formigas (r^2 >0.9). All, temperature, salinity and density resulted in most cases very good predictors for the species´ presence and abundance, with minimal differences among them. Therefore, in these cases, we have selected the explanatory variable that explain in higher percentage the variability and displayed narrower confidence intervals, since difference in model AIC variables were usually negligible.

Lophelia pertusa

In general, the model results for *L. pertusa* presence/absence and abundance data were in agreement among the different formulations used, besides the type of response (linear-non linear), Fig. 32). However, the low sample size (n=14 presence data) prevent from applied the hurdle model for *L. pertusa*. Dissolved oxygen (DO) seems to be determinant for the occurrence of this species (DO was also a significant variable for the occurrence of the white corals in Gazul Mud Volcano), whereas water density seems to drive its abundance. Despite the high correlation among water variables only density resulted significant in the abundance GAM. However, abundance results should be taken with caution due to the low number of data used in this model. It is worth noticing that all models provided a quite reasonable data fit (~ 50% of the explained variance). The abundance GLM and the zero-inflated model also detected significant effects of water density, temperature and salinity, respectively. In the case of temperature, the range in the explored areas of Formigas is much wider than in the Gazul Mud Volcano and in Seco de los Olivos, covering from ca. 5 to ca 12ºC. However, the effect of temperature detected by the zero inflate model formulation (see section 4.4.2.1) cannot be clearly differentiated for presence or abundance.

Abundances of *L. pertusa* slightly decreased as the temperature increases above 9 ºC. The results from Gazul for the white corals (considering *Lophelia* and *Madrepora* together), reveal a distribution depth range of 400 to 465 m for these two species, being partially under the influence of the MOW (slightly higher temperatures); however the results from Gazul displayed higher

abundances in relatively shallower areas of the transect (420-430 m) close to the depth where both water masses NACW and MOW encounter. In the case of Formigas, it seems that the depth distribution range of *Lophelia pertusa* is associated to the confluence zone of the MOW and the NADW.

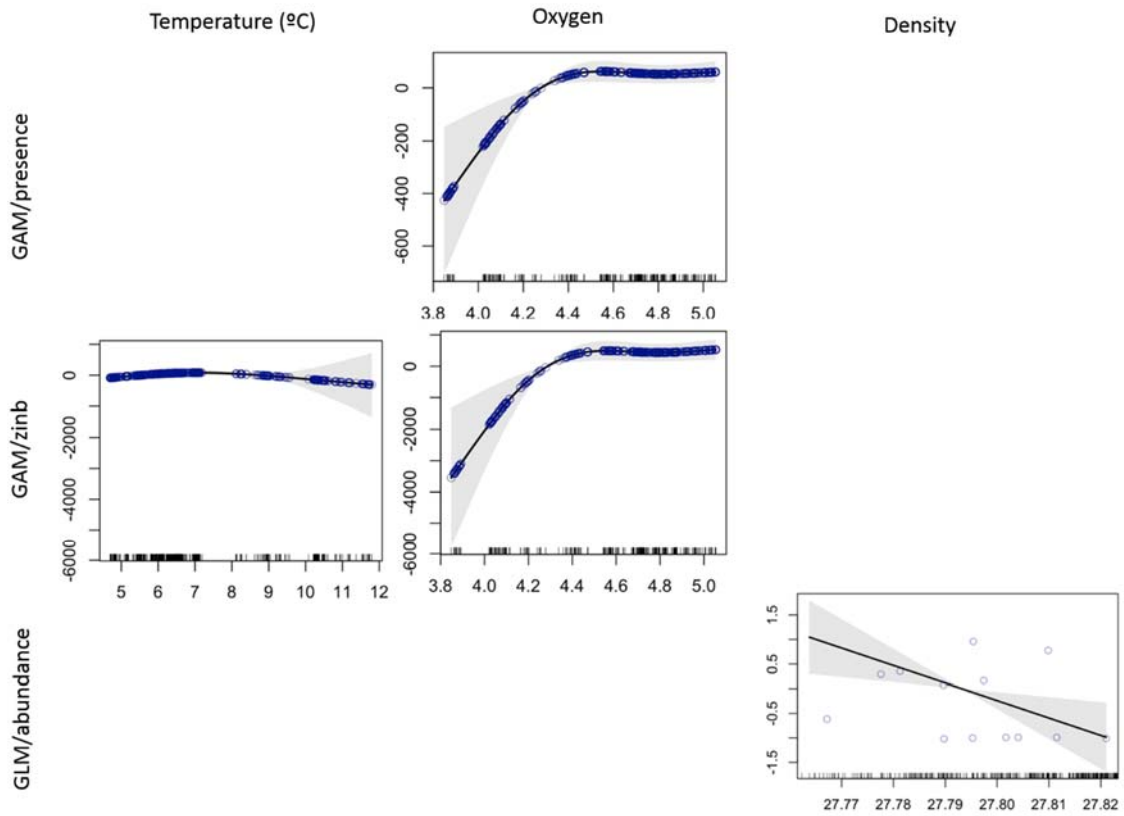

Figure 32. *Models outputs for* Lophelia pertusa *in Formigas seamount. From the upper to the lower part of the image: GAM for presence/absence, zero-inflated GAM and GLM for abundance. From the left to the right the tested variables: oxygen, temperature and density.*

Effects of Oxygen

The outputs of the GAM for presence and zero inflated models show DO as the main factor defining the presence of *L. pertusa*. In general, a threshold point at 4.3 mL L^{-1} can be observed in these model outputs, above which the positive effect of DO disappears, indicating that the presence of *L. pertusa* increases with DO until this threshold to remain then constant. Although this result should be taken with caution due to the low number of data used and a possible entangle effect oxygen-depth, it is worthy to mention that the results obtained in Gazul for the white corals showed similar threshold value. The oxygen concentrations documented in Formigas, as well as in Gazul are above the values documented for other areas where *L. pertusa* is present. Overall DO levels of 4.8–

6.7mL L^{-1} have been recorded for *L. pertusa* occurrences at 100 m depth in the Swedish Kosterfjord (Wisshak et al. 2005), however according to Freiwald (2002), most *L. pertusa* records in the NE Atlantic coincide with zones of relatively low oxygen cc of around 3–5 mL L^{-1}. Indeed, for the NE Atlantic (including the Mediterranean Sea) values of ~3.7 mL L^{-1} have been recorded (Dullo et al. 2008, Freiwald et al. 2009) whereas lower values have been registered in the NW Atlantic (~2 mL L^{-1}; including the Gulf of Mexico, Brooke and Ross 2014, Georgian et al. 2016, Hebbeln et al. 2014) as well as in the SE Atlantic (1.1 ml L^{-1} which are the lower values ever recorded for a *Lophelia* reef, Hebbeln et al. 2016). Consequently, considering the currently available information the *L. pertusa* specimens in Formigas seems to be within the oxygen cc higher ranges natural for the species.

Effects of Water Mass Density

The GLM for abundance found significant effect of density for *L. pertusa*. However, an optimal density range cannot be extracted from the model due to the low number and dispersal of the sample size. As previously mentioned in the Gazul section, forthcoming results on the chemical parameters of the water column will be included in these analyses in the coming months in order to explore other potential factors influencing the occurrence and abundances of *L. pertusa*.

Acanthogorgia armata

This species occurs always associated to hard substrates: rock and hard-flagstone, but none of them contribute to explain the variability observed in the data. The highest contribution to explained variability between locations in all model formulations has been given by salinity (Fig. 33). GAM for presence, the zero-inflated and the hurdle models also detected significant but minor effects of oxygen, and in a less extend of temperature in the latter one. The goodness of fit was reasonable in all models (~60% explained variability), except for the abundance GAM which only accounted for ~20% of the variance.

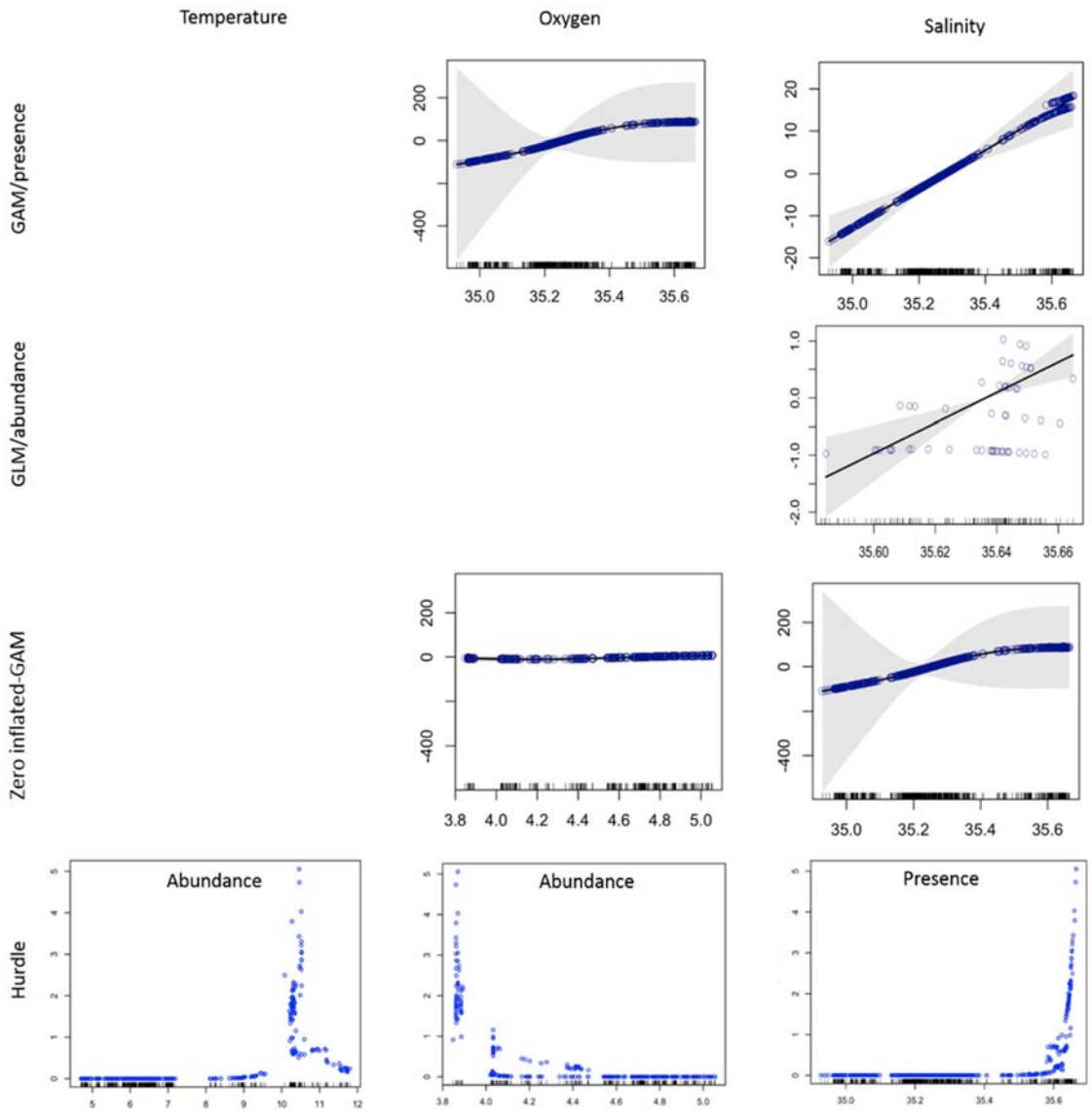

Figure 33. *Models outputs for Acanthogorgia armata in Formigas seamount. Outputs of the 4 models tested are display, from the upper to the lower part of the image: GAM for presence/absence, GLM for abundance, zero-inflated GAM and Hurdle model. From the left to the right the tested variables: temperature, oxygen, and salinity.*

Acanthogorgia armata occur in the explored areas of Formigas only in the SE flank of the seamount in the depth range comprised between 511-937 m water depth. The lack of presence in the NW flank can be explained by the fact that the depth range covered by the ROV transects in the NW flank was deeper. The depth range where the gorgonian species appear corresponds mostly to the influence of the MOW but also of the encounter zone of MOW and NACW; in the case of Gazul, the *Acanthogorgia*-like morphotype display a decrease in presence in the depth range of ca. 440-480 m, being more frequent in shallower areas, however it is important to remind that the taxonomical

identification in the case of Gazul was not clear and several species could be included in this morphotype. The model from Formigas displays a higher occurrence of the *A. armata* at higher concentrations of oxygen, as it was also observed in Gazul, however the variation range for oxygen CC values is very narrow and the absence of information on the biology of this species make it difficult to interpret the observed trend. The increasing presence and abundance linked to higher salinity values is a trend showed by *A. armata* in Formigas but not detected for the *Acanthogorgia*-like morphotype in Gazul, although this could be related to the narrow variation range documented for this parameter in Gazul. A significant effect of temperature has been detected only by the Hurdle model for abundance. The recorded temperature across the transects analysed for *A. armata* in Formigas was remarkable (from ca 5 to ca 12ºC), contrary to the temperature range in the analysed transects of Gazul for the *Acanthogorgia*-like morphotype which was very small (12.8 to 13.5ºC). However, in both cases it appears that *A. armata* and *Acanthogorgia*-like are more abundant and more frequent respectively when temperature reach values of 10 to 12 ºC degrees in Formigas and higher than 12ºC in Gazul.

Forthcoming ATLAS results on biogeography will contribute to enlarge our knowledge on the geographical distribution of the species allowing identifying the degree of Mediterranean-Atlantic distribution and contributing to better interpret the results obtained here. For instance, *Acanthogorgia hirsuta*, which is most probably included in the *Acanthogorgia*-like category here analysed, present a Mediterranean-Atlantic distribution and seems to be (at least in the Mediterranean) a more common species than *Acanthogorgia armata*. *A. hirsuta* bathymetric range has been documented as from 70 to 470 meters and it is frequent in the Mediterranean as well as in the Atlantic (see Otero et al. 2017 and references therein, UICN Mediterranean Red list). *A. armata* is a more Atlantic species which occur in the Mediterranean only in the Alborán Sea (Otero et al. 2017 and references therein, UICN Mediterranean Red list); The upper depth limit in the Mediterranean has been documented at 150 m, whereas in the Atlantic it is found deeper than 200 meters and it has been registered below 2,000 m (Bachman et al. 2012). *Acanthogorgia armata* has been found together with crinoids' assemblages of *Leptometra celtica* (Fonseca et al. 2013) and in Formigas it has also been detected the presence of crinoids with the species, further in this study the co-occurrence of *Acanthogorgia* spp. with crinoids has been also documented in Gazul.

Narella bellissima

The species occurs in a very specific depth range (740-780 meters) and display a clear preference for hard substrates. The results of the model formulations tested (GAM, GLM, zero

inflated and Hurdle) for *N. bellissima* presence/absence and abundance data (Fig. 34) showed a strong effect of salinity. Temperature and density individually also explained a high proportion (70%) of variance, but model inspections reveal salinity presented narrower confidence intervals and higher variability. Thus, salinity itself explained 80% of the variability in the presence of this species, although only 20% of its abundance. The depth range where *N. bellissima* occurs corresponds to the upper limits of the area of influence of the MOW (from ca.730-1250 m depth). The lack of information on the biology of the species prevent to extract any clear conclusions, but it is interesting to mention that *N. bellisima* only occurred, and in high numbers, at salinity values ~35.6. However, it is surprising that a purely Atlantic species, such as *N. bellissima*, occurs under the area of influence of the MOW and in such a narrow bathymetric range. Nevertheless, other factors as competence cannot be disregarded to explain this distribution pattern displayed by this species.

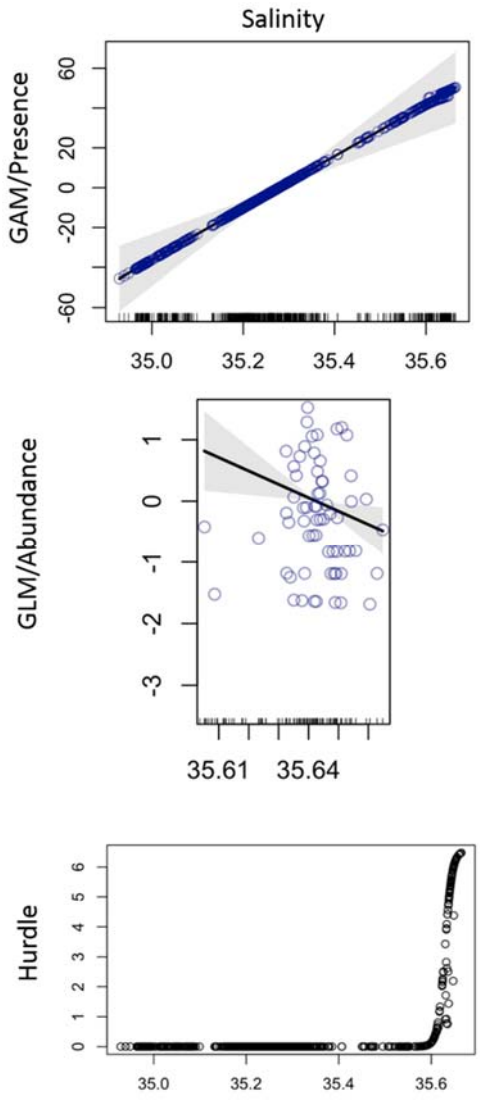

Figure 34. *Models outputs for* Narella bellissima *in Formigas seamount. Outputs of the 3 models tested are display for water density, from the upper to the lower part of the image: GAM for presence/absence, GLM for abundance and Hurdle model.*

Narella versluysi

The species occurs in much wider depth range (1300 meters) than *N. bellissima* but display similar preference for hard substrates. The results of the model formulations tested (GAM, GLM, zero inflated and Hurdle) for *N. versluysi* were similar as those for *N. bellissima*, in terms of all oceanographic variables were individually significant (Fig. 35). However, the best fits were obtained with density or temperature as explanatory variables, depending on the model formulation. Water density explained 60% of the presence variability observed for the species, whereas abundance has been better explained by temperature for both GAM, the zero-inflated and the hurdle models. Significant effects were also detected for

hard substrate variables in most of the models, but with a contribution of less than 10% in the explained variability. A remarkable difference between the results of the two *Narella* species is that *N. versluysi* can grow under a wider temperature and water density ranges, in agreement with the much wider bathymetric range that *N. versluysi* presents in the explored areas of Formigas. The forthcoming in depth analyses of the species occurrence and abundances and the oceanographic factors (physical and chemical) as well as terrain variables will contribute to better understand the distribution patterns that the first video analyses started to reveal.

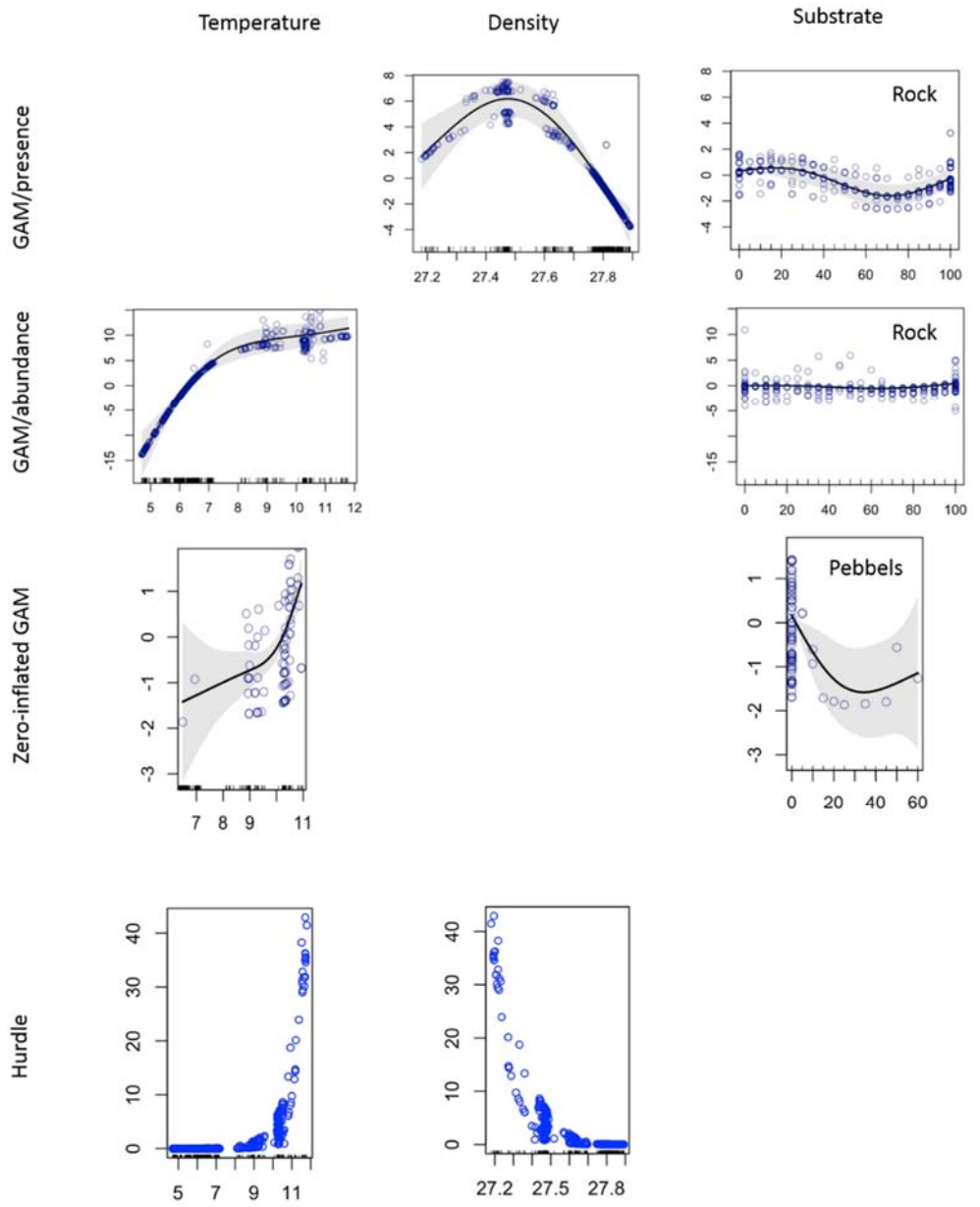

Figure 35. *Models outputs for* Narella verluysi *in Formigas seamount. Outputs of the 4 models tested are display, from the upper to the lower part of the image: GAM for presence/absence, GAM for abundance, zero-inflated GAM and Hurdle model. From the left to the right results are presented for temperature, density and substrate.*

Acanella arbuscula

This is the most ubiquitous of the analysed species. It occurs in all substrate types, covering a depth range of ca. 930 to 1400 meters. Despite the high number of records of *A. arbuscula* the results of the tested models did not offer any clear pattern, due to the opportunistic character of the species. Regarding presence of the species, less than 5% of the variance was explained by substrate type and around 20% by water parameters considered individually. Abundance patterns cannot be explained by substrate and less than 5% of the variability was explained by the water parameters analysed. The zero-inflate model showed the best results with significant effects of water density and depth; this suggests that a bathymetric (900-1100 m) and/or water density range (27.6-27.90) might be preferred by this species. The Hurdle model also captured a similar optimal density range. No graphics have been included for this species due to the los relevance of the results obtained in this analysis.

Effects of environmental factors on the foraminiferal fauna from Alborán Sea to Azores

The results of this study are focused in the foraminifer species *Globorotalia truncatulinoides* (d'Orbigny, 1839), which is a subtropical cosmopolitan species that is abundant in mid latitudes (Be 1977, Kucera 2007). It is likely to be the deepest plankton foraminifera because it has been found alive at depths of about 2000 meters (Schmuker and Schiebel 2002). However, its greatest abundance is between 100 and 300 meters deep (Schiebel and Hemleben 2005). This organism is considered to be one morphospecies consisting of 4 cryptopsecies. Among them, *G. truncatulinoides* type II is exclusive of the Atlantic Ocean and the Mediterranean Sea. It is the only species that has dextral and sinistral forms (Fig. 36); while the other cryptospecies are predominantly sinistral. In the South Atlantic type II is only dextral, nevertheless, in North Atlantic both morphotypes are present (de Vargas et al. 2001).

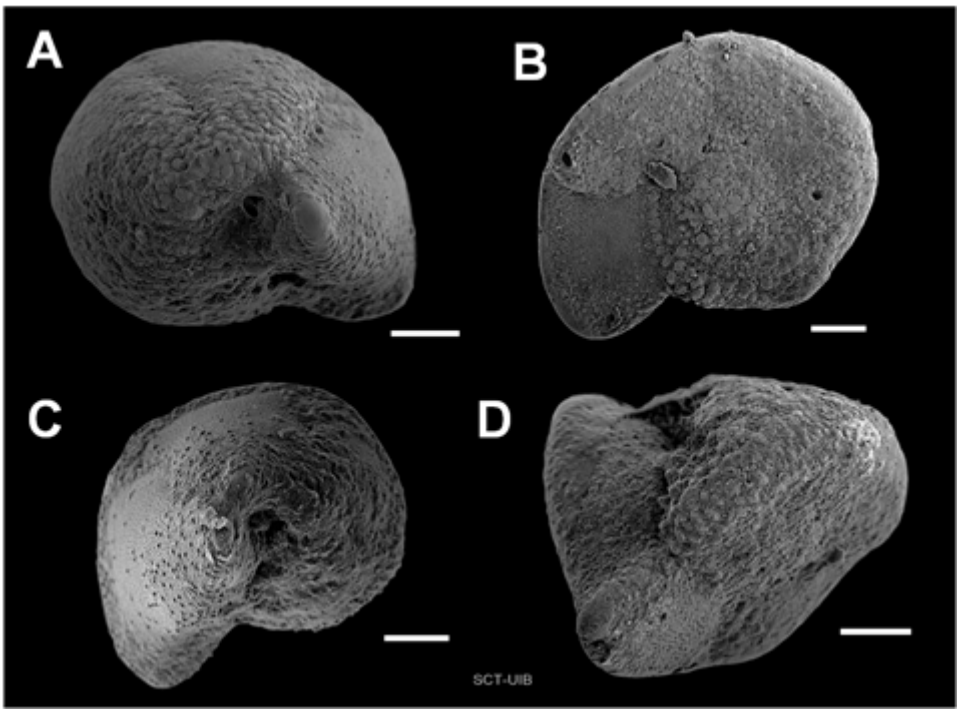

Figure 36. Globorotalia truncatulinoides*. Sinistral form, umbilical zone (A) and hélix (B); dextral form umbilical zone (C) and hélix (D). Scale bar: 100 µm.*

In this area, three regions were differentiated depending on the dominant coiling gyre. Left-coiling gyre dominated the central zone from North Africa to North America and Mediterranean Sea (Thunell 1978). Right-coiling gyre dominated the two other zones. It included the equatorial Atlantic, and extended through the Caribbean, the Gulf of Mexico and back into the Atlantic through the Florida Straits. Moreover, the Northeast quadrant of the North Atlantic is dominated by dextral forms too (Ericson et al. 1955). Furthermore, *G. truncatulinoides* ecology varies depending on the morphotype. For example, sinistral forms dwell at greater depths than dextral forms (Lohmann and Schweitzer 1990). Thus, the sinistral from of *G. truncatulinoides* type II could be exported from the Mediterranean Sea to the North Atlantic being, therefore, an indicator of the MOW.

From Gazul Mud Volcano, three samples collected at depths between 444 and 470 meters were analysed. Two samples presented a similar percentage of each form (dextral and sinistral). On the other hand, one sample has been mostly represented by sinistral forms (90%). This heterogeneity results from the low number of specimens of *G. truncatulinoide*s per sample. A total of 44 individuals have been found in the Gazul seamount. In this region, an equitable proportion of sinistral and dextral forms have been found, slightly biased in favor of left-coiling individuals (57%).

In Ormonde seamount, six samples were obtained. In the shallowest sample (1142 m), located at the west of the seamount, 55% of the 11 of the *G. truncatulinoides* presented sinistral form. On the other hand, the central and the northern parts of the seamount have shown a similar proportion of left-coiling individuals (35 and 38% respectively). Despite the wide depth range (between 1235 to 1936 m deep), no significant differences are detected between both areas. To sum up, Ormonde has presented a total of 105 individuals of *G. Truncatulinoides* and sinistral forms are not dominant in Ormonde (39%).

The Formigas seamount is represented by 13 different samples. The southeastern part corresponds to six samples. A total of 252 individuals have been found, which present mostly dextral forms (only 33% with left-coiling gyre). The northern sector is represented by seven samples that include 186 individuals. There was a slightly higher proportion of sinistral forms (40%) than in the southern sector. On the other hand, percentages of sinistral vs. dextral forms seem to be depth-related. The deepest samples (>1300 meters deep) present a greater proportion of sinistral forms (40%) than the shallow samples (1000- 1300 meters deep) (33%). A total of 438 *G. truncatulinoides* have been found, mostly corresponding to dextral forms (only 36% with left-coiling gyre).

Finally, in the Seco de los Olivos, 11 samples have been collected and analysed. Left-coiling direction clearly dominated 10 of the samples (100% in nine of them and 83% in the other). Only one sample (VV35) has been constituted exclusively of dextral form. However, all samples presented few individuals (between one to six individuals per sample), which makes the comparison quite unreliable. From a general point of view, in Seco de los Olivos left-coiling forms predominate (94%, 31 individuals).

Globorotalia truncatulinoides as a proxy of the MOW

A clear gradient of decrease in the proportion of levorotatory (sinistral) forms of *G. truncatulinoides* was observed from the Strait of Gibraltar to Formigas (Fig. 37). These data reveal that *G. truncatulionoides* with sinistral form is exported from Mediterranean Sea to Northeastern Atlantic. For this reason, *G. truncatulinoides* seems to be a good bioindicador of the MOW in this area.

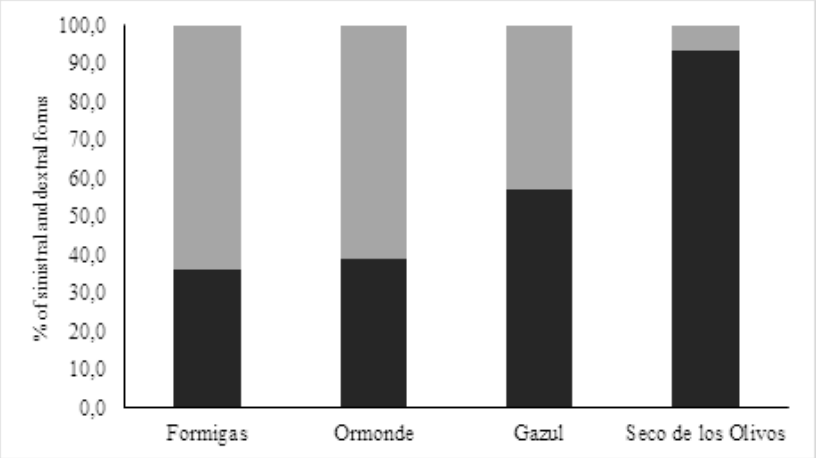

Figure 37. *Percentage of G. truncatulinoides with sinistral (black) and dextral forms (gray) in each geomorphological feature investigated during MEDWAVES.*

Gazul displayed a similar proportion of sinistral and dextral forms (57%), whereas Ormonde was dominated by dextral forms (39% with left-coiling gyre). In this seamount the greatest abundance of sinistral forms has been found on the western side of the seamount, coinciding with the shallowest sample (1142 meters deep). The central and northern parts of Ormonde have presented a similar proportion of left-coiling individuals (35 and 38% respectively). No significant differences have been detected through the depth gradient in these parts (from 1235 to 1936 m). Samples from Formigas were dominated by dextral forms (33% with sinistral forms) as it was the case in Ormonde. In the northern part, the proportion of sinistral forms (40%) was slightly higher than in the Southeast sector (33%). Moreover, the deeper samples (<1300 m) show a higher proportion of left-coiling individuals (40%) than the shallower samples (1000- 1300 meters deep) (33%). Finally, Seco de los Olivos was dominated by sinistral forms (94%).

References

Abad E, Preciado I, Serrano A, Baro J (2007) Demersal and epibenthic assemblages of trawlable grounds in the northern Alboran Sea (western Mediterranean) Sci Mar 71(3): 513-524

Arantes RCM, Castro CB, Pires DO, Seoane JCS (2009) Depth and water mass zonation and species associations of cold-water octocoral and stony coral communities in the southwestern Atlantic. Mar Ecol Progr Ser 397: 71-79

Bachman M, Clifford N, Packer D, Stevenson D, Auster P, Valentine P, Ford K (2012) Essential fish habitats (EFH) omnibus amendment “Deep-sea corals of the north east region: species, habitats and proposed coral zones, and vulnerability of fishing impacts. NewEnglandFisheryManagementCounci, 97 p.

Baker KD, Wareham VE, Snelgrove PVR, Haedrich RL, Fifield DA, Edinger EN, Gilkinson KD (2012) Distributional patterns of deep-sea coral assemblages in three submarine canyons off New found land, Canada. Mar Ecol Prog Ser 445: 235–249. http://dx.doi.org/10.3354/meps09448

Ballesteros M, Rivera J, Muñoz A, Muñoz-Martín A, Acosta J, Carbó A, Uchupi E (2008) Alboran Basin, southern Spain—Part II: Neogene tectonic implications for the orogenic float model. Mar. Pet. Geol. 25, 75–101. doi:10.1016/j.marpetgeo.2007.05.004

Be A (1977) A taxonomic and zoogeographic review of Recent planktonic foraminifera. In: Ramsay, A. T., Ed., Oceanic micropaleontology. London: Academic Press, 2 vols.

Braga-Henriques A, Pereira JN, Tempera F, Porteiro FM, Pham C, Morato T, Santos RS (2011) Cold-water coral communities on Condor Seamount: initial interpretations. In: Giacomello E, Menezes G (eds) CONDOR observatory for long-term study and monitoring of azorean seamount ecosystems. Final Project Report, Arquivos do DOP, Série Estudos 1/2012, Horta, Portugal, pp 105–114

Braga-Henriques A, Porteiro FM, Ribeiro PA, Matos V de, Sampaio Í, Ocaña O, Santos RS (2013) Diversity, distribution and spatial structure of the cold-water coral fauna of the Azores (NE Atlantic). Biogeosciences, 10, 4009–4036

Brooke S, Ross S (2014) First observations of the cold-water coral *Lophelia pertusa* in mid-Atlantic canyons of the USA. Deep Sea Res II 104: 245-251

Bryan TL, Metaxas A (2006) Distribution of deep-water corals along the North American continental margins: relationships with environmental factors. Deep-Sea Research Part I – Oceanographic Research Papers, 53, 1865–1879.

Bryan TL, Metaxas A (2007) Predicting suitable habitat for deep-water gorgonian corals on the Atlantic and Pacific Continental Margins of North America. Mar Ecol Progr Ser 330: 113–126
Cairns SD, Bayer FM (2003) Studies on western Atlantic Octocorallia (Coelenterata: Anthozoa). Part 3: The genus Narella Gray, 1870. Proc Biol Soc Was 116(3):617- 648. 2003

Cairns SD, Bayer FM (2008) A Review of the Octocorallia (Cnidaria: Anthozoa) from Hawai and Adjacent Seamounts: The Genus Narella Gray, 1870. Pacific Science 62 (1): 83–115

Candela J (2001) Mediterranean water and global circulation. International Geophysics. 77:419-XLVIII

De la Torriente A, Serrano A, Fernández-Salas LM, García M, Aguilar R (2018) Identifying epibenthic habitats on the Seco de los Olivos Seamount: species assemblages and environmental characteristics. Deep-Sea Res Part I. doi.org/10.1016/j.dsr.2018.03.015

De Mol B, Henriet J-P, Canals M (2005) Development of coral banks in Porcupine Seabight: do they have Mediterranean ancestors? Cold-Water Corals and Ecosystems: Springer; p. 515-33

de Vargas C, Renaud S, Hilbrecht H, Pawlowski J (2001) Pleistocene adaptive radiation in *Globorotalia truncatulinoides*: genetic, morphologic, and environmental evidence. Paleobiology 27(1): 104-125

Doughty CL, Quattrini AM, Cordes EE (2014) Insights into the population dynamics of the deep-sea coral genus Paramuricea in the Gulf of Mexico. Deep Sea Res. PartII Top. Stud. Oceanogr. 99: 71–82. http://dx.doi.org/10.1016/j. dsr2.2013.05.023

Dullo WC, Flögel S, Rüggeberg A (2008) Cold-water coral growth in relation to the hydrography of the Celtic and Nordic European continental margin. Mar Ecol Progr Ser 371: 165-176

Edinger EN, Sherwood OA, Piper DJW, Wareham VE, Baker KD, Gilkinson KD, Scott DB (2011) Geological features supporting deep-sea coral habitat in Atlantic Canada. Cont Shelf Res 31: S69–S84. http://dx.doi.org/10.1016/j. csr.2010.07.004

Elith J, Leathwick JR (2009) Species Distribution Models: Ecological Explanation and Prediction Across Space and Time. Ann Rev Ecol Evol Syst 40:677–697. DOI: 10.1146/annurev.ecolsys.110308.120159

Ericson DB, Wollin G, Wollin J (1955) Coiling direction of *Globorotalia truncatulinoides* in deep-sea cores. Deep Sea Research 2(2): 152-158

Fonseca P, Abrantes F, Aguilar R, Campos A, Cunha M, Ferreira D, Fonseca TP, Henriques V, Machado M, Mecho A, García S, Relvas P, Rodrigues CF, Salgueiro E, Vieira R, Weetman A, Castro M (2013) A deep-water crinoid *Leptometra celtica* bed off the Portuguese south coast. Marine Biodiversity 44: 223-228 pp.

Freiwald A (2002) Reef-forming cold-water corals. In: Wefer, G, Billett, D, Hebbeln, D, Jorgensen, BB, Schlüter, M, van Weering, TCE (eds.), Ocean Margin Systems. Springer, Berlin, Heidelberg, pp. 365-385.

Freiwald A, Beuck L, Rüggeberg A, Taviani M, Hebbeln D, R/V Meteor Cruise M70-1 participants (2009) The white coral community in the central Mediterranean Sea revealed by ROV surveys. Oceanography 22: 58-74

Georgian SE, DeLeo D, Durkin A, Gomez CE, Kurman M, Lunden JJ, Cordes EE (2016) Oceanographic patterns and carbonate chemistry in the vicinity of cold-water coral reefs in the Gulf of Mexico: Implications for resilience in a changing ocean. Limnol Oceanogr 61: 648-665

Hastie T, Tibshirani R (1990) Generalized additive models. London: Chapman and Hall. DOI: 10.1002/sim.4780110717

Hebbeln D, Wienberg C, Wintersteller P, Freiwald A, Becker M, Beuck L, Dullo C, Eberli GP, Glogowski S, Matos L, Forster N, Reyes-Bonilla H, Taviani M (2014) Environmental forcing of the Campeche cold-water coral province, southern Gulf of Mexico. Biogeosciences 11, 1799-1815

Hebbeln et al. (2016) METEOR-Berichte ANNA. Cold-Water Coral Ecosystems off Angola and Namibia. Cruise No. M122 December 30, 2015 . January 31, 2016. Walvis Bay (Namibia) . Walvis Bay (Namibia), 66 p.

Henry LA, Vad J, Findlay HS, Murillo J, Milligan R, Roberts JM (2014) Environmental variability and biodiversity of megabenthos on the Hebrides Terrace Seamount (Northeast Atlantic). Scientific Reports 4: 5589

Jackman S (2017). pscl: Classes and Methods for R Developed in the Political Science Computational Laboratory. United States Studies Centre, University of Sydney. Sydney, New South Wales, Australia. R package version 1.5.2. https://github.com/atahk/pscl/

Kucer M (2007) Chapter six planktonic foraminifera as tracers of past oceanic environments. Developments in marine geology 1: 213-262

Lacombe H, Richez C (1982) The regime of the Strait of Gibraltar. Elsevier Oceanography Series. 34: 13-73

Loeys T, Moerkerke B, de Smet O, Buysse A (2012) The analysis of zero-inflated count data: Beyond zero-inflated Poisson regression. British Journal of Mathematical and Statistical Psychology 65:163–180. DOI: 10.1111/j.2044-8317.2011.02031.x.

Lohmann GP, Schweitzer PN (1990) *Globorotalia truncatulinoides'* growth and chemistry as probes of the past thermocline: 1. Shell size. Paleoceanography 5(1): 55-75

Lo Iacono C, Gràcia E, Bartolomé R, Coiras E, Dañobeitia JJ, Acosta J (2012) Habitats of the Chella Bank, Eastern Alboran Sea (Western Mediterranean). doi:10.1016/B978-0-12-385140-6.00049-9
Long DJ, BacoAR (2014) Rapid change with depth in megabenthic structure- forming communities of the Makapu'u deep-sea coral bed. Deep Sea Res.Part II Top. Stud. Oceanogr. 99: 158–168. http://dx.doi.org/10.1016/j.dsr2.2013.05.032.

Machado F (1959) Submarine pits of the azores plateau. Bulletin Volcanologique 21 (1): 109–116

Madeira J, Ribeiro A (1990) Geodynamic models for the Azores triple junctiun: a contribution from tectonics. Tectonophysic. 184: 405-41

Marcon Y, Purser A (2017) PAPARA(ZZ)I: An open-source software interface for annotating photographs of the deep-sea. URL/DOI: 10.1016/j.softx.2017.02.002

Messing CG, Neumann CA, Lang JC (1990) Biozonation of deep-water lithoherms and associated hardgrounds in the northeastern Straits of Florida. Palaios 5:15–33

Naumann MS, Orejas C, Ferrier-Pagès C (2014) Species-specific physiological response by the cold-water corals *Lophelia pertusa* and *Madrepora oculata* to variations within their natural temperature range. Deep Sea Research Part II: Topical Studies in Oceanography 99:36-41

Oksanen J, Guillaume Blanchet F, Friendly M, Kindt R, Legendre P, McGlinn D, Minchin PR, O'Hara RB, Simpson GL, Solymos P, Henry M, Stevens H, Szoecs E, Wagner H (2018) vegan: Community Ecology Package. R package version 2.5-2. https://CRAN.R-project.org/package=vegan

Orejas C, Addamo A, Álvarez M, Aparicio A, Alcoverro D, Arnaud-Haond S, et al. (2017) Cruise report MEDWAVES survey. (MEDiterranean out flow WAter and Vulnerable EcosystemS) ATLAS Project H2020. 211 pp and Appendixes

Otero MM, Numa C, Bo M, Orejas C, Garrabou J, Cerrano C, Kružic´ P, Antoniadou C, Aguilar R, Kipson S, Linares C, Terrón-Sigler A, Brossard J, Kersting D, Casado-Amezúa P, García S, Goffredo S, Ocaña O, Caroselli E, Maldonado M, Bavestrello G, Cattaneo-Vietti R, Özalp B (2017) Overview of the conservation status of Mediterranean anthozoans. In: UICN (ed), Málaga, Spain

Paliy O, Shankar V (2016) Application of multivariate statistical techniques in microbial ecology. Molecular Ecology 25:1032–1057. DOI: 10.1111/mec.13536

Palomino D, López-González N, Vázquez JT, Fernández-Salas LM, Rueda JL, Sánchez-Leal R, Diaz-del-Rio V (2016). Multidisciplinary study of mud volcanoes and diapirs and their relationship to seepages and bottom currents in the Gulf of Cádiz continental slope (northeastern sector). Mar Geol 378: 196-212.

Pardo E, Aguilar R, García S, de la Torriente A, Ubero J (2011) Documentación de arrecifes de corales de agua fría en el Mediterráneo occidental (Mar de Alborán). Chron Naturae 1: 20–34.

Patarnello T, Volckaert FAMJ, Castilho R (2007) Pillars of Hercules: is the Atlantic– Mediterranean transition a phylogeographical break? Mol Ecol16: 4426– 4444

Pham CK, Ramirez-Llodra E, Amaro T, Bergmann M, Canals M, Company JB et al. (2014) Marine litter distribution and density in European seas from the shelves to deep basins. PLoS ONE 9(4): e95839. https://doi.org/10.1371/journal.pone.0095839

Potts JM, Elith J (2006) Comparing species abundance models. Ecological Modelling 199:153–163. DOI: 10.1016/j.ecolmodel.2006.05.025

Quattrini AM, Georgian SE, Byrnes L, Stevens A, Falco R, Cordes EE (2013) Niche divergence by deep-sea octocorals in the genus *Callogorgia* across the continental slope of the Gulf of Mexico .Mol. Ecol. 22: 4123–4140. http://dx.doi. org/10.1111/mec.12370.

Quattrini AM, Baums IB, Shank TM, Morrison C, Cordes EE (2015) Testing the depth-differentiation hypothesis in a deep water octocoral. Proc. R. Soc. B Biol. Sci. 282, 20150008. http://dx.doi.org/10.1098/rspb.2015.0008

Radice VZ, Quattrini AM, Wareham VE, Edinger EN, Cordes EE (2016) Vertical water mass structure in the North Atlantic influences the bathymetric distribution of species in the deep-sea coral genus *Paramuricea*. Deep-Sea Research I 116 (2016): 253–263

R Core Team. (2018) R: A language and environment for statistical computing. R Foundation for Statistical Computing, Vienna, Austria. URL https://www.R-project.org/

Rueda, JL, Díaz-del-Río V, Sayago-Gil M, López-González N, Fernández-Salas LM, Vázquez JT (2012) Fluid Venting Through the Seabed in the Gulf of Cadiz (SE Atlantic Ocean, Western Iberian Peninsula):

Geomorphic Features, Habitats, and Associated Fauna. Seafloor Geomorphology as Benthic Habitat. GeoHAB Atlas of Seafloor Geomorphic Features and Benthic Habitats, pp 831-841

Rueda JL, González-García, Krutzky C, López-Rodriguez FJ, Bruque G, López-González N, Palomino D, Sánchez RF, Vázquez JT, Fernández-Salas LM, Díaz-del-Río V (2016). From chemosynthesis-based communities to cold-water corals: Vulnerable deep-sea habitats of the Gulf of Cádiz. Mar Biodiv 46(2): 473-482.

Sampaio Í, Freiwald A, Mora-Porteiro F, Menrzes G, Carreiro-Silva M (2019) Census of Octocorallia (Cnidaria: Anthozoa) of the Azores (NE Atlantic) with a nomenclature update. Zootaxa 4550 (4): 451–498

Schiebel R, Hemleben C (2005) Modern planktic foraminifera. Paläontologische Zeitschrift 79(1): 135-148

Schmuker B, Schiebel R (2002) Planktic foraminifers and hydrography of the eastern and northern Caribbean Sea. Marine Micropaleontology 46(3-4): 387-403

Tempera F, Hipólito A, Madeira J, Vieira S, Campos AS, Mitchell NC (2013) Condor seamount (Azores, NE Atlantic): A morpho-tectonic interpretation. Deep Sea Res. Part II Top. Stud. Oceanogr. 98, 7–23. doi:10.1016/j.dsr2.2013.09.016

Thunell RC (1978) Distribution of recent planktonic foraminifera in surface sediments of the Mediterranean Sea. Marine Micropaleontology 3(2): 147-173

van den Beld IMJ, Bourillet J-F, Arnaud-Haond S, de Chambure L, Davies JS, Guillaumont B, Olu K, Menot L (2017) Cold-water coral habitats in submarine canyons of the Bay of Biscay. Front Mar Sci 4:118. https ://doi.org/10.3389/fmars .2017.00118

Wisshak M, Gektidis M, Freiwald A, Lundalv T (2005) Bioerosion along a bathymetric gradient in a cold-temperate setting (Kosterfjord, SW Sweden): an experimental study. Facies 51:93-117

Wood SN (2017) Generalized Additive Models: An Introduction with R (2nd edition). Chapman and Hall/CRC.

Wood SN, Pya N, Saefken B (2016) Smoothing parameter and model selection for general smooth models (with discussion). Journal of the American Statistical Association 111:1548-1575

Yesson C, Taylor, ML, Tittensor DP, Davies AJ, Guinotte J, Baco A, Black J, Hall-Spencer JM, Rogers AD (2012) Global habitat suitability of cold-water octocorals. J. Biogeogr. 39: 1278–1292. http://dx.doi.org/10.1111/ j.1365-2699.2011.02681.x.

Zuur AF, Ieno EN, Saveliev AA, Smith GM eds. (2009) Mixed effects models and extensions in ecology with R. New York: Springer.

Annex I: *Taxa analysed from still images for Seco de los Olivos (Table 1), Gazul mud volcano (Table 2) and Formigas seamount (Table 3). Abbreviations used in the analyses and displayed in the graphs included in the text are indicated in each table. Number of records per dive are also included.*

Table 1 Seco de los Olivos. (Abb = Abbreviation, D= Dive).

Taxa	Abb.	D 22	D 23	D 24	D 25
Porifera					
Asconema sp		3	0	0	3
Cladocroce	Cla	24	0	0	5
Geodia like		0	0	0	1
Pachastrella spp		2	0	0	0
Phakellia sp1		0	0	0	2
Phakellia sp2		0	0	0	4
Rhizaxinella	Rhiz	3	5	0	0
Stylocordyla spp		10	4	0	2
Sympagella spp		2	0	0	0
Porifera glass sp1		0	0	0	0
Porifera massive	Pmas	1	7	0	9
Porifera encrusting blue		3	2	2	0
Porifera encrusting	Pinc	27	55	7	34
Porifera lamellate		1	3	0	0
Porifera pedunculate sp1		1	0	0	0
Porifera pedunculate sp2		0	0	1	0
Cnidaria					
Anthozoa					
Ceriantharia		0	0	2	0
Zoanthidae		0	1	0	0
Octocorallia					
Acanthogorgia spp	Acanth	0	33	0	1
Callogorgia verticillata		0	0	0	0
Kophobelemnon sp		0	0	0	1

Alcyonacea sp1	Alcy	0	7	0	2
Hexacorallia					
Dendrophyllia cornigera	Dcor	3	10	0	4
Lophelia pertusa		0	0	0	1
Madrepora oculata		2	1	0	1
Scleractinia sp1		1	0	0	0
Scleractinia sp2		0	0	0	0
Anthipataria					
Parantipathes sp	Para	5	4	0	2
Gastropoda					
Charonia spp		0	1	0	0
Gastropoda		0	1	0	0
Echinodermata					
Cidaris sp		0	2	4	0
Echinus melo		0	0	0	0
Parastichopus sp		0	0	2	0
Crustacea					
Munida sp		1	0	0	3
Pagurus spp		1	0	0	0
Paramola spp		0	0	1	0
Pisces					
Chondrichthya					
Scyliorhinus canicula		1	0	0	0
Osteichthya					
Anthias anthias		0	0	0	0
Callionymus sp		2	0	1	0
Capros aper		0	0	1	0
Coelorinchus caelorhincus		1	0	1	0
Gadiculus argenteus	Garg	22	0	1	94
Helicolenus dactylopterus	Hdac	7	3	4	1

Hymenocephalus italicus		1	0	1	0
Micromesistius poutassou		0	0	0	0
Pagellus bogaraveo		0	0	0	0
Scorpaena elongata		1	1	0	1
Tigla lyra		0	0	1	0
Trachurus trachurus		7	0	0	0
Fish sp1		3	0	0	4

Aggregated spp	Taxa	Abb.
Porifera pedunculate	*Stylocordyla* spp	Pped
	Sympagella spp	
Porifera lamellate	*Phakellia* sp2	Plam
	Phakellia sp1	
	Pachastrella spp	
	Porifera lamellate	

Table 2 Gazul mud volcano (Abb = Abbreviation, D= Dive).

Taxa	Abb.	D 1	D 2
Porifera			
Asconema setubalense	Aset	10	2
Leiodermatium		4	0
Porifera Encrusting sp1		2	3
Porifera massive yellow	Pye	87	8
Porifera globular	Pglo	7	5
Pachastrella spp		24	13
Porifera massive sp3		123	49
Porifera massive sp2		2	9
Porifera pedunculate		1	1
Phakellia spp		0	0
Porifera sp1		4	0
Porifera sp2		10	0
Porifera arborescent sp1		0	0
Porifera lamellate		1	0
Porifera massive sp4		9	0
Porifera tubular sp1		0	0
Cnidaria			
Anthozoa			
Octocorallia			
Acanthogorgia sp	Acanth	89	156
Plexauridae	Plex	6	9
Callogorgia sp		2	0
Acanella arbuscula		1	0
Bebryce mollis		10	0
Alcyonacea		0	0
Hexacorallia			
Dendrophyllia cornigera		1	2

Lophelia pertusa		7	0
Madrepora oculata		93	1
Flabellum chunii	Flab	55	7
Desmophyllum sp		1	5
Actinauge richardi	Arich	0	1117
Hydrozoa			
Aglaopheniidae	Aglao	12	1
Stylasteridae		3	0
Gastropoda		1	0
Bivalvia		2	0
Pseudamussium peslutrae		0	0
Polychaeta			
Sabellidae		1	3
Echinodermata			
Echinoidea		0	1
Cidaris sp	Cid	20	31
Crinoidea	Crin	66	15
Ophiuroidea		1	1
Parastichopus regalis		1	0
Hacelia superba		0	0
Chaetaster longipes		2	0
Gracilechinus acutus		2	3
Crustacea			
Munida sp		10	6
Palinurus mauritanicus		1	0
Tunicata			
Ascidiacea	Asci	4	63
Cephalopoda			
Eledone cirrhosa		3	2
Pisces			

Teleostea			
Gadiculus argenteus		0	1
Helicolenus dactylopterus		0	1
Coelorhynchus coelorhynchus		0	0

aggregated spp	Taxa	abbreviation
White corals	*Lophelia pertusa*	Wcor
	Madrepora oculata	
Porifera massive	Porifera massive sp3	Pmas
	Porifera massive sp2	
	Porifera massive sp4	
Porifera lamellate	*Phakellia* spp	Plam
	Pachastrella spp	
	Porifera lamellate	

Table 3 Formigas seamount (Abb = Abbreviation, D= Dive)

Taxa	Abb.	D 4	D 5	D 6	D 7	D 8	D 9	D 10
Porifera								
cf. *Aphrocalister beatrix*		0	0	0	1	0	0	0
cf. *Ertwigia falcifera*		0	0	0	0	0	0	0
cf. *Farrea occa*	Focc	2	1	127	6	8	0	0
cf. *Haliclona magna*		0	0	0	1	5	0	0
cf. *Hymedesmia curvichela*		0	0	1	0	1	0	0
cf. *Macandrewia azorica*		0	0	2	0	1	0	0
cf. *Pachastrella monilifera*		2	0	0	0	0	1	0
cf. *Phakellia robusta*		0	0	2	0	0	0	0
cf. *Phakellia ventilabrum*		0	0	2	0	0	0	0
cf. *Poecillastra compressa*		2	0	2	0	0	1	0
cf. *Polymastia* sp1	Poly	0	0	45	41	11	0	0
cf. *Polymastia* sp2		0	0	0	0	0	0	0
cf. *Sceptrulophora* sp1	Scep	1	0	10	9	16	0	0
Euplactella sp		2	0	0	0	0	1	0
Pheronema carpenteri	Pcar	0	3	1	28	5	1	0
Porifera Encrusting Beige	PenB	0	0	0	4	292	0	0
Porifera Encrusting Bright Yellow	PenBY	0	0	0	0	15	0	0
Porifera Encrusting Dark Grey		0	0	0	0	0	0	0
Porifera Encrusting Grey		0	0	1	0	1	0	0
Porifera Encrusting Orange	PenO	0	0	6	1	19	0	0
Porifera Encrusting Pale Yellow	PenPY	0	0	0	0	27	0	0
Porifera Encrusting Red	PenR	0	0	0	35	3	0	0
Porifera Encrusting Transparent	PenT	27	57	28	128	79	76	43
Porifera Encrusting White	PenW	0	0	1	23	97	0	0
Porifera Flabellate Beige		1	0	0	0	0	0	0
Porifera Glass sp2	Pgla2	0	0	0	0	20	0	0
Porifera Glass sp3	Pgla3	0	0	1	2	24	0	0

Porifera Glass sp5		0	0	0	0	0	0	0
Porifera Massive sp1	Pmas1	0	0	5	2	0	3	0
Porifera Pedunculate sp1	Pped1	0	1	19	25	1	0	0
Porifera Pedunculate sp2		1	1	2	1	0	1	0
Porifera Tubular sp1		0	0	0	0	2	0	0
Porifera digitate sp1	Pdig1	0	0	95	217	39	0	0
Porifera digitate sp2	Pdig2	0	0	1	36	17	0	0
Porifera digitate sp3	Pdig3	0	0	11	6	9	0	0
Regradella phoenix		0	0	1	0	0	0	0
Rosselidae sp		0	0	0	0	2	0	0
Stylocordyla pellita	Spell	1	0	182	0	4	0	0
Cnidaria								
Hydrozoa								
Crypthelia sp	Crypt	4	0	8	0	0	2	0
Hydrozoa sp1		0	0	3	0	0	0	0
Hydrozoa sp5		0	0	0	0	0	1	0
Lytocarpia myriophyllum		0	0	4	0	3	0	0
Stylasteridae sp2		1	0	0	0	0	0	0
Stylasteridae sp1		0	0	2	2	0	0	0
Ceriantharia								
Cerianthus sp1	Ceri	2	7	0	5	0	1	2
Octocorallia								
Acanella arbuscula	Aarb	17	56	99	0	0	46	1
Alcyonacea sp1		1	0	0	0	0	1	0
Alcyonacea sp3		0	0	0	0	0	0	0
Alcyonacea sp4		0	0	0	0	0	0	0
Alcyonacea sp5		2	1	0	0	0	4	0
Alcyonacea Yellow		1	2	1	2	0	0	0
Anthomastus sp	Antho	2	0	0	11	0	0	0
Anthoptilum cf. *murrayi*		0	0	0	0	0	0	0
Bamboo coral sp1		0	0	0	0	0	1	0
Candidella imbricata	Cimb	0	0	128	0	0	0	0

cf. *Alcyonium grandiflorum*		2	0	0	0	0	1	0
cf. *Acanthogorgia armata*	Aarm	0	0	3	151	12	0	0
cf. *Gyrophyllum hirondellei*		4	0	0	0	0	0	0
cf. *Dentomuricea meteor*		0	0	0	0	0	0	0
cf. Keratoisis	Kera	2	3	0	0	0	6	0
cf. Lepidisis		0	0	1	0	0	0	0
cf. *Paramuricea* sp1		0	0	0	0	0	0	0
cf. *Swiftia* sp	Swif	16	7	3	5	0	3	0
cf. *Villogorgia bebrycoides*		0	0	0	1	0	0	0
cf. Anthothelidae		0	0	0	0	0	0	0
Chrysogorgia agassizi	Caga	3	4	0	0	0	19	0
Corallium johnsoni		0	0	1	1	1	0	0
Corallium niobe		2	0	2	1	0	0	0
Corallium tricolor	Ctri	0	0	19	19	2	2	0
Iridogorgia cf *pourtalesii*	Ipou	7	3	1	0	0	2	0
Narella bellissima	Nbel	0	0	0	365	51	0	0
Narella versluysi	Nver	0	0	84	374	193	4	0
Nidaliidae	Nida	0	0	0	0	38	0	0
Placogorgia terceira		0	1	0	0	0	2	0
Plexauridae Orange sp1		2	0	0	0	0	0	0
Plexauridae Purple sp1	Plexp1	1	1	3	0	9	9	0
Plexauridae White sp1	Plexw1	156	122	97	0	86	26	1
Radicipes cf *gracilis*	Rgra	10	3	1	0	0	2	0
Hexacorallia								
Anthipatharian sp3		0	0	1	0	0	0	0
Anthipathes cf *erinaceus*		0	0	0	0	0	3	0
Anthipathes dichotoma	Adic	4	5	4	0	0	2	0
Bathypathes patula		2	3	0	0	0	3	0
Caryophyllia sp	Cary	1	1	19	0	0	1	0
cf. Stauropathes		0	0	0	0	0	0	0
Desmophyllum dianthus	Ddya	7	1	0	0	0	2	0
Enallopsammia rostrata		1	0	0	0	0	0	0

Flabellum sp		0	0	0	0	0	1	0
Leiopathes glaberrima	Lgla	5	2	25	0	0	16	0
Leptopsammia formosa	Lfor	0	0	0	35	5	0	0
Lophelia pertusa	Lper	2	0	0	0	0	44	0
Madrepora oculata	Mocu	0	0	0	0	0	18	0
Parantipathes cf *hirondelle*	Phir	2	0	2	0	12	2	0
Scleractinian Yellow		2	0	0	0	0	0	0
Stichopathes sp1	Stich	5	0	0	0	2	6	1
Thouarella sp		6	0	0	0	0	0	0
Zoantharia sp2		0	0	0	0	1	0	0
Bryozoa								
Bryozoa sp1		0	2	0	0	0	2	0
Bryozoa sp2		0	0	1	0	1	0	0
Bryozoa sp3		0	0	3	0	0	0	0
Arthropoda								
Aristaeopsis edwarsiana		0	0	0	0	0	0	0
Barnacle sp1	Barn	0	0	44	3	0	0	0
cf. *Chaceon affinis*		0	0	0	2	0	0	0
cf. Galatheoidea sp1		0	1	1	0	0	2	0
cf. *Paromola cuvieri*		0	0	1	0	0	0	0
Crab sp2		0	0	0	0	0	0	0
Shrimp sp4		0	0	3	4	1	0	0
Echinodermata								
Asteroidea								
Asteroidea Orange sp1		0	0	1	0	1	0	0
Asteroidea Orange sp2		1	0	0	0	0	0	0
Asteroidea White sp1		4	2	0	0	0	0	0
Asteroidea White sp3		0	0	0	0	0	0	0
Ophiuroidea								
cf. Gorgonocephalus sp1		0	0	0	0	1	0	0
Ophiuroidea sp5		0	0	0	0	6	0	0
Ophiuroidea sp6		3	0	3	0	2	1	0

Crinoidea								
cf. *Cyathidium foresti*		0	0	0	8	0	0	0
Crinoidea Orange sp1		0	0	3	1	0	0	0
Crinoidea Purple sp1		2	0	0	0	0	0	0
Crinoidea stalcked sp1		4	0	0	0	0	0	0
Crinoidea Small sp1	Crino	0	0	3	0	71	0	0
Echinoidea								
Cidaris cidaris	Ccid	0	6	3	1	0	2	0
Echinus sp1		0	0	0	0	0	0	0
Holothuroidea								
Anemona sp1		0	0	0	0	0	0	0
Anemona sp2		0	0	0	0	0	0	0
Anemona sp3	Anem	1	0	1	0	0	10	2
Foraminifera								
Xenophyophore		1	0	0	0	0	0	8

3.5 Davis Strait, Rockall Bank, Azores: effects of organic matter supply on VME biodiversity

Authors: Lea-Anne Henry, Laurence de Clippele, Dick van Oevelen, Berta Ramiro Sánchez, Karline Soetaert

Contributors: Ellen Kenchington, Dierk Hebbeln (for VME data supplied to the ATLAS WP3 Data Call)

Abstract

Alongside projections of changes to physical quantities in the North Atlantic by the century's end, changes to biological parameters such as food supply, organic matter and particulate organic carbon are also likely to occur. However, the potential for a drained food supply to impact the biodiversity of VMEs and their associated biological communities has not often been directly investigated. This study quantified the importance of particulate organic carbon (POC) across three ATLAS Case Studies in the Davis Strait (Canada), Rockall Bank (UK and High Seas), and the Azores, as well as the role that organic matter (OM) supply plays in structuring biodiversity of non-scleractinian corals in area of the High Seas, at the Logachev Mound Province at Rockall. Gaussian Mixture Models were used to group areas in each of the 3 Case Studies according to low, medium and high POC levels. Analysis of variance (ANOVA) showed that POC class had statistically significant effects on VME indicator taxon richness only in the Azores (SS=2686, F=4.030, p=0.022), the Case Study with the relatively lowest POC daily flux (0.672-1.053 mg C m^{-2} d^{-1}). Here, the richness of taxa was positively related to higher POC flux, whereas VME indicator taxa richness did not exhibit any strong or significant trends directly related to POC flux; in these 2 Case Studies where mean POC fluxes were relatively higher (and probably not a critically limiting factor). In contrast to the Azores, diversity and evenness of octocorals and black corals decreased with increasing OM supply estimated from a Regional Ocean Model System (ROMS) at the Logachev Mound Province of Rockall in the High Seas. Here, mean POC levels were far higher than at the Azores (2.189 – 88.288 0.672-1.053 mg C m^{-2} d^{-1}) so are not likely critically limited, however, density of these corals positively increased with higher OM suggesting that some coral taxa may thrive and even dominate areas with very high OM levels. Although these results are caveated with the fact that multiple environmental drivers create community structure in VMEs (e.g., substrate heterogeneity, seafloor topography, oceanographic properties), the present study identified a potentially important correlation with POC, whether direct or indirect, with VME diversity. With projected decreases of >50% of POC to regions like the Azores,

and the potential for critical limitations in OM supply to VME indicator taxa in the Azores, it stands to reason that out of all three Case Studies, projected perturbations to OM supply could cause loss of species in the central Atlantic.

Introduction

By the next century, climate change will have impacted much of the deep and open-ocean Atlantic. Besides changes to physical quantities such as sea temperatures, salinities, carbonate chemistry and oxygen concentrations, projections of changes to biological parameters such as food supply, organic matter and particulate organic carbon are also likely to occur (Sweetman et al., 2017; see Section 3.1 in this Deliverable 3.2). Together, these changes could radically impact marine ecosystems from the bottom of the food chain, to the microbes and sponges and corals of interest to the Blue Biotechnology sector, to top ocean predators such as tuna and billfish that have high energetic and oxygen demands but which are of great interest to the Maritime and Coastal Tourism sector.

The potential for a drained food supply to impact the biodiversity and biogeography of VMEs and their associated biological communities has not often been directly investigated. Observational and modelling studies demonstrate that present-day climate change could lead to a decline by up to 40% of the food supply (Particulate Organic Carbon or POC flux) to the deep interior of the ocean and seafloor in some regions, particularly the central gyres, by the year 2100 (Sweetman et al., 2017). Predicted changes in the euphotic zone (e.g., increased stratification, ocean acidification) may even amplify effects of declining POC by causing shifts from fast-sinking diatoms to slow-sinking picoplankton, leading to enhanced water column POC degradation and declines in the quality of the organic matter quality eventually reaches the seafloor (Jones et al., 2014; Sweetman et al., 2017). It is particularly important to examine these effects, because as we approach the next century, by which time VMEs will be vulnerable and likely impacted by multiple stressors. With the fact that most of the deep sea and abyssal plains in particular are already characterised by severe food limitation (Smith et al., 2008, 2009; Watling et al., 2013; Sweetman et al., 2017), it is urgent we improve our understanding of how sensitive VMEs in the North Atlantic may be to changing POC dynamics as many marine organisms may require extra energy (food) in order to cope with the effects of climate change (Wood et al., 2008).

For this in-depth analysis of Deliverable 3.2, three ATLAS Case Studies were pre-selected to examine effects of organic matter supply on VMEs. These 3 Case Studies are also the subject of *in situ* lander deployments for eddy covariance studies examining effects of VME versus non-VME

habitat type on ecosystem functioning (WP2) and organic matter supply, so the empirical results derived in Deliverable 3.2 help build a big picture for ATLAS about how organic matter affects ecosystem structure (biodiversity and biogeography). With the remotely operated vehicle (ROV) and lander cruise delayed by one year to the Davis Strait, and the ROV deployment at Rockall experiencing difficulties in conducting quantitative transects, it was decided to use other data sources compiled for ATLAS to build the biodiversity datasets to be analysed for this aspect of Deliverable 3.2 congruent, and harmonise these with correctly scaled estimates of organic matter supply from existing models that would cover the same spatial extent as the biodiversity data.

Additionally, one in-depth study was also made possible using an existing regional ocean model system (ROMS) of organic matter supply for an area in the High Seas of Rockall that was matched with a corresponding, also correctly-scaled, ROV video survey of octocoral and black coral biodiversity to give even more insight into the importance of food supply on these VME types. This study investigated the environmental drivers of diversity, evenness and density of the non-scleractinian cold-water corals on the Logachev Mound Province of Rockall Bank where the coral communities are known to play an important part in the biogeochemical cycling of carbon (van Oevelen et al. 2009).

In some cases, a topography supporting live cold-water corals is the result of the growth of the corals themselves, giving rise to cold-water coral carbonate mounds. When the morphology of a mound reflects that of the dominant hydrodynamic controls, Wheeler et al. 2007 classified these mounds as having a 'developed' morphology (Darwin Mounds, Logachev Mounds). These large mound structures have developed over glacial-interglacial time periods (Kenyon et al. 2003, van Weering et al. 2003, Mienis et al. 2007). In the Rockall Case Study area, there is a significant interaction between tidal currents and cold-water coral formed mounds, which induce downwelling events of surface water that brings the organic matter to 600 m deep (Soetaert et al. 2016). The influence of topography on current patterns, and consequently on the food supply, is thought to determine the distribution of cold-water corals and their associated fauna on both broader and finer scales (Sebens 1998, Mortensen et al. 2001, Davies et al. 2009, Soetaert et al. 2016). The goal of this aspect of the organic matter studies, besides the broader comparison between Davis Strait, Rockall and the Azores, was to provide an in-depth analysis of the role that organic matter plays relative to other factors (substrate, seafloor geomorphology) on the diversity, evenness and density of non-scleractinian corals in the Logachev Mound Province in the High Seas.

Methods

Data Sources

The effect of POC flux to the seafloor on VME species richness and composition was examined across three areas of study in the North Atlantic. The areas encompassed the marine region of the Davis Strait in the Canadian Exclusive Economic Zone (EEZ) waters, the marine region of the Azores EEZ, and the Rockall region encompassing both an Area Beyond National Jurisdiction (ABNJ) and part of the United Kingdom's EEZ.

Data records of VME indicator taxa were collated from a variety of taxa, including stony and lace corals, gorgonians, crinoids, sponges and chemosynthetic species. Data were collated from the Ocean Biogeographic Information System (OBIS), the International Council for the Exploration of the Sea (ICES) Working Group on Deepwater Ecology (WGDEC) and National Oceanic and Atmospheric Administration (NOAA) public repositories, the literature [Cairns (2006), Tabachnick and Collins (2008), Molodtsova et al. (2008), Hestetun et al. (2015), Howell et al. (2016)] and data compiled during ATLAS's Data Call for VME records under WP3. These included unpublished databases from the University of Edinburgh, the Spanish Institute of Oceanography, the University of Bremen, and the Canadian Department of Fisheries and Oceans.

Prior to analysis, the taxonomic names were matched to the World Register of Marine Species and were manually inspected for errors, identifying synonyms and misspellings, and excluding any locations recorded on land. A total of 25 taxa in the Davis Strait, 271 in the Azores EEZ, and 56 in Rockall were retained for analysis.

The global ocean model GEBCO's gridded bathymetric data (https://www.gebco.net/) at 30 arc-second interval grid were used to map the North Atlantic bathymetry. Estimated Particulate Organic Carbon (POC) flux to the seafloor was obtained from Sweetman et al. (2017), calculated using an equation from (Lutz et al., 2007) based on the seasonal variability of primary productivity over a 12-year period and the export depth below the euphotic zone. The spatial resolution of the POC flux layer was 0.65° by 0.65° per grid cell, which was also selected for the data analysis as a compromise between the lack of spatial resolution of a larger 1° dataset and the increased number of cells with just one record at a 0.083° data set (i.e. the same resolution as the bathymetric data).

Taxonomic and POC Database

All analyses and maps were performed in ArcGIS 10.6.1. For calculating taxon richness per cell, a 0.65° global grid was first created at the same resolution as the POC flux raster layer. The tool Spatial Join (Spatial Analyst toolbox) allowed to join the taxa point dataset to the grid, joining each taxon to an indexed grid. Next, regardless of the amount of times a taxon was recorded in a location

(i.e. grid cell), it was represented by one grid cell record. The tool Summary Statistics was used to count the number of taxa per grid cell. Finally, the resulting table was joined back to the original 0.65° grid. For each study area, taxon richness per 0.65° cell was shown over the POC flux layer, and extracted for each grid cell for further analysis.

Statistical Analyses

For each Case Study Area, a Gaussian mixture model (GMM) was used to help predict the potential for taxonomic richness to vary across groups of low, medium and high POC values. Unlike other clustering methods such as K-means, GMM does not assume a fixed numbers of clusters, and allows for each cluster having unconstrained variance. In the present study, a GMM was conducted in each Case Study to group records of POC values into low, medium and high, with the Bayesian Information Criterion (BIC) used to find the optimum structure of clusters. Each POC group or "class" was then used as a qualitative categorical variable for which we then used in an analysis of variance (ANOVA) that tested whether taxon richness differed between classes of POC values. Pairwise comparisons between POC classes were perfomed using Tukey's multiple comparison tests.

In-depth ROMS study at the Logachev Mound Province, High Seas

The Logachev Mound Province is located on the south-eastern slope of Rockall Bank in the northeast Atlantic (Kenyon et al. 2003) (Figure 1).

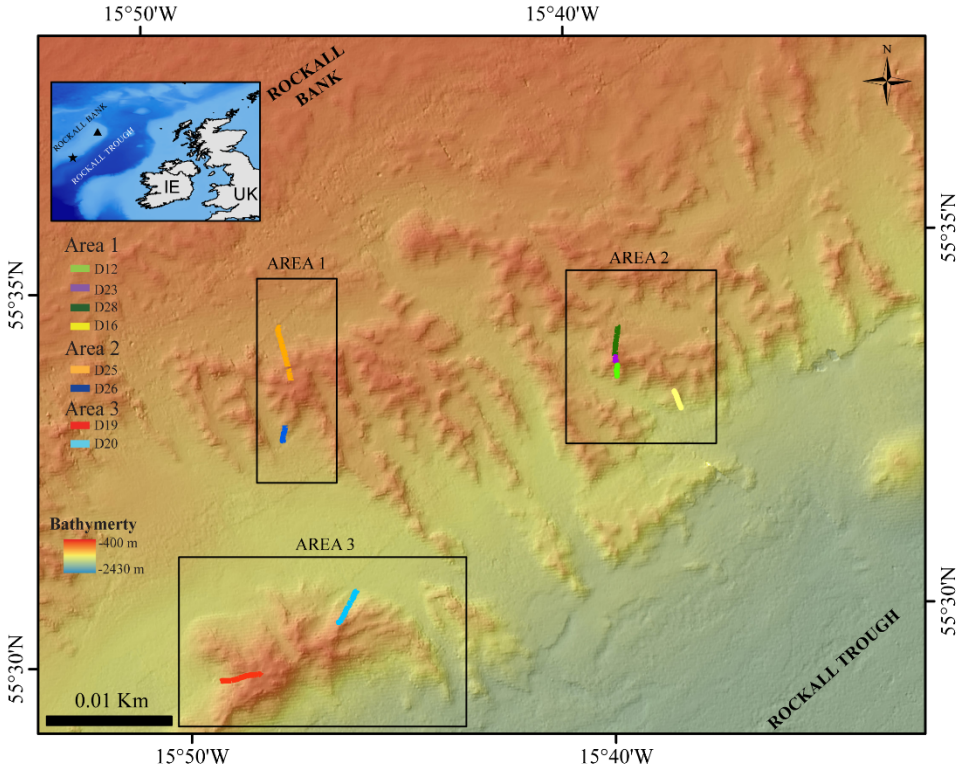

Figure 1. *(A) Location map of the Logachev Mound Province (star), and Rockall Island (triangle) on Rockall Bank. IE: Ireland, UK: United Kingdom (B) Location of the three study areas 1 – 3, and ROV dives in the Logachev Mound Province on the southeast side of Rockall Bank.*

Within Rockall Trough, the upper layers down to 1,200-1,500 m are occupied by Eastern North Atlantic Water (ENAW) (Holliday et al. 2000). The cold-water coral carbonate mounds are between 5 and 360 m tall, up to a few kilometres long and located between 600-1000 m depth, which is within the boundaries of the ENAW (Kenyon et al. 2003, Mienis et al. 2007, 2009, de Haas et al. 2009). The ENAW circulates through an anticyclonic gyre in Rockall Trough with a net northward flow direction, while around the mounds there is a local residual current flow towards the south-west that ranges between 5-15 cm s-1 (Holliday et al. 2000, Huthnance 1986, Mienis et al. 2007, White et al. 2007, Soetaert et al. 2016). There is also a stronger bottom-magnified diurnal tidal flow of 15-28 cm s-1. It is these strong northwest-southeast directed currents that affect the growth direction of the mounds, which is perpendicular to the regional contours (Mienis et al. 2007, White et al. 2007).

The Logachev Mound Province consist of a cluster of mounds that are built of accumulated fine sediments baffled by coral reef framework, dead coral fragments and live coral on the summit. The mound bases are covered by bio- and siliciclastic sands with various amounts of pebbles, cobbles and boulders (de Haas et al. 2009). The flanks of the mounds are covered with patches of coral rubble, dead coral branches and living corals, while the summits of the mounds are characterised by dense *L. pertusa* patches at 500-600 m depth (Kenyon et al. 2003, Van Weering et al. 2003, de Haas et al. 2009).

Food and organic matter is supplied to the suspension-feeding corals through different mechanisms. First, the presence of the coral framework will slow down the currents allowing the corals to gather food, but also trap sediments, which can then accumulate between the coral branches ensuring further growth of the mounds as a whole (Roberts et al. 2006, Dorschel et al. 2007, de Haas et al. 2009, Mienis et al. 2009, Roberts et al. 2009). Secondly, the interaction of the diurnal tidal currents with the slope of Rockall Bank and the topographies of the cold-water coral mounds themselves, induces downwelling of the productive Rockall Bank surface waters due to the formation of internal waves (Davies et al. 2009, Kenyon et al. 2003, Wagner et al. 2011, Findlay et al. 2013, Cyr et al. 2016, Soetaert et al. 2016). Thirdly, the interaction of internal waves and tidal currents with seabed sediments also causes nepheloid layers, which contain increased amounts of suspended seabed sediment that can supply the corals with food at deeper depths (Kenyon et al. 2003, Mienis et al. 2007). Intermediate Nepheloid Layers (INL) have been identified as turbidity clouds between 450 and 900 m depth and varied in depth and shape coincidingly with the diurnal cycle. The largest turbidity cloud can be found between 200-500 m depth, just above the carbonate mounds. A second

smaller turbidity cloud can be found 25 km from Rockall Bank between 500-700 m depth (White et al. 2003, Mienis et al. 2006, 2007).

High-definition video

During the Changing Oceans Expedition (RRS *James Cook* Cruise 073, 18 May-15 June 2012), a total of eight video transects were recorded in the Logachev Mound Province with a total length of ~3.4 km and an average width of 2.74 m +/- 0.5 m. These eight video transects only covered small parts, on alternating sides of three large clustered cold-water coral carbonate mounds within the Logachev Mound Province (Figure 1, Table 1). Since the transects only covered a section and not the whole of the clustered mound, they are referred to as area 1, 2 and 3.

Table 1. *ROV dive information. Average aspect represents the side of the area/clustered mound at which the video transects were collected.*

Dive (area)	Start Lon (decimal degrees)	Start Lat (decimal degrees)	End Lon (decimal degrees)	End Lat (decimal degrees)	Aspect/ flank	Depth range (min-max) (m)	Length/ Width (m)
25 (1)	-15.78718	55.57206	-15.78421	55.56013	NW	[547-705]	1040/ 3.37
26 (1)	-15.78795	55.55020	-15.78918	55.54672	SW	[702-768]	360/ 2.79
23 (2)	-15.65630	55.55847	-15.65571	55.55965	NE	[563-584]	40/ 2.55
28 (2)	-15.65585	55.56014	-15.65389	55.56674	S	[575-701]	240/ 2.91
19 (3)	-15.82089	55.49419	-15.80442	55.49478	NE	[559; 801]	880/ 2.62
20 (3)	-15.76447	55.51220	-15.77232	55.50529	NW	[610-873]	360/ 2.97

Using the remotely operated vehicle (ROV) *Holland-1*, the data were recorded with a combination of cameras mounted on the ROV: an HD Insite mini-Zeus video camera with a direct

HDSDI fibre output, a Kongsberg 14-366 pan and tilt camera and an Insite Pegasus-plus fixed zoom camera. Four lights were used: two 400-W deep-sea power and light SeaArc2 HMI lights and two 25,000 lumen Cathx ocean APHOS LED lights. Two lasers spaced 10 cm were also mounted on the HD camera. The position and depth of the ROV were determined by USBL (Sonardyne) underwater positioning system and recorded using the OFOP (Ocean Floor Observation Protocol) software.

Coral identification and associated fauna

The presence of the non-scleractinian coral species were counted and noted in an Excel spreadsheet alongside video time, latitude and longitude (example fauna shown in Figure 2).

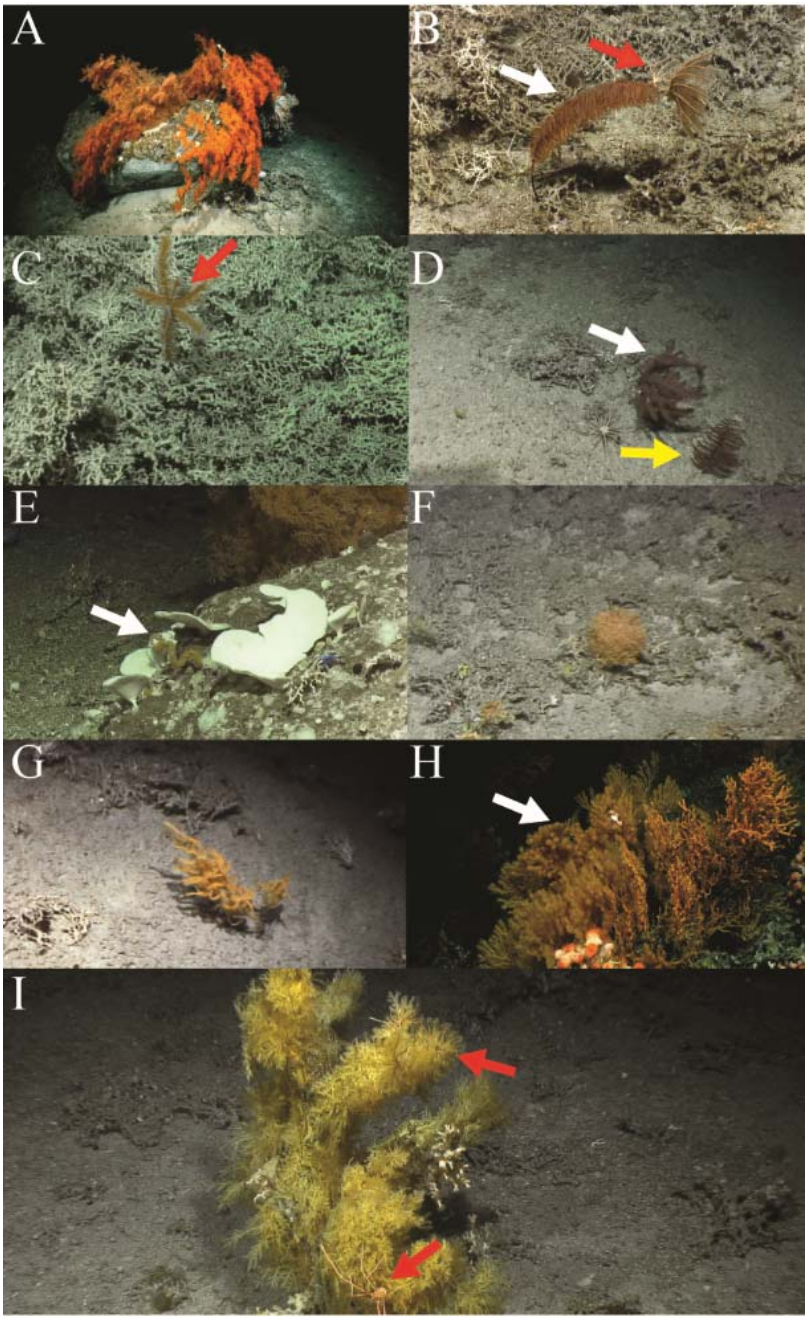

Figure 1. *(A)* Leiopathes *sp. (B)* Parantipathes *sp. 1 (white arrow) with two crinoids sp attached to the top (red arrow) (C)* Parantipathes *sp. 2 (D)* Trissopathes *sp. 1 (white arrow)* Bathypathes *sp. (yellow arrow) (E)* Stichopathes *cf.* gravieri *(F)* Acanella *sp. (G)* Antipathes *sp. 2 (H)* Paramuricea *sp. (white arrow) with* Gorgonocephalus *sp. (red arrow) (I)* Antipathes *sp. 1 with crinoids (top red arrow) and* Gastropyctus *sp. (bottom red arrow)*

Environmental Data Sources

Substratum information was obtained from video data (see section substrate below), while the bathymetry dataset was provided by the Irish National Seabed Survey programme (INSS) at a 20 x 20 m resolution (www.gsiseabed.ie). Several topographic variables were derived from the bathymetric grid using the ArcGIS 10.1, ESRI Software and the Benthic Terrain Modeler (Wright et al. 2012): slope,

aspect (eastness and northness), rugosity (using a square kernel window of 9x9 pixels) and bathymetric positioning index (BPI; using an annulus kernel window with inner and outer radius of 3x6). More information on these variables can be found in De Clippele et al. (2017) and in for example in Wilson et al. (2007), Guinan et al. (2009) and Henry et al. (2010). Substrate types were identified from the HD videos according to the classes listed in table 2 (see Table 2, Figure 3). The dominant substrate class was noted every meter from the HD videos in Excel. The number of glacial dropstones (boulder > 1m) was also noted.

ROMS to Derive Organic Matter Supply

A coupled numerical model was used to infer the organic matter supply for the Logachev mound province at Rockall Bank. The 3D-hydrodynamic model has been developed in the Regional Ocean Modeling System (ROMS) and generated flow fields in a model domain covering an area of 60 × 90 km, which extends from the shallow bank (200 m) down into the deep Rockall Trough (2000 m) (Mohn ea 2014). It is important to note that although non-linear internal wave generation is not explicitly resolved by the model, the evolution of internal lee waves and associated large-amplitude up- and downwelling events are well represented and time-scale was chosen such that impacts of tidal pumping above the CWC mounds are included.

The resulting hydrodynamic simulations, stored at 6-hour intervals, was used offline to drive organic matter dynamics in the water column, including production at the upper boundary, advective horizontal and vertical transport, constant decay and passive sinking. Zero-gradient conditions were imposed at the lower and horizontal domain boundaries. At the upper boundary, a constant flux of 12 mmol C m^{-2} d^{-1} was imposed. This is equivalent to an export carbon flux of about 50 g C m^{-2} yr^{-1}, consistent with estimates of new production in the nearby Goban Spur area. The sinking velocity (w) and the decay rate (k) were chosen such that the e-folding depth (w/k) was around 500–700 m, a value often used in biogeochemical ocean general circulation models. The sinking velocity of 20 m d^{-1} and the first-order decay rate of 0.03 d^{-1} are representative for the decay of freshly produced organic matter. Note that with this input flux and sinking speed, the maximal organic matter concentration in the water column is 0.6 mmol C m^{-3}. This is below measured organic matter concentrations at northwestern Atlantic margins, however, our model results are representative for reactive, freshly-produced organic matter, while the *in-situ* measurements include refractory organic matter.

The presence of CWCs in the area was inferred from a habitat suitability model, which predicts coral occurrence at the Logachev province from a generalised linear modelling approach based on a

set of bathymetric, hydrodynamic and environmental variables (Rengstorf et al., 2014). Deposition of organic matter from the water column to the seafloor is modelled as passive sinking. In the CWC areas (as predicted by the habitat suitability model) however, deposition of organic matter is due to both passive sinking and suspension-feeding. The passive sinking velocity in the bottom grid cells overlying the CWCs was therefore enhanced by a factor 10 to account for the suspension feeding activity. The enhancement factor of 10 can be justified by the following three arguments. Firstly, the metabolic activity of a cold-water coral community is 5 to 10 times higher as compared to the adjacent barren seafloor (Van Oevelen et al. 2009) and the enhancement factor is needed to ensure that sufficient organic matter is taken up to sustain this elevated metabolic activity. Secondly, while *in situ* estimates of passive sinking + filtration activity above CWC reefs are not available, our enhancement factor compares favourably with data from tropical coral reefs (Monismith ea Limnology and Oceanography 55, 1881–1892 2010). Thirdly, an order of magnitude calculation of the capturing efficiency shows that the enhancement factor is not unrealistic. The mean current velocity is roughly 0.3 m s−1 above the CWCs. Assuming that suspension feeders feed from 20 cm of water above the sediment (a lower estimate, as corals are usually higher than 20 cm), this means that a m^2 of CWC reef can extract resources from 5184 m^3 d^{-1}. With the imposed passive sinking + suspension feeding activity of 200 m d^{-1}, this implies that they have a capturing efficiency of less than 4%.

Statistical Analyses

Species counts of non-scleractinian VME indicator fauna were grouped per 40 m sub-transects. A length of 40 m sub transects was chosen as this length gave the best representation of the substrate and species variability in relation to a changing bathymetry and rugosity. The percentage cover for each substrate class were also calculated per 40 m sub-transect. Sampes that fell outside the organic matter infered cold-water coral presence zone were not included in the analyses, to allow relevant comparision for organic matter between the samples.

Species diversity, density and evenness of the megafauna were calculated in Excel per 40 m transects. The Shannon diversity index (H') and Pielou value were used to calculate the diversity and evenness of the non-scleractinian corals in the study area. The Pielou's evenness value can range from 0 to 1 and gives an indication of dominant species being present in a sample (~0) or if there is an equal abundance of all species (~1). Density was calculated by dividing the total number of individuals per square meter of the transect.

The diversity, density and evenness of the megafauna was also calculated per area. No statistical analyses are yet performed to compare differences between the areas, but boxplots of the environmental variables that were important in the RF (bellow) are created.

Random forest (RF) classification (Breiman 2001) is used here as a modelling technique. A random forest consists of a number of simple decision trees. Each tree is based on a bootstrapped sample of the biological and environmental data set. This group of simple trees vote for the most popular class, which is capable of predicting a response when presented with a set of explanatory variables. More background information about the application can be found in Cutler et al. (2007) and Rogan et al. (2008). All classifications were carried out in R version 3.2.2 (R Development Core Team 2013) using the random forest package v.1.6-7 (Liaw and Wiener 2002). Here, the 40m sub-transects are used as samples. The RF classification models were assessed based on random separation of training and test (validation) data. This was done by leaving 15 of the 136 random samples out for model training and subsequently using them to test the model. The model is evaluated based on the mean of squared error (MSE), which is better closer to 0, together with the percentage variance explained. The root mean square error (rmse) is used to assess the accuracy of the observed versus the predicted values (using the test data), where the lower the value, the better the fit. Response curves for the partial dependence on the three dominant explanatory variables are also given.

Results

Comparison across Davis Strait, Rockall, and Azores

POC flux varied considerably between Case Studies. GMM classes demonstrated considerably higher mean values for POC in Davis Strait and at Rockall, with lowest values in the Azores EEZ (Table 2). Both the Azores and Rockall POC classes showed statistically significant structuring of POC values in the data (normalised entropy criterion, NEC, value = 0.932 and 0.182, respectively, each of which is < 1), meaning that the POC classes are statistically different from one another, whereas the classes in Davis Strait did not exhibit as strong structuring, yet these were the highest values.

Table 2: GMM class means for daily POC flux in each Case Study area.

Case Study	**Low POC class mean (mg C m^{-2} d^{-1})**	**Medium POC class mean (mg C m^{-2} d^{-1})**	**High POC class mean (mg C m-2 d-1)**
Davis Strait	8.916	14.000	17.624
Rockall Bank	2.189	3.219	88.288
Azores	0.672	0.873	1.053

Notably, differences between POC classes in terms of taxon richness were not statistically significant in the Davis Strait or at Rockall, but they were in the Azores EEZ (Sum of squares (SS)=5.477, F=1.571, p=0.213 for Davis Strait; SS=3.045, F=0.052, p=0.949 for Rockall; SS=2686, F=4.030, p=0.022 for Azores; Figure 2). This is notable because the Azores EEZ also had relatively lower mean POC values than the other two case study areas.

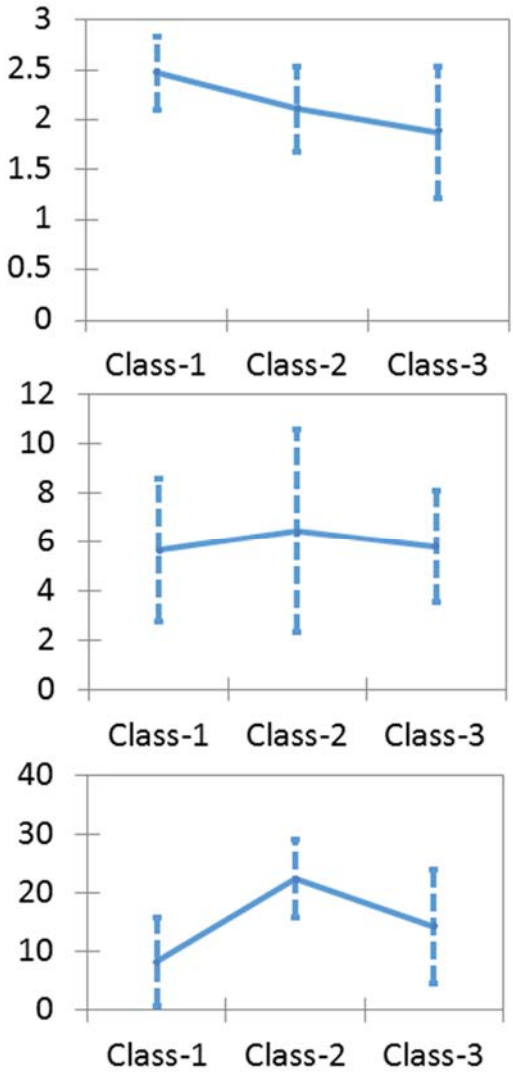

Figure 2: *Results of ANOVA tests to determine whether taxon richness in each Case Study area (Davis Strait – top; Rockall – middle; Azores – bottom) showed statistically significant different across classes of POC flux. Taxon richness was only statistically significantly at higher at medium to high levels of POC flux relative to areas with lower flux in the Azores EEZ.*

Although taxon richness did not statistically differ between POC classes in the Davis Strait, at Rockall Bank, considerable variability did exist in the biodiversity of VME indicator taxa across the study region (Figures 3 and 4). Pairwise Tukey tests did not indicate any significant pairwise differences between POC classes in these areas either, it was only between the lowest and middle/higher POC classes in the Azores that richness was statistically lower (Figure 1, bottom), and where spatial variability in VME indicator richness could also been seen (Figure 5).

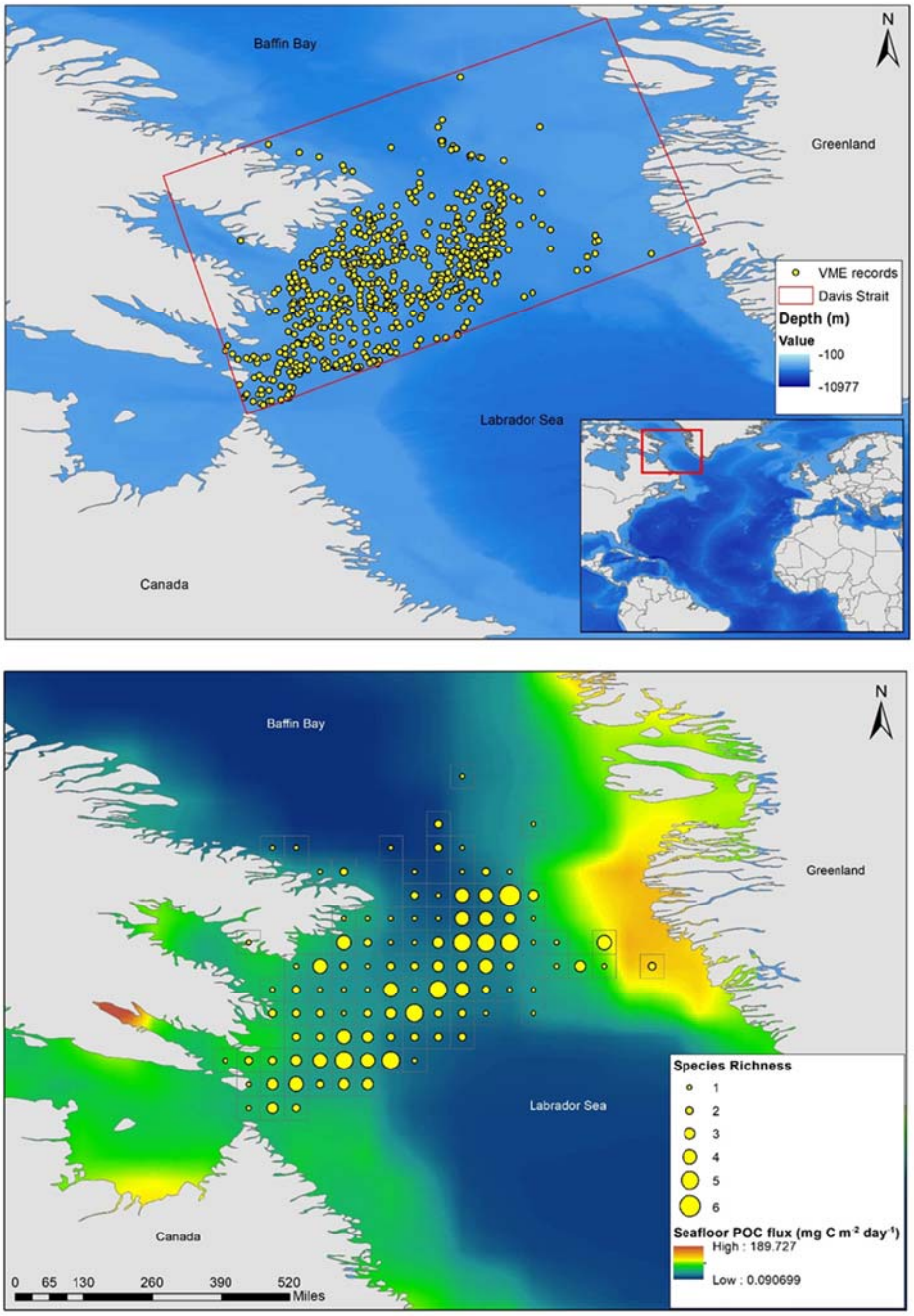

***Figure 3**: Effects of organic matter supply on VME biodiversity in the Davis Strait. VME records across the region (top) and VME taxon richness by grid cell (bottom) are shown.*

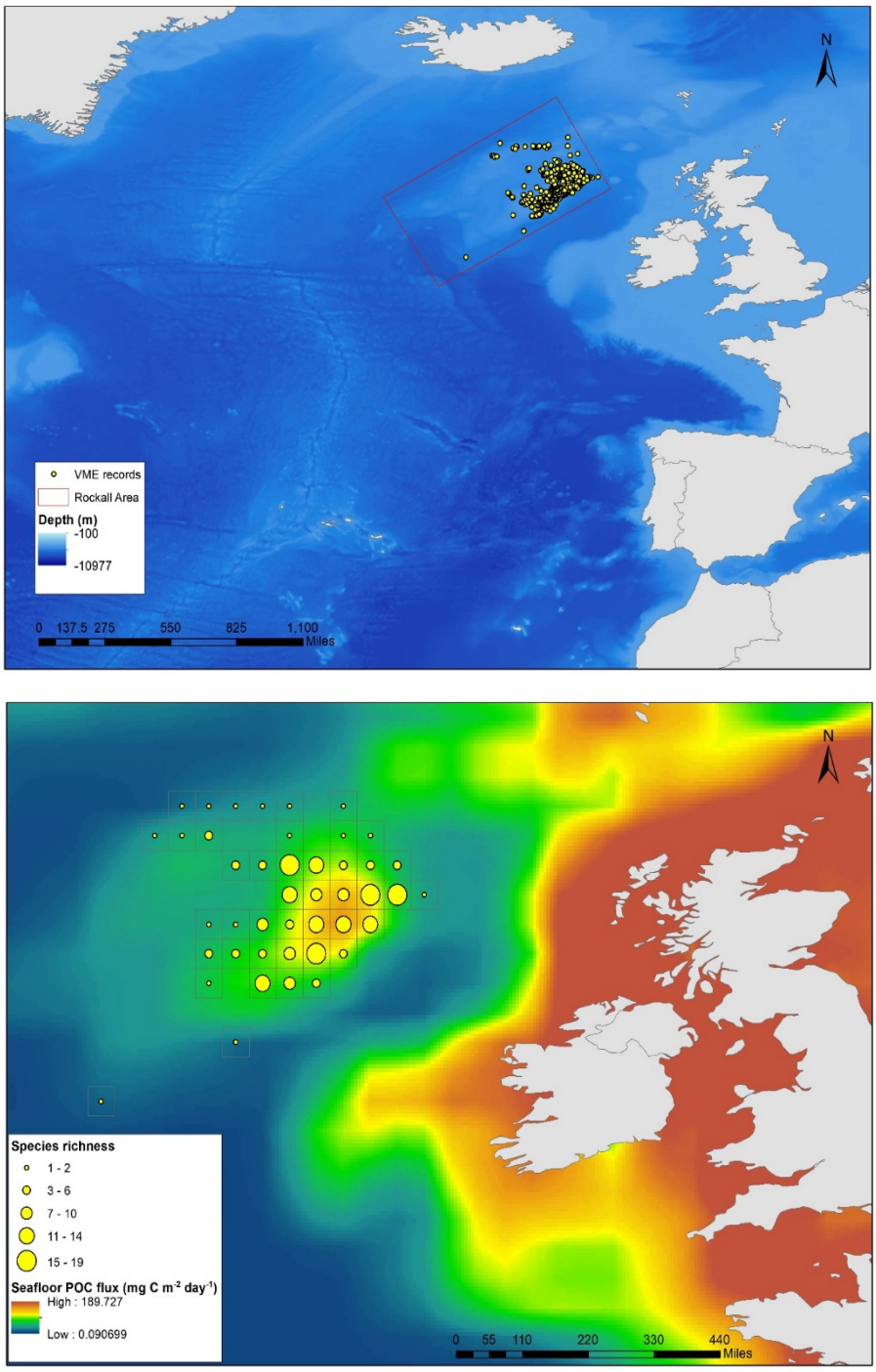

***Figure 4**: Effects of organic matter supply on VME biodiversity at Rockall. VME records across the region (top) and VME taxon richness by grid cell (bottom) are shown.*

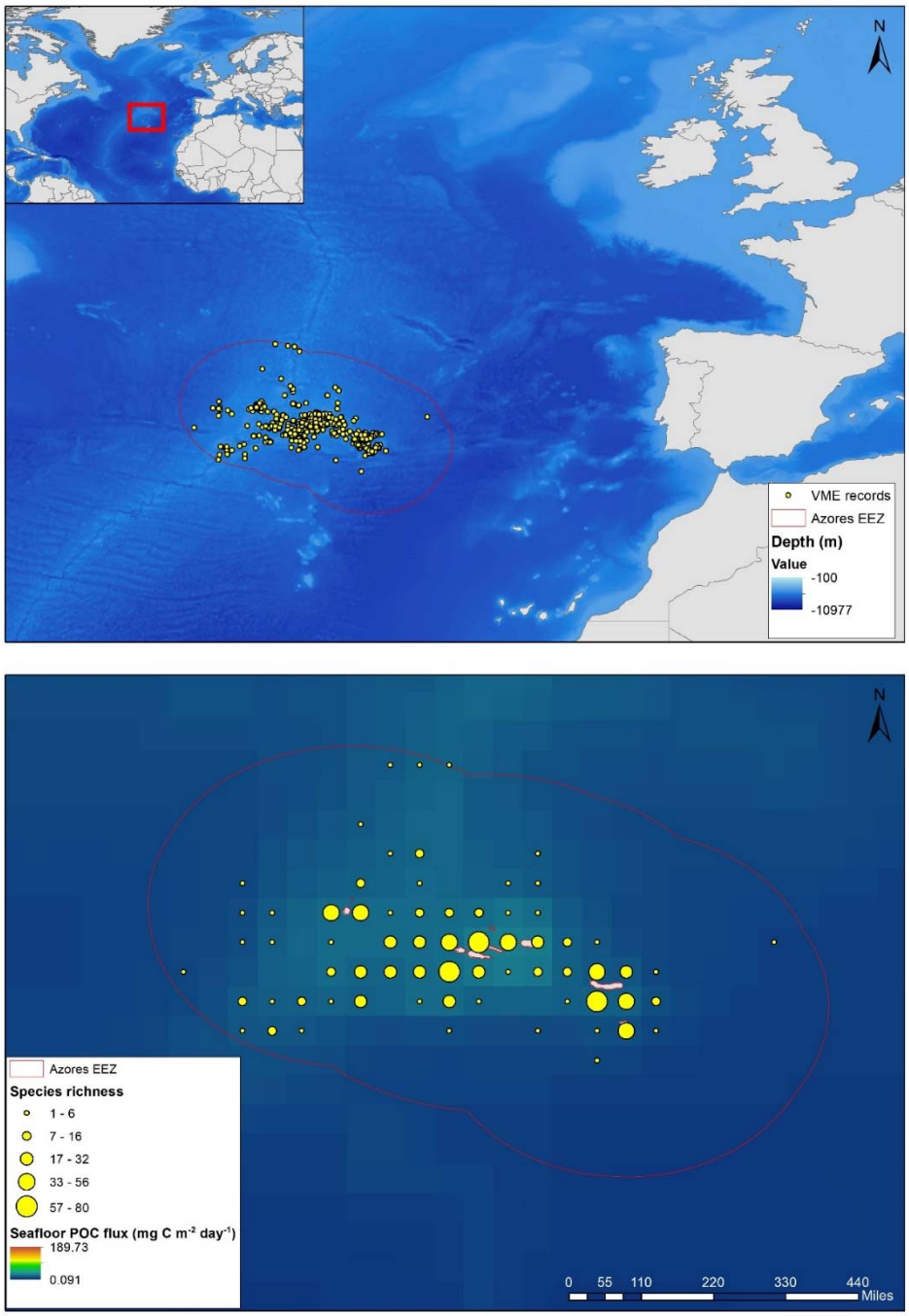

***Figure 5**: Effects of organic matter supply on VME biodiversity in the Azores EEZ. VME records across the region (top) and VME taxon richness by grid cell (bottom) are shown.*

In-depth analysis on effects of organic matter supply at the Logachev Mound Province

Non-scleractinian diversity, evenness and density the percentage variance explained was around 18-27% for all the models. The mean square error was between 0.4-0.6 for all models, with all predictions close to 0.1 (Table 3).

Table 1. *Results from random forest analyses, with mtry=6 and ntree=1500 for models on diversity, density and evenness for all megafauna counted, and for only non-scleractinian corals.*

Non-scleractinians	Mean of squared error	% Variance explained	rmse
Diversity	0.05348098	27.47	0.10823
Evenness	0.0666336	18.85	0.1183756
Density	0.04877137	22.43	0.1081599

For the non-scleractinians, patterns in diversity and evenness, and to some extent density, are strongly driven by organic matter, as well as occurrence of dropstones and dead exposed coral framework (Figure 6).

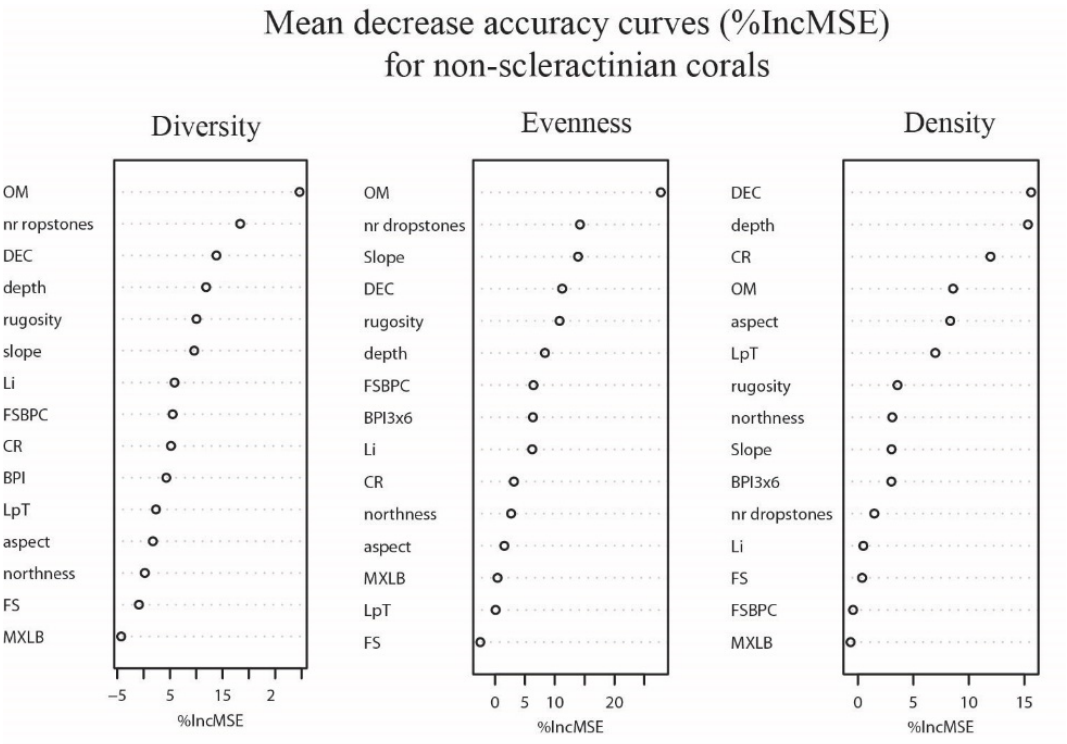

Figure 6. *Mean decrease on accuracy plot indicating the contribution of each variable to the model performance.*

The response curves (Figure 7) indicated that non-scleractinian diversity and density both increase with lower organic matter concertation, and an increasing number of dropstones and dead

exposed coral framework. In contrast, non-scleractinian coral density increases with increasing organic matter concentration, and with increasing amounts of dead exposed coral framework, depth and coral rubble.

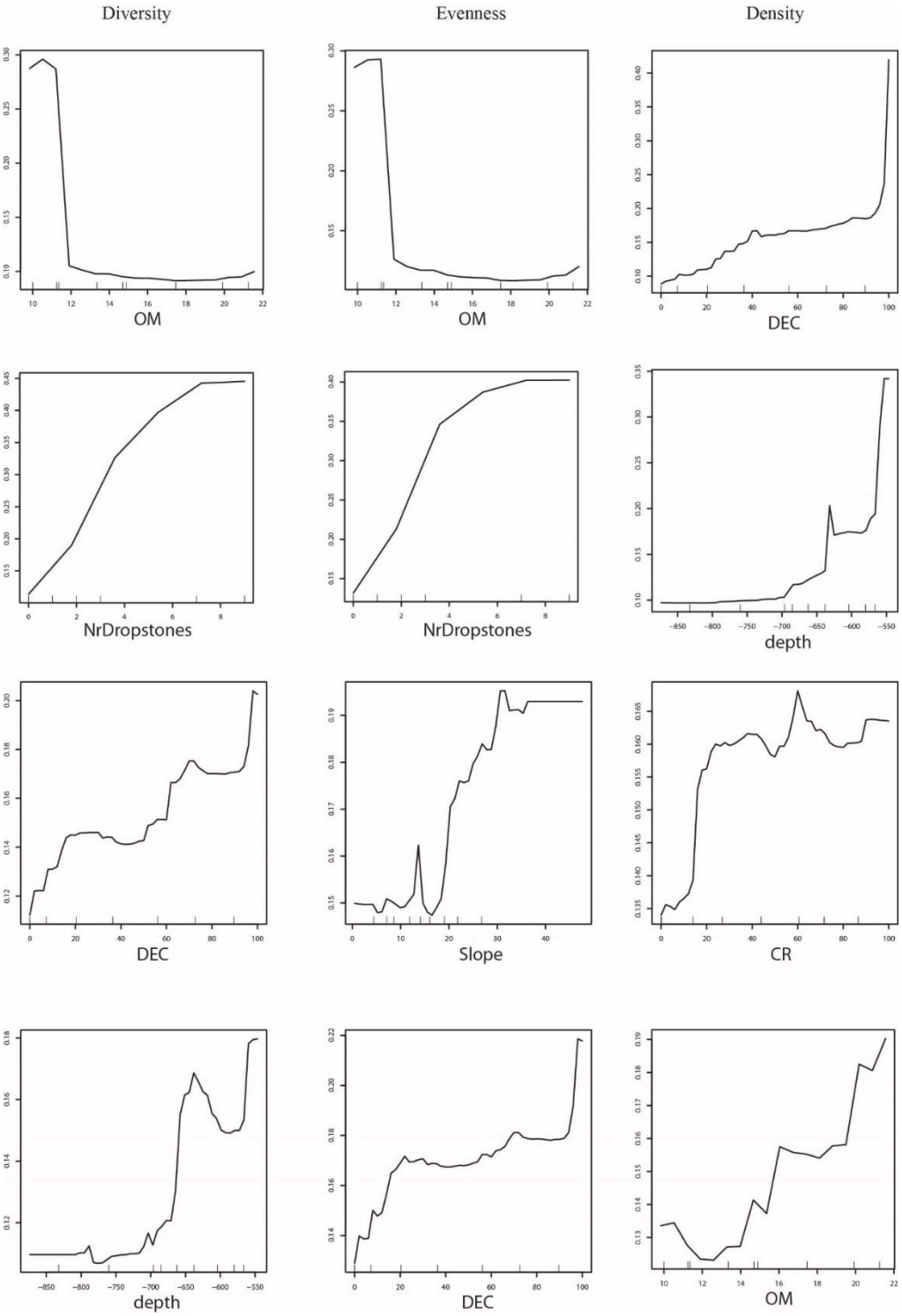

Figure 7. *Response curves for the non-scleractinian RF models diversity, evenness and density (values on the y-axis) versus the explanatory variables (x-axis).*

Discussion

In the North Atlantic, the supply of organic matter via particulate organic carbon can exert strong bottom-up controls on VME biodiversity. Section 2 of this Deliverable 3.2 reviewed the hydrographic mechanisms by which OM and POC can reach VMEs on the deep seafloor, highlighting strong links to large scale and local hydrodynamics, and the variety of physical mechanisms by which food reaches VMEs via

features that enhance current velocities, e.g., downstream of upwelled water, cascading, internal waves). Section 2 also synthesised the importance of OM for many areas in the North Atlantic, revealing close links between the distribution of VME habitat-formers and indicator taxa, as well as a means for coupling whereby, e.g., cold-water coral mound growth creates more turbulence and downwelling, which promotes carbon transfer back down to the seafloor VMEs.

However, the synthesis and review in the first part of Deliverable 3.2 (section 2) also showed that a critical decrease in POC flux (>50 % reduction) by 2100 was predicted to occur in the central-eastern Atlantic, including around the Azores Case Study, and a part of the Rockall Case Study. While North Atlantic-wide reductions in food supply were predicted by the models in Section 2 in general, e.g, also for the Davis Strait Case Study area, critical reductions in the Azores Case Study and around Rockall are concerning in light of the new empirical evidence shown in this comparative and in-depth studies presented here in Section 3.5.

POC flux rates are already a critically limiting factor in the Azores, unlike Davis Strait and Rockall, at least to VME indicator taxa. In these other two Case Studies from the Atlantic-Arctic interface and from the UK/High Seas area, VME distribution exhibits spatial structure (varies across space), but here, the occurrence and biomass of VME taxa is more likely limited and structured by other environmental factors because POC is not (currently) limiting. For example, the presence of deep-sea sponge grounds in the Hudson Strait and Ungava Bay region near Davis Strait are primarily structured by mean surface currents, minimum surface temperature and minimum summer chlorophyll, whereas depth and salinity help predict sponge occurrence best in the Davis Strait itself (Beazley et al. 2016). Notably (relevant to the in-depth analysis at Logachev Mound Province discussed next), surface salinity, bottom sea temperatures and mixed layer depth best predict sponge biomass (Beazley et al. 2016). However, with the supply of OM and POC playing a crucial role structuring VME biodiversity across the whole of the Azores marine EEZ, a projected POC flux reduction >50% by 2100 will have devastating consequences to future VME biodiversity in the central Atlantic, even without the cumulative impacts of multiple other stressors that the Azores EEZ could experience such as the shoaling (shallowing) of the aragonite saturation horizon to 2000 m water depth, anomalously cooler oceans at depths, and human activites such as deep seabed mining.

The in-depth analysis at the Logachev Mound Province in the UK EEZ and High Seas off Rockall showed signficiant effects of other environmental variables on controlling VME biodiversity (Shannon's diversity, and evenness), with higher biodiversity in areas on Logachev that had lower

POC flux values. In contrast (and now linking back to observations of sponge grounds in the Davis Strait where POC is also not limiting) is that octocoral and black coral density were higher in areas with the highest POC flux: more corals equals more biomass, but not necessarily higher biodiversity. Thus, while any critical reduction in POC flux in the area of Rockall would not likely affect coral diversity, decreased food supply could limit coral biomass of those species that do prefer higher amounts of POC for feeding. In ATLAS WP2, the integrated model of hydrodynamics, biomass and organic matter supply will further investigate what impacts loss of VME biomass could mean for ecosystem functioning in these three Case Study areas.

References

Beazley, L., Murillo, J., Kenchington, E., Guijarro-Sabaniel, J., Lirette, C., Siferd, T., Treble, M., Baker, E., Bouchard Marmen, M., Tompkins-MacDonald, G. (2016) Species distribution modelling of corals and sponges in the eastern Arctic for use in the identification of significant benthic areas. Canadian Technical Report of Fisheries and Aquatic Sciences 3175.

Breiman L (2001) Random forests. Machine Learning 45: 5-32.

Cairns, S.D. 2006. Studies on western Atlantic Octocorallia (Coelenterata: Anthozoa). Part 3: The genus *Narella* Gray, 1870. *Proceedings of the Biological Society of Washington*, 116 (3):617–648.

Cutler DR, Edwards TC, Beard KH, Cutler A, Hess KT (2007) Random forests for classification in ecology. Ecology 88: 783-2792.

Cyr F, Van Haren H, Mienis F, Duineveld G. and Bourgault D (2016) On the influence of cold-water coral mound size on flow hydrodynamics, and vice versa. Geophysical Research Letters 43.

Davies AJ, Duineveld GC, Lavaleye MSS, Bergman MJN, Van Haren H, Roberts JM (2009) Downwelling and deep-water bottom currents as food supply mechanisms to the cold-water coral *Lophelia pertusa* (Scleractinia) at the Mingulay Reef complex. Limnology and Oceanography 54: 620-629.

De Clippele LH, Gafeira J, Robert K, Hennige S, Lavaleye MS, Duineveld GCA, et al. (2017) Using novel acoustic and visual mapping tools to predict the small-scale spatial distribution of live biogenic reef framework in cold-water coral habitats. Coral Reefs 36(1): 255-268. doi: 10.1007/s00338-016-1519-8.

de Haas H, Mienis F, Frank N, Richter TO, Steinacher R, de Stigter H, et al. (2009) Morphology and sedimentology of (clustered) cold-water coral mounds at the south Rockall Trough margins, NE Atlantic Ocean. Facies 55(1): 1-26. doi: 10.1007/s10347-008-0157-1.

Dorschel B, Hebbeln D, Foubert A, White M and Wheeler AJ (2007) Hydrodynamics and cold-water coral facies distribution related to recent sedimentary processes at Galway Mound west of Ireland. Marine Geology 244(1-4): 184-195. doi: 10.1016/j.margeo.2007.06.010.

Douarin M, Sinclair DJ, Elliot M, Henry L-A, Long D, Mitchison F and Roberts JM (2014) Changes in fossil assemblage in sediment cores from Mingulay Reef Complex (NE Atlantic): Implications for coral reef build-up. Deep-Sea Research Part II: Topical Studies in Oceanography 99: 286-296.

Findlay HS, Artioli Y, Moreno-Navas J, Hennige SJ, Wicks LC, Huvenne VA, Woodward EM, Roberts JM (2013) Tidal downwelling and implications for the carbon biogeochemistry of cold-water corals in relation to future ocean acidification and warming. Global Change Biology19(9): 2708-19.

Guinan J, Grehan AJ, Dolan MFJ, Brown C (2009) Quantifying relationships between video observations of cold-water coral cover and seafloor features in Rockall Trough, west of Ireland. Marine Ecology Progress Series 375: 125-138.

Henry L-A, Davies AJ and Roberts JM (2010) Beta diversity of cold-water coral reef communities off western Scotland. Coral Reefs 29: 427-436.

Hestetun, J.T, Fourt, M., Vacelet, J., Boury-Esnault, N. & Rapp, H.T. 2015. Cladorhizidae (Porifera, Demospongiae, Poecilosclerida) of the deep Atlantic collected during Ifremer cruises, with a biogeographic overview of the Atlantic species. *Journal of the Marine Biological Association of the United Kingdom*, 95 (7): 1311–1342. DOI: 10.1017/S0025315413001100

Howell, K-L., Piechaud, N., Downie, A-L. & Kenny, A. 2016. The distribution of deep-sea sponge aggregations in the NA and implications for their effective spatial management. *Deep-Sea Research I*, 115: 309–320. DOI: 10.1016/j.dsr.2016.07.005

Huthnance JM (1986) The Rockall slope current and shelf-edge processes. Proceedings of the Royal Society of Edinburgh 88B: 83-101. doi: 10.1017/S0269727000004486.

Jones, D.O., Yool, A., Wei, C.L., Henson, S.A., Ruhl, H.A., Watson, R.A. and Gehlen, M. 2014. Global reductions in seafloor biomass in response to climate change. Global change biology, 20(6):1861-1872.

Kenyon NH, Akhmetzhanov Am, Wheeler AJ, van Weering TCE, de Haas H and Ivanov MK (2003) Giant carbonate mud mounds in the southern Rockall Trough. Marine Geology 195(1-4): 5-30.

Liaw A and Wiener M (2002) Classification and regression by random forest. R News 2(3): 18-22.

Lutz, M.J., Caldeira, K., Dunbar, R.B. & Behrenfeld, M.J. 2007. Seasonal rhythms of net primary production and particulate organic carbon flux to depth describe the efficiency of biological pump in the global ocean. *Journal of Geophysical Research*, 112: C10011.
DOI: https://doi.org/10.1029/2006JC003706

Mienis F, de Stigter HC, White M, Duineveld G, de Haas H, van Weering TCE (2007) Hydrodynamic controls on cold-water coral growth and carbonate-mound development at the SW and SE Rockall Trough Margin, NE Atlantic Ocean. Deep-Sea Research I 54(9): 1655-1674.

Mienis F, van Weering T, de Haas H, de Stigter H, Huvenne VAI and Wheeler A (2006) Carbonate mound development at the SW Rockall Trough margin based on high resolution TOBI and seismic recording. Marine Geology 233(1-4): 1-1.

Mohn C and Beckmann A (2002) Numerical studies on flow amplification at an isolated shelf break bank, with application to Porcupine Bank. Continental Shelf Research 22: 1325-1338.

Molodtsova, T., Sanamyan, N. & Keller, N. 2008. Anthozoa from the northern Mid-Atlantic Ridge and the Charlie-Gibbs Fracture Zone. Marine Biology Research, 4 (1-2): 112-130. DOI: 10.1080/17451000701821744

Mortensen PB (2001) Aquarium observations on the deep-water coral *Lophelia pertusa* (L., 1758) (Scleractinia) and selected associated invertebrates. *Ophelia* 54: 83-104.

Proulx R, Bohn K, Dyke JG, Kleidon A, Pavlick R and Schmidtlein S (2011) The role of climate and plant functional trade-offs in shaping global biome and biodiversity patterns. Global Ecology and Biogeography 20(4) pp. 570-581.
Roberts JM, Wheeler AJ, Freiwald A (2006) Reefs of the deep: the biology and geology of cold-water coral ecosystems. Science 312: 543-547. doi: 10.1126/science.1119861.

Rogan J, Franklin J, Stow D, Miller J, Woodcock C, Roberts D (2008) Mapping land-cover modifications over large areas: A comparison of machine learning algorithms. Remote Sensing of Environment 112: 2272-2283.

Sebens KP, Grace SP, Helmuth B, Maney EJ and Miles JS (1998) Water flow and prey capture by three scleractinian corals, *Madracis mirabilis*, *Montastrea cavernosa* and *Porites porites* in a field enclosure. Marine Biology 131(2): 347-360. doi: 10.1007/s002270050328.

Smith, C.R., De Leo, F.C., Bernardino, A.F., Sweetman, A.K. and Arbizu, P.M. 2008. Abyssal food limitation, ecosystem structure and climate change. *Trends in Ecology & Evolution* 23: 518–528. DOI: https://doi.org/10.1016/j. tree.2008.05.002

Smith, K.L., Ruhl, H.A., Bett, B.J., Billett, D.S.M., Lampitt, R.S. and Kaufmann, R.S. 2009. Climate, carbon cycling, and deep-ocean ecosystems. Proc Nat Acad S USA 106: 19211–19218. DOI: https://doi.org/10.1073/ pnas.0908322106

Soetaert K, Mohn C, Rengstorf A, Grehan A and van Oevelen D (2016) Ecosystem engineering creates a direct nutritional link between 600-m deep cold-water coral mounds and surface productivity. Scientific Reports 6: 35057.

Sweetman, A.K., Thurber, A.R., Smith, C.R., Levin, L.A., Mora, C., Wei, C.-L., Gooday, A. J., Jones, D.O.B., Rex, M., Yasuhara, M., Ingels, J., Ruhl, H.A., Frieder, C.A., Danovaro, R., Würzberg, L., Baco, A., Grupe, B.M., Pasulka, A., Meyer, K.S., Dunlop, K.M., Henry, L.-A. & Roberts, J.M. 2017. Major impacts of climate change on deep-sea benthic ecosystems. *Elementa Science of the Anthropocene*, 5: 4. DOI: https://doi.org/10.1525/elementa.203

Tabachnick, K. & Collins, A. 2008. Glass sponges (Porifera, Hexactinellida) of the northern Mid-Atlantic Ridge. *Marine Biology Research*, 4 (1-2):25-47. DOI: 10.1080/17451000701847848.

van Oevelen F, Duineveld G, Lavaleye M, Mienis F, Soetaert K and Heip CHR (2009) The cold-water coral community as a hot spot for carbon cycling on continental margins: A food-web analysis from Rockall Bank (northeast Atlantic). Limnology and Oceanography 54(6): 1829-1844.

Van Weering TCE, de Haas H, de Stigter HC, Lykke-Andersen H and Kouvaev I (2003) Structure and development of giant carbonate mounds at the SW and SE Rockall Trough margins, NE Atlantic Ocean. Marine Geology 198(1-2): 67-81.

Wagner D, Pochon X, Irwin L, Toonen RJ and Gates RD (2011). Azooxanthellate? Most Hawaiian black corals contain *Symbiodinium*. Proceedings of the Royal Society B 278: 1323-1328. doi: 10.1098/rspb.2010.1681.

Watling, L., Guinotte, J., Clark, M.R. and Smith, C.R. 2013. A proposed biogeography of the deep ocean floor. *Progress in Oceanography*, 111:91-112.

White M, Roberts JM and van Weering T (2007) Do bottom-intensified diurnal tidal currents shape the alignment of carbonate mounds in the NE Atlantic? Geo-Marine Letters 27(6): 391-397. doi: 10.1007/s00367-007-0060-8.

Wilson MFJ, O'Connel B, Brown C, Guinan JC and Grehan AJ (2007) Multiscale Terrain Analysis of Multibeam Bathymetry Data for Habitat Mapping on the Continental Slope. Marine Geodesy 30: 3-35.

Wood, H.L., Spicer, J.I. and Widdicombe, S. 2008. Ocean acidification may increase calcification rates, but at a cost. Proceedings of the Royal Society B: Biological Sciences, 275(1644):1767-1773.

Wright, D.J., Pendleton, M., Boulware, J., Walbridge, S., Gerlt, B., Eslinger, D., Sampson, D. and Huntley, E., 2012. ArcGIS Benthic Terrain Modeler (BTM), v. 3.0, Environmental Systems Research Institute, NOAA Coastal Services Center, Massachusetts Office of Coastal Zone Management. Available onlineat http://esriurl.com/5754.

Appendix: Document Information

EU Project N°	678760	Acronym	ATLAS
Full Title	A trans-Atlantic assessment and deep-water ecosystem-based spatial management plan for Europe		
Project website	www.eu-atlas.org		

Deliverable	N°	3.2	Title	Oceanographic and hydrographic controls on North Atlantic Vulnerable Marine Ecosystem biodiversity and biogeography
Work Package	N°	3	Title	Biodiversity and Biogeography

Date of delivery	Contractual
Dissemination level	Public

Authors (Partner)	UEDIN			
Responsible Authors	Name	Lea-Anne Henry	Email	l.henry@ed.ac.uk

Version log			
Issue Date	Revision N°	Author	Change